Universidade de Aveiro Departamento de Engenharia Cerâmica e do Vidro, **2000**

José Martinho Marques de Oliveira

desenvolvimento de vidros e de vidros cerâmicos sílico-fosfatados com elevado teor de alcalino-terrosos para aplicações biomédicas

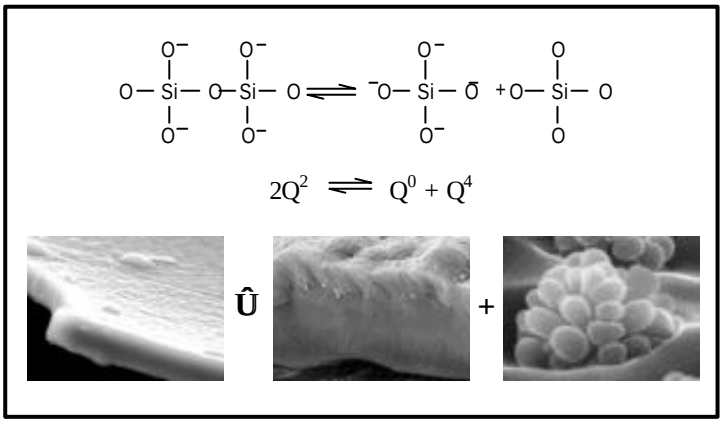

Universidade de Aveiro Departamento de Engenharia Cerâmica e do Vidro, **2000**

José Martinho Marques de Oliveira

desenvolvimento de vidros e de vidros cerâmicos sílico-fosfatados com elevado teor de alcalino-terrosos para aplicações biomédicas

tese apresentada à Universidade de Aveiro para cumprimento dos requisitos necessários à obtenção do grau de Doutor em Ciência e Engenharia dos Materiais, realizada sob a orientação científica da Dra. Maria Helena Figueira Vaz Fernandes, Professora Auxiliar do Departamento de Engenharia Cerâmica e do Vidro e do Dr. Rui Nunes Correia, Professor Associado do mesmo departamento.

o júri

presidente

Prof. Doutor Celso de S. Figueiredo Gomes

professor catedrático da Universidade de Aveiro

Prof. Doutor Jorge Ribeiro Frade

professor catedrático da Universidade de Aveiro

Prof. Doutor José Domingos dos Santos

professor associado da Faculdade de Engenharia da Universidade do Porto

Prof. Doutora Maria Clara Henriques Baptista Gonçalves

professora auxiliar do Instituto Superior Técnico da Universidade Técnica de Lisboa

Prof. Doutora Maria Helena Figueira Vaz Fernandes

professora auxiliar da Universidade de Aveiro

Prof. Doutor José Maria Fernandes Navarro

professor de investigação, Consejo Superior de Investigaciones Científicas, Fundação Centro Nacional del Vidrio, Espanha

agradecimentos

É com enorme satisfação que deixo aqui expresso um profundo agradecimento aos meus supervisores Professores Doutores Helena Fernandes e Rui Correia pelas preciosas orientação, ajuda e compreensão prestadas ao longo deste trabalho.
À Prof. Helena Fernandes, que me iniciou num novo mundo – os VIDROS, desejo ainda, em virtude da grande simpatia, da amizade e direi mesmo do carinho com que sempre me presenteou, exprimir-lhe ainda a minha especial gratidão.

Agradeço à minha esposa, Cristina, a compreensão, o amor e o apoio demonstrado ao longo deste percurso.

Do ambiente humano existente no DECV, à data de início dos trabalhos de doutoramento, sublinho a camaradagem e amizade existentes e endereço um especial abraço ao Rogério Lopes.

Agradeço à Junta Nacional de Investigação Científica e Tecnológica a Bolsa Ciência BD/2762/93 e a atitude tomada aquando da minha renuncia à mesma, em virtude da instabilidade provocada pela transição para o Programa Praxis XXI.

À Universidade de Aveiro e a todo o pessoal do DECV os meus sinceros agradecimentos.

A minha dívida para com todos é muito grande. Obrigado.

resumo

A presente tese dá seguimento ao trabalho de mestrado realizado pelo mesmo autor. Pretendeu-se estudar os processos de separação de fases amorfas e de cristalização em vidros do sistema base SiO_2-CaO-P_2O_5-MgO obtidos por fusão. Avaliou-se também como o comportamento *in vitro* de vidros e de vidros cerâmicos desse sistema, em especial a influência da estrutura nos primeiros e de características morfológicas nos segundos.

A tese é constituída por um conjunto de artigos científicos apresentados em revistas da especialidade e em congressos. Os artigos estão agrupados em 3 capítulos (capítulos 2, 3 e 4) sendo a primeira secção de cada um deles constituída por uma introdução ao tema.

No primeiro capítulo faz-se uma breve referência à evolução histórica da investigação em biovidros e biovidros cerâmicos e apresentam-se os materiais que foram objecto de estudo nesta tese.

O segundo capítulo respeita a estudos de separação de fases amorfas e de cristalização em vidros. Os vidros bifásicos apresentam uma fase dispersa constituída por sílica amorfa, a qual tem uma morfologia peculiar – formações do tipo mórula. O desenvolvimento destas formações depende de parâmetros como a temperatura, o tempo de fusão e a composição química da matriz. Concluiu-se que a formação das mórulas resulta de um processo rápido de coalescência a partir de um número de formações existentes no fundido, característico da temperatura de fusão mas independente do tempo, e que as suas dimensões médias finais são função da viscosidade da fase contínua. Estudos com TiO_2 permitiram concluir que a sua adição a um vidro monofásico do sistema SiO_2-$_3$CaO.P_2O_5-MgO provoca separação de fases amorfas e facilita a sua posterior cristalização. Com base na técnica de análise térmica diferencial (ATD) foram realizados estudos cinéticos de cristalização a temperatura variável num vidro bifásico (V4) de composição (% ponderal) SiO_2 30, CaO 28,61, P_2O_5 24,14 e MgO 17,25. Através da aplicação de modelos teóricos concluiu-se que o processo de cristalização é constituído por duas etapas: nucleação (a ≈ 730 °C) e crescimento de cristais (para temperaturas superiores a

800 °C), sendo a energia de activação do processo de crescimento de cristais elevada (≈ 763 kJ/mol) mas inferior à energia de activação de fluxo viscoso (≈ 1000 kJ/mol). Concluiu-se ainda ser aconselhável adaptar os modelos cinéticos às condições experimentais usadas na ATD.

No terceiro capítulo são apresentados estudos de natureza estrutural subjacentes à compreensão do comportamento dos vidros em meio fisiológico sintético acelular. Através do recurso à técnica de ressonância magnética nuclear (RMN) foi identificada uma reacção de desproporcionação do silício, $2Q^2 \rightleftharpoons Q^0 + Q^4$, em vidros com elevado teor de óxidos alcalino-terrosos. Esta reacção torna-se mais extensa à medida que a razão MgO/CaO aumenta. O fósforo está presente sob a forma de orto-fosfato. Neste capítulo é apresentado um outro estudo realizado com o objectivo de desenvolver um vidro monofásico com composição e estrutura idênticas às da matriz do vidro bifásico V4. O estudo da matriz do vidro V4 tem interesse na compreensão do processo de cristalização e da viscosidade (determinante do tamanho final das mórulas).

O quarto capítulo é dedicado ao comportamento *in vitro* de vidros e de vidros cerâmicos. Analisou-se a influência da especiação do silício na bioactividade de vidros com a mesma conectividade de rede, tendo-se concluído que a sua presença modifica o comportamento *in vitro* destes materiais em virtude da diferente solubilidade das espécies Q^n. Este comportamento promove os estágios 1-3 do mecanismo proposto por Hench. Embora seja um modificador, concluiu-se que o magnésio tem um papel estrutural diferente do desempenhado pelo cálcio, provocando um aumento da solubilidade dos vidros. O estudo do efeito da topografia e da presença de fases cristalinas no comportamento bioactivo dos vidros cerâmicos encerra esta tese. A existência de flutuações microestruturais e topográficas associada à presença de hidroxiapatite é responsável pela nucleação *in vitro* de apatite à superfície de vidros cerâmicos.

abstract

This work extends the subject of the master thesis by the same author, its main aims being the study of the amorphous phase separation process and crystallisation in melted glasses of the SiO_2-CaO-P_2O_5-MgO system. The *in vitro* behaviour of glasses and glass-ceramics was also evaluated, especially the influence of structure and morphological characteristics.

This thesis is mainly composed by sets of scientific articles published in international journals and congresses. The papers are gathered in 3 chapters (Chapters 2, 3 and 4), the first section of each chapter being a introduction.

In the first chapter a short historical overview of the development of bioactive glasses and glass-ceramics is presented together with the materials that were used in this investigation.

The second chapter is dedicated to the amorphous phase separation and crystallisation in glasses. The two-phase glasses show a dispersed phase that is amorphous silica with a peculiar morphology – morular type formations. The development of these formations depends on melting temperature and time and on the chemical composition of the matrix. It was concluded that a fast coalescence process of a fixed amount of individual droplets was responsible for morulae formation. This fixed amount of droplets depends on melting temperature but is independent of the melting time. The final average morulae dimensions are a function of the matrix viscosity. Additions of TiO_2 to an otherwise monophasic glass of the SiO_2-$3CaO.P_2O_5$-MgO system were able to increase the overall crystallisation rates and to promote amorphous immiscibility in the system. The differential thermal analysis (DTA) technique coupled with theoretical models was used to study the non-isothermal crystallisation kinetics of a phase-separated glass (V4) of nominal composition (wt. %) 30 SiO_2, 28.61 CaO, 24.14 P_2O_5, 17.25 MgO. It was concluded that the kinetics of crystallisation comprises two stages: a nucleation stage at about 730 °C and a particle growth stage for temperatures higher that 800 °C, the activation energy for growth being very high (≈ 763 kJ/mol) but still lower than the activation energy for viscous flow (≈ 1000 kJ/mol). It was also

concluded that it is necessary to introduce modifications in the kinetic models in order to get a good agreement with the experimental DTA conditions. Chapter three reports structural studies of glasses in order to understand the bioactive properties of these materials. By magic-angle spinning (MAS) nuclear magnetic resonance (NMR) technique a silicon desproportionation reaction, $2Q^2 \rightleftharpoons Q^0 + Q^4$, in alkaline-earth rich glasses was identified. This reaction is more extensive as the MgO/CaO ratio increases. Besides Q species these glasses are composed by orthophosphate species. This chapter presents further work pursued in order to develop a monophasic glass with the same composition and structure of the matrix in two-phase glass V4. The interest for such material stems from the important role of the V4 glass matrix in the crystallisation behaviour and in the viscosity (which determines the final dimensions of the dispersed phase).

The forth chapter presents *in vitro* studies of glasses and glass-ceramics. The influence of silicon speciation in the bioactivity of glasses with the same network connectivity is analysed and it is concluded that this phenomenon changes the behaviour of glasses due to the different solubilities of Q^n species. This behaviour promotes the stages 1-3 of Hench's mechanism. Although magnesium behaves as a modifier, it plays a structural role different from that played by calcium, the final result being an increase in glass solubility as the MgO/CaO ratio augments. The influence of morphology and nature of crystalline phases on the bioactive behaviour of some glass-ceramics was the last field addressed. It is proposed that microstructural fluctuations together with the presence of crystalline hydroxyapatite are responsible for *in vitro* apatite nucleation in glass-ceramics.

Para a Cristina e para a Inês

ÍNDICE

1 - PREÂMBULO I

1.1 - Breve história do desenvolvimento de biovidros e biovidros cerâmicos 3

1.2 - Os biovidros e os biovidros cerâmicos comercialmente mais utilizados 4

1.3 - Projecto das composições vítreas 5

Referências Bibliográficas 9

2 - ESTUDOS DE SEPARAÇÃO DE FASES E DE NUCLEAÇÃO E CRESCIMENTO DE CRISTAIS EM VIDROS 11

2.1 - Introdução 13

2.1.1 - Estruturas "morulares" 13

2.1.2 - Nucleação e crescimento de cristais em vidros – alguns aspectos cinéticos 16

Referências Bibliográficas 20

2.2 - Phase Separation and Crystallisation in $3CaO.P_2O_5$-SiO_2-MgO Glasses 25

2.3 - TiO_2-induced Amorphous Phase Separation and Crystallization in a Glass of the System SiO_2-$3CaO.P_2O_5$-MgO 31

2.4 - Effect of MgO Additions on Amorphous Phase Separation in Silico-Phosphate Glasses 43

2.5 - Formation of Convoluted Silica Precipitates During Amorphous Phase Separation in the $Ca_3(PO_4)_2$-SiO_2-MgO System 51

2.6 - Crystallization of Whitlockite From a Glass in the System CaO-P_2O_5-SiO_2-MgO 59

3 - ESTRUTURA VÍTREA 83

3.1 - Introdução 85

Referências Bibliográficas 88

3.2 - Effect of SiO_2 on Amorphous Phase Separation of CaO-P_2O_5-SiO_2-MgO Glasses 89

3.3 - Influence of the CaO/MgO Ratio on the Structure of Phase-separated Glasses: a Solid State ^{29}Si and ^{31}P MAS NMR study 99

4 - COMPORTAMENTO *IN VITRO* DE VIDROS E VIDROS CERÂMICOS 115

4.1 - Introdução 117

4.1.1 - A formação de apatite in vitro e mecanismos explicativos 117

O mecanismo de Hench 118

O mecanismo de Kokubo 119

O mecanismo de Andersson 120

O mecanismo de Li *121*
Os pontos fundamentais dos vários mecanismos *122*
4.1.2 - A composição e o papel dos vários componentes do vidro *123*
O silício 124
O fósforo 125
Os outros elementos 125
4.1.3 - O papel das fases vítreas e cristalinas *127*
4.1.4 - A topografia e as características químicas da superfície *128*
4.1.5 - A estrutura da matriz vítrea *129*
Referências Bibliográficas 131
4.2 - Effects of Si Speciation on the *in vitro* Bioactivity of Glasses 141
4.3 - In vitro Bioactivity of Glass and Glass-ceramics of the $3CaO.P_2O_5$-$CaO.SiO_2$-$CaO.MgO.2SiO_2$ System 161
4.4 - Role of Acid Attack in the *in vitro* Bioactivity of a Glass-ceramic of the $3CaO.P_2O_5$-$CaO.SiO_2$-$CaO.MgO.2SiO_2$ System 177
5 - CONCLUSÕES E SUGESTÕES 193
5.1 - Conclusões 195
5.2 - Sugestões para trabalhos futuros 199

1 - PREÂMBULO

1.1 - Breve história do desenvolvimento de biovidros e biovidros cerâmicos

A utilização clínica de materiais no ser humano é uma prática que remonta, pelo menos, ao tempo das civilizações egípcia, grega e hindu. Dos materiais cerâmicos, o gesso e, já neste século, o fosfato tri-cálcico foram os mais procurados.[1-4]

A utilização do vidro como biomaterial é mais recente. O trabalho pioneiro neste domínio data do início da década de 70 e deve-se a Larry Hench, responsável pelo projecto de desenvolvimento do Bioglass® 45S5.[5] A principal característica diferenciadora deste material biocompatível[6] é a sua capacidade para promover uma rápida e durável ligação química, através de uma interface apatítica, com o tecido ósseo, o que lhe valeu a designação de vidro bioactivo. Com o seu desenvolvimento nasceu o conceito de bioactividade e acelerou-se toda a investigação realizada no campo dos materiais para implantes ósseos.

Materiais como o Bioglass® 45S5 e outros vidros, vidros cerâmicos (obtidos por cristalização controlada de vidros) e ainda materiais cerâmicos à base de fosfatos de cálcio constituem um vasto grupo de materiais designados por biocerâmicos. Os biocerâmicos são geralmente classificados em bioinertes (exemplo: alumina), absorvíveis (exemplo: tri-fosfato de cálcio) e porosos (cerâmicos porosos) para além dos bioactivos já referenciados[4].

Dos vidros cerâmicos bioactivos o Ceravital®[7,8,9] foi o primeiro a ser comercializado mas o Cerabone A/W®[10,11], desenvolvido por Kokubo, rapidamente se tornou mais "popular" dadas as suas melhores propriedades mecânicas. Os Bioverit®[12], desenvolvidos por Vogel *et al*., apresentam a vantagem de serem maquináveis devido à presença de cristais curvos do tipo mica (flogopite) na respectiva microestrutura[13].

Actualmente os vidros são utilizados em três situações clínicas distintas: como material bioinerte para aplicações em medicina dentária (vidros do tipo alumino-silicato com elementos alcalinos e/ou alcalino-terrosos, dos quais se destacam os ionoméricos[14,15,16]), como veículos de agentes radioactivos para tratamentos localizados de tumores, em especial do fígado, por radioterapia (vidros do tipo alumino-silicato com elementos terras-raras, sendo o ítrio o elemento mais frequente) e como material

bioactivo para implantologia (vidros de sílica do tipo Bioglass®) especificamente em ortopedia, em cirurgias do ouvido médio, como espaçador intervertebral e em reconstruções maxilo-faciais e ósseas diversas[4,17,18]. É precisamente este último tipo de vidros que foi objecto do presente projecto.

Embora muitos dos biovidros e biovidros cerâmicos existentes tenham sido desenvolvidos pelo *método de tentativa e erro*, actualmente é já possível melhorar a bioactividade de uma composição vítrea através do seu correcto projecto. O principal obstáculo à sua utilização generalizada no ser humano é o fraco desempenho mecânico, dada as inerentes fragilidade e, como na maioria dos materiais inorgânicos, a elevada rigidez destes materiais.

1.2 - Os biovidros e os biovidros cerâmicos comercialmente mais utilizados

De entre os vidros e vidros cerâmicos desenvolvidos para aplicações biomédicas apenas quatro famílias destes materiais atingiram algum sucesso comercial: os vidros Bioglass® e os vidros cerâmicos Ceravital®, Cerabone® A/W e Bioverit®, cujas composições mais frequentes são apresentadas na Tabela 1.I.

As principais características composicionais destes biovidros, em relação aos vidros tradicionais, são o seu baixo conteúdo em sílica, a presença de fósforo e um elevado teor de elementos alcalinos e/ou alcalino-terrosos, o que lhes confere uma grande tendência para desvitrificarem. O processo de fusão tradicionalmente utilizado no fabrico destes vidros tem-se revelado limitativo quando se pretende alargar a gama de composições químicas, pelo que a preparação por via sol-gel pode ser útil no estudo de novas composições, aumentando também o nível de homogeneidade dos materiais e permitindo um melhor controlo de porosidade e da reactividade da superfície.[22]

Tabela 1.I. Composições ponderais típicas de vidros e vidros cerâmicos bioactivos comercializados.

(%)	Bioglass® 45S5[4]	Ceravital® KG Cera[19]	Ceravital® Mina 13[19]	Cerabone® A/W[10]	Bioverit® I[20]	Bioverit® II[20]	Bioverit® III[21]
SiO_2	45,0	46,2	46,0	34,0	30,5	44,5	
P_2O_5	6,0	18,3	11,5	16,2	11,4	0,2	51,4
CaO	24,5	27,4	37,5	44,7	14,4	0,2	16,0
MgO		2,9	5,0	4,6	14,8	11,8	
Na_2O	24,5	4,8			2,3	4,4	14,6
K_2O		0,4			5,8	4,9	
Al_2O_3					15,9	29,7	9,0
CaF_2				0,5			
F					4,9	4,2	1,8
Cl						0,1	
ZrO_2							4,5
TiO_2							2,7
Fases	Amorfa	Amorfa Apatite	Amorfa Apatite	Amorfa Apatite Wollastonite	Amorfa Apatite Flogopite	Amorfa Flogopite Cordierite	Amorfa Apatite $AlPO_4$

1.3 - Projecto das composições vítreas

Ao longo da realização do trabalho experimental conducente a esta tese, foi necessário projectar vários vidros base. No projecto das composições sílico-fosfatadas manteve-se um elevado teor de elementos alcalino-terrosos e, em especial, procurou-se estudar o efeito do magnésio na estrutura vítrea e sua relação com o comportamento *in vitro*.

Todos os materiais estudados pertencem ao sistema SiO_2-P_2O_5-CaO-MgO. Em alguns trabalhos foram ainda utilizadas pequenas quantidades de CaF_2 e TiO_2 como agentes dopantes.

Com base no conhecimento prévio[23] da zona de formação vítrea no ternário $3CaO.P_2O_5$-SiO_2-MgO (Fig. 1.1) e das principais características dos materiais desenvolvidos, foram inicialmente seleccionados dois vidros para diferentes estudos: o

vidro bifásico V4 e o monofásico V5, cujas composições são apresentadas na Tabela 1.II.

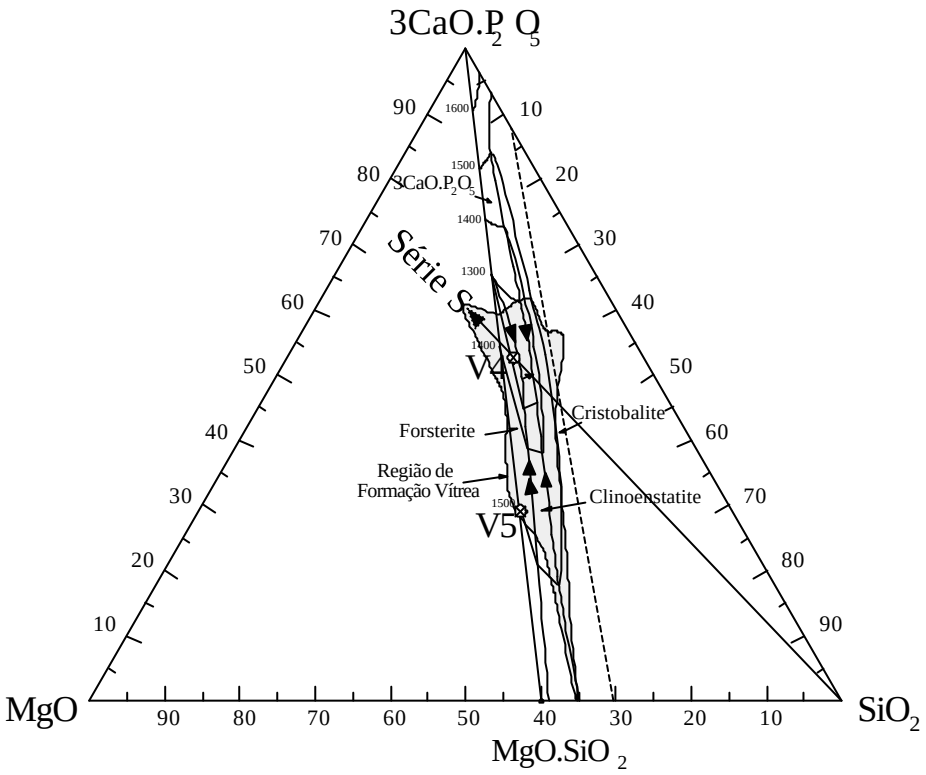

Fig. 1.1. Diagrama de fases do sistema $3CaO.P_2O_5$-SiO_2-MgO com sinalização das composições estudadas (adaptado de Sata[24]).

Tabela 1.II. Composições ponderais dos vidros V4 e V5.

	$3CaO.P_2O_5$	SiO_2	MgO
V4	52,75	30,00	17,25
V5	29,43	42,67	28,00

Nos trabalhos apresentados nas secções 2.2, 2.5 e 2.6 foi utilizado o vidro V4 e na secção 2.3 o V5 dopado com diferentes quantidades de TiO_2.

Foi também desenvolvido um conjunto de vidros, denominado "Série CM" no qual se procedeu à substituição de CaO por MgO. A composição molar é $31SiO_2$-$11P_2O_5$-(58-*x*)CaO-*x*MgO, com *x* a variar desde 0 a 32 (Fig. 1.2). Esta série tem a

particularidade de conter a composição V4, sendo aí denominada CM6 (x = 26,6) e foi alvo de estudos apresentados nas secções 2.4, 3.3 e 4.2.

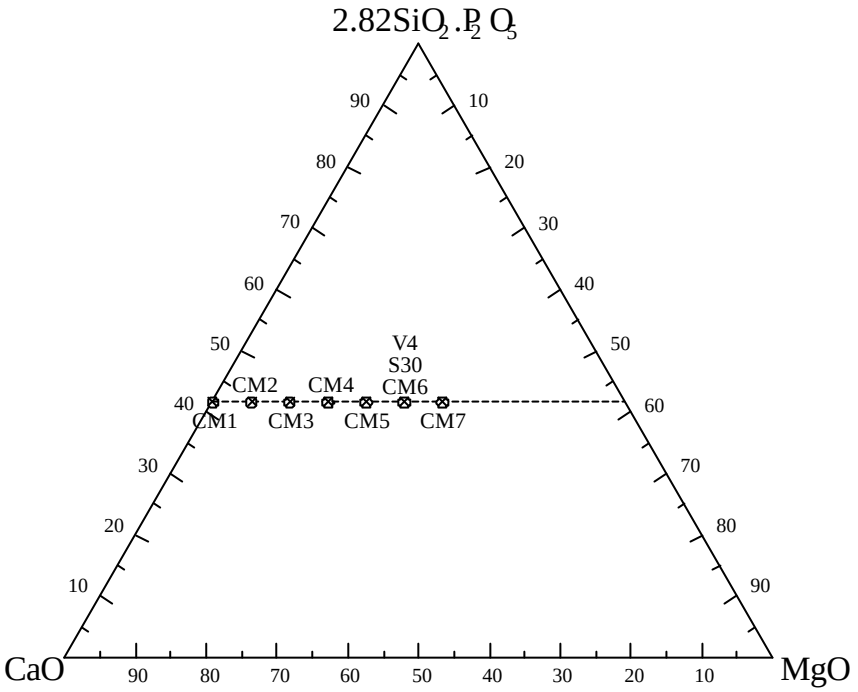

Fig. 1.2. Composições dos vidros da Série CM.

Com o objectivo de desenvolver um vidro monofásico de composição e estrutura iguais às da matriz do vidro bifásico V4 projectou-se um outro conjunto de vidros – "Série S" de composição ponderal: $52{,}75(1+x/70)CaO.P_2O_5$-$17{,}25(1+x/70)MgO$-$(30-x)SiO_2$. Esta série foi desenvolvida a partir da composição V4 que aqui adopta a designação S30 (x = 0). A linha de composição desta série está indicada no diagrama da Fig. 1.1 e os resultados são apresentados na secção 3.2.

Por fim, e sempre com o intuito de estudar a influência do MgO, apresentam-se nas secções 4.3 e 4.4 trabalhos realizados com o vidro e vitrocerâmicos de composição G13 (Tabela 1.III), desenvolvido no sistema $3CaO.P_2O_5$-$CaO.SiO_2$-$CaO.MgO.2SiO_2$ a partir da composição Cerabone A/W® de Kokubo[10] (Fig. 1.3). Este estudo permitiu analisar a influência da topografia provocada por ataque ácido e da presença da hidroxiapatite no comportamento *in vitro* dos vidros cerâmicos.

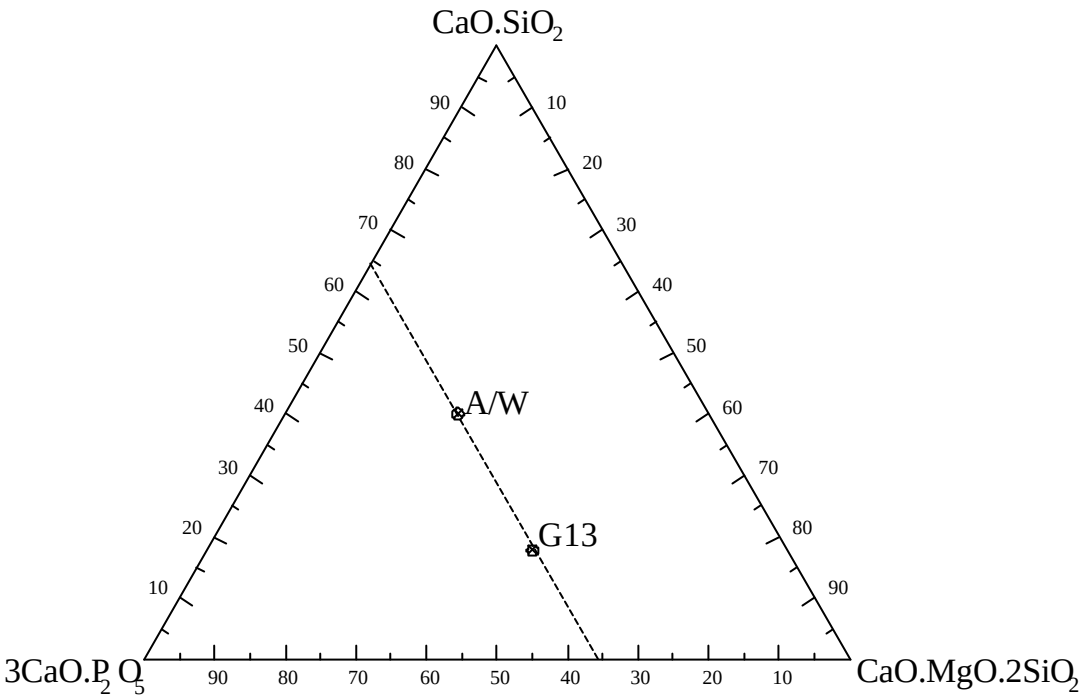

Fig. 1.3. Composição estudada no sistema $CaO.SiO_2$-$CaO.MgO.2SiO_2$-$3CaO.P_2O_5$ (G13).

Tabela 1.III. Composições ponderais dos vidros G13 e A/W.

	CaO	SiO_2	P_2O_5	MgO	CaF_2
G13	**40,01**	34,53	16,49	**8,46**	0,51
A/W	**44,68**	34,03	16,21	**4,58**	0,50

Em termos experimentais esta tese é constituída por um capítulo dedicado ao estudo da separação de fases amorfas em alguns dos vidros estudados. Nesse capítulo são ainda apresentados estudos de cristalização em vidros.

Nos dois capítulos seguintes são apresentados estudos de natureza estrutural realizados em vidros e de comportamento *in vitro* de vidros e de vidros cerâmicos.

Em todos estes capítulos a primeira secção é constituída por uma breve introdução, a qual no capítulo 4 assume a forma de uma revisão bibliográfica.

No último capítulo são enumeradas as principais conclusões desta tese e apresentadas algumas sugestões para trabalhos futuros.

Referências Bibliográficas

[1] Hench, L. L. – "La Fabbricazione dei Bioceramici", *Ceramurgia*, VII, 1977, 253-266.

[2] Hulbert, S. F.; Hench, L. L.; Forbers, D.; Bowman, L. S. – "History of Bioceramics", *Ceramics International*, 8, 1982, 131-140.

[3] Hench, L. L. – "The Processing of Bioceramics", Advances in Ceramics Processing – *Proceedings of the 3rd CIMTEC*, 1978, 92-100.

[4] Hench, L. L. – "Bioceramics", *Journal of the American Ceramic Society*, 81, 1998, 1705-1728.

[5] Hench, L. L.; Splinter, R. J.; Allen, W. C.; Greenlee, T. K. – "Bonding Mechanisms at the Interface of Ceramic Prosthethic Materials", *Journal of Biomedical Materials Research Symposium*, 36, 1971, 117-141.

[6] Wilson, J.; Pigott, G. H.; Hench, L. L. – "Toxicology and Biocompatibility of Bioglasses", *Journal of Biomedical Materials Research*, 15, 1981, 805-817.

[7] Bromer, H.; Deutscher, K.; Blencke, B.; Pfeil, E.; Strunz, V. – "Properties of the Bioactive Implant Material *Ceravital*", *Science of Ceramics*, 9, 1977, 219-225.

[8] Ohtsuki, C.; Kushitani, H.; Kokubo, T.; Kotani, S.; Yamamuro, T. – "Apatite Formation on the Surface of Ceravital-type Glass-ceramic in the Body", *Journal of Biomedical Materials Research*, 25, 1991, 1363-1370.

[9] Gross, U. M.; Müller-Mai, C. – "Hard Materials-Tissue Interface: General Considerations and Examples for Bone Bonding and for Epithelial Attachment", *in* Yamamuro, T.; Hench, L. L.; Wilson, J. – *CRC Handbook of Bioactive Ceramics*, 1, Boca Raton, CRC Press, 1990, 25-39.

[10] Kokubo, T.; Shigematsu, M.; Nagashima, Y.; Tashiro, M.; Nakamura, T.; Yamamuro, T.; Higashi, S. – "Apatite -and Wollastonite-Containing Glass-ceramic for Prosthetic Application", *Bullettin of the Institute of Chemical Research Kyoto University*, 60, 1982, 260-268.

[11] Kokubo, T. – "Bonding Mechanism of Bioactive Glass-ceramic A-W to Living Bone", *in* Yamamuro, T.; Hench, L. L.; Wilson, J. – *CRC Handbook of Bioactive Ceramics*, 1, Boca Raton, CRC Press, 1990, 41-49.

[12] Vogel, W.; Holand, W.; Naumann, K.; Gummel, J. – "Development of Machineable Bioactive Glass-ceramics for Medical Uses", *Journal of Non-Crystalline Solids*, 80, 1986, 34-51.

[13] Holand, W.; Vogel, W.; Mortier, W. J.; Duvingneaud, P. H.; Naessens, G.; Plumat, E. – "A New type of Phlogopite Crystal in Machineable Glass-ceramics", Glass Technology, 24, 1983, 318-322.

[14] Wilson, A. D. – "Glass-Ionomer Cements - Origins, Development and Future", *Clinical Materials*, 7, 1991, 275-282.

[15] McLean, J. W. – "The Clinical Use of Glass-Ionomer Cements - Future and Current Developments", *Clinical Materials*, 7, 1991, 283-288.

[16] Nicholson, J. W. – "Chemistry of Glass Ionomer Cements: A Review", *Biomaterials*, 19, 1998, 485-494.

[17] Day, D. – "Using Glass in the Body", *The American Ceramic Society Bulletin*, 74, 1995, 64-68.

[18] Day, D. E.; Day, T. E. – "Radiotherapy Glasses" *in* Hench, L. L.; Wilson, J. – *An Introduction to Bioceramics*, 1, Singapore, World Scientific, 1993, 305-317.

[19] Gross, U. M.; Müller-Mai, C.; Voigt, C. – "Ceravital® Bioactive Glass-ceramics" *in* Hench, L. L.; Wilson, J. – *An Introduction to Bioceramics*, 1, Singapore, World Scientific, 1993, 105-123.

[20] Höland, W.; Vogel, W. – "Machinable and Phoshate Glass-ceramics" *in* Hench, L. L.; Wilson, J. – *An Introduction to Bioceramics*, 1, Singapore, World Scientific, 1993, 125-137.

[21] Verné, E.; Ferraris, M.; Jana, C. – "Pressureless Sintering of Bioverit® III/Ti Particle Biocomposites", *Journal of the European Ceramic Society*, 19, 1999, 2039-2047.

[22] Hench, L. L. – "Summary and Future Directions" in Hench, L. L.; Wilson, J. – *An Introduction to Bioceramics*, 1, Singapore, World Scientific, 1993, 365-374.

[23] Oliveira, J. M. – "Vidros Cerâmicos do Sistema MgO-3CaO.P_2O_5-SiO_2 para Implantologia Óssea", *Tese de Mestrado*, Universidade de Aveiro, Aveiro, 1994.

[24] Sata, T. – "Phase Relationships in the System 3CaO.P_2O_5-MgO-SiO_2", *Bulletin of the Chemical Society of Japan*, 31, 1958, 408-413.

2 - ESTUDOS DE SEPARAÇÃO DE FASES E DE NUCLEAÇÃO E CRESCIMENTO DE CRISTAIS EM VIDROS

2.1 - Introdução

2.1.1 - Estruturas "morulares"

O conhecimento do processo de separação de fases em vidros abriu novas possibilidades de processamento destes materiais, como é o caso da produção industrial dos vidros Vycor®.[1]

A imiscibilidade líquido-líquido em vidros tem sido largamente estudada, nomeadamente em termos termodinâmicos. A separação de fases amorfas pode ocorrer através de dois mecanismos distintos: por nucleação e crescimento ou por decomposição *spinodal.* A microestrutura final dos vidros é condicionada pelo tipo de processo envolvido. Quando o processo é do tipo nucleação e crescimento o vidro é formado por uma matriz e uma ou mais fases dispersas, as quais apresentam tendência para adquirir a forma esférica; neste caso as fases dispersas não apresentam conectividade nem variação composicional e os seus contornos são bem definidos, distribuindo-se aleatoriamente na matriz, quer em tamanho quer em posição. Quando o processo é o de decomposição *spinodal* o vidro é formado por uma matriz e uma ou mais fases que apresentam uma tendência preferencial para adquirir uma forma não esférica de elevada conectividade; estas fases apresentam variação composicional e distribuem-se regularmente na matriz, quer em tamanho quer em posição.[2-23]

Alguns vidros com imiscibilidade líquida têm fases dispersas que apresentam estruturas muito convolutas, do tipo "morular" ou "amora"[i]. Em trabalhos realizados no sistema $3CaO\text{-}P_2O_5\text{-}SiO_2\text{-}MgO$ Oliveira[2] observou a existência de mórulas amorfas e ricas em silício (ver Fig. 2.1). Embora não frequentes, este tipo de formações tem sido detectado num número crescente e diverso de sistemas químicos.

O mecanismo de formação das mórulas não está ainda completamente compreendido, existindo actualmente várias opiniões.

[i] Estas designações são aqui sugeridas em razão de uma semelhança morfológica.

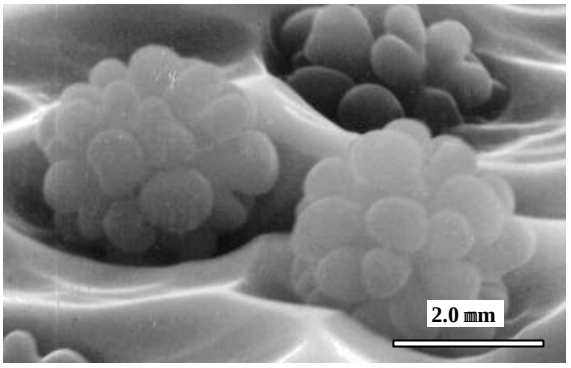

Fig. 2.1. Micrografia da superfície de fractura do vidro V4, atacada com HNO_3 1M durante 10s, (microscopia electrónica de varrimento)[2]. A morfologia da fase dispersa é do tipo morular.

Baylor e Brown[25] detectaram a presença de formações morulares amorfas, ricas em silício, em vidros do sistema $SrO\text{-}B_2O_3\text{-}SiO_2$ e atribuíram a sua morfologia à grande diferença de viscosidades existente entre a matriz e a fase dispersa. Segundo os autores, a fase dispersa apresenta uma viscosidade tão elevada que impede que a forma esférica correspondente ao estado de equilíbrio seja atingida.

Outros autores detectaram formações morulares amorfas em vidros dos sistemas Mg-Si-Al-O-N[26] e Mg-Si-O-N[27] cuja fase dispersa é também rica em silício e atribuíram a sua formação ao agrupamento de formações esféricas dispersas – gotas – existentes nos fundidos, ocorrido durante o processo de arrefecimento. Materiais desenvolvidos em sistemas do tipo Y-Si-Al-O-N apresentam também formações do tipo morular ricas em SiO_2, embora os autores[28] refiram que são entidades cristalinas.

Vogel[29] propõe que as mórulas se formam durante o arrefecimento de vidros, do sistema $CaO\text{-}P_2O_5\text{-}SiO_2$, na sequência de um processo secundário de separação de fases amorfas envolvendo agrupamento, i.e., numa primeira separação de fases formam-se regiões ricas em silício e cálcio dispersas numa matriz rica em fósforo e cálcio e com o arrefecimento progressivo estas duas fases voltam a sofrer uma separação de fases: na fase rica em fósforo e cálcio desenvolvem-se formações ricas em silício e na região rica em silício e cálcio desenvolvem-se formações ricas em fósforo. As entidades ricas em silício formadas durante a segunda separação são do tipo morular e, segundo o autor, a sua formação deve-se à agregação de gotas. A *driving force* responsável por esta agregação foi atribuída à diferença de composição entre as gotas e os compostos estequiométricos $CaO.SiO_2$ e $3CaO.P_2O_5$.

A presença de mórulas foi também detectada em vários vidros do sistema ZnO-B_2O_3-SiO_2. O mecanismo de formação sugerido difere dos anteriormente expostos e faz uma analogia com o desenvolvimento de instabilidades durante o crescimento de cristais em processos de solidificação. Baseado na elevada diferença de viscosidades entre a matriz e a fase dispersa (usualmente sílica), Taylor[30,31] propõe que a elevada fluidez da matriz (fase nutriente), que permite o desenvolvimento de um gradiente de difusão a distâncias de muitos mícron, e a existência de uma fase dispersa em crescimento suficientemente viscosa para reter as instabilidades, são responsáveis pelo desenvolvimento deste tipo de morfologia durante o arrefecimento de fundidos, o qual tem de ser necessariamente rápido para que esta seja preservada.

Uma interpretação que, em grande parte, não se enquadra nos mecanismos anteriores, é apresentada por Milyukov[32]. Este autor trabalhou com vidros do sistema SrO-B_2O_3-SiO_2 e sugeriu, por analogia com o comportamento de emulsões, que a formação de mórulas ocorre por um processo rápido de coagulação e coalescência de gotas.

Mais recentemente, ao trabalhar com vidros desenvolvidos nos sistemas sem sílica TeO_2-B_2O_3, TeO_2-B_2O_3-GeO_2 e TeO_2-GeO_2-V_2O_5 Kashchieva e Dimitriev[33] encontraram o mesmo tipo de entidades morfológicas amorfas, sendo a fase dispersa, mais viscosa, rica em B_2O_3 ou GeO_2. Os autores são também da opinião que a formação das mórulas se deve à agregação de gotas e a sua preservação às diferenças de viscosidade existentes entre a fase dispersa e a matriz.

Em conclusão, não existe uma explicação clara para o mecanismo responsável pelo desenvolvimento das formações morulares. Mazurin *et al.*[34], autores que estudaram aspectos de natureza morfológica em vidros com imiscibilidade líquida, referem a necessidade de se realizar experimentação para melhor se compreender a formação deste tipo de entidades; contudo, não são conhecidos trabalhos científicos desenvolvidos especificamente com este objectivo. Todos os resultados acima apresentados são pequenas contribuições colaterais de outros estudos.

Em virtude da abundância deste tipo de entidades em muitos dos vidros estudados no presente projecto apresentam-se, nas secções seguintes, vários trabalhos realizados com o objectivo de se compreender a formação desses precipitados.

2.1.2 - Nucleação e crescimento de cristais em vidros – alguns aspectos cinéticos.

A desvitrificação, enquanto processo de cristalização não controlada, é extremamente prejudicial no processamento de vidro. No século XVII realizaram-se as primeiras tentativas de produção de materiais policristalinos a partir da cristalização controlada de vidros. Contudo, o primeiro vidro cerâmico comercial só foi desenvolvido em 1950[35]. Hoje é possível encontrar este tipo de materiais nos mais diversos e exigentes ambientes desde as aplicações térmicas, eléctricas, espaciais, até às medicinais.[36-43]

A preparação de vidros cerâmicos resulta do apertado controlo de um processo físico-químico constituído por duas etapas: nucleação e crescimento de cristais. A nucleação pode ser *homogénea* ou *heterogénea*. Diz-se homogénea se os núcleos se formam a partir de constituintes do fundido e têm a mesma composição química da fase cristalina a desenvolver. Diz-se heterogénea se os núcleos são constituídos por partículas de composição diferente da do fundido (caso comum das impurezas). Geralmente, quando se pretende provocar uma nucleação do tipo heterogéneo utilizam-se agentes nucleantes – na presente tese serão apresentados estudos envolvendo TiO_2 e CaF_2 como nucleantes. O crescimento de cristais não é mais do que a deposição sucessiva de matéria sobre os núcleos, após estes terem atingido um tamanho crítico.[1] Os tratamentos termodinâmico e cinético destes processos encontram-se descritos em vários livros de referência, como os da autoria de McMillan[44], Vogel[16], Navarro[1], etc..

A cinética de cristalização em vidros é de extrema importância no controlo da microestrutura de vidros cerâmicos.

Em processos isotérmicos, e não obstante do avanço registado no desenvolvimento de microscopia e de processamento digital de imagem, o estudo da cinética de cristalização é bastante penoso face às características da componente experimental (recorde-se que estão envolvidas sucessivas e repetidas contagens do número de cristais em diferentes materiais). Para além da morosidade inerente à técnica existe ainda o problema de se analisarem zonas muito localizadas das amostras, o que por si só pode falsear os resultados. O recurso a técnicas alternativas envolvendo processos

não-isotérmicos, como é o caso das técnicas termo-analíticas, veio dinamizar esta área.[45,46,47]

A análise térmica diferencial (ATD) é uma técnica muito utilizada no estudo cinético de transformação de fases em materiais, nomeadamente em vidros. Esta técnica é relativamente simples, de ampla divulgação, requer um reduzido tempo de execução e pode ser aplicada continuamente, sem cuidados especiais, até temperaturas da ordem dos 1500 °C utilizando apenas uma pequena quantidade de amostra (tipicamente 100-300 mg). Neste tipo de técnica, contrariamente a uma técnica isotérmica em que é realizada uma medida pontual, tem-se informação sobre o global de uma amostra.

A base teórica para a interpretação dos fenómenos cinéticos ocorridos durante uma cristalização é a que se descreve na *teoria cinética de transformações de fase* desenvolvida por Johnson, Mehl e Avrami (JMA); contudo, a equação JMA[48,49,50] (Eq. 2.1), que traduz a dependência temporal da fracção volúmica cristalizada de material, α, só é aplicável em condições isotérmicas.

$$\alpha = 1 - \exp(-K t^{n}) \qquad (2.1)$$

ou

$$\ln[-\ln(1-\alpha)] = \ln(K) + n \ln(t) \qquad (2.2)$$

sendo: t – tempo

α – fracção volúmica de matéria transformada ao fim de t

n – parâmetro de Avrami (função dos mecanismos de nucleação e crescimento e de dimensionalidade geométrica)

K – constante cinética da reacção, função da temperatura. Usualmente descrita por uma lei do tipo Arrhenius:

$$K = K_0 \exp(-E/RT)$$

K_0 – factor pré-exponencial

E – energia de activação da cristalização

R – constante dos gases perfeitos

T – temperatura

Naturalmente, esta descrição só é verdadeira se as taxas de nucleação e crescimento de cristais seguirem, também elas, a referida lei.

Para situações não-isotérmicas, como é o caso do processo envolvido na técnica de ATD, foram propostos múltiplos modelos cinéticos para interpretação das transformações de fase, alguns dos quais criticamente revistos por Yinnon e Uhlmann[51].

Contrariamente às técnicas envolvidas no processo isotérmico, que recorrem a medidas directas para determinação das taxas de nucleação e crescimento, as técnicas usadas no processo não isotérmico baseiam-se em medidas indirectas. Por vezes os resultados provenientes dos dois processos não são concordantes e os parâmetros cinéticos calculados com base nos métodos não isotérmicos são de difícil interpretação.

A grande maioria dos métodos, como é o caso dos que a seguir são apresentados, derivam da equação de JMA e são particularmente úteis para a determinação da energia de activação da cristalização e do parâmetro de Avrami. Um dos modelos mais utilizado, baseado no método de Nakamura[52,53,54], foi desenvolvido por Matusita e Sakka[45,46]. Este modelo cinético traduz a dependência existente entre a fracção volúmica cristalizada e a temperatura conhecida a taxa de aquecimento, β (Eq. 2.3) e é utilizado na determinação do parâmetro de Avrami.

$$\ln [-\ln (1 - \alpha)] = \text{constante} - n \ln (\beta) - E/(RT) \qquad (2.3)$$

sendo: $\boldsymbol{b}$ – taxa de aquecimento

O efeito que a alteração da taxa de aquecimento provoca na temperatura do pico exotérmico numa ATD ($d^2\alpha/dt^2=0$) pode avaliar-se através do modelo proposto por Kissinger[55] (Eq. 2.4). Este modelo cinético é vulgarmente utilizado para a determinação da energia de activação e verificou-se ser válido apenas quando o processo de cristalização dominante é do tipo superficial.

$$\ln (\beta/T_p^2) = -E_{ck}/(RT_p) + \text{constante} \qquad (2.4)$$

sendo: T_p – temperatura correspondente ao pico exotérmico de cristalização

E_{ck} – energia de activação do processo de cristalização (Kissinger)

Matusita e Sakka[56] sugeriram uma correcção a este modelo por forma a alargar a sua aplicabilidade a processos envolvendo cristalização em volume (Eq. 2.5).

$$\ln (\beta^n/T_p^2) = -mE_{cm}/(RT_p) + \text{constante} \qquad (2.5)$$

sendo: m – factor numérico, função do mecanismo de nucleação

E_{cm} – energia de activação do processo de cristalização (Matusita)

As equações (2.4) e (2.5) são iguais quando $n = m = 1$, sendo então $E_{ck} = E_{cm}$. Segundo Xu *et al.*[57] a energia de activação verdadeira do processo é dada pela seguinte equação:

$$E_c \approx n/mE_{ck} \qquad (2.6)$$

Estes métodos têm sido alvo de sucessivos melhoramentos por introdução de diversos factores correctivos visando, nomeadamente, uma descrição mais ajustada às condições experimentais utilizadas durante uma ATD.

A partir da equação JMA (Eq. 2.1) Marotta *et al.*[58,59] e Xu *et al.*[57] alargaram o estudo cinético por ATD ao processo de nucleação em vidros. Com base nos desvios da posição dos picos exotérmicos das curvas de ATD estes autores, utilizando sempre as mesmas quantidades de amostra e taxa de aquecimento, determinaram os valores de temperatura e de tempo para os quais a nucleação é máxima recorrendo à (Eq. 2.7).

$$\ln N = -E/R\ (1/T_p - 1/T_p^0) + \text{constante} \qquad (2.7)$$

sendo: N – número de núcleos formados por unidade de volume (numa ATD)

T_p – temperatura do pico de ATD após tratamento térmico de nucleação

T_p^0 – temperatura do pico de ATD de uma amostra não tratada termicamente

De notar que T_p é função da temperatura de nucleação, T_n, e portanto a representação gráfica de $(1/T_p - 1/T_p^0)$ *versus* T_n permite determinar a temperatura à qual a taxa de formação de núcleos é máxima, mantendo-se para o efeito o tempo de nucleação, t_n, constante. Determinada a temperatura máxima de nucleação, analogamente pode-se obter uma dependência isotérmica da taxa de formação de núcleos com o tempo de nucleação uma vez que T_p é também função de t_n.

Referências Bibliográficas

[1] Navarro, J. M.F. – *El Vidrio*, Madrid, C.S.I.C., 1991.

[2] Roy, R. – "Metastable Liquid Immiscibility and Subsolidus Nucleation", *Journal of the American Ceramic Society*, 43, 1960, 670-671.

[3] Cahn, J.W.; Charles, R. J. – "The Initial Stages of Phase Separation in Glasses, *Physics and Chemistry of Glasses*, 6, 1965, 181-191.

[4] Moriya, Y.; Warrington, D. H.; Douglas, R. W. – "A Study of Metastable Liquid-Liquid Immiscibility in Some Binary and Ternary Alkali Silicate Glasses", *Physics and Chemistry of Glasses*, 8, 1967, 19-25.

[5] Zarzycki, J.; Naudin, F. – "A Study of Kinetics of the Metastable Phase Separation in the $PbO-B_2O_3$ System by Small-Angle Scattering of X-Rays", *Physics and Chemistry of Glasses*, 8, 1967, 11-18.

[6] Haller, W.; Macedo, P. B. – "The Origin of Phase Connectivity in Microheterogeneous Glasses, *Physics and Chemistry of Glasses*, 9, 1968, 153-155.

[7] Charles, R. J. – "The Origin of Immiscibility in Silicate Solutions", *Physics and Chemistry of Glasses*, 10, 1969, 169-178.

[8] Tomozawa, M.; MacCrone, R. K.; Herman, H. – "A Study of Phase Separation of Na_2O-SiO_2 Glass by X-Ray Small Angle Scattering", *Physics and Chemistry of Glasses*, 11, 1970, 136-150.

[9] Burnett, D. G.; Douglas, R. W. – "Liquid-Liquid Phase Separation in the Soda-Lime-Silica System", *Physics and Chemistry of Glasses*, 11, 1970, 125-135.

[10] Utsumi, Y.; Sakka, S.; Tashiro, M. – "Experimental Study on the Bending Strength of Glass in Relation to Liquid-Liquid Phase Separation", *Glass Technology*, 11, 1970, 80-85.

[11] Shahid, K. A.; Glasser, F. P. – "Phase Equilibria in the Glass Forming Region of the System $Na_2O-CaO-MgO-SiO_2$", *Physics and Chemistry of Glasses*, 13, 1972, 27-42.

[12] Nakagawa, K.; Izumitani, T. – "Effect of a Third Component upon the Immiscibility of Binary Glass", *Physics and Chemistry of Glasses*, 13, 1972, 85-90.

[13] James, P. F. – "Review: Liquid-Phase Separation in Glass-Forming Systems", *Journal of Materials Science*, 10, 1975, 1802-1825.

[14] Uhlmann, D. R.; Kolbeck, A. G. – "Phase Separation and the Revolution in Concepts of Glass Structure", *Physics and Chemistry of Glasses*, 17, 1976, 146-158.

[15] Finn, C. W. F.; Fray, D. J.; King, T. B.; Ward, J. G. – "Some Aspects of Structure in Glassy Silicophosphates", *Physics and Chemistry of Glasses*, 17, 1976, 70-76.

[16] Vogel, W. – "Phase Separation in Glass", *Journal of Non-Crystalline Solids*, 25, 1977, 170-214.

[17] Kumar, B.; Rindone, G. E. – "Phase Separation in a Soda-Lime-Silica Glass as Affected by Silica Purity", *Physics and Chemistry of Glasses*, 20, 1979, 148-149.

[18] Kreidl, N. – "Phase Separation in Glasses", *Journal of Non-Crystalline Solids*, 129, 1991, 1-11.

[19] Shepilov, M. P. – "Calculations of Kinetics of Metastable Liquid-liquid Phase Separation for the Model with Simultaneous Nucleation of Particles", *Journal of Non-Crystalline Solids*, 146, 1992, 1-25.

[20] Weinberg, M. C.; Shneidman, V. A.; Osborne, Z. A. – "On the Composition of the Critical Nucleus in Phase Separating Glasses", *Physics and Chemistry of Glasses*, 37, 1996, 49-50.

[21] Hoel, A.; Kranold, R.; Lembke, U.; Aures, J. – "Effect of Fining with Sodium Chloride on the Phase Separation of a Soda Lime Silica Glass", *Journal of Non-Crystalline Solids*, 208, 1996, 294-302.

[22] Deubener, J.; Osborne, Z. A.; Weinberg, M. C. – "Determination of the Liquid-Liquid Surface Energy in Phase Separating Glasses", *Journal of Non-Crystalline Solids*, 215, 1997, 252-261.

[23] Inoue, S.; Wada, K.; Nukui, A.; Yamane, M.; Shibata, S.; Yasumori, A.; Yano, T.; Makishima, A.; Inoue, H.; Soga, K. – "Estimation of Phase Separation Rates of $BaO-B_2O_3$ Melts under Cooling", *Physics and Chemistry of Glasses*, 38, 1997, 197-200.

[24] Oliveira, J. M. – "Vidros Cerâmicos do Sistema $MgO-3CaO.P_2O_5-SiO_2$ para Implantologia Óssea", *Tese de Mestrado*, Universidade de Aveiro, Aveiro, 1994.

[25] Baylor, R.; Brown, J. J. – "Phase Separation of Glasses in the System $SrO-B_2O_3-SiO_2$", *Journal of the American Ceramic Society*, 59, 1976, 131-136.

[26] Loehman, R. E. – "Oxynitride Glasses", *Journal of Non-Crystalline Solids*, 42, 1980, 433-446.

[27] Shaw, T. M.; Thomas, G.; Loehman, R. E. – "Formation and Microstructure of Mg-Si-O-N Glasses", *Journal of the American Ceramic Society*, 67, 1984, 643-647.

[28] Hampshire, S.; Nestor, E.; Flynn, R.; Besson, J.-L.; Rouxel, T.; Lemercier, H.; Goursat, P.; Sebai, M.; Thompson, D. P.; Liddell, K. – "Yttrium Oxynitride Glasses: Properties and Potencial for Crystallization to Glass-ceramics", *Journal of the European Ceramic Society*, 14, 1994, 261-273.

[29] Vogel, W. – *Glass Chemistry*, Springer-Verlag, Berlin, 1994, 114-117.

[30] Taylor, P.; Owen, D. G. – "Liquid Immiscibility in the System $Na_2O-ZnO-B_2O_3-SiO_2$", *Journal of the American Ceramic Society*, 64, 1981, 360-367.

[31] Taylor, P. – "Peculiar Morphology in Some Phase-Separated Multicomponent Silicate Glasses", *Journal of the American Ceramic Society*, 75, 1992, 1276-1277.

[32] Milyukov, E. M. – "Morphological Features of Two-Phase Glasses", *Fizika i Khimiya Stekla*, 3, 1977, 576-579 (em russo).

[33] Kashchieva, E. P.; Dimitriev, Y. B. – "Unusual Immiscibility Structures in Tellurite Glasses", *Journal of the American Ceramic Society*, 80, 1997, 1588-1590.

[34] Mazurin, O. V.; Porai-Koshits, E. A.; Andreev, N. S. – *Phase Separation in Glass*, Mazurin, O. V.; Porai-Koshits, E. A., Amsterdan, North-Holland, 1984.

[35] Stookey, S. D. – "Catalyzed Crystallization of Glass in Theory and Practice", *Industrial and Engineering Chemistry*, 51, 1959, 805-808.

[36] James, P. F. – "Glass Ceramics: New Compositions and Uses", *Journal of Non-Crystalline Solids*, 181, 1995, 1-15.

[37] Frischat, G. H. – "Glass and Glass-ceramic in the Extreme Environment of Space", *Journal of Non-Crystalline Solids*, 183, 1995, 92-99.

[38] Partridge, G. – "An Overview of Glass-ceramics. Part 1. Development and Principal Bulk Applications", *Glass Technology*, 35, 1994, 116-127.

[39] Partridge, G. – "An Overview of Glass-ceramics. Part 2. Joining, Minor Applications and the Future", *Glass Technology*, 35, 1994, 171-182.

[40] Beall, G. H. – "Synthesis and Design of Glass-ceramics", *Journal of Materials Education*, 14, 1992, 315-361.

[41] McMillan, P. W. – "Advances in the Technology and Applications of Glasses", *Physics and Chemistry of Glasses*, 17, 1976, 193-204.

[42] Russel, C. – "Oriented Crystallization of Glass. A Review", *Journal of Non-Crystalline Solids*, 219, 1997, 212-218.

[43] Donald, I. W.; Metcalfe, B. L.; Taylor, R. N. – "Review: The Immobilization if high Level Radioactive Wastes Using Ceramics and Glasses", *Journal of Materials Science*, 32, 1997, 5851-5887.

[44] McMillan, P. W. – *Glass-ceramics*, London, Academic Press, 1964.

[45] Matusita, K.; Sakka, S.; Matsui, Y. – "Determination of the Activation Energy for Crystal Growth by Differential Thermal Analysis", *Journal of Materials Science*, 10, 1975, 961-966.

[46] Matusita, K.; Sakka, S. – "Kinetic Study of the Crystallization of Glass by Differential Scanning Calorimetry", *Physics and Chemistry of Glasses*, 20, 1979, 81-84.

[47] Briggs, J.; Carruthers, T. G. – "A DTA Technique for the Determination of the Crystal Growth Kinetics of some Inorganic Glasses", *Physics and Chemistry of Glasses*, 17, 1976, 30-34.

[48] Avrami, M. - "Kinetics of Phase Change. I - General Theory", *Journal of Chemical Physics*, 7, 1939, 1103-1112.

[49] Avrami, M. – "Kinetics of Phase Change. II - Transformation-Time Relations for Random Distribution of Nuclei", *Journal of Chemical Physics*, 8, 1940, 212-224.

[50] Avrami, M. – "Kinetics of Phase Change. III - Granulation, Phase Change, and Microstructure", *Journal of Chemical Physics*, 9, 1941, 177-184.

[51] Yinnon, H.; Uhlmann, D. R. – "Applications of Thermoanalytical Techniques to the Study of Crystallization Kinetics in Glass-Forming Liquids, Part I: Theory", *Journal of Non-Crystalline Solids*, 54, 1983, 253-275.

[52] Nakamura, K.; Watanabe, T.; Katayama, K.; Amano, T. – "Some Aspects of Nonisothermal Crystallization of Polymers. I – Relationship Between Crystallization Temperature, Crystallinity, and Cooling Conditions", *Journal of Applied Polymer Science*, 16, 1972, 1077-1091.

[53] Nakamura, K.; Watanabe, T.; Katayama, K.; Amano, T. – "Some Aspects of Nonisothermal Crystallization of Polymers. II – Consideration of the Isokinetic Condition", *Journal of Applied Polymer Science*, 17, 1973, 1031-1044.

[54] Nakamura, K.; Watanabe, T.; Amano, T.; Katayama, K. – "Some Aspects of Nonisothermal Crystallization of Polymers. III – Crystallization During Melt Spinning", *Journal of Applied Polymer Science*, 18, 1974, 615-623.

[55] Kissinger, H. E. – "Reaction Kinetics in Differential Thermal Analysis", *Analytical Chemistry*, 29, 1957, 1702-1706.

[56] Matusita, K.; Sakka, S. – "Kinetic Study on Crystallization of Glass by Differential Thermal Analysis - Criterion on Application of Kissinger Plot", *Journal of Non-Crystalline Solids*, 38&39, 1980, 741-746.

[57] Xu, X. J.; Ray, C. S.; Day, D. E. – "Nucleation and Crystallization of $Na_2O.2CaO.3SiO_2$ Glass by Differential Thermal Analysis", *Journal of the American Ceramic Society*, 74, 1991, 909-914.

[58] Marotta, A.; Buri, A.; Branda, F. – "Nucleation in Glass and Differential Thermal Analysis", *Journal of Materials Science*, 16, 1981, 341-344.

[59] Marotta, A.; Buri, A.; Branda, F.; Saiello, S. – "Nucleation in Glass-Forming Systems. A DTA Study", *Thermochimica Acta*, 85, 1985, 231-234.

2.2 - Phase Separation and Crystallisation in $3CaO.P_2O_5$-SiO_2-MgO Glasses

A. L. Oliveira, J. M. Oliveira, R. N. Correia, M. H. Fernandes

Departamento de Engenharia Cerâmica e do Vidro, Universidade de Aveiro, 3810-193 Aveiro, PORTUGAL

(Glastechnische Berichte Glass Science and Technology, 67C, 1994, 367-370)

1. Introduction

This paper reports a preliminary study on phase transformations of a nominal composition (wt%) 52.75 $3CaO.P_2O_5$-30.00 SiO_2-17.25 MgO, whose devitrified form has previously[1] shown reasonable mechanical strength and ability to develop an adherent apatite deposit after immersion in SBF, making it a potential candidate for biomedical applications.

2. Experimental

The glass was prepared from reagent-grade $Ca(H_2PO_4)_2$, $CaCO_3$, SiO_2 and MgO, ground, remelted in platinum crucibles for 30 min at 1525, 1560 and 1595 °C in air, water-quenched to room temperature and microstructurally analysed under SEM after chemical etching. DTA crystallisation studies have been performed only in glasses fabricated at 1525 °C. These were crushed in an agate mortar and sieved to collect a coarse fraction (between 180 and 250 μm) assumed to ensure essentially bulk crystallisation[2]. Samples of 300 mg were used in all DTA runs, according to a cycle of 50 $K.min^{-1}$ up to the nucleation temperature T_n, halting at T_n for 2 hours and immediately heating up to 1000 °C at 10 $K.min^{-1}$. A DTA curve was previously obtained for the non-nucleated glass, to have an indication of the transition temperature T_g and of the location of the crystallisation peaks.

3. Results and Discussion

The microstructure of the as-quenched glass shows separation of amorphous silica[1,3]. The size and morphology of the silica precipitates varies with quenching temperature. Spherical droplets of ~0.3 μm are present at higher temperatures (Fig.1) some of them coalescent, and become progressively morular-shaped as the temperature decreases (Figs. 2 and 3). A sample cooled from 1560 °C onto a metal plate and annealled at 700 °C showed an agglomeration of droplets into morulae of ~3 μm (Fig. 4).

The mechanism accounting for the morphological change is not clear, but it seems that the size of the spherical individual droplets is nearly constant (~3 μm). The phenomenon of phase separation is due to the immiscibility gap characteristic of the SiO_2-containing systems; according to the present microstructural evidence it does not play any role in the nucleation process of crystalline phases.

The non-nucleated glass shows T_g ~ 730 °C (as determined by DTA) and two exotherm peak temperatures at 829 °C (T^o_{p1}) and 936 °C (T^o_{p2}). The latter were used as reference temperatures for the analysis of the crystallisation kinetics according to the procedure of Marotta *et al.*[4,5]. Previous studies[1] showed that the first peak corresponds to the formation of Mg-substituted β-tricalcium phosphate (whitlockite) $3(Ca,Mg)O.P_2O_5$ and the second to the precipitation of a Ca-substituted enstatite, $(Mg,Ca)O.SiO_2$. The first peak is sharp, whereas the second is broadened; it is not yet know if this broadening is due to an interference of surface nucleation[2].

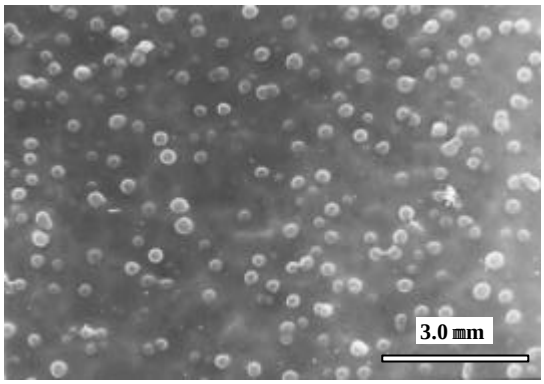

Fig. 1. Quenched from 1595 °C.

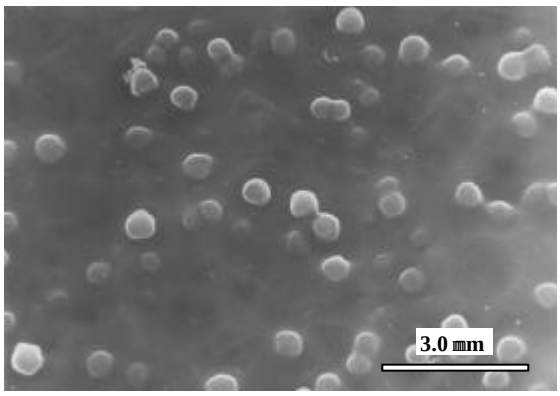

Fig. 2. Quenched from 1560 °C.

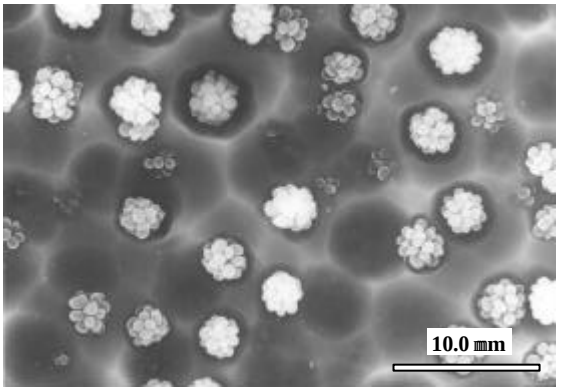

Fig. 4. Cooled from 1560 °C onto a metal plate and annealled at 700 °C.

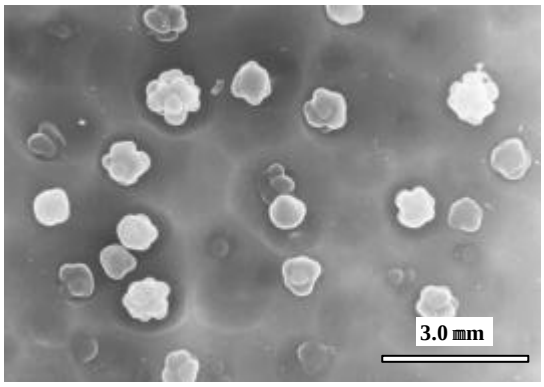

Fig. 3. Quenched from 1525 °C.

Figure 5 shows the plot of nucleation rate of whitlockite, as measured by the parameter $1/T_{p1}-1/T^{o}_{p1}$ at constant nucleation time (2 hours in our case, where T_{p1} is the temperature of the first exothermic peak in previously-nucleated samples), as a function of the nucleation temperature T_n. It is seen that the maximum nucleation rate of whitlockite occurs at 730°C. For T_n greater than 770 °C the whitlockite crystallisation exotherm disappears, indicating that all the precipitate had formed during heat treatment, which means that the crystallisation kinetics of the phosphate is sufficiently high for nucleation and growth to occur simultaneously at temperatures of 770 °C or higher. Figure 6 shows that for T_n = 730 °C a constant density of nuclei is attained for nucleation times greater than 2 hours.

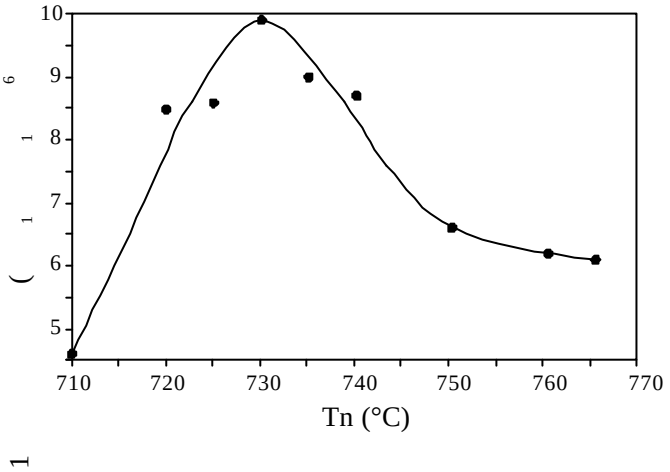

Fig. 5. Nucleation rate of whitlockite vs. Temperature. Nucleation Time = 2 hours.

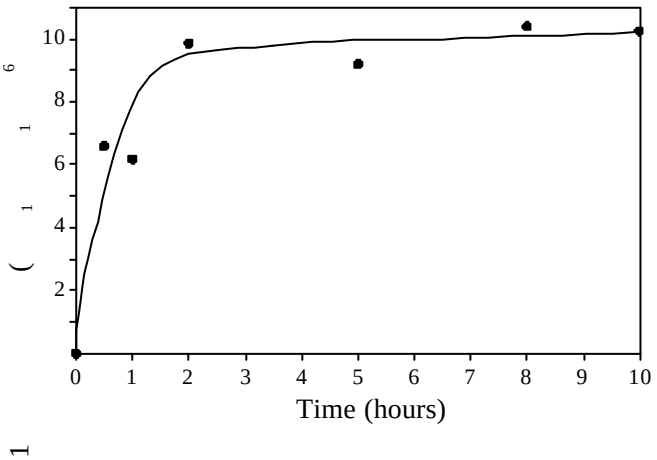

Fig. 6. Density of nuclei of whitlockite .vs. nucleation time. Nucleation temperature = 730 °C

The applicability of the previous analysis to the crystallisation of enstatite is not so evident. No relative maximum of the nucleation rate was detected, and it is likely that the net rate of transformation will simply increase with temperature. Within the limits of the DTA method the transformation is already completed after 2 hours at 850 °C. It is not excluded that diffusion of Mg and Si away from the growing phosphate crystals, instead of nucleation, might be the rate controlling step for the precipitation of enstatite. The formation of this second phase seems to be a distinct event occurring after the crystallization of the phosphate; this is evidentiated on micrographs which show triangular or quadrangular crystals formed in areas left after precipitation of the whitlockite needles (Fig. 7).

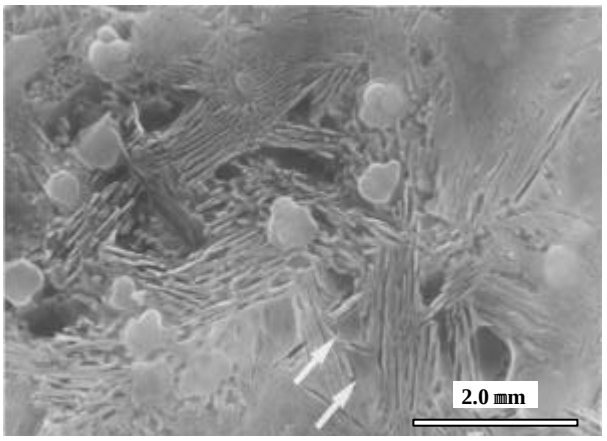

Fig. 7. SEM micrograph of devitrified glass showing separated SiO_2 morulae, whitlockite needles and enstatite crystals (arrows). DTA heat treatment schedule as in text (T_n=770 °C, 2h).

Acknowledgements

This work has been financially supported by JNICT under Project PBIC/C/CTM/1425/92. One of the authors (J. M. Oliveira) is currently supported by a JNICT grant (BD/2762/93).

References

[1] Oliveira, J. M.; Fernandes, M. H.; Correia R. N. – "Development of a New Glass-ceramic in the System MgO-3CaO.P_2O_5-SiO_2", *Bioceramics*, 5, 1992, 7-14.

[2] Xu, X. J.; Ray, C. S.; Day, D. E. – "Nucleation and Crystallisation of Na_2O.2CaO.3SiO_2 Glass by Differential Thermal Analysis", *Journal of the American Ceramic Society*, 74(5), 1991, 909-914.

[3] Oliveira, J. M.; Correia R. N.; Fernandes, M. H. – "Surface Modifications of a Glass and a Glass-ceramic of the MgO-3CaO.P_2O_5-SiO_2 System in a Simulated Body Fluid", *Biomaterials*, 16(11), 1995, 849-854.

[4] Marotta, A.; Buri, A.; Branda, F. – "Nucleation in Glass and Differential Thermal Analysis", *Journal of Materials Science*, 16, 1981, 341-344.

[5] Cioffi, R.; Pernice, P.; Aronne, A.; Marotta, A.; Quattroni, G. – "Nucleation and Crystal Growth in a Fly Ash Derived Glass", *Journal of Materials Science*, 28, 1993, 6591-6594.

2.3 - TiO_2-induced Amorphous Phase Separation and Crystallization in a Glass of the System SiO_2-$3CaO.P_2O_5$-MgO

S. R. Lacerda, J. M. Oliveira, R. N. Correia, M. H. V. Fernandes

Department of Ceramics and Glass Engineering, University of Aveiro, 3810-193 Aveiro, PORTUGAL

(Journal of Non-Crystalline Solids, 221, 1997, 255-260)

Abstract

The effect of 1 to 5 wt% TiO_2 additions on the microstructural and crystallization behaviour of a glass with base composition (wt%) 42.6 SiO_2; 29.4 $3CaO.P_2O_5$; 28.0 MgO has been studied. The added amounts produced separation of amorphous SiO_2 in the glass and volume crystallization during ceramming.

Heat treatments up to 1100 ºC resulted in simultaneous crystallization of β-$3(Ca,Mg)O.P_2O_5$ and clino-enstatite ($MgO.SiO_2$) in TiO_2-free glasses and the occurrence of a third phase, forsterite ($2MgO.SiO_2$), in all TiO_2-containing glasses.

Crystallization peak temperatures suggested that overall crystallization rates increase with increasing TiO_2 content up to 3% and that further changes do not occur for higher contents.

***Keywords**: nucleation, crystallization, phase-separation, phosphate glasses, titania*

1. Introduction

The first studies on glass-ceramics of the SiO_2-CaO-P_2O_5-MgO system were made by Kokubo and co-workers[1,2], who produced a bioactive material with apatite and β-wollastonite ($CaO.SiO_2$) as crystalline phases in a MgO-CaO-SiO_2 matrix. The section SiO_2-$3CaO.P_2O_5$-MgO in this system has been recently investigated for the first time by the present authors and some of the glass-ceramics obtained, containing β-$3(Ca,Mg)O.P_2O_5$ and Mg-silicates as crystalline phases, were found to have potential to be used as biomaterials[3,4]. Some glasses in the SiO_2-$3CaO.P_2O_5$-MgO system exhibit precipitates of amorphous silica, which remain in the crystallized material. Processing of monolythic crack-free glass-ceramics by heat treatment of glass blocks has been possible whenever the base glasses were phase-separated, but not so when phase separation did not occur. The promising mechanical properties and bioactivity exhibited by glass-ceramics obtained from phase-separated glasses led us to attempt induction of phase separation in an otherwise monophasic glass, by the introduction of small amounts of titania in the glass composition.

TiO_2 is used as a bulk nucleating agent, namely in silica-based glasses. This compound is miscible in the glassy network at high temperatures but induces phase separation during cooling of the melt, due to coordination incompatibility with the silicate network[5,6]. Titania is known particularly to prevent calcium-phosphate surface nucleation in CaO-P_2O_5-based systems. Hosono *et al.*[7,8] used significant amounts of TiO_2 in such systems for the purpose of producing porous glass-ceramics with applications in the field of biotechnology, in which the volume nucleated β-$Ca_3(PO_4)_2$ phase is leached with HCl, leaving a $CaTi_4(PO_4)_6$ skeleton.

Since TiO_2 is considered to be harmless when in contact with native human tissues it has gained interest in the field of biomaterials, namely in the production of glass-ceramics of the SiO_2-CaO-P_2O_5 system[9]. Ceramming of glasses in this system usually gives rise to biocompatible phases, such as β-$Ca_2P_2O_7$ (calcium pyrophosphate) and Ti P_2O_7.

This paper reports a preliminary study on the crystallization effects of different TiO_2 additions to a glass V5 of composition (wt%) 42.6 SiO_2; 29.4 $3CaO.P_2O_5$; 28.0 MgO, with the main objective of producing bulk crystallized monolythic specimens. Phase separation caused by TiO_2 was followed by Scanning Electron Microscopy (SEM) observation of

phase-separated microstructures and by Transmission Electron Microscopy (TEM) with Energy Dispersive Spectroscopy (EDS) analysis of the separated amorphous phase without matrix interference. Crystallization behaviour was evaluated from Differential Thermal Analysis (DTA) traces, by studying the effect of varying TiO_2 contents on crystallization peak shifts. Crystalline phases precipitated during DTA runs were identified by X-Ray Diffraction (XRD).

2. Experimental

Glasses were melted from reagent-grade $Ca(H_2PO_4)_2$, $CaCO_3$, SiO_2, MgO and TiO_2. The nominal compositions are shown in Table I where the numbers before Ti mean that percentages from about 1 to 5% in weight of TiO_2 have been added to the base composition.

Table I. Glass compositions (wt% oxides).

	Glass samples					
Oxide	V5	V5-1Ti	V5-2Ti	V5-3Ti	V5-4Ti	V5-5Ti
SiO_2	42.6	42.2	41.8	41.3	41.0	40.6
$3CaO.P_2O_5$	29.4	29.1	28.8	28.5	28.3	28.0
MgO	28.0	27.7	27.4	27.2	26.9	26.6
TiO_2	-	1.0	2.0	3.0	3.8	4.8

After weighing, the powders were thoroughly mixed in ethanol for 30 minutes, dried at 60 °C and subsequently melted at 1550 °C in a platinum crucible. In order to homogenize the melt, a double melting procedure was adopted. The first melt was poured into water to obtain a frit. The frit was dried and then remelted at 1550 °C for two hours in the same platinum crucible. This melt was poured onto a preheated metal plate and the obtained glass annealed for 30 minutes at 730 °C and then slowly cooled to room temperature.

After polishing on diamond-impregnated polymeric films, followed by lapping on a colloidal silica-impregnated cloth, samples of the obtained glasses were prepared for SEM observation in a microscope Hitachi S-4100.

Carbon extraction replicas of fracture surfaces of all phase-separated glasses were prepared for TEM observation in a microscope Hitachi H9000-NA, using immersion for a few seconds in a mixture of 50% HNO_3 1M + 50% HF 1M.

DTA runs on powders obtained by crushing the glasses in an agate mortar were performed by heating these powders in alumina crucibles at a rate of 10 $K.min^{-1}$ from room temperature to 1100 °C in air; alumina powder was used as the reference material. Monolythic, bulk crystallized samples which did not exhibit any cracking or fractures were obtained at the end of the DTA runs. These were ground in an agate mortar and the crystalline phases identified by X-ray powder diffraction in a diffractometer Rigaku PMG-VH operating with Cu K_α radiation.

3. Results

Additions of titania to the initial transparent base glass V5 caused phase separation in all glass compositions, as indicated by the opal white colour of all TiO_2-containing glasses. The separated phase has a morphology previously described as "morular"[10] (Figs. 1 and 2) and the glass microstructure is similar to that found in other separated glasses of the same system[3,4].

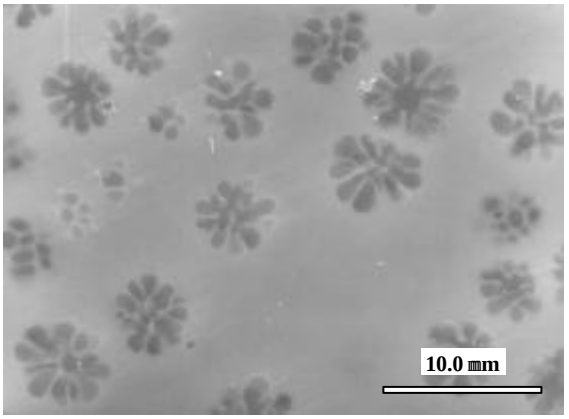

Fig. 1. SEM micrograph of annealed glass V5-1Ti (polished sample)

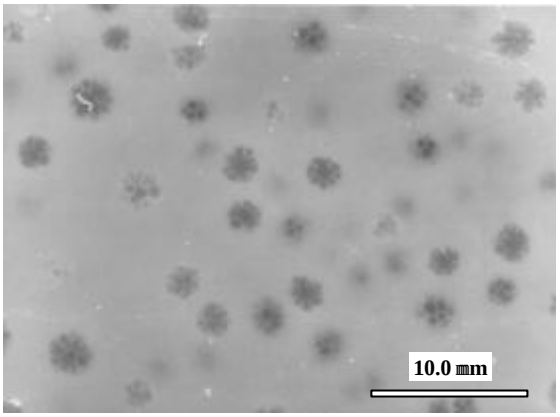

Fig. 2. SEM micrograph of annealed glass V5-5Ti (polished sample)

Selected area electron diffraction on TEM extraction replicas showed that these precipitates are amorphous and EDS microanalysis indicated that they consist of pure SiO_2. Composition V5-1Ti heat treated at 10 $K.min^{-1}$ from room temperature to 1200 ºC and held at this temperature for 1 hour gave rise to a glass-ceramic with the microstructure shown in Fig. 3.

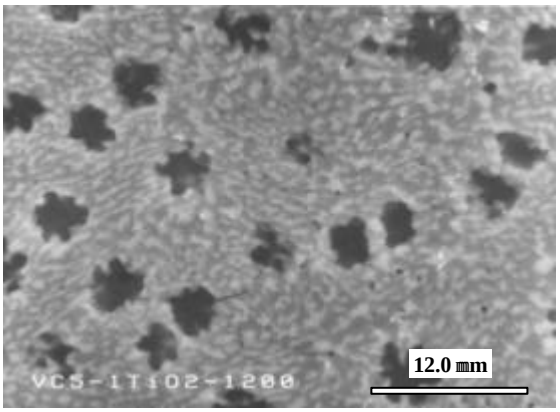

Fig. 3. Back-scattered electron image of V5-1Ti heat treated at 1200 ºC for 1 hour (polished surface). Dark phase is dissolving silica, light phase is β-$3CaO.P_2O_5$ and grey formations are enstatite and forsterite, undistinguished due to very close electronic densities. Vitreous silica has the same mean atomic number but is darker because of its lower atom packing density.

Table II gives the values of glass transition temperatures (T_g) and cystallization peak temperatures (T_c) of all glass compositions, as obtained by DTA of powdered glasses (Fig. 4).

n

Table II. Glass transition temperatures (Tg) and crystallization temperatures (Tc).

	Glass samples					
	V5	V5-1Ti	V5-2Ti	V5-3Ti	V5-4Ti	V5-5Ti
T_g (ºC)	732	732	726	727	730	730
T_c (ºC)	944	934	928	916	916	916

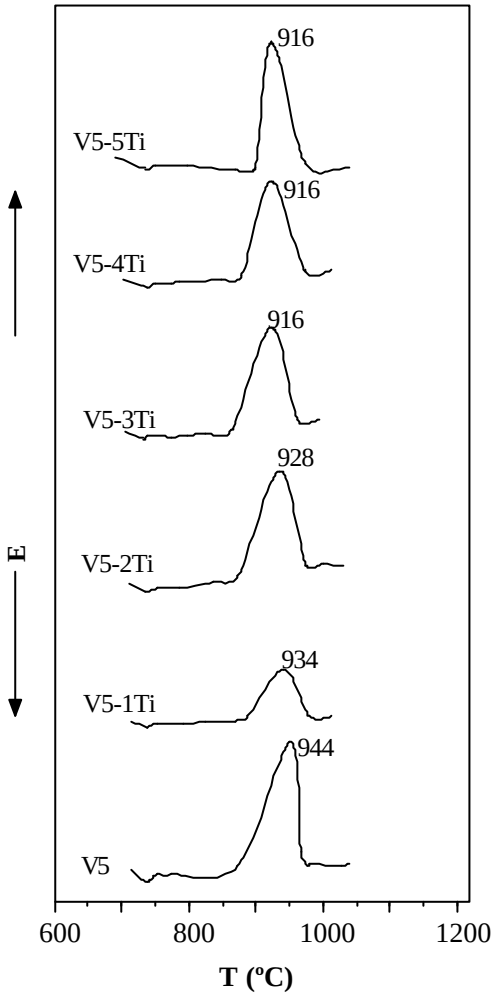

Fig. 4. DTA curves for annealed glasses (heating rate 10 K.min^{-1})

After DTA runs all samples were analysed by XRD. Diffractographs are shown in Fig. 5.

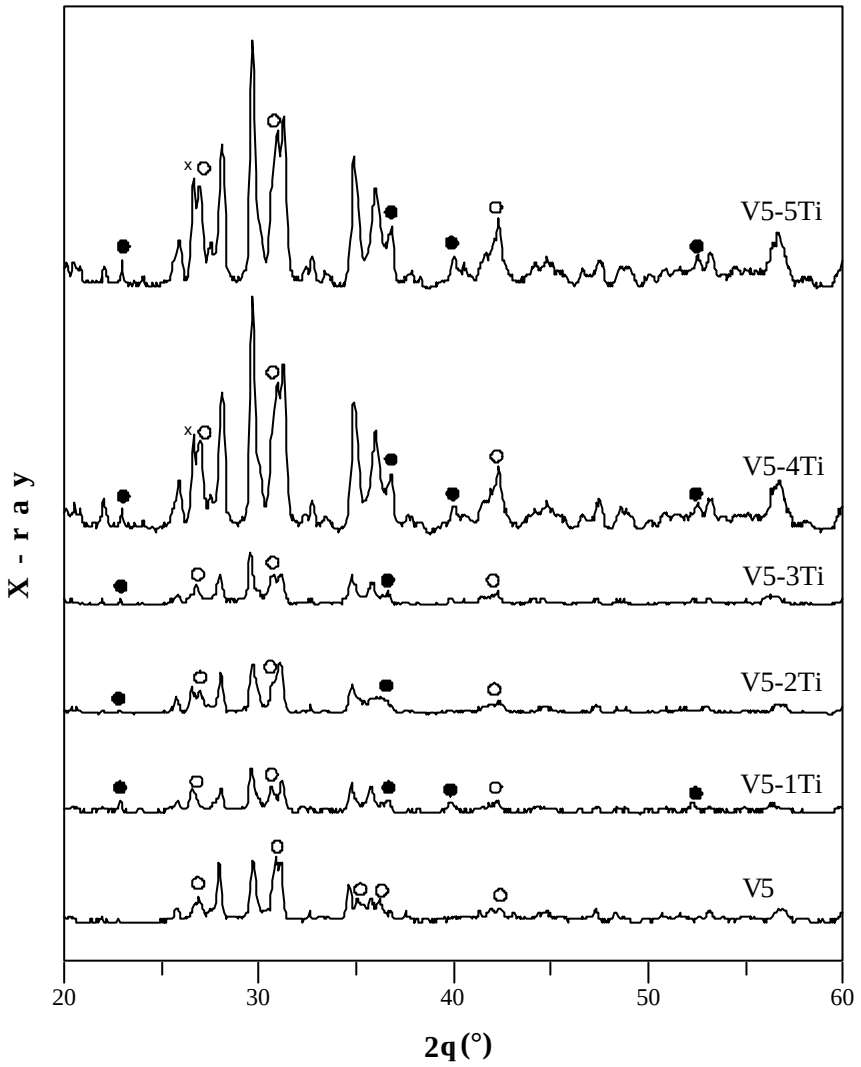

Fig. 5. XRD patterns (CuK_α) after DTA runs up to 1100 ºC.(x - non-identified; o - clino-enstatite characteristic lines; ● - forsterite characteristic lines; all other peaks - β-$3CaO.P_2O_5$).

4. Discussion

4.1. Microstructure

The formation of silica-rich agregates of peculiar morphology was also detected by other authors[11-15] in multicomponent silicate systems without TiO_2. Amorphous silica precipitates were found in the systems SiO_2-ZnO-B_2O_3[12], SiO_2-SrO-B_2O_3[14] and Si-Mg-(Al)-O-N[11,13]. Hampshire *et al.*[15] also found what they called "flower-like" silica agregates in the Y-Si-Al-O-N system, but with a crystalline structure. The origin of the peculiar

morphology is not clear for any of the authors, although most of them tend to attribute it to large differences (several orders of magnitude) in viscosity between the separated phases.

In the system we have been studying, silica separation is common to other compositions, even in the absence of phase separation inducers[16]. It is a metastable precipitation related with the liquid immiscibility field found near the SiO_2 composition in equilibrium diagrams involving silica and oxides of divalent cations (CaO, MgO) above ca. 1700 ºC. The author's experience suggests that the peculiar shape of these aggregates is due to incipient coalescence of silica droplets with formation of relatively stable necks, probably hindered by the viscosity of the matrix[17]. With thermal treatment in the vicinity of 1200-1300 ºC, well below the stable liquid immiscibility plateau, these precipitates re-dissolve, in some cases with previous spheroidization and, possibly, crystallization to cristobalite[17]. An example of such a microstructure obtained by heat treatment is shown in Fig. 3, which shows a facetting of dissolving silica precipitates, which suggests crystallization.

Observation of several micrographs of phase-separated amorphous samples exemplified by Figs. 1 and 2 showed that the size of silica aggregates may vary noticeably across the same polished surface. Due to uncertainty in defining the contour of the morulae/matrix interface, no quantitative image treatment was attempted, but a rough assessment showed that the average morular size decreases from about 6 μm in V5-1Ti (Fig. 1) to 1-2 μm in the remaining samples (see Fig. 2). Under visual observation no variation of volume fraction of aggregates with Ti content could be noticed, which would imply that the change in morular spacing follows the change in size.

The shape of morulae does not systematicaly vary with Ti content, whereas the degree of coalescence within aggregates varies within each sample and also with composition. More refined research is needed to separate effects due to sample thickness and melt cooling rates.

The role of titania in the observed phase separation is not yet clear. It is generally noted in the literature that phase separation in silicate glasses is usually complex and the available information is conflicting[18,19]. Apart from the lack of structural information in the nucleation stage, it remains to be understood as to why the immiscibility promoted by TiO_2 leads in this case to the separation of amorphous silica precipitates with the observed peculiar morphology.

4.2. Differential Thermal Analysis

As shown in Table II the glass transition temperature is 730 ± 3 °C, and does not change significantly with TiO_2 additions, indicating that viscosity should be about the same in all cases. A single exothermic crystallization peak was detected in all DTA traces. The crystallization peak temperature T_c shifts gradually from 944 °C in TiO_2-free glass, to 916 °C in V5-3Ti, remaining constant for higher Ti-containing compositions (Fig. 4). Additions of TiO_2 up to 3 wt% seem thus to make crystallization easier but higher contents do not promote further changes.

4.3. X-Ray Diffraction

Although only one peak was evident in DTA traces, XRD showed that crystallization of several phases (tricalcium phosphate and silicates) occurs (Fig. 5); these observations imply that crystallization of those phases is simultaneous. At the heating rate of 10 $K.min^{-1}$ used in DTA up to 1100 ºC, β-$3(Ca,Mg)O.P_2O_5$ and clino-enstatite ($MgO.SiO_2$) precipitate in TiO_2-free samples. In all TiO_2-containing powders there is evidence for the additional crystallization of forsterite ($2MgO.SiO_2$), as concluded from the presence of new lines at 2θ (± 0.3º) = 22.8º (reflection 120) and 40º (041) together with an increase in intensity of the 36.5 º line, common to forsterite (211) and enstatite. On the other hand, weakening of some lines (28.1, 31.2, 35.3 and 36.2 º) with respect to the strongest β-$3(Ca,Mg)O.P_2O_5$ line suggests a decrease in the clino-enstatite fraction.

The results in Fig. 5 are consistent with the obtained microstructures, in which it is seen that even the smallest amount of titania produces separation of amorphous silica. Since this phase does not easily re-dissolve in the matrix even at high temperatures, it remains in the sample during DTA runs, although with some morphological alterations, shifting the matrix composition from the $3CaO.P_2O_5$-$MgO.SiO_2$ line of the equilibrium diagram towards the $3CaO.P_2O_5$-$MgO.SiO_2$-$2MgO.SiO_2$ compatibility triangle (Fig. 6). This enables the co-precipitation of the two silicates in TiO_2-doped glass, whereas in TiO_2-free material, with no silica separated, only clino-enstatite is detected.

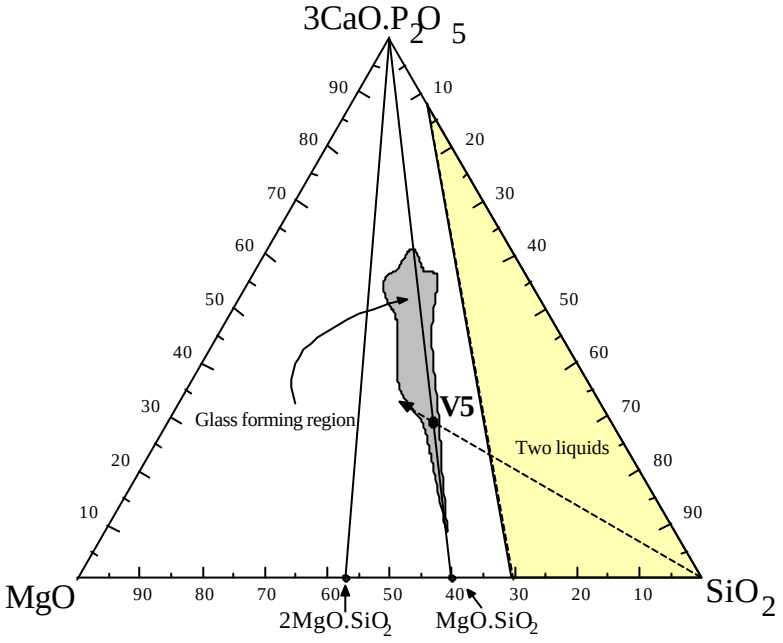

Fig. 6. Position of V5 composition in the equilibrium diagram $3CaO.P_2O_5$-MgO-SiO_2, adapted from Sata[20], and compositional shift of matrix produced by SiO_2 separation.

5. Conclusions

(i) TiO_2 additions of 1 wt% or greater promoted amorphous phase separation in glasses of the SiO_2-$3CaO.P_2O_5$-MgO system. Phase separated glass powders partially bulk-crystallized by heating at 10 $K.min^{-1}$ up to 1100 ºC.

(ii) Evolution of peak temperatures in DTA traces suggest that overall crystallization rates are increased by TiO_2 contents up to 3 wt%. Higher contents do not promote further changes.

(iii) At the heating rate of 10 $K.min^{-1}$ simultaneous crystallization of ß-tricalcium phosphate and silicate(s) occurs. TiO_2-free glasses exhibit clino-enstatite crystallization but Ti additions induce the precipitation of forsterite together with clino-enstatite.

(iv) DTA runs on powders to 1100 ºC produce monolythic blocks of glass-ceramic without cracking, which indicates potential for a sintering route in the processing of these materials.

Acknowledgements

This work has been financially supported by JNICT (Junta Nacional de Investigação Científica e Tecnológica) under Project PBIC/C/CTM/1425/92. One of the authors, J. M. Oliveira, was also supported by a JNICT grant, BD/2762/93.

References

[1] Kokubo, T. – "Bioactive Glass-ceramics: Properties and Applications", *Biomaterials*, 12, 1991, 155-163.

[2] Kokubo, T.; Ito, S.; Sakka, S.; Yamamuro, T. – "Formation of a High-strength Bioactive Glass-ceramic in the System MgO-CaO-SiO_2-P_2O_5", *Journal of Materials Science*, 21, 1986, 536-540.

[3] Oliveira, J. M.; Correia, R. N.; Fernandes, M. H. – "Surface Modifications of a Glass and Glass-ceramic of the System MgO-3CaO.P_2O_5-SiO_2 in a Simulated Body Fluid", *Biomaterials*, 16, 1995, 849-854.

[4] Oliveira, J. M. – "Glass-ceramics of the MgO-3CaO.P_2O_5-SiO_2 System for Bone Implants", Master´s Thesis, Aveiro, Universidade de Aveiro, 1994 *(in Portuguese)*.

[5] Vogel, W. – *Glass Chemistry*, Berlin, Springer-Verlag, 1994.

[6] McMillan, P. W. – *Glass-ceramics*, London, Academic Press, 1964.

[7] Hosono, H.; Abe, Y. – "Porous Glass-ceramics Composed of a Titanium Phosphate Crystal Skeleton: a Review", *Journal of Non-Crystalline Solids*, 190, 1995, 185-197.

[8] Hosono, H.; Zhang, Z.; Abe, Y. – "Porous Glass-ceramic in the CaO-TiO_2-P_2O_5 System", *Journal of the American Ceramic Society*, 72, 1989, 1587-1590.

[9] Nan, Y.; Lee, W. E.; James, P. F. – "Crystallization Behaviour of CaO-P_2O_5 Glass with TiO_2, SiO_2 and Al_2O_3 Additions", *Journal of the American Ceramic Society*, 75, 1992, 1641-1647.

[10] Oliveira, J. M.; Fernandes, M. H.; Correia, R. N. – "Development of a New Glass-ceramic in the System MgO-3CaO.P_2O_5-SiO_2", *Bioceramics*, 5, 1992, 7-14.

[11] Shaw, T. M.; Thomas, G.; Loehman, R. E.; "Formation and Microstructure of Mg-Si-O-N Glasses", *Journal of the American Ceramic Society*, 67, 1984, 643-647.

[12] Taylor, P.; Owen, D. – "Liquid Immiscibility in the System Na_2O-ZnO-B_2O_3-SiO_2", *Journal of the American Ceramic Society*, 64, 1981, 360-367.

[13] Loehman, R. E.; "Oxynitride Glasses", *Journal of Non-Crystalline Solids*, 42, 1980, 433-446.

[14] Baylor, R.; Brown, J. J. – "Phase Separation of Glasses in the System SrO-B_2O_3-SiO_2", *Journal of the American Ceramic Society*, 59, 1976, 131-136.

[15] Hampshire, S.; Nestor, E.; Flynn, R.; Besson, J.-L.; Rouxel, T.; Lemercier, H.; Goursat, P.; Sebai, M.; Thompson, D. P.; Liddell, K. – "Yttrium Oxynitride Glasses: Properties and Potencial for Crystallization to Glass-ceramics", *Journal of the European Ceramic Society*, 14, 1994, 261-273.

[16] Oliveira, A. L.; Oliveira, J. M.; Correia, R. N.; Fernandes, M. H. – "Phase Separation and Crystallisation of 3CaO.P_2O_5-MgO-SiO_2 Glasses", *Glastechnische Berichte Glass Science and Technology*, 67C, 1994, 367-370.

[17] Oliveira, J. M.; Oliveira, A. L.; Fernandes, M. H.; Correia, R. N. – "Comparative Study of Two 50 wt% Whitlockite Glass-ceramics of the 3CaO.P_2O_5-SiO_2-MgO System", Euroceram Seminar on Biomaterials, Limerick, 1995.

[18] Lecomte, A.; Petrault, P.; Vesteghem, A.; Dauger, A. – "Small Angle X-Ray Scattering Study of Phase Separation in Cordierite-Based Glasses Containing TiO_2 and Na_2O", *Science of Ceramics*, 14, 1988, 395-400.

[19] Alberto, H. V.; Campos, A. N.; Mysen, B. O. – "The Structural Role of Titanium in Silicate Glasses: a Raman Study of the System CaO-SiO_2-TiO_2", *Physics and Chemistry of Glasses*, 36, 1995, 114-122.

[20] Sata, T. – "Phase Relationship in the System 3CaO.P_2O_5-MgO-SiO_2", *Bulletin of the Chemical Society of Japan*, 31, 1958, 408-413.

2.4 - Effect of MgO Additions on Amorphous Phase Separation in Silico-Phosphate Glasses

J. M. Oliveira, R. N. Correia, M. H. V. Fernandes

Department of Ceramics and Glass Engineering, University of Aveiro, 3810-193 Aveiro, PORTUGAL

(Proceedings of the XVIII International Congress in Glass - D5: Glass Properties III; Glass Melts (CD-ROM), The American Ceramic Society, Ohio, M. K. Choudhary, N. T. Huff, C. H. Drummond III, 1998, 80-85)

Abstract

Previous research has shown that MgO additions induce amorphous phase separation in the system SiO_2-CaO-P_2O_5-MgO. This work reports a study on the effect of MgO additions on the microstructure of glasses with composition (mol %) 31SiO_2-11P_2O_5-(58-*x*)CaO-*x*MgO, with *x* ranging from 0 to 32.

All MgO-containing glasses exhibited phase separation. The dispersed phase consists of clusters of pure, amorphous SiO_2 droplets with average size increasing with MgO content. Glass transformation temperatures (T_g) decrease with increasing MgO content. Apatite crystallizes on heating the MgO-free composition, whereas all the MgO-containing compositions crystallize to β-tricalcium phosphate and magnesium silicates.

Differences in the observed microstructures are discussed on the basis of T_g values and available viscosity data for pure amorphous SiO_2 and for a particular glass of this series.

1. Introduction

In a previous study[1] it was observed that some glasses of the $3CaO.P_2O_5$-SiO_2-MgO system showed phase separation, morphologically characterized by the clustering of pure, amorphous silica. The characteristic morphology of the separated phase has similar to that reported by other authors: silica-rich phase separation was detected in the systems SiO_2-P_2O_5-CaO[2], SrO-B_2O_3-SiO_2[3], MgO-SiO_2-Si_3N_4[4,5], ZnO-B_2O_3-SiO_2[6,7] and Y-Si-Al-O-N[8] and in the systems TeO_2-B_2O_3[9], TeO_2-B_2O_3-GeO_2[9] and TeO_2-GeO_2-V_2O_5[9] a B_2O_3- or GeO_2- rich phase was found.

So far, a clear explanation for the observed morphology has not been proposed. However most authors[4,7] agree that the growing and grouping of individual droplets is somehow related to differences in viscosity between the separated phase and the glassy matrix.

2. Experimental Procedure

The glasses were prepared from reagent-grade $Ca(H_2PO_4)_2$, $CaCO_3$, SiO_2 and MgO. The raw materials were wet mixed (in ethanol) for 30 minutes and dried at 60 °C. Batches of 50-70 g were melted in a platinum crucible at temperatures in the range 1500-1530 °C for 2 hours, a schedule which was found to be adequate to ensure a good homogeneity and fining. The glass compositions investigated are listed in Table I.

Table I. Glass compositions.

	Composition (mol %)			
Sample	SiO_2	CaO	P_2O_5	MgO
CM1	31.1	58.4	10.6	0.0
CM2	31.1	52.9	10.6	5.5
CM3	31.1	47.6	10.6	10.8
CM4	31.1	42.3	10.6	16.0
CM5	31.1	37.0	10.6	21.4
CM6	31.1	31.7	10.6	26.6
CM7	31.1	26.4	10.6	32.0

All the glasses except CM1 were cast into metal moulds, annealed at T_g temperatures for 30 minutes and slowly cooled to room temperature. As composition CM1 devitrified on casting, it was necessary to pour it into water to obtain an amorphous frit.

Differential Thermal Analysis (DTA) runs were performed on powders with particle size below 38 μm, by heating them in alumina crucibles at a rate of 10 $K.min^{-1}$ from room temperature to 1100 °C in air. Calcined alumina powder was used as the reference material.

Powdered samples, either from base glasses or from glasses cerammed during DTA runs, were analyzed by X-Ray Diffraction (XRD) with Cu K_α radiation.

Microstructures of the obtained glasses were observed by Scanning Electron Microscopy (SEM) of fresh fracture surfaces etched with HNO_3 1 M for 10 seconds.

3. Results and Discussion

3.1 Glass Formation

Composition CM1 crystallized on pouring into the mould (a frit was needed to obtain an amorphous material) and composition CM2 still exhibited some tendency for surface devitrification giving rise to cloudy specimens. All other compositions were very homogeneous, yielding white opaque specimens. Compositions with MgO contents higher than that of CM7 did not melt up to 1550 °C.

XRD runs on the base materials showed that all the samples were amorphous.

SEM observation indicated that phase separation did not occur in the frit CM1, while a separated phase was present in all other glasses of the series.

Figure 1 shows micrographs of the glasses CM2, CM3, CM5 and CM7.

The separated cluster was previously identified as pure amorphous silica[10]. An increase in average size of aggregates with MgO content is evident.

3.2 DTA runs

The most significant events in DTA runs (Fig. 2) are deflections due to glass transitions and exothermic crystallization peaks. Composition CM1 exhibited a single

crystallization peak corresponding to apatite, as identified by XRD (a minor amount of calcium silicate pseudowollastonite is also possible). All other compositions exhibited two crystallization peaks, the first one attributed to the precipitation of whitlockite (β-$Ca_3(PO_4)_2$) and the second one to the crystallization of magnesium silicates (enstatite and forsterite). Figure 2 also shows that the amount of magnesium silicates, with respect to that of phosphate, increases with MgO content.

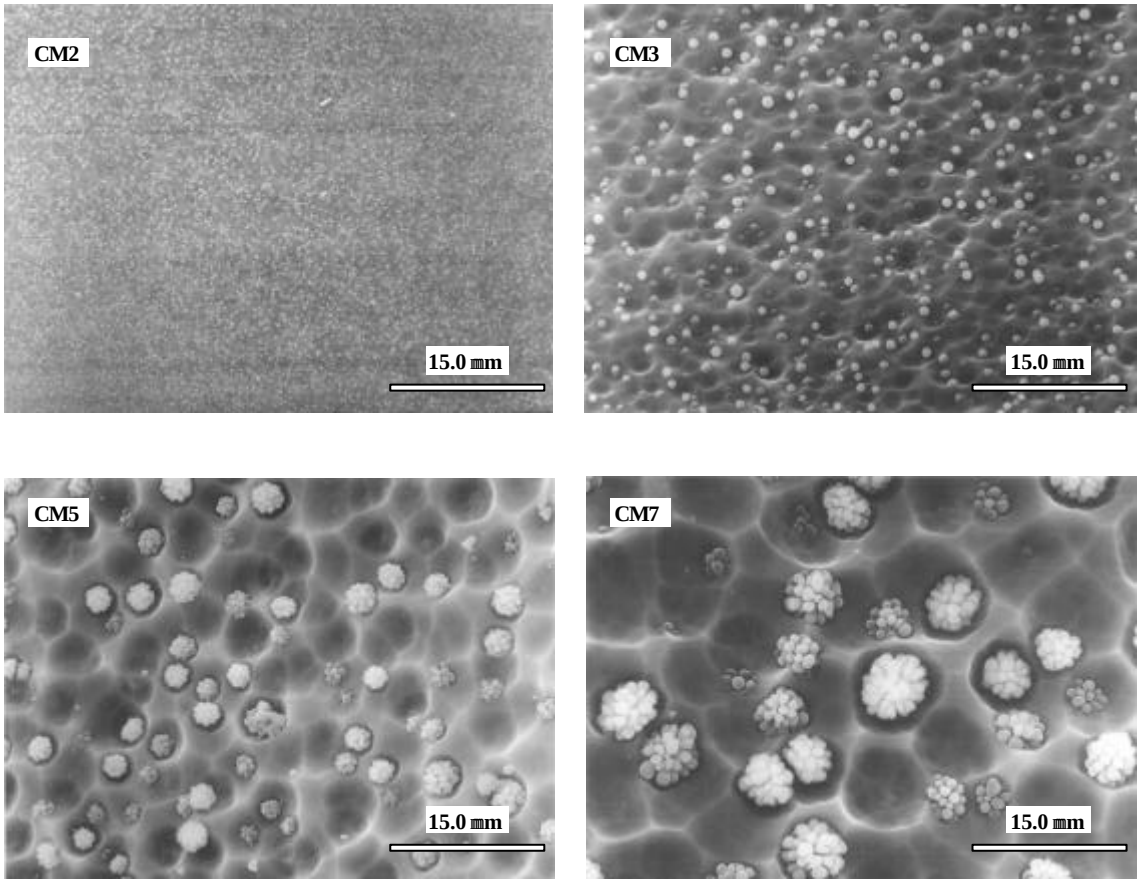

Fig. 1. SEM micrographs of etched, fracture CM glasses.

It is known that Mg^{2+} substitution for Ca^{2+} in phosphates stabilizes tricalcium phosphate, rathar than apatite[11]. It is thus natural that magnesium-free compositions crystallize to apatite, whereas magnesium-containing materials produce whitlockite. Also an increase in magnesium silicate(s) concentration is expected with increasing MgO contents of the parent composition.

Transformation temperatures T_g decrease with increasing MgO content, as shown in Fig. 3. This behaviour may be rationalized if, as suggested by preliminary nuclear

magnetic resonance spectroscopy work[12], Mg^{2+} is able to disrupt Si-O-Si bonds, thus increasing the concentration of non-bridging oxygens and weakening the glass network.

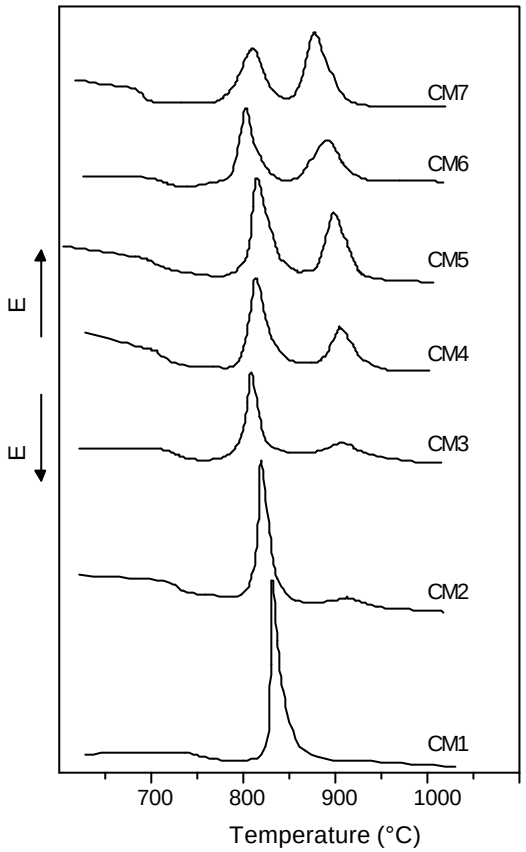

Fig. 2. DTA traces for $31SiO_2$-(58-*x*)CaO-$11P_2O_5$-*x*MgO compositions.

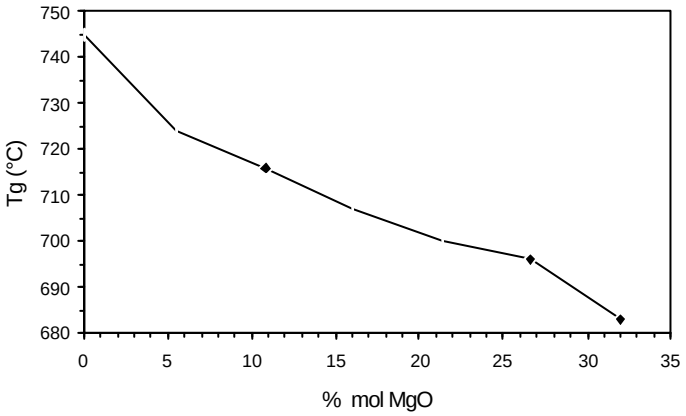

Fig. 3. T_g dependence on MgO content.

3.3 Phase Separation

The viscosity curve for the phase-separated glass CM6 has been previously determined up to 800 ºC[13]. Based on this curve and on the fact that at T_g the viscosity of glasses is approximately the same (10^{12} - $10^{12.5}$ dPa.s)[14] the variation of viscosity with temperature for the CM series was estimated (Fig. 4). Lines referring to amorphous SiO_2 were assessed from published data[15].

In a previous work[1] it has been found that quenching composition CM6 from melting temperatures results in a glass with spherical separated droplets, and that grouping of individual droplets occurs at lower quenching temperatures (but higher than T_g). These findings provide support to the assumption that individual droplets precipitate at higher temperatures and group on cooling. In this case, mobility of droplets, hence the viscosity of the glass matrix, should be particularly important in an intermediate range of temperatures, above T_g, such as that covered in Fig. 4.

In all cases the amount of precipitated silica is relatively small (assessed as lower than 10%), and is not much sensitive to MgO content, so that the comparison of viscosity values will provide reasonable information on matrix viscosity variations. Assuming the viscosity on temperature suggested in Fig. 4, it becomes obvious that, at a given temperature matrix viscosity decreases with increasing MgO content (in agreement with T_g depression) and that matrix viscosities of the end-members of the series, CM7 and CM1, are separated by two orders of magnitude. Matrix / silica viscosity differential ranges from 6 to 8 orders magnitude as the MgO content increases from CM1 to CM7.

Lower matrix viscosities, (or higher viscosity differentials) obtained with increasing MgO contents, would explain easier aggregation and increasing size of aggregates, at a given temperature). Neither the mechanism nor the driving force for aggregation are yet clear, and so the relative importance of matrix viscosity in itself or, rather, the matrix/precipitate viscosity differential, cannot be established at this stage.

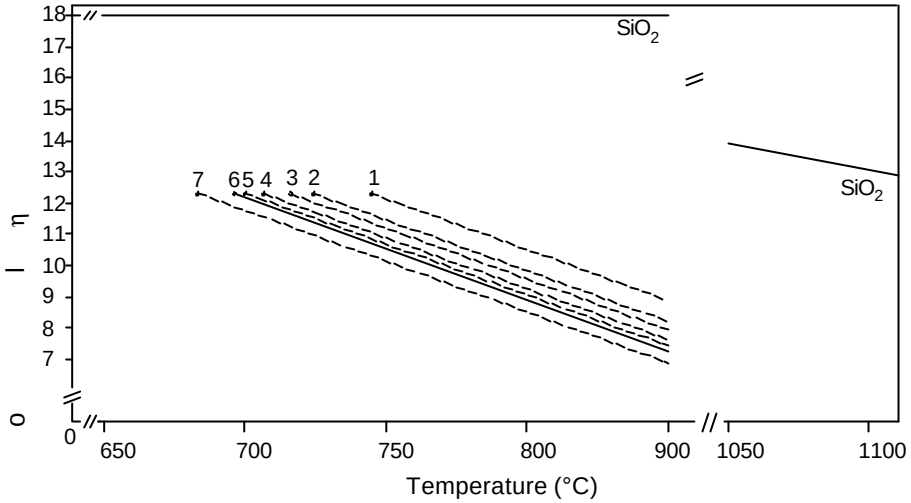

Fig. 4. Effects of MgO additions on the viscosity of CM glasses.

4. Conclusions

Replacing CaO by MgO in the series $31SiO_2$-$11P_2O_5$-(58-*x*)CaO-*x*MgO promotes separation of pure amorphous SiO_2 consisting of aggregates of droplets with average sizes increasing with increasing MgO content.

The size of the aggregates increases with MgO content and this trend is tentatively explained in terms of the effect of MgO in glassy matrix viscosity.

MgO-free CM glasses heated up to 1100°C precipitate apatite, while in MgO containing compositions whitlockite is the stable phosphate phase. The fraction of magnesium silicate(s) increases relatively to that of whitlockite, as MgO content increases.

References

[1] Oliveira, A. L.; Oliveira, J. M.; Correia, R. N.; Fernandes, M. H. – "Phase Separation and Crystallization of $3CaO.P_2O_5$-SiO_2-MgO Glasses", *Glastechenische Beriche Glass Science and Technology*, 67C, 1994, 367-370.

[2] Vogel, W. – *Glass Chemistry*, 2nd ed., Berlin Heidelberg, Springer-Verlag, 1994.

[3] Baylor, R.; Brown, J. J. – "Phase Separation of Glasses in the System $SrO-B_2O_3-SiO_2$", *Journal of the American Ceramic Society*, 59, 1976, 131-136.

[4] Shaw, T. W.; Thomas, G.; Loehman, R. E. – "Formation and Microstructure of Mg-Si-O-N Glasses", *Journal of the American Ceramic Society*, 67, 1984, 643-647.

[5] Loehman, R. E. – "Oxynitride Glasses", *Journal of Non-Crystalline Solids*, 42, 1980, 433-446.

[6] Taylor, P.; Owen, D. G. – "Liquid Immiscibility in the System $Na_2O-ZnO-B_2O_3-SiO_2$", *Journal of the American Ceramic Society*, 64, 360-367.

[7] Taylor, P. – "Peculiar Morphology in Some Phase-Separated Multicomponent Silicate Glasses", *Journal of the American Ceramic Society*, 75, 1992, 1276-1277.

[8] Hampshire, S.; Nestor, E.; Flynn, R.; Besson, J.-L.; Rouxel, T.; Lemercier, H.; Goursat, P.; Sebai, M.; Thompson, D.; Liddell, K. – "Yttrium Oxynitride Glasses: Properties and Potencial for Crystallization to Glass-ceramics", *Journal of the European Ceramic Society*, 14, 1994, 261-273.

[9] Kashchieva, E. P.; Dimitriev, Y. B. – "Unusual Immiscibility Structures in Tellurite Glasses", *Journal of the American Ceramic Society*, 80, 1997 1588-1590.

[10] Oliveira, J. M; Fernandes, M. H.; Correia, R. N. – "Surface Modifications of Glasses and Glass-ceramics of the System $MgO-3CaO.P_2O_5-SiO_2$ in a Simulated Body Fluid", *Biomaterials*, 16, 1995, 849-854.

[11] Correia, R. N.; Magalhães, M. C.; Marques, P. A.; Senos, A. M. – "Wet Synthesis and Characterization of Modified Hydroxyapatite Powders", *Journal of Materials Science: Materials in Medicine*, 7, 1996, 501-505.

[12] Oliveira, J. M; Correia, R. N.; Fernandes, M. H. – unpublished work.

[13] Oliveira, A. L.; Oliveira, J. M.; Correia, R. N.; Fernandes, M. H.; Frade, J. R. – "Crystallization of Whitlockite From a Glass in the System $CaO-P_2O_5-SiO_2-MgO$", *Journal of the American Ceramic Society*, 81, 1998, 3270-3276.

[14] Navarro, J. M. F. – *El Vidrio*, 2nd ed., Consejo Superior de Investigaciones Científicas - Fundación Centro Nacional del Vidrio, Madrid, 1991.

[15] Shand, E. B – *Glass Engineering Handbook*, 2nd ed., MacGraw-Hill, New York, 1958.

2.5 - Formation of Convoluted Silica Precipitates During Amorphous Phase Separation in the $Ca_3(PO_4)_2$-SiO_2-MgO System

J. M. Oliveira, R. N. Correia, M. H. V. Fernandes

Department of Ceramics and Glass Engineering, UIMC, University of Aveiro, 3810-193 Aveiro, PORTUGAL

(Journal of the American Ceramic Society, 83(5), 2000, 1296-1298)

Abstract

Dispersed aggregates of peculiar morphology have been obtained in phase-separated glasses of the system $Ca_3(PO_4)_2$-SiO_2-MgO, where the separated phase is amorphous silica. The formation of such convoluted aggregates is tentatively explained in terms of a fast coalescence process of initial isolated quasi-spherical droplets which behave as a dispersed phase in an emulsion-like system.

1. Introduction

Liquid immiscibility is well known in multicomponent glasses[1-4], particularly in those containing silica and whose compositions lie near the silica-rich liquid immiscibility dome of the corresponding equilibrium diagrams. The separated phase appears as uniformly dispersed spherical droplets[4] or as convoluted structures of peculiar morphologies[5-12], whose origin has been assigned either to grouping of individual droplets[9,13] or to growth instabilities leading to a dendritic-like growth[11]. Whatever the underlying mechanism, most authors agree in that the formation of these convoluted aggregates is somehow related to differences in viscosity between the separated phase and the matrix.[8,11,12]

Convoluted aggregates have been obtained in phase-separated glasses of the system $Ca_3(PO_4)_2$-SiO_2-MgO, where the separated phase is amorphous silica. In this case it appears that separation is already present at melting temperatures, below 1600ºC.[13]

In this work, a discussion on the probable mechanisms of formation of convoluted silica precipitates in $Ca_3(PO_4)_2$-SiO_2-MgO glasses is made, and it is suggested that they form by a fast coalescence process of individual droplets, taking place on cooling the glass down to temperatures where the viscosity of silica becomes so high that any further arrangements can no longer occur.

2. Experimental Procedure

Glasses of nominal composition (wt%) 52.75 $Ca_3(PO_4)_2$ 30 SiO_2 17.25 MgO were prepared from reagent-grade $Ca(H_2PO_4)_2$, $CaCO_3$, SiO_2 and MgO. Batches with 80 g were obtained by mixing the raw materials in ethanol for 30 minutes, drying at 60 °C and melting in a platinum crucible. Three sets of experiments were then performed:

(1) Melting at different temperatures for a certain time and quenching: glasses were melted at 1595, 1560 and 1525 ºC for 30 minutes and then directly plunged into water at room temperature.

(2) Fixed melting temperature and quenching after different melting times: melted glasses at 1560 ºC were kept at this temperature for 5 minutes, 15 minutes, 2, 6 and 14 hours and then quenched in water.

(3) Fixed melting temperature and time, and quenching from different stages along the cooling cycle: after melting at 1560 °C for 2 hours, small amounts of glass were quickly poured onto a metallic mould, after roughly calculated cooling times of 1, 5, 10, 15, 30 and 120 seconds and then quenched in water at room temperature.

Fresh fracture surfaces were observed by Scanning Electron Microscopy (SEM) after etching with HNO_3 1 M for 15 seconds. An extraction replica of a fresh fracture surface of annealed glass was prepared for observation by Transmission Electron Microscopy (TEM) and for evaluation of chemical composition by Energy Dispersive Spectroscopy (EDS). EDS profiles for Si, P, Ca and Mg were also obtained in polished

samples, with no etching, in order to assess any composition gradients around silica precipitates.

The amount of precipitated silica was quantitatively determined by digesting the glass in HCl 1 M, ultracentrifuging, and analysing the dissolved Si, P, Ca and Mg in the remaining liquid by Inductively Coupled Plasma (ICP) spectroscopy. SEM/EDS analysis of the residue was used to confirm that, within the detection limits of EDS analysis, it mainly consisted of unattacked aggregates containing only silica. The amount of precipitated silica was calculated by difference between the nominal amount of Si and the Si content in the liquid.

3. Results and Discussion

Figure 1 shows the microstructures of the glasses quenched from 1595, 1560 and 1525 ºC, according to the first set of experiments, and the microstucture of the same glasses after slow cooling in the annealing furnace.

TEM electron diffraction of an isolated aggregate extracted by replication from an annealed sample revealed the amorphous nature of the separated phase (Fig. 2). EDS of the aggregate indicated the presence of only two elements, silicon and oxygen, thus confirming that the separated phase consisted of amorphous silica.

Figure 1 shows that the separated phase is homogeneously dispersed in the matrix, with droplets of average diameter around 300 nm at 1595 ºC and around 500 nm at 1560 ºC, whereas at 1525 ºC some convoluted precipitates are already present. However, independently of the melting temperature, all microstructures obtained after annealing consisted of homogeneously dispersed convoluted aggregates with average sizes around 2.5 μm.

The micrographs indicate that the mean size of precipitates increases as the melting temperature decreases. Moreover, the particle size, as noted in SEM micrographs, did not vary with melting times from 5 minutes to 14 hours at 1560 °C (second set of experiments). Thus, at each constant temperature a characteristic size of precipitate should occur, being essentially independent of time.

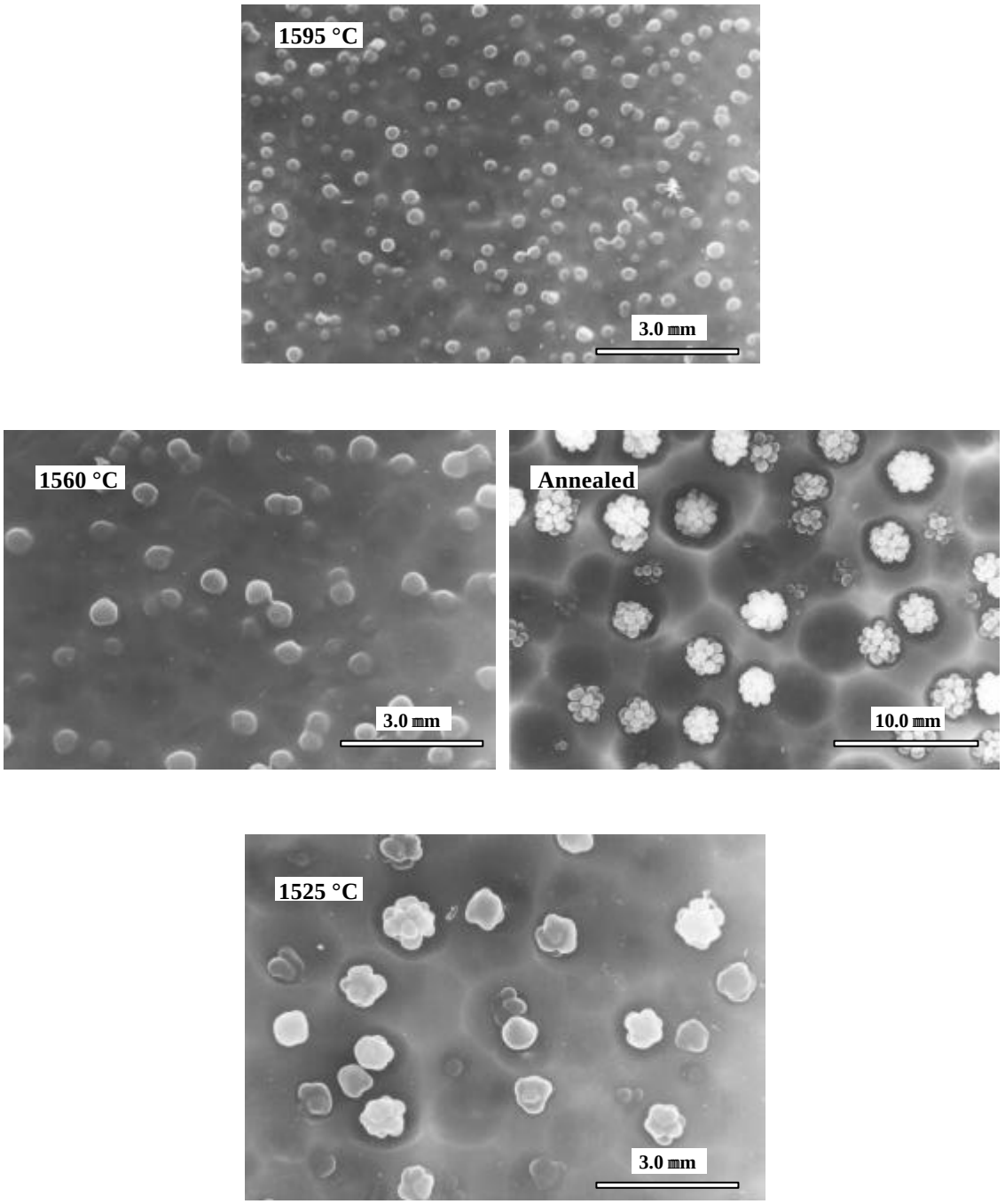

Fig. 1. SEM micrographs of etched glass samples quenched from 1595, 1560 and 1525 °C (first set of experiments) and annealed.

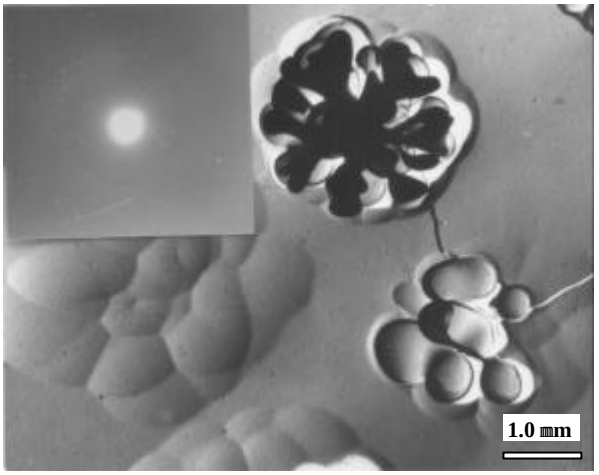

Fig. 2. TEM extraction replica micrograph with diffraction pattern of an annealed sample.

Micrographs in Fig. 3, corresponding to decreasing transient temperatures (third set of experiments), show that the precipitates formed at 1560 ºC consist of fairly uniform isolated droplets, and that the morphology progresses towards convoluted agglomerates whose mean size increases as temperature falls.

A dendritic growth mechanism by transport of Si from the matrix may explain the origin of the observed morphology, but this may also be the result of a mere rearrangement of an initial amount of silica precipitates. The first hypothesis could not be confirmed by EDS, since no compositional gradient was detected at either side of the precipitate/matrix boundary. To assess the possibility of the second hypothesis we determined the amounts of precipitated silica in the samples quenched from 1595, 1560 and 1525 ºC (containing quasi-spherical formations) and in the annealed sample (containing silica aggregates). The values obtained ranged from 7 to 7.5 wt% for all the samples, suggesting that at those temperatures the amount of separated silica is very similar and that it is kept along the cooling process. This points towards the possibility of formation of the convoluted aggregates from a fixed amount of initial separated silica, without significant contribution of the Si from the matrix. An additional conclusion is that the immiscibility dome of the equilibrium diagram of the present system should have a quasi-infinite temperature vs. composition slope in the range of temperatures tested, a situation not uncommon in other silica-based systems exhibiting liquid - liquid immiscibility.[2,14-16]

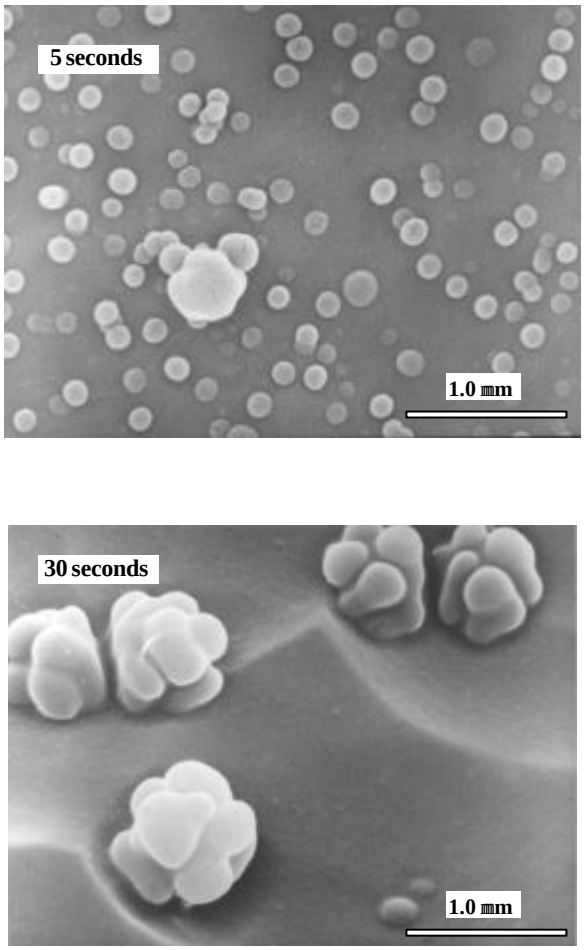

Fig. 3. SEM micrographs of etched glass samples melted at 1560 °C and quenched after cooling times of 5 and 30 seconds (third set of experiments).

If the growth instability hypothesis is abandoned, one is left to consider the coalescence of individual entities, as it would happen in an uniformly sized emulsion. An interesting feature that strongly suggests an emulsion-like behaviour for this system is the apparent flattening of closely spaced entities (pairs of droplets in Fig. 1 and pairs of aggregates in Fig. 3). Moreover, the size of individual entities permits us to hypothesize brownian motion as responsible for particle collisions.

From the microstructures it is seen that precipitates tend to become more convoluted as temperature falls. At higher temperatures the rate of neck growth is high enough to make the identification of particle coalescence difficult. It is believed that the process of neck growth is mainly governed by a viscous sintering mechanism which is halted on cooling because the viscosity of the separated silica significantly increases in

comparison with the viscosity of the surrounding matrix. The authors have shown in another paper[17] that partial substitution of CaO by MgO in these glasses depresses the transition temperature, and thus the matrix viscosity (that is increases the difference for the separated silica viscosity) and leads to an increase in the average dimension of the aggregates formed at a given temperature.

4. Conclusions

Convoluted amorphous silica precipitates have been found in phase-separated glasses of the $Ca_3(PO_4)_2$-SiO_2-MgO system. It is suggested that the formation of such aggregates is due to a fast coalescence process of a fixed amount of individual droplets, which takes place in a low viscosity matrix as temperature decreases, and is halted by a significant increase in the viscosity of the silica separated phase.

Acknowledgements

The authors acknowledge FCT (Portuguese Foundation for Science and Technology) for financial support.

References

[1] Vogel, W. – "Phase Separation in Glass", *Journal of Non-Crystalline Solids*, 25, 1977, 170-214.

[2] James, P. F. – "Review Liquid-Phase Separation in Glass-forming Systems", *Journal of Materials Science*, 10, 1975, 1802-1825.

[3] Kreidl, N. – "Phase Separation in Glasses", *Journal of Non-Crystalline Solids*, 129, 1991, 1-11.

[4] Mazurin, O. V.; Porai-Koshits, E. A.; Andreev, N. S. – *Phase Separation in Glass*, Mazurin, O. V.; Porai-Koshits, E. A., Amsterdan, North-Holland, 1984.

[5] Vogel, W. – *Glass Chemistry*, Springer-Verlag, Berlin Heidelberg, 1994.

[6] Milyukov, E. M. – "Morphological Features of Two-Phase Glasses", *Fiz. Khim. Stekla*, 3, 1977, 576-579 *(in Russian)*.

[7] Baylor, R.; Brown, J. J. – "Phase Separation of Glasses in the System $SrO-B_2O_3-SiO_2$", *Journal of the American Ceramic Society*, 59, 1976, 131-136.

[8] Shaw, T. M.; Thomas, G.; Loehman, R. E. – "Formation and Microstructure of Mg-Si-O-N Glasses", *Journal of the American Ceramic Society*, 67, 1984, 643-647.

[9] Loehman, R. E. – "Oxynitride Glasses", *Journal of Non-Crystalline Solids*, 42, 433-446 (1980).

[10] Taylor, P.; Owen, D. – "Liquid Immiscibility in the System $Na_2O-ZnO-B_2O_3-SiO_2$", *Journal of the American Ceramic Society*, 64, 1981, 360-367.

[11] Taylor, P. – "Peculiar Morphology in Some Phase-Separated Multicomponent Silicate Glasses", *Journal of the American Ceramic Society*, 75, 1992, 1276-1277.

[12] Kashchieva, E. P.; Dimitriev, Y. B. – "Unusual Immiscibility Structures in Tellurite Glasses", *Journal of the American Ceramic Society*, 80, 1997, 1588-1590.

[13] Oliveira, A. L.; Oliveira, J. M.; Correia, R. N.; Fernandes, M. H. – "Phase Separation and Crystallization of $3CaO.P_2O_5-SiO_2-MgO$ Glasses", *Glastechenische Beriche Glass Science and Technology*, 67C, 1994, 367-370.

[14] Cahn, J. W.; Charles, R. J. – "The Initial Stages of Phase Separation in Glasses", *Physics and Chemistry of Glasses*, 6, 1965, 181-191.

[15] Nakagawa, K.; Izumitani, T. – "Effect of a Third Component upon the Immiscibility of Binary Glass", *Physics and Chemistry of Glasses*, 13, 1972, 85-90.

[16] Tomozawa, M. – "Phase Separation in Glasses", *in* Tomozawa, M.; Doremus, R. H. – *Treatise on Materials and Technology: Glass II*, 17, New York, Academic Press, 1979, 71-113.

[17] Oliveira, J. M.; Correia, R. N.; Fernandes, M. H. – "Effect of MgO Additions on Amorphous Phase Separation in Silicophosphate Glasses"; *in* Choudhary, M. K.; Huff, N. T.; Drummond III, C. H. – *Proceedings of the XVIII International Congress on Glass*, D5: Glass Properties III; Glass Melts (CD-ROM), Ohio, American Ceramic Society, 1998, 80-85.

2.6 - Crystallization of Whitlockite From a Glass in the System $CaO-P_2O_5-SiO_2-MgO$

A. L.Oliveira, J. M. Oliveira, R. N. Correia, M. H. Fernandes, J. R. Frade

Departamento de Engenharia Cerâmica e do Vidro, Universidade de Aveiro, 3810-193 Aveiro, PORTUGAL

(Journal of the American Ceramic Society 81(12), 1998, 3270-3276)

Abstract

The kinetics of crystallization of a glass with composition $30SiO_2$-$24.14P_2O_5$-28.61CaO-17.25MgO (wt%) was studied with variable temperature, by differential thermal analysis. These results were interpreted according to revised theoretical models which describe the dependence of fraction crystallized on temperature and on the heating rate, and the dependence of the peak temperature on the rate of change in temperature. These models emphasize the differences in crystallization behaviour between "as prepared" glass samples, and the corresponding previously nucleated samples. These differences in behaviour suggest that the kinetics of crystallization comprises a nucleation stage at temperatures of about 730 °C, and particle growth for temperatures higher than 800 °C. The temperature dependence of the fraction crystallized corresponds to a very high value of activation energy for growth (≈763 kJ/mol), but this is still lower than the activation energy evaluated from the temperature dependence of viscosity.

1. Introduction

The kinetics of crystallization must be properly understood to obtain glass-ceramic materials with controlled microstructure and properties. These studies are usually based on the dependence of fraction reacted on time and/or temperature, and this may be evaluated under isothermal conditions or with variable temperature. Experiments performed with variable temperature require much less time than what is needed to perform several isothermal experiments for different temperatures and times. This is possible because crystallization is exothermic and changes in fraction crystallization can thus be evaluated in real time by differential thermal analysis (DTA) or differential scanning calorimetry (DSC).

Sound theoretical models are also needed to interpret experimental data obtained with variable temperature. These models describe the dependence of fraction crystallized on temperature and on the rate of change in temperature for a variety of different mechanisms. However, designing materials with controlled fractions crystallized require several parameters such as the activation energy and pre-exponential factor, for describing the temperature dependence, and an exponent *n* for describing the effects of the rate of change in temperature. This exponent *n* depends on the dimensionality of particle growth, and also on the controlling mechanisms (diffusion control or phase boundary controlled growth). It is thus sometimes difficult to attribute a physicochemical meaning to every fitting parameter obtained from DTA or DSC results.

The meaning of the activation energy obtained by fitting is not always straightforward, especially because this may comprise contributions of nucleation (E_g) and growth (E_n). In addition, most theoretical models are based on assuming that the rates of nucleation and growth follow the Arrhenius law, which may fail in real cases. For example, the growth rate tends to vanish on approaching the melting temperature (after reaching a peak). This effect is accounted for by a classical model for the growth rate with phase boundary control[1]

$$U = U_o \exp[-E_g/(RT)] \{1-\exp[\Delta G/(RT)]\} \quad (1)$$

where U_o is a preexponential factor, E_g is an activation energy for transport across the interface, R is the perfect gas constant, T is absolute temperature, and ΔG is the transformation free energy. The factor 1-exp[$\Delta G/(RT)$] drops to zero at the melting temperature, due to the temperature dependence of $\Delta G=\Delta H-T\Delta S$, and the growth rate thus vanishes in identical conditions. On the other hand, one may expect $|\Delta G| << RT$ at sufficiently low temperatures, and in this case Eq. (1) reduces to a typical Arrhenius law $U \approx U_o \exp[-E_g/(RT)]$, as assumed by most models proposed to describe the temperature dependence of fraction crystallized with variable temperature.

The nucleation rate usually reaches a peak at even lower temperature, and a classical model can be written[2]

$$I = I_o \exp[-E_N/(RT)] \exp[-W^*/(kT)] \quad (2)$$

where I_o is the preexponential factor, E_N is a typical activation energy for nucleation (kinetic barrier), W^* is the Gibbs free energy to form the nucleus, and k is the Boltzmann constant. The thermodynamic barrier W^* varies with ΔG^{-2}, and tends to increase rapidly on approaching the melting temperature. At sufficiently low temperatures one expects $W^*/(kT) << 1$, and a simpler Arrhenius law can also be assumed for the nucleation rate $I \approx I_o \exp[-E_N/(RT)]$.

The experimental conditions must be carefully planned to avoid exceeding the growth rate peak temperature, and thus to be able to assume that the Arrhenius law is nearly true. For example, experiments performed with low heating rates might ensure that high fractions crystallized are attained before reaching the growth peak temperature. Avoiding the nucleation peak is less critical, and relatively simple model can be obtained at least for the following cases:

Case A – when the nucleation peak occurs at temperatures which are lower than required for the onset of growth, the growth rate being described by the Arrhenius law for the entire temperature range (Fig. 1).

Case B – for simultaneous nucleation and growth in a temperature range where the nucleation rate and growth rate are both described by Arrhenius laws.

Case A comprises stages of nucleation and growth, and these stages can be separately adjusted by changing suitable experimental variables. For example, the number of nuclei

formed during an isothermal nucleation stage will increase with time, prior to the onset of growth; this will be refered to as case A1 as shown in Fig. 1. Alternatively, the number of nuclei formed with variable temperature will increase with decreasing heating rate for temperatures lower than the onset of crystallization[3]; this corresponds to case A2 in Fig. 1.

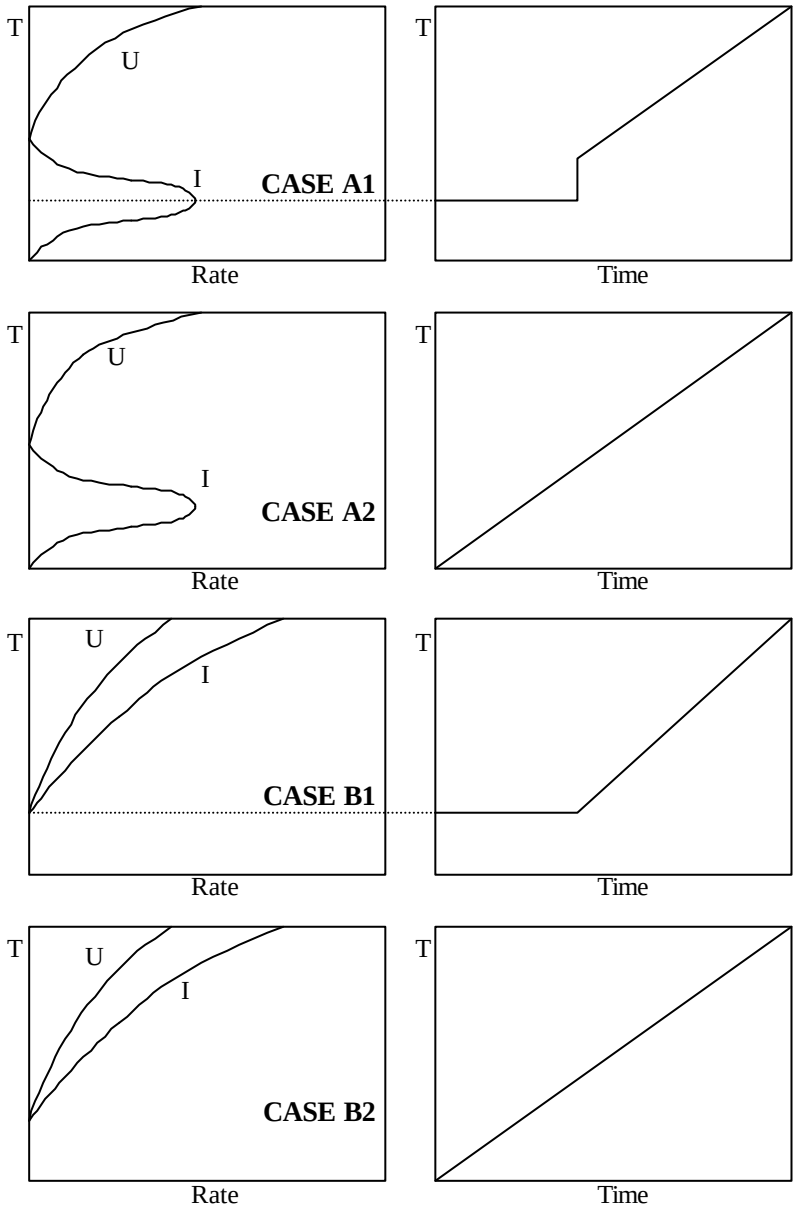

Fig. 1. Schematic representation of the temperature dependence of the rates of nucleation (I) and growth (U) for selected cases and suitable heat treatments for studying the overall kinetics of crystallization.

In cases A1 and A2 the nucleation rate vanishes before reaching significant values of the fraction crystallized, and the temperature dependence thus depends on the activation

energy for growth only. The activation energy of the overall crystallization process is not expected to be altered by changing the nucleation time, or the rate of change in temperature during the nucleation stage. In addition, narrow particle size distributions are expected in cases A1 and A2 because the onset of growth is nearly simultaneous for every particle. Nevertheless, the nucleation time or other variables which are likely to change the number of nuclei are also expected to effect the values of fraction crystallized attained at a given temperature. The crystallization peak (observed by DTA or DSC) is thus expected to be shifted to lower temperatures with increasing nucleation time (for isothermal nucleation), or decreasing heating rate (for variable temperature). The average particle size attained on reaching a given fraction crystallized must decrease in identical conditions.

Simultaneous nucleation and growth (case B) implies that the relevant experimental variables affect both stages. Particles may nucleate at different temperatures (or times), thus yielding a broad particle size distribution. The fraction crystallized will not be affected by changing the heat treatment for temperatures lower than the onset of crystallization T_{oc}, and the alternative heat treatments shown in Fig. 1 (cases B1 and B2) should provide nearly identical temperature dependence for the fraction crystallized.

2. Revised Avrami-Nakamura models

The original JMA equation has been used to interpret the kinetics of crystallization in isothermal conditions, and has been applied to a great variety of conditions, including cases when nucleation and growth are simultaneous, and other cases when nucleation precedes particle growth (or is nearly instantaneous). However, the JMA equation cannot be used to fit experimental results obtained with variable temperature, and several authors have thus proposed solutions to deal with the temperature dependence of fraction crystallized, based on a method derived by Nakamura[4,5,6]. The most widely used model for the crystallization of glasses with variable temperature is[7-10]

$$\ln [-\ln (1-\alpha)] = \text{constant} - n \ln (\beta) - E/(RT) \qquad (3)$$

where α is the fraction crystallized, β is the rate of change in temperature, n is the so-called Avrami parameter (as shown in Table I), and E is a fitting parameter which should be close to the true activation energy for the overall crystallization process (E_c in Table I). Actually, the value of E obtained by fitting tends to be overestimated, as recognized by some authors (Matusita and coauthors[10]; Kemeny and Šesták[11]). These authors proposed a correcting factor $E/E_c = 1.052$ to recover a better evaluation of the activation energy of crystallization E_c. However, this is an oversimplification because the relative difference between E and E_c increases with decreasing values of activation energy[3].

Table I. Relevant Parameters for the Generic Solution for Crystallization with Variable Temperature (Eqs. (4) and (5) or (6)), for Systems Where Nucleation Precedes Growth (Case A), and for Simultaneous Nucleation and Growth (Case B).

Nucleation	Growth	Dimensionality	n	E_c
Case A	Phase Boundary	1	1	E_g
	Phase Boundary	2	2	$2E_g$
	Phase Boundary	3	3	$3E_g$
Case B	Phase Boundary	1	2	$E_N + E_g$
	Phase Boundary	2	3	$E_N + 2E_g$
	Phase Boundary	3	4	$E_N + 3E_g$
Case A	Diffusion	1	1/2	$E_g/2$
	Diffusion	2	1	E_g
	Diffusion	3	3/2	$3E_g/2$
Case B	Diffusion	1	3/2	$E_N + E_g/2$
	Diffusion	2	2	$E_N + E_g$
	Diffusion	3	5/2	$E_N + 3E_g/2$

Some authors proposed the following improved solution to account for the temperature dependence [3, 12]

$$\ln [-\ln (1-\alpha)/T^{2n}] \approx \ln (K_v) - n \ln (\beta) - E/(RT) \qquad (4)$$

where K_v is a preexponential factor for crystallization with variable temperature. This is a constant for simultaneous nucleation and growth (case B), and increases with the number of particles when nucleation precedes growth (cases A1 and A2). This number of nuclei formed after isothermal nucleation increases with time t_N (case A1), and in this case the corresponding preexponential factor is also dependent on the nucleation time $K_v(t_N)$. However, one must know the nucleation peak to be able to adjust the number of nuclei under isothermal conditions (case A1). Otherwise, one may resort to variable temperature (case A2), and the number of nuclei should increase with decreasing heating rate β_N thus yielding a pre-exponential factor $K_v = K_v'/\beta_N^3$. In this case Eq. (4) becomes

$$\ln [-\ln (1-\alpha)/T^{2n}] \approx \ln (K_v') - \ln (\beta_N) - n \ln(\beta_g) - E/(RT) \quad (5)$$

and can be used for conditions when different heating rates are selected for nucleation (β_N) and growth (β_g). When the heating rate remains the same for both stages of nucleation and growth Eq. (5) becomes

$$\ln [-\ln (1-\alpha)/T^{2n}] \approx \ln (K_v') - (n+1) \ln(\beta) - E/(RT) \quad (6)$$

Equations (4) and (6) are useful to interpret experimental results describing the dependence of fraction crystallized on temperature, and on the rate of change in temperature. The fitting parameters obtained in this way will then be useful to adjust the experimental conditions to design new materials with different values of fraction crystallized, and possibly also differences in average particle size.

For relatively high activation energies the fitting parameter E is nearly identical to the activation energy for the overall crystallization process ($E \approx E_c$), which is related to the activation energies for nucleation (E_N) and/or growth (E_g), as recognized by Šesták and coauthors[11,13]. The solutions shown in Table I ($E_c = nE_g$ for cases when nucleation precedes growth, or $E_c = nE_g + E_N$ for simultaneous nucleation and growth) can be used for sufficiently high values of activation energy. Otherwise, one may also use the following corrections proposed by Frade[3]:

$$E_c \approx n f_{2g} E_g \quad (7)$$

for cases when nucleation precedes growth, or

$$E_c \approx n f_{2g} E_g + f_{2N} E_N \quad (8)$$

for simultaneous nucleation and growth, where f_{2g} and f_{2N} are correcting factors.

These correction factors $f_{2g} = f_2(RT/E_g)$, and $f_{2N} = f_2(RT/E_N)$ increase with the average dimensionless temperature (RT_{av}/E_g or RT_{av}/E_N), and are close to unit for low dimensionless temperatures. Typical values are $f_2(RT/E_a)$ = 0.996, 0.985, 0.970, 0.952, 0.932, 0.909, ... for RT/E_a = 0.05, 0.1, 0.15, 0.2, 0.25, 0.3, ... respectively, E_a being a generic activation energy. One can thus assume that $E \approx nE_g$ for $RT/E_g < 0.1$, or $E = nE_g + E_N$ for $RT/E_g < 0.1$ and $RT/E_N < 0.1$. These criteria correspond to activation energies higher than about 83 kJ/mol with a typical temperature of 1000 K.

The effect of the heating rate is suitable to evaluate the Avrami exponent n[8,10]. This method is based on results attained on reaching a given upper temperature T_u, for several experiments performed at different heating rates. In this case Eq. (4) reduces to

$$\ln [-\ln (1-\alpha)] = B(T_u) - n \ln (\beta) \quad (9)$$

where $B(T_u) = \ln (K_v T_u^{2n}) - E/(RT_u)$ is a function of the upper temperature. The slope of plots $\ln [-\ln (1-\alpha)]$ versus $\ln (\beta)$ reduces to $-n$, thus giving the Avrami exponent. The limiting upper temperature should be identical for every heating rate, which is sufficient to maintain the same value of $B(T_u)$ for simultaneous nucleation and growth (case B). Otherwise, one must avoid changing the heat treatment for temperatures lower than the onset of crystallization when nucleation precedes growth. For example, the isothermal nucleation time (in case A1) must remain the same for every experiment to avoid changing the number of nuclei, thus ensuring that $B(T_u)$ is identical for every experiment.

Equation (9) fails to describe the effects of heating rate during a previous nucleation stage performed with variable temperature, rather than in isothermal conditions. On selecting different heating rates for nucleation and growth Eq. (5) yields[3]

$$\ln [-\ln (1-\alpha)] = B'(T_u) - \ln(\beta_N) - n \ln(\beta_g) \quad (10)$$

This equation is equivalent to Eq. (9) for experiments performed with different heating rates for growth β_g (at temperatures higher than the onset of crystallization), but identical heating rate β_N during the nucleation stage. When the rates of change in temperature are identical for both stages ($\beta = \beta_N = \beta_g$) Eq. (10) becomes

$$\ln [-\ln (1-\alpha)] = B'(T_u) - (n+1) \ln (\beta) \qquad (11)$$

In this case, the slope obtained on plotting ln [-ln (1-α)] versus ln (β) is -(n + 1) rather than -n. One should thus be cautious about selecting suitable experimental conditions to obtain the so-called Avrami exponent n, which is required to obtain the relation between the activation energy of crystallization and the activation energy of growth (Table I).

The interpretation of experimental data may proceed on using plots of ln [-ln (1-α)/T^{2n}] versus T^{-1} to obtain the activation energy. However, it is advantageous to combine different sets of data for several heating rates on plotting ln [-ln (1-α)/T^{2n}] + n ln (β) versus T^{-1}; this is straightforward at least for simultaneous nucleation and growth (case B), or without changing the nucleation stage (case A1). Such plots should yield better estimates of the activation energy and preexponential factor by increasing the amount of experimental data in a single line, and spreading the experimental data over wider scales.

Significant differences between the nucleation and growth peaks appears to be suitable for obtaining materials with differences in fraction crystallized and/or microstructures as discussed above. Suitable experiments should thus be performed to assess whether this is the case. For example, one may select an initial experiment with identical heating rates for the nucleation and growth stages ($\beta_N = \beta_g$), to evaluate the temperature required for the onset of crystallization T_{oc}, and then perform additional experiments with different values of β_N (for $T < T_{oc}$), without changing the heating rate for growth (β_g), at temperatures $T > T_{oc}$. The results obtained must be nearly independent of β_N for materials with simultaneous nucleation and growth. On the contrary, the crystallization peak is expected to vary with β_N when nucleation precedes growth. Similarly, one might conclude that nucleation precedes growth when an isothermal nucleation stage yields results which are significantly different from those obtained on heating at constant rate.

In addition to designing the heat treatment one can resort to microstructural image analysis to investigate the particle size distribution. Note that broad size distributions

suggest simultaneous nucleation and growth, as discussed above, and narrow distribution suggests that nucleation precedes growth.

The effects of heating rates on the maximum temperature of the relevant exothermic peak T_p have also been used to extract the relevant kinetic parameters. The original method was proposed by Kissinger[14] to interpret the kinetics of decomposition of solids (solid A $\rightarrow$ solid B + gas), and reduces to

$$\ln (\beta/T_p^2) = \text{constant} - E_a/(RT_p) \tag{12}$$

where E_a is the relevant activation energy.

The applicability of the Kissinger equation to crystallization was revised by Matusita at al.[9] who proposed the following extended solution for cases when the dimensionality is higher than 1

$$\ln [\beta^n/T_p^2) = \text{constant} - E/(RT_p) \tag{13}$$

where E is the same as in Eq. (4). Nevertheless, most authors still resort to the original Kissinger equation to interpret experimental results, even for dimensionalities higher than 1[13,15,16] and Frade[3] has demonstrated the following solution for the generic case.

$$\ln (\beta/T_p^2) = n^{-1} \ln (K_v) - (E/n)/(RT_p) \tag{14}$$

where K_v and E are still given by Eq. (4); this can be used for simultaneous nucleation and growth (case B), and also for conditions when the samples are heated at constant rate β after previous nucleation (case A1). Otherwise, one must take into account the effects of heating rates β_N during the nucleation, even for cases when nucleation precedes growth (case A2). The value of K_v increases with the number of nuclei, and thus varies as $1/\beta_N$. Therefore, Eq. (14) must be replaced by the following alternative solution for a correct interpretation of the effects of heating rates

$$\ln (\beta_g/T_p^2) + n^{-1} \ln (\beta_N) = n^{-1} \ln (K_v) - (E/n)/(RT_p) \tag{15}$$

This is suitable for being able to interpret experiments performed with different rates of change in temperature for the stages of nucleation and growth, and the solution for experiments performed with identical rates ($\beta_g = \beta_N = \beta$) becomes

$$\ln [\beta/T_p^{2n/(n+1)}] = (n+1)^{-1} \ln (K_v) - [E/(n+1)]/(RT_p) \quad (16)$$

Note that $E = nE_g$ is still valid in this case A2, and Eq. (16) thus shows that the slope of a Kissinger plot is not necessarily identical to $-E_g/R$, even for cases when the nucleation rates peaks before the onset of growth.

3. Experimental Procedure

A glass of nominal composition $30SiO_2$-$24.14P_2O_5$-28.61CaO-17.25MgO (wt%) was prepared from reagent grade $Ca(H_2PO_4)_2$, $CaCO_3$, SiO_2, and MgO. These powders were thoroughly mixed with ethanol for 45 min, and dried; 80 g batches were melted in an electric furnace at 1525 °C, for 2 hours and in a platinum crucible. The melt was poured into water, ground and screened to sizes smaller than 250 μm. A small platinum crucible was then used to remelt 0.5 g batches, at 1525 °C and for 30 min. These melts were quenched to room temperature by introducing the crucible in water. The resulting glass sample was easily detached from the platinum crucible, crushed in an agata mortar and screened to particle sizes in the range 180 to 250 μm. These powders were stored at 120 °C to prevent moisture attack until used for DTA analysis. The particle size range was selected as a criterion for low surface area to prevent significant contributions of surface nucleation, and thus ensure that bulk nucleation prevails[17].

Remelted samples were also polished, etched with HNO_3 (1 M) for about 10 s, and observed by scanning electron microscopy (SEM). These SEM micrographs reveled that phase separation takes place on cooling, yielding spheres with typical diameter of about 0.3 μm after quenching from melting temperatures, or larger sizes for slower cooling. These spheres were amorphous, and SiO_2-rich as found by EDS. Details were given elsewhere[18].

Samples of glass powder (300 mg) were used for DTA measurements, in a Linseis type L81/077 equipment, in alumina crucibles in air, and with α-Al_2O_3 as the reference material. Some samples were heated at 50 K/min from room temperature up to 730 °C, held at this temperature for 2 hours for nucleation, and then immediately heated up to 1000 °C at different heating rates (5, 10, 15 and 20 K/min). These samples will be called "nucleated samples". The nucleation peak was previously found[18]. Other samples were heated from room temperature at 5, 10, 15 and 20 K/min, without the isothermal nucleation stage. These samples will be called "as prepared samples".

The DTA analyses revealed an exothermic peak for temperatures in the range 800 to 850 °C, and a second exothermic peak at temperatures higher than about 900 °C. The first peak could be ascribed to the crystallization of whitlockite (as detected by X-Ray diffraction), was printed on paper, and area fractions were used to evaluate the fractions crystallized as a function of temperature and heating rate. These printouts were also used to evaluate the relation between peak temperatures and heating rates.

A three point beam bending method was used to evaluate the viscosity of 5 cm long glass bars, with a square cross section of about 25 mm^2, which were cut from glass blocks. The measurements were performed in a Bahr Thermoanalyse equipment (type 401) on heating from room temperature at 10, 20 and 40 K/min, and loading the samples with 40 or 80 g.

4. Results and Discussion

The DTA results shown in Fig. 2 for "nucleated" and "as prepared" samples demonstrate that previous isothermal nucleation (at 730 °C) shifts the first exothermic peak to lower temperatures. In addition, the XRD of a sample which had been heat-treated at 730 °C/min for 2 hours and then cooled to room temperature was typical of a fully amorphous material, suggesting that crystal growth remains negligible during this nucleation stage at 730 °C. The onset of crystallization occurs for temperatures higher than 800 °C both for nucleated and as prepared samples, and the first exothermic peak (for temperatures in the range 800-850 °C) could be ascribed to the crystalization of Mg-substituted β-tricalcium phosphate (whitlockite), $3(Ca,Mg)O\text{-}P_2O_5$.

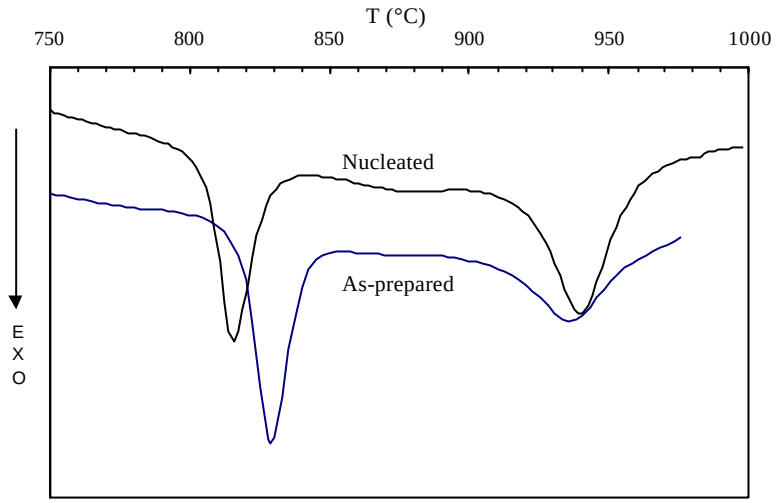

Fig. 2. DTA analysis of "as-prepared" and previously nucleated (at 730 °C) glass samples.

The differences between the results obtained for nucleated and as prepared samples also suggest than nucleation precedes growth, and the models proposed for case A1 should thus be used to fit the experimental results for the so-called nucleated samples, and models for case A2 should apply for "as prepared" samples. For example, this may be investigated by analysing the effects of the heating rate on the fraction crystallized (Figs. 3 and 4).

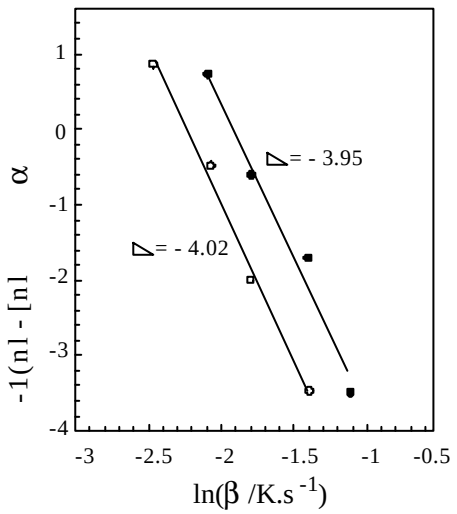

Fig. 3. Effects of heating rate on the fraction crystallized reached at 822 °C (O), and 828 °C (•), for "as-prepared" samples.

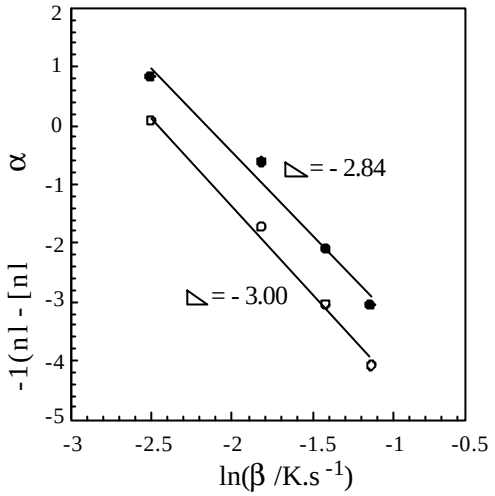

Fig. 4. Effects of heating rate on the fraction crystallized reached at 810 °C (O), and 815 °C (•), for "previously nucleated" samples.

The difference in slopes (≈3 for nucleated samples and ≈4 for "as prepared" samples) suggest that nucleation precedes growth as predicted by Eqs. (9) and (11). Note that the results expected for materials with simultaneous nucleation and growth should be nearly independent of changes for temperatures lower than the onset of crystallization. The value of the Avrami exponent obtained for previously "nucleated" samples ($n \approx 3$) suggests that growth is phase boundary controlled with dimensionality 3 (see Table I).

The value of n is also required to be able to use the improved Eqs. (4) to (6) instead of Eq. (3), and typical plots of ln [-ln (1-α)/T^{2n}] versus T^{-1} are shown in Fig. 5 for "as prepared" samples, crystallized at different heating rates. These results confirm the expected temperature dependence for low to moderate values of the fraction crystallized but deviate from Eq. (6) for relatively high values of α. Note also that the onset of these deviations is shifted to higher temperatures on increasing the heating rate. Possible reasons for the deviations from Avrami-Nakamura models are discussed in Section V, and the data for high values of fractions crystallized were excluded to be able to evaluate the activation energy of the crystallization process. The values of activation energy E obtained in this way are very high, and the average value is about 2722 kJ/mol, which suggests that growth might be controlled by viscous relaxation. The relative differences between the values of E obtained for different heating rates are within about 10%, which might be attributed to data scattering (especially for low values of α), and/or the onset of deviations from Eq. (6) (for

high or moderate values of the fraction crystallized). Note that several experiments performed with different heating rates should yield identical values of activation energy if nucleation precedes growth (Eq. (6) and (7)).

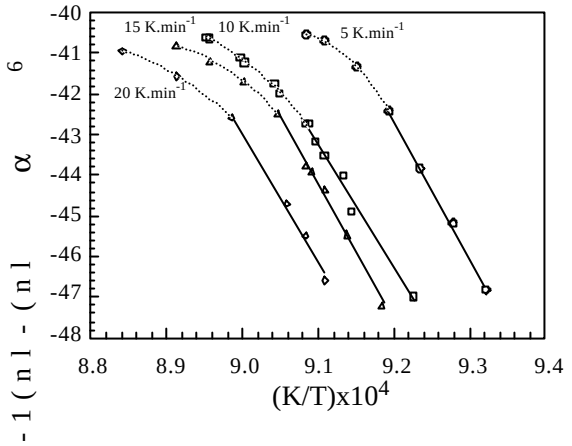

Fig. 5. Temperature dependence of the fraction crystallized for "as-prepared" samples, with different heating rates.

The results obtained for previously nucleated samples (Fig. 6) confirm the trends observed for "as prepared" samples, including the deviations observed for high values of the fraction crystallized. The relative differences between the values of activation energy obtained for different heating rates are within about 15%, and the average value is 2167 kJ/mol.

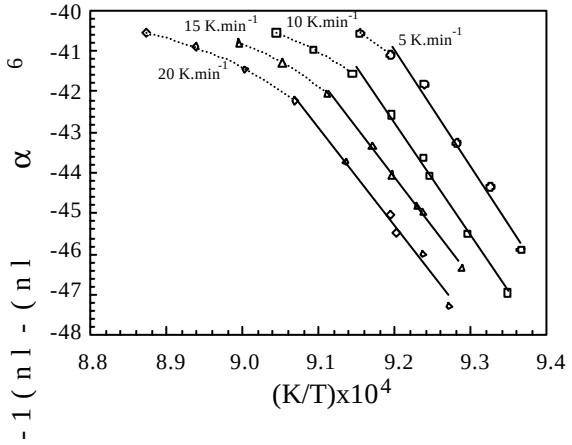

Fig. 6. Temperature dependence of the fraction crystallized for "previously nucleated " samples, with different heating rates.

The difference between this average value and the average activation energy obtained for "as prepared" samples might raise some doubts about our conclusion that nucleation precedes growth in both cases. Note that the values of activation energies should be nearly identical for "as prepared" and previously nucleated samples when the nucleation rate peaks before the onset of growth. One should thus obtain improved evaluation of the activation energies before attempting to find an explanation for this. For example, plots of $\ln [-\ln (1-\alpha)/T^{2n}] + n \ln(\beta)$ versus T^{-1}, for previously "nucleated" samples, or $\ln [-\ln (1-\alpha)/T^{2n}] + (n+1) \ln (\beta)$ versus T^{-1}, for "as prepared" samples (Eq. (6)), are expected to yield improved evaluation of the activation energies. These alternative representations are shown in Figs. 7 and 8, and the slopes were used to evaluate the activation energies obtained in this way (2428 kJ/mol for "as prepared" samples, and 2290 kJ/mol after previous nucleation); this confirms that the activation energy is higher for "as-prepared" than for previously nucleated samples but differences between those cases are much smaller than from Figs. 5 and 6.

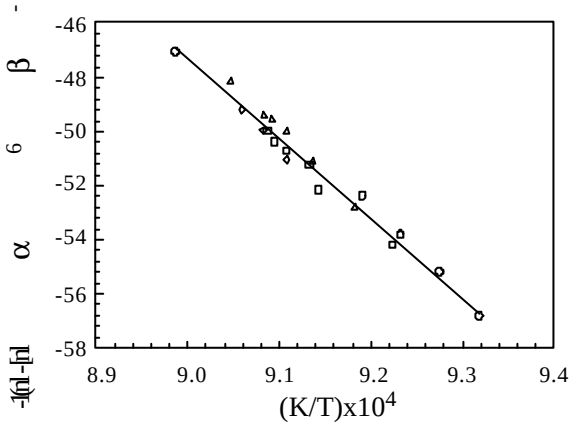

Fig. 7. Alternative plots for describing the temperature dependence of the fraction crystallized in "as-prepared" samples. Different symbols were used for the following heating rates (°C/min): 20 (◊), 15 (Δ), 10 (□), and 5 (O).

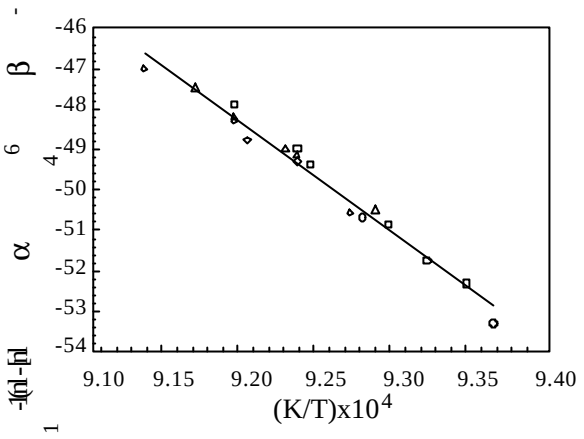

Fig. 8. Alternative plots for describing the temperature dependence of the fraction crystallized in "previously nucleated" samples. Different symbols were used for the following heating rates (°C/min): 20 (◊), 15 (Δ), 10 (□), and 5 (O).

Modified Kissinger plots also provide a second alternative for evaluating the activation energies for "as prepared" samples (Eq. (16)) or previously nucleated samples (Eq. (14)), as shown in Figs. 9 and 10.

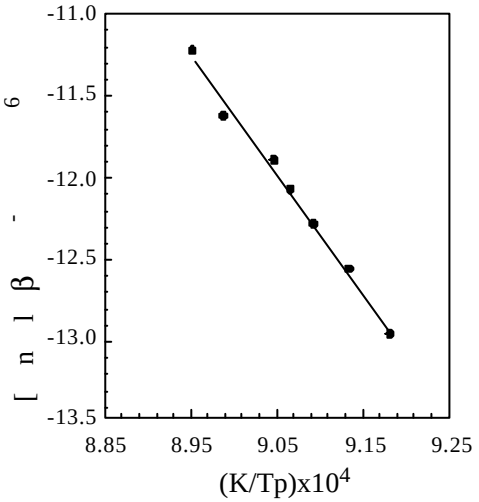

Fig. 9. Dependence on peak temperature on the heating rate for "as-prepared" samples.

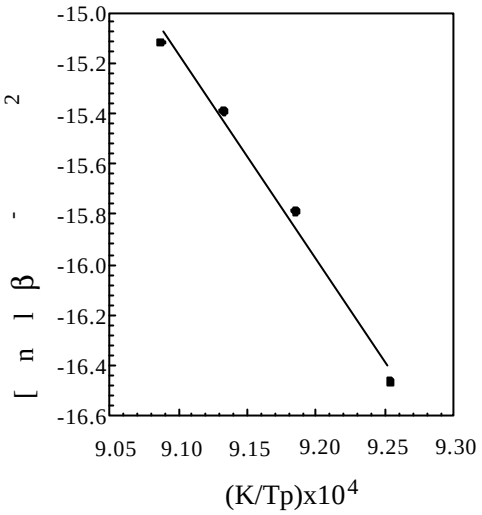

Fig. 10. Dependence on peak temperature on the heating rate for "previously nucleated" samples.

The slopes are $-[E/(1 + n)]/R = 74.0 \times 10^3$ K in Fig. 9, and $-E/(nR) = -80.90 \times 10^3$ K in Fig. 10, yielding the corresponding values of activation energy E = 2461 kJ/mol for "as-prepared" samples, and E = 2018 kJ/mol for previously nucleated samples. The value obtained for "as prepared" samples is very close to the estimate obtained from Fig. 7, and the differences between the values obtained from Fig. 8 and 10 (for previously nucleated samples) might be due to insufficiency of data in Fig. 10.

Overlapping of the nucleation peak with growth corresponds to a transition from case A (when nucleation precedes growth) to case B (simultaneous nucleation and growth). In this case the activation energy of the overall crystallization process obtained for the "as prepared" samples should be higher than nE_g and lower $nE_{gv} + E_N$; this might provide an explanation for the differences in activation energy between "as prepared" and previously nucleated samples. Nevertheless, is seems that an isothermal nucleation stage (2 h at 730 °C) excludes any significant contribution of overlapping to nucleation (on heating previously nucleated samples to higher temperatures). Otherwise, the effects of heating rate on the so-called "nucleated" samples should be nearly identical to those observed for "as prepared samples". The activation energy was thus evaluated from the slope of Fig. 8 ($E_g = E/3$ = 763 kJ/mol), and one can also evaluate a typical value of the dimensionless temperature ($RT_{av}/E_g \approx 8.314 \times 1083/763 \times 10^3$) = 0.0119, at about 815 °C. Under these conditions, one can neglect the correcting factor in Eq. (7), as discussed above.

The high value of activation energy for growth suggests that viscous relaxation might control the kinetics of crystallization. Note that several authors have suggested a relation between the growth rate and viscosity[19-21] on assuming that the activation energy for growth (E_g) is in fact an activation energy for diffusion across the crystal/glass interface, and on combining with the Stokes-Einstein equation. The validity of this assumption is still debatable but the results obtained for different systems suggest that the activation energy for viscous flow is usually an upper limit for the activation energy of crystal growth[21], and our results are consistent with this finding. The temperature dependence of viscosity is nearly described in the Arrhenian dependence $\eta = \eta_o \exp[-E_\eta/(RT)]$, with activation energy E_η of about 1000 kJ/mol. However, these results also depend on the experimental conditions of load and/or heating rate (Fig. 11).

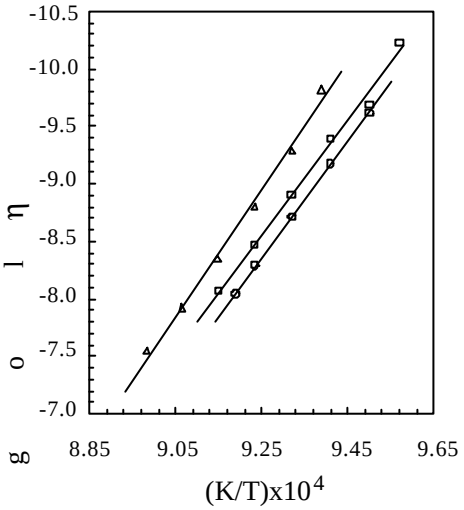

Fig. 11. Temperature dependence of viscosity measured under the following conditions: (Δ) heating rate = 40 °C/min, load = 40 g; (□) heating rate = 20 °C/min, load = 80 g; (O) heating rate = 10 °C/min, load = 40 g.

The effects of heating rate and/or load on viscosity measurements suggest that the dynamic of viscous relaxation might thus be affected after a previous isothermal nucleation stage; this raises an additional hypothesis for explaining the differences in activation energy of previously nucleated and "as prepared" samples, on assuming that viscous relaxation plays some effect on the kinetics of crystallization. However, viscosity measurements obtained with the beam bending method may be affected by differences

between the true sample temperature and the sensor reading. Increasing heating rates may thus give slightly values of viscosity for identical sensor readings, as observed in Fig. 11. In addition, these viscosity measurements were performed in the temperature range of crystallization, implying that the residual glass composition is changing; this raises some uncertainty about the true values of viscosity, and activation energy E_η.

5. Deviations from the Avrami-Nakamura type of models

Figures 5 and 6 show clear deviations from the expected trend, and one can propose some explanations for these deviations, including crystallization for temperatures which exceed the growth rate peak (Fig. 1), or exhaustion of some components in the residual glass matrix. The first hypothesis is likely to affect the results obtained for low heating rates, because high temperatures might be needed to attain relatively small values of the fraction crystallized. An inspection of the results shown in Figs. 5 and 6 shows that the relevant temperature ranges are very narrow, raising doubts about this argument.

The second hypothesis should also be considered because the composition of the crystalline phase, $3(Ca,Mg)O.P_2O_5$, is markedly different from the original glass composition. The growth rate is thus expected to be halted when the content of a controlling species drops to a given minimum in the residual glass phase; this corresponds to an equilibrium condition. Actually, the driving force for crystal growth might drop gradually as the relevant chemical potential difference decreases. The deviations from the Avrami-Nakamura models should become effective on approaching a critical fraction crystallized which is independent of the heating rate. In this case, DTA results might be misinterpreted because the base line is recovered on reaching a limiting volume fraction crystallized (α_{max}), rather then a fully crystalline material. The area fraction obtained in this away thus represents a ratio α/α_{max} rather than the true volume fraction, and neglecting this difference corresponds to overestimating the preexponential factor in Eqs. (4) to (6).

Finally, Tobin[22,23] suggested that the original JMA equation and the corresponding solutions for variable temperature might be poor descriptions of the interactions between growing particles. Nevertheless, the Avrami-Nakamura solutions are usually simpler and have provided efficient fitting for the kinetics of crystallization of many inorganic glasses.

6. Conclusions

The crystallization of glass in the system SiO_2-P_2O_5-CaO-MgO was used to demonstrate that proper theoretical models should take into account the experimental conditions. Several alternative equations were used to verify the consistency of fitting parameters, including a method which combines experimental data obtained for different heating rates. This method is suitable to minimize the experimental errors for very low or high values of the fraction crystallized. Revised models were also used to reexamine the effects of the rate of change in temperature on the fraction crystallized, and on the crystallization peak. The value of activation energy evaluated from crystal growth is very high (≈763 kJ/mol) but still lower than the activation energy of viscous relaxation (about 1000 kJ/mol).

Acknowledgments

This work was supported by Junta Nacional de Investigação Científica e Tecnológica, Portugal, under Contract No. PBIC/C/CTM/1425/92, and in the form of a Ph.D. Grant (BD/2762/93). Additional funding was provided by the Programme PRAXIS XXI, and by Portuguese-German Integrated Action (A-32/94). Viscosity measurements were performed in the Otto-Schott Institute of the University of Jena, Germany.

References

[1] Rawson, H. – *Inorganic Glass-Forming Systems*, London, Academic Press, 1967.

[2] Rowlands, E. G.; James, P. F. – "Analysis of Steady State Crystal Nucleation Rates in Glasses", *Physics and Chemistry of Glasses*, 20, 1979, 1-14.

[3] Frade, J. R. – "Crystallization with Variable Temperature: Corrections for the Activation Energy", *Journal of the American Ceramic Society*, 81, 1998, 2654-2660.

[4] Nakamura, K.; Watanabe, T.; Katayama, K.; Amano, T. – "Some Aspects of Nonisothermal Crystallization of Polymers. I – Relationship Between Crystallization Temperature, Crystallinity, and Cooling Conditions", *Journal of Applied Polymer Science*, 16, 1972, 1077-1091.

[5] Nakamura, K.; Watanabe, T.; Katayama, K.; Amano, T. – "Some Aspects of Nonisothermal Crystallization of Polymers. II – Consideration of the Isokinetic Condition", *Journal of Applied Polymer Science*, 17, 1973, 1031-1044.

[6] Nakamura, K.; Watanabe, T.; Amano, T.; Katayama, K. – "Some Aspects of Nonisothermal Crystallization of Polymers. III – Crystallization During Melt Spinning", *Journal of Applied Polymer Science*, 18, 1974, 615-623.

[7] Matusita, K.; Sakka, S.; Matsui, Y. – "Determination of the Activation Energy for Crystal Growth by Differential Thermal Analysis", *Journal of Materials Science*, 10, 1975, 961-966.

[8] Matusita, K.; Sakka, S. – "Kinetic Study of the Crystallization of Glass by Differential Scanning Calorimetry", *Physics and Chemistry of Glasses*, 20, 1979, 81-84.

[9] Matusita, K.; Sakka, S. – "Kinetic Study on Crystallization of Glass by Differential Thermal Analysis - Criterion on Application of Kissinger Plot", *Journal of Non-Crystalline Solids*, 38-39, 1980, 741-746.

[10] Matusita, K.; Komatsu, T.; Yokota, R. – "Kinetic of Non-Isothermal Crystallization Process and Activation Energy for Crystal Growth in Amorphous Materials", *Journal of Materials Science*, 19, 1984, 291-296.

[11] Kemeny, T.; Šesták, J. – "Comparison of Crystallization Kinetics Determined by Isothermal and Nonisothermal Methods", *Thermochimical Acta*, 110, 1987, 113-129.

[12] Yinnon H.; Uhlmann, D. R. – "Applications of Thermoanalytical Techniques to the Study of Crystallization Kinetics in Glass-forming Liquids, Part I: Theory", *Journal of Non-Crystalline Solids*, 54, 1983, 253-275.

[13] Koga, N.; Šesták, J.; Strnad, Z. – "Kinetics of Crystallization in the Soda-Lime-Silica System. Part I: Na_2O-CaO-$2SiO_2$ and Na_2O-CaO-$3SiO_2$ Glasses by DTA", *Thermochimical Acta*, 203, 1992, 361-372.

[14] Kissinger, H. E. – "Reactive Kinetics in Differential Thermal Analysis", *Analytical Chemistry*, 29, 1957, 1702-1706.

[15] Hayward, P. J.; Vance, E. R.; Doern, D. C. – "DTA/SEM Study of Crystallization in Sphene Glass-ceramics", *American Ceramic Society Bulletin*, 66, 1987, 1620-1626.

[16] Xu, X. J.; Ray, C. S.; Day, D. E. – "Nucleation and Crystallization of Na_2O-2CaO-3SiO_2 Glass by Differential Thermal Analysis", *Journal of the American Ceramic Society*, 74, 1991, 909-914.

[17] Xiaojie, J. X.; Ray, C. S.; Day, D. E. – "Nucleation and Crystallization of Na_2O-2CaO-3SiO_2 Glass by Differential Thermal Analysis", *Journal of the American Ceramic Society*, 74, 1991, 909-914.

[18] Oliveira, J. M.; Oliveira, A. L.; Correia, R. N.; Fernandes, M. H. – "Phase Separation and Crystallization in 3CaO.P_2O_5-SiO_2-MgO Glasses", *Glastechnishe Berichte Glass Science and Technology*, 67C, 1994, 367-70.

[19] Avramov, I.; Gutzow, I.; Grantscharova, E. – "Crystallization Kinetics and Rheology of Undercooled Melts", *Journal of Crystal Growth*, 87, 1988, 305.

[20] Henderson, D. W.; Ast, D. G. – "Viscosity and Crystallization Kinetics of As_2Se_3", *Journal of Non-Crystalline Solids*, 64, 1984, 43-70.

[21] Mora, N. D.; Ziemath, E. C.; Zanotto, E. D. – "Viscous Flow and Crystal Growth in Glasses", *Cerâmica*, 39, 1993, 7-10. *(in Portuguese)*

[22] Tobin, M. C. – "Theory of Phase Transition Kinetics with Growth Site Impingement. I. Homogeneous Nucleation", *Journal of Polymer Science*, 12, 1974, 399-406.

[23] Tobin, M. C. – "Theory of Phase Transition Kinetics with Growth Site Impingement. II. Heterogeneous Nucleation", *Journal of Polymer Science*, 14, 1974, 2253-2257.

3 - ESTRUTURA VÍTREA

3.1 - Introdução

Neste capítulo são apresentados dois trabalhos realizados com objectivos diferentes. O primeiro (secção 3.2) foi efectuado com o objectivo de se desenvolver um vidro com a composição e estrutura da matriz do vidro V4. Este vidro, monofásico, possibilitará a determinação experimental da viscosidade (importante no processo de formação das mórulas) e será útil para futuros estudos de cristalização. O segundo trabalho foi realizado com o objectivo de relacionar o comportamento *in vitro* com a estrutura de vidros sílico-fosfatados com elevado teor de elementos alcalino-terrosos, nomeadamente MgO.

A estrutura de um vidro tem sido alvo de diferentes interpretações. De entre os vários modelos estruturais propostos[1,2,3], a aproximação polimérica efectuada por Stevels[2,3] revela-se particularmente útil na análise estrutural do fenómeno da bioactividade.

Um modelo universal deve considerar o comportamento dos diferentes elementos que constituem um vidro: formadores, modificadores ou intermediários[1]. Um formador tem um número de coordenação, *NC*, de 3 ou 4 e uma força de campo, $Z/a^2 > 1,5$ (Z – valência; a – distância inter-iónica); num modificador $NC = 6$ ou 8 e $Z/a^2 < 0,4$; num intermediário $NC = 4$, 6 ou 8 e Z/a^2 situa-se entre os dois valores anteriores.[2,3,4]

Estruturalmente, um vidro não exibe ordem a longa distância, mas a curta distância a ordem é já considerável. Esta é conferida pela presença de poliedros de coordenação, que no caso de vidros de sílica são tetraedros SiO_4^{4-}, em que Si^{4+} ocupa a posição central e os oxigénios os vértices, e cuja regularidade de frequência determina o grau de ordem a média distância. Quando um oxigénio está ligado a dois silícios é designado por *ligante*; caso contrário é classificado como *não ligante.*

Segundo Stevels, um vidro pode ser visto como um polímero inorgânico em que os formadores são os responsáveis pela polimerização da rede e os modificadores pela sua despolimerização; os intermediários podem comportar-se como formadores ou como modificadores.

Em vidros bioactivos contendo silício e fósforo, o silício funciona como formador. O fósforo, muito embora origine estruturas do tipo PO_2 e seja considerado um formador, na realidade tende a formar agregados isolados do tipo orto-fosfato. O boro

funciona como formador em unidades do tipo BO_3^{3-} ou BO_4^{5-}, requerendo neste último caso a presença de um catião monovalente para compensar a carga. O Al^{3+} funciona quase sempre como intermediário mas introduz deficiência de carga em redes SiO_4, pelo que requer a presença de outros catiões na sua vizinhança os quais, nestas circunstâncias, não devem ser considerados modificadores. Os catiões alcalinos e alcalino-terrosos funcionam praticamente sempre como modificadores de rede (ver Fig. 3.1).

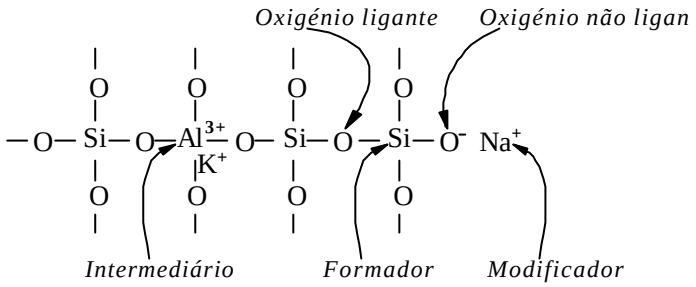

Fig. 3.1. Representação planar da estrutura de uma rede vítrea.

A conectividade da rede (grau de polimerização) pode ser definida como o número de oxigénios ligantes, *BO* ("Bridging Oxygens"), por catião formador, *T*. A razão *BO/T* numa estrutura tridimensional completamente polimerizada, como a da sílica, é 4 e numa estrutura totalmente despolimerizada, caso dos orto-silicatos (SiO_4^{4-}), é 0.

Os parâmetros de Stevels *Y* e *X* permitem determinar o número médio de oxigénios ligantes por tetraedro e o número médio de oxigénios não ligantes por tetraedro, respectivamente. Estes parâmetros são calculados a partir da composição vítrea molar, segundo:

$$Y = 8 - 2R \tag{3.1}$$

$$X = 2R - 4 \tag{3.2}$$

sendo *R* a razão entre o número total de moles de oxigénios e o número total de moles de catiões formadores. O parâmetro *Y* traduz a conectividade de rede de um vidro. Por

exemplo, os vidros de composição $CaO.SiO_2$ e $Na_2O.SiO_2$ apresentam $Y = 2$ pelo que são estruturalmente análogos.

Em silicatos as unidades estruturais são frequentemente designadas por Q^n, onde Q representa o silício e n o número de oxigénios ligantes. Assim, as espécies Q^0 representam um tetraedro isolado, cuja unidade estrutural é $\left[SiO_4\right]^{4-}$, as espécies Q^1 dímeros, cuja unidade estrutural é $\left[Si_2O_7\right]^{6-}$, as espécies Q^2 estruturas lineares, por exemplo[ii] $\left[SiO_3\right]_x^{2-}$ ou $\left[Si_3O_9\right]^{6-}$ (anelar), as espécies Q^3 estruturas bidimensionais, por exemplo $\left[Si_2O_5\right]_x^{2-}$, $\left[Si_2O_5\right]_{xx}^{2-}$ e as espécies Q^4 estruturas tridimensionais, como é o caso das unidades $\left[SiO_2\right]_{xxx}$.

Como se verifica na literatura, o tipo de notação empregue para descrever as entidades estruturais está associado à técnica experimental utilizada. Assim, a notação Q^n é mais usada em ressonância magnética nuclear e as expressões estequiométricas são mais utilizadas em espectroscopias vibracionais, nomeadamente espectroscopia de Raman.

[ii] x – em cadeia (“chain silicates”); xx – em camada (“layer silicates”); xxx – rede “network silicates”

Referências Bibliográficas

[1] Zarzycki, J. – *Glasses and the Vitreous State*, Cambridge University Press, Cambridge, 1991.

[2] Navarro, J. M.F. – *El Vidrio*, Madrid, C.S.I.C., 1991.

[3] Vogel, W. – *Glass Chemistry*, Springer-Verlag, Berlin, 1994.

[4] Rawlings, R.D. – "Composition Dependence of the Bioactivity of Glasses", *Journal of Materials Science Letters*, 11, 1992, 1340-1343.

3.2 - Effect of SiO_2 on Amorphous Phase Separation of $CaO-P_2O_5-SiO_2-MgO$ Glasses

J. M. Oliveira, R. N. Correia, M. H. Fernandes

UIMC, Department of Ceramics and Glass Engineering, University of Aveiro, 3810-193 Aveiro, PORTUGAL

(Journal of Non-Crystalline Solids, in press)

Abstract

Scanning and transmission electron microscopy, differential thermal analysis and Raman spectroscopy were used to investigate glasses of the $52,75(1+x/70)3CaO.P_2O_5$-$17,25(1+x/70)MgO$- $(30-x)SiO_2$ (wt%) series (with x=0 to 10). In glasses for which the silica content is 24 wt% or larger a dispersed amorphous silica phase was present. Differential thermal analysis showed that the transition temperature and the second exothermic peak temperature are independent of silica content between 30 and 23 wt%. The first crystallization peak is independent of silica content in all the range investigated. Raman spectroscopy showed that the structure of the 20 wt% SiO_2 glass differs from the others. We conclude that for a silica content <23 wt% the single-phase glass becomes more de-polymerised as the silica content decreases and for a silica content >23 wt% the glasses are phase separated and the degree of polymerisation of the matrix is constant; the monophasic glass with 23 wt% SiO_2 has the same composition and structure as the matrices of all other phase-separated glasses.

***PACS**: 81.70.Pg, 64.75.+g, 61.43.Fs, 64.70.Pf, 82.80.Ch.*

1. Introduction

Development of glasses from the CaO-P_2O_5-MgO-SiO_2 system has received increased attention, specially during the past two decades, because they are suitable for biomedical applications[1-3]. One of the major factors that determines the bioactive properties of glasses is the silica content[1]. Several compositions have been developed with the aim of improving bioactivity and mechanical properties[4-6].

Phase separation and crystalization of a two-phase bioactive glass, S30, from the $3CaO.P_2O_5$-MgO-SiO_2 system were investigated in a previous work[7,8] and one of the conclusions was that the matrix phase plays an important role in the crystallization process. Isolation of matrix composition is relevant to understand the crystallization process and assess the effect of matrix viscosity in the formation of the dispersed phase[9].

In the present work a glass series containing the S30 composition was studied. In this series the silica content decreased from 30 to 20 wt%, with the (Ca+Mg)/P ratio constant. The effect of silica is analysed with respect to amorphous phase separation, transition temperature (Tg), crystallization temperatures, and structure, by using electron microscopy, differential thermal analysis (DTA) and Raman spectroscopy.

2. Experimental Procedure

Glasses from the $52.75(1+x/70)3CaO.P_2O_5$-$17.25(1+x/70)MgO$-$(30-x)SiO_2$ (wt%) series (with x=0 to 10) were prepared from reagent-grade $Ca(H_2PO_4)_2$, $CaCO_3$, SiO_2 and MgO. The raw materials were mixed in ethanol for 30 minutes and dried at 60 °C. Batches of 40 g were melted in a platinum crucible at temperatures in the range 1500-1550 °C for 1 hour, a schedule which was adequate to ensure good homogeneity and fining. The glass compositions investigated are listed in Table I.

Table I. Nominal glass compositions.

		Composition (wt%)			
Sample	*x*	SiO_2	CaO	P_2O_5	MgO
S30	0	30.0	28.6	24.1	17.3
S29	1	29.0	29.0	24.5	17.5
S28	2	28.0	29.4	24.8	17.8
S27	3	27.0	29.8	25.2	18.0
S26	4	26.0	30.3	25.5	18.2
S25	5	25.0	30.6	25.9	18.5
S24	6	24.0	31.1	26.2	18.7
S23	7	23.0	31.5	26.5	19.0
S22	8	22.0	31.9	26.9	19.2
S21	9	21.0	32.3	27.2	19.5
S20	10	20.0	32.7	27.6	19.7

All glasses were cast to blocks in heated metal molds and annealed for 30 minutes at the transition temperature, previously determined by DTA, and cooled to room temperature.

Powders for DTA experiments were prepared by crushing cast glass in an agate mortar, sieving and collecting the fraction of particles <38 μm. The runs (3 per composition) were performed by heating these powders in alumina crucibles at a rate of 10 K min^{-1} from room temperature to 1200 °C in air, using calcined α-alumina powders as reference materials. X-Ray Diffraction (XRD) was used to identify crystalline phases forming during DTA runs, by using a Rigaku PMG-VH diffractometer with Cu K_α radiation.

For scanning electron microscopy (SEM) observation (Hitachi S-4100) fresh etched fractures of glass were prepared by etching them in HNO_3 1M for 10 s. Replica of fracture surfaces of glass samples S23 to S20 were prepared for transmission electron microscopy (TEM) observation (Hitachi H9000-NA).

Raman spectral measurements (3 per composition) were performed on polished samples (α-alumina, 0.25μm) using a micro-Raman spectrometer (Renishaw 2000) equipped with a microscope (in phase separated glasses the matrix phase was selected). A HeNe laser source with the power ~25 mW was used (wavelength 632 nm). The spectra were collected in the frequency region between 300 and 1500 cm^{-1} with a resolution of 1 cm^{-1}.

3. Results

Along this series the cast glasses change from opaque white (x=0) to transparent ($x \geq 6$). A sample of S25 has a slightly white cloudy color. Samples S25 to S20 had some tendency to surface devitrification.

Figure 1 shows SEM micrographs of the sample of S30, S28, S26 and S25. In these samples a dispersed phase is present with average diameter decreasing from 2.5 μm to 20 nm as x increases from 0 to 6.

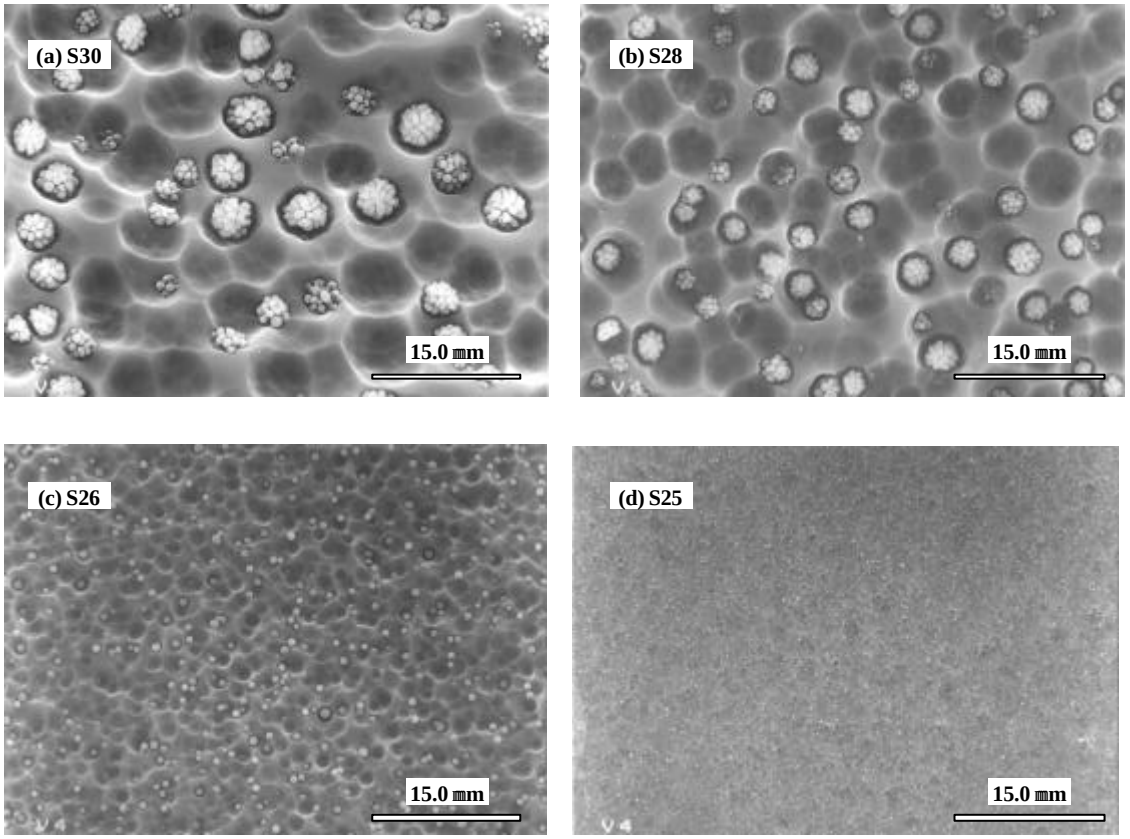

Fig. 1 - SEM micrographs of (a) S30, (b) S28, (c) S26 and (d) S25 glasses. The decrease of the SiO_2 content in the glass produces a significant increase in the number of aggregates (dispersed phase) per unit volume and the reduction of their average size. The morphology of the aggregates is kept along the glass series.

Oliveira *et al.*[10] working with extraction replicas of non-etched fracture surfaces of a sample of S30, examined by TEM/EDS (energy dispersive spectroscopy), found that the precipitates are amorphous silica. In sample S24 (not shown) the number of

dispersed formations is the smallest and they have a diameter ~20 nm. In TEM replica observation of samples of S23 to S20 dispersed phase was not detected indicating that phase separation did not occur.

All the samples were measured by DTA. In Figure 2 the DTA traces of samples of S30, S28, S26, S24, S23, S22 and S20 are shown. The DTA curves for samples of S30 through S21 (not shown) have three deflections, one due to the glass transition (extrapolated start temperature) and two to exothermic crystallization peaks, the first being sharper than the second one. DTA of a sample of S20 has an extra small exothermic peak at higher temperature (1014 °C). The curves for samples from S30 to S23 are similar, the T_g being 698 ± 2 °C, the first crystallization peak 820 ± 5 °C and the second 897 ± 4°C.

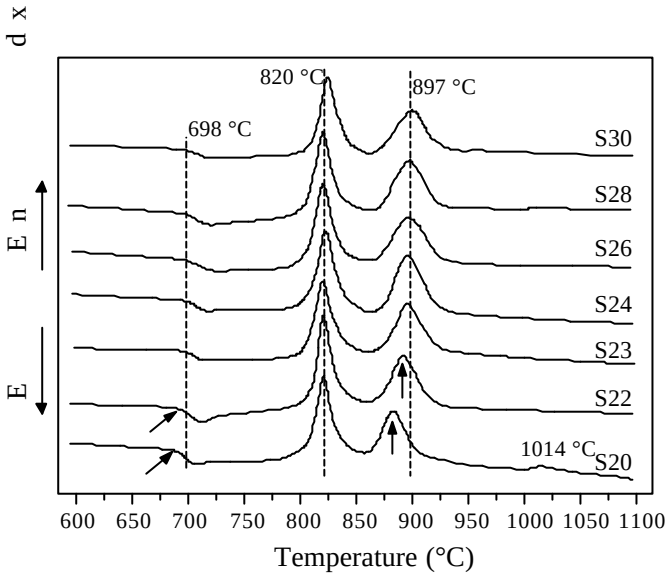

Fig. 2. DTA curves for annealed glasses S30, S28, S26, S24, S23, S22 and S20 (heating rate 10 $Kmin^{-1}$).

Figure 3 shows the Raman spectra of samples of S30, S28, S26, S24, S22 and S20 for wavenumbers ranging from 300 cm^{-1} to 1200 cm^{-1}. The bands are characteristic of glass materials[11]. A peak centered at 950 ± 3 cm^{-1} has the largest amplitude. There are also two smaller amplitude bands with greater width between 400-620 cm^{-1} which are larger in the S20 sample spectrum. The S20 sample spectrum has another band in the region 850-900 cm^{-1}.

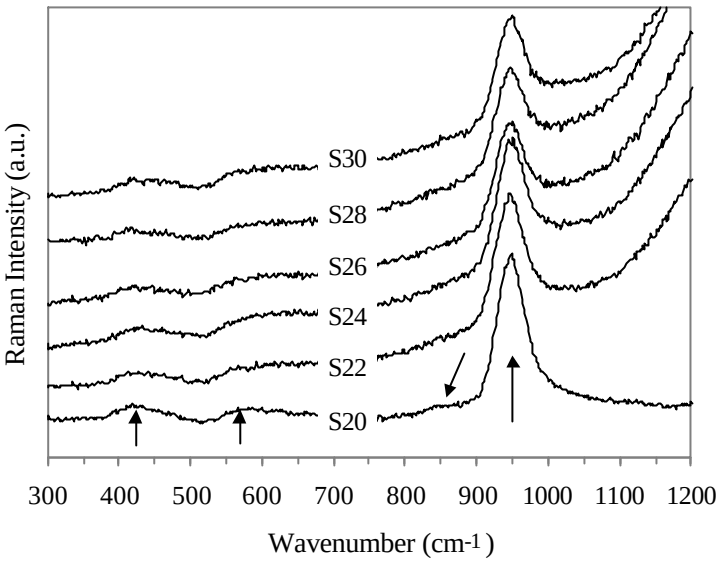

Fig. 3. Raman spectra of S30, S28, S26, S24, S22 and S20 glasses.

4. Discussion

In samples with <23 wt% SiO_2 the glasses are single-phase. In samples with >23 wt% we observe particles of increasing average size, identified by Oliveira *et al.*[10] as amorphous silica (Figure 1).

DTA traces (Figure 2) show a transition temperature around 698°C; normally, a second glass transition temperature, corresponding to the silica particles should be expected[12] at approximately 1108°C[13], but, given the amount of silica involved – a few per cent – and the thermal effect that accompanies the transition, this one was not observed. The transitions detected are, therefore, attributable to the glass matrix. Within the experimental error, the matrix Tg‘s found by extrapolation of DTA traces are independent of SiO_2 content for samples from S30 to S23 and decrease with decreasing amounts of SiO_2 for samples from S22 to S20. This independence should be interpreted as due to a common structure for matrices in samples with separated silica phases and so, composition S23, in which no separation is detected by TEM, should approximately coincide with that of a silica saturated matrix.

The first DTA exothermic peak, corresponding to an orthophosphate ($Ca_7Mg_2P_6O_{24}$[8]) is essentially independent of glass composition, whereas the second exothermic effect, attributed to silicates (forsterite and enstatite), shifts to lower

temperatures as the silica content decreases to less than 23 wt% (S22 to S20); this effect will be discussed further. A third exothermic peak is observed in S20 at 1014°C. However it was not possible to identify a crystalline phase associated to this effect by XRD. Apart from the usual scattering due to experimental errors, the observed effect was repeatedly confirmed.

The largest amplitude present in the Raman spectra (Figure 3) is at 950 cm^{-1} independent of composition, and its amplitude increases with decreasing silica content. It is known[14-16] that the $P\text{-}O^-$ stretch bond in a PO_4^{3-} structural unit has a band near 950 cm^{-1}. Oliveira *et al.*[17] have shown by ^{31}P magic-angle spinning (MAS) nuclear magnetic resonance (NMR) that in a sample of S30 phosphorus is present in an orthophosphate structure. Thus, the band around 950 cm^{-1} is assigned to $P\text{-}O^-$ stretch motions in a PO_4^{3-} structural unit. Therefore, along this series the phosphorus is always present in an orthophosphate structure, and will accordingly crystallize as such.

The structural interpretation of Raman spectra for silicate anionic species is more difficult. In silicates the stretching bands are located at higher frequencies and these depend on the degree of polymerization[15,16]. In accordance with previous ^{29}Si MAS NMR studies with a sample of S30[17] SiO_3^{2-} species are expected. SiO_3^{2-} structural unit has a Raman band[16] ($Si\text{-}O^-$ stretch) in the range 960-970 cm^{-1} which, in Figure 3, is not identified due to overlap with the orthophosphate band. In the spectrum of a sample of S20 a band in the range 850-900 cm^{-1}, assigned to $Si_2O_7^{6-}$ and SiO_4^{4-} structural units[18] indicates a glass de-polymerisation, consistent with the decrease in Tg. Increasing concentration of SiO_4^{4-} units will, in turn, favour the crystallization of the orthosilicate forsterite during DTA experiments, as confirmed by XRD, displacing the second exothermic peak to lower temperatures, as observed in samples S22 to S20. The magnitude of the experimental errors is thought not to affect the exhibited trend.

In the low frequency region the spectra have bands with greater width which overlap. These bands are assigned to bending motions and Ca,Mg-O vibrations in silicates (400-600cm^{-1}) and bending motions in orthophosphates (550-600cm^{-1}).[15,16,18]

With the exception of the spectrum of glass S20 Raman spectra are almost identical which we suggest is indicative of structural similarity among them.

5. Conclusions

Glasses with a silica content ranging from 24 to 30 wt% are phase separated and their structure is not affected by changing silica content. The phase with the largest volume fraction has an approximate composition corresponding to x=7.

For $x \geq 7$ the glasses are single-phase and de-polymerize as x increases.

De-polymerization increases the concentration of SiO_4^{4-} groups and the crystallization of forsterite during thermal treatment.

References

[1] Hench, L. L. – "Bioceramics: From Concept to Clinic", *Journal of the American Ceramic Society*, 74, 1991, 1487-1510.

[2] Kokubo, T.; Shigmatsu, M.; Nagashima, Y.; Tashiro, M.; Nakamura, T.; Yamamuro, T.; Higashi, S. – "Apatite and Wollastonite-containing Glass-ceramics for Prosthetic Application", *Bulletin of the Institute for Chemical Research Kyoto University*, 60, 1982, 260-268.

[3] Oliveira, J. M.; Fernandes, M: H.; Correia, R. N. – "Surface Modifications of a Glass and a Glass-ceramic of the MgO-3CaO.P_2O_5-SiO_2 System in a Simulated Body Fluid", *Biomaterials*, 16, 1995, 849-854.

[4] Shyu, J. J.; Wu, J. M. – "Effects of Composition Changes on the Crystallization Behavior of MgO-CaO-SiO_2-P_2O_5 Glass-ceramics", *Journal of the American Ceramic Society*, 74, 1991, 2123-2130.

[5] Lacerda, S. R.; Oliveira, J. M.; Fernandes, M. H.; Correia, R. N. – "TiO_2-induced Amorphous Phase Separation and Crystallization in a Glass of the System SiO_2-3CaO.P_2O_5-MgO", *Journal of Non-Crystalline Solids*, 221, 1997, 255-260.

[6] Kokubo, T. – "Surface Chemistry of Bioactive Glass-ceramics", *Journal of Non-Crystalline Solids*, 120, 1990, 138-151.

[7] Oliveira, A. L.; Oliveira, J. M.; Correia, R. N.; Fernandes, M. H.; Frade, J. R. – "Crystallization of Whitlockite from a Glass in the System CaO-P_2O_5-SiO_2-MgO", *Journal of the American Ceramic Society*, 81, 1998, 3270-3276.

[8] Oliveira, A. L.; Oliveira, J.M.; Correia, R. N.; Fernandes, M. H. – "Phase Separation and Crystallization in $3CaO.P_2O_5$-SiO_2-MgO Glasses", *Glastechnishe Berichte Glass Science and Technology*, 67C, 1994, 367.

[9] Oliveira, J. M.; Correia, R. N.; Fernandes, M. H. – "Effect of MgO Additions on Amorphous Phase Separation in Silico-Phosphate Glasses", *Proceedings of the XVIII International Congress on Glass* (CD-ROM), Ohio, D5, 1998, 80-85.

[10] Oliveira, J. M.; Correia, R. N.; Fernandes, M. H. – "Formation of Convoluted Silica Precipitates during Amorphous Phase Separation in the $Ca(PO_4)_2$-SiO_2-MgO System", *Journal of the American Ceramic Society*, in press.

[11] Wong, J.; Angell, C. A. – *Glass Structure by Spectroscopy*, New York, Marcell Dekker Inc., 1976.

[12] Mazurin, O. V.; Porai-Koshits, E. A.; Andreev, N. S. – *Phase Separation in Glass*, Amesterdam, Elsevier Science Publishers B. V., 1984.

[13] Turkdogan, E. T. – *Physicochemical Properties of Molten Slags and Glasses*, London, The Metals Society, 1983.

[14] Farmer, V. C. – *The Infrared Spectra of Minerals*, London, Mineralogical Society, 1974.

[15] Brawer, S. A.; White, W. B. – "Raman Spectroscopic Investigation of the Structure of Silicate Glasses. I. The Binary Alkali Silicates", *The Journal of Chemical Physics*, 63, 1975, 2421-2432.

[16] Mysen, B. O.; Ryerson, F. J.; Virgo, D. – "The Structural Role of Phosphorus in Silicate Melts", *American Mineralogist*, 66, 1981, 106-117.

[17] Oliveira, J. M.; Correia, R. N.; Fernandes, M. H.; Rocha, J. – "Influence of the CaO/MgO ratio on the structure of phase-separated glasses: a solid state ^{29}Si and ^{31}P MAS NMR study", *Journal of Non-Crystalline Solids*, 265, 2000, 221-229.

[18] Meysen, B. O. – "Iron and Phosphorus in Calcium Silicate Quenched Melts", *Chemical Geology*, 98, 1992, 175-202.

3.3 - Influence of the CaO/MgO Ratio on the Structure of Phase-separated Glasses: a Solid State ^{29}Si and ^{31}P MAS NMR study

J. M. Oliveira [a], R. N. Correia [a], M. H. Fernandes [a], J. Rocha [b]

[a] UIMC, Department of Ceramics and Glass Engineering, University of Aveiro, 3810-193 Aveiro, PORTUGAL

[b] Department of Chemistry, University of Aveiro, 3810-193 Aveiro, PORTUGAL

(Journal of Non-Crystalline Solids, 265(3), 2000, 221-229)

Abstract

^{29}Si and ^{31}P magic-angle spinning (MAS) nuclear magnetic resonance (NMR) spectroscopy was used to investigate structural aspects of glasses of the series (mol %) $31SiO_2$-$11P_2O_5$- (58-*x*)CaO-*x*MgO, with *x* ranging from 0 to 32, in which precipitation of amorphous silica occurs. As expected for alkaline-earth silicates, a strong ^{29}Si MAS NMR peak was recorded, shifting to higher frequencies with decreasing CaO/MgO molar ratios. Q^2 species predominate in the alkaline-earth rich phase and the observed shift in the ^{29}Si spectra is attributed to a decrease in the average degree of Si polymerization in the matrix. The experimental evidence suggests that Mg^{2+} replaces Ca^{2+} and also promotes the disruption of Si-O-Si bonds. Substitution of CaO by MgO increases the amount of dispersed phase. ^{29}Si MAS NMR showed the presence of Q^4 species in the dispersed phase and also suggested the presence of Q^0 species. A disproportionation reaction $2Q^2 \rightleftharpoons Q^0 + Q^4$ is proposed to balance the silicate charges. ^{31}P MAS NMR showed that phosphorus is present in an orthophosphate environment. The shift of the ^{31}P MAS NMR peak was attributed to the replacement of Ca by Mg.

***PACS**: 61.43.Fs; 61.18.Fs; 64.75.+g*

1. Introduction

The development of new silica-phosphate glasses and glass-ceramics containing a large amount of alkaline and alkaline-earth ions occurred in the last two decades, namely for biomedical applications[1-8].

The biomedical performance of glasses and glass-ceramics is influenced by many factors: tissue compatibility, hydrolytic stability, chemical, physical and mechanical properties of the material[2]. When implanted in a living organism these materials can be bioactive, that is, they can develop at the surface an hydroxycarbonate apatite layer, which is formed by a sequence of reactions between the material and the surrounding tissues[8]. Due to ethical concerns, clinical experiments are preceded by standard *in vitro* tests performed in the so-called simulated body fluids (SBF), which have a chemical composition close to that of human plasma[9]. These tests usually give reliable indications of the surface reactivity of the materials, which determine whether there is a formation of the surface apatite layers responsible for the bioactivity.

The surface reactivity of an implant depends on the rate of release of constituents from the material. Li *et al.*[10] proposed that the formation of the apatite layer on the surface of a bioglass-ceramic is mainly caused by the glassy phase, and can be prevented if the glass-ceramic is completely crystallized. The knowledge of the structure of the glass and of the remaining glassy phase in the glass-ceramic may thus be of major importance, because the rate of release of constituents is mainly determined by its structure.

A number of researchers have tried to quantify the relationship between the composition and the structure and bioactivity of glasses and glass-ceramics[11-14]. Strnad[13], using Stevels' structural parameters which measure the mean number of bridging oxygens and non-bridging oxygens in a polyhedron, correlated these parameters with the bioactivity of glasses and glass-ceramics. Later, Hill[14] using the network polymeric approach in inorganic glass structures proposed the cross-linking density as a measure of the network connectivity, in order to predict the glass reactivity.

Magnesium and calcium ions are usually classified as network modifiers, but there are some reports discussing the possibility of a network former role for magnesium, specially in alumino-silicate glasses[15,16]. Many papers on phosphate glasses containing

magnesium ions refer anomalous properties[17-20]. It is thus important to clarify the role of magnesium in the structure of glasses.

NMR is a powerful technique in structural studies of glasses and it has been used in the study of bioactive glasses[21-25]. In silica-based glasses silicon occupies the centre of an oxygen tetrahedron. A silicate unit is usually represented by Q^n, where Q refers to the silicon atom and n is the number of bridging oxygens. The different Q species have resonances in separate regions of the ^{29}Si MAS NMR spectrum[26]. In amorphous silicates the ^{29}Si NMR resonance spectrum presents a larger linewidth than in crystalline materials due to geometrical differences among silicate units, and overlapping can occur, rendering interpretation more difficult[27-29]. The ^{29}Si MAS NMR chemical shifts occur at lower frequencies as the degree of polymerization of the silicate anions increases. Other structural factors such as cation characteristics or geometric features can also influence the spectrum[29].

The ^{29}Si MAS NMR spectra of alkaline-earth silicate glasses usually exhibit only one broad peak. Schneider *et al.*[28] reported that two glasses of compositions $(Na_2O)_{0.4}(SiO_2)_{0.6}$ and $(CaO)_{0.4}(SiO_2)_{0.6}$ display distinct spectra. The alkaline-containing glass spectrum displayed two peaks assigned to Q^2 and Q^3 species, while the alkaline-earth-containing glass exhibited only one broad peak which was assigned to Q^2 species and explained on the basis of the existence of a distribution of bond angles and bond lengths, rather than being due to variations in the number of bridging oxygens.

Introduction of phosphorus in alkaline-earth silicate glasses increases the degree of polymerization of the silicate network. Yang *et al.*[30] determined that the ^{31}P MAS NMR chemical shifts in alkaline-earth silicate glasses containing phosphorus ranged from 3.9 to 0.4 ppm, decreasing from Sr to Mg orthophosphates.

This paper reports a study on the structural effects in a separated silica-phosphate glass containing 58 mol % alkaline-earth oxides, in which Ca ions were gradually replaced by Mg ions. The glass microstructures were examined by scanning electron microscopy (SEM). The amount of dispersed phase was assessed by both induced coupled plasma (ICP) emission spectroscopy and ^{29}Si MAS NMR. The effect of the substitution of Ca by Mg on the structural features of the glasses was studied by ^{29}Si and ^{31}P MAS NMR.

2. Experimental Procedure

2.1 Glass preparation

Seven glasses of the series $31SiO_2$-$11P_2O_5$-(58-*x*)CaO-*x*MgO were prepared from reagent-grade $Ca(H_2PO_4)_2$, $CaCO_3$, SiO_2 and MgO. The raw materials were mixed in ethanol for 30 minutes and dried at 60 °C. Batches of 50-70 g were melted in a platinum crucible at temperatures in the range 1500-1530 °C for 2 hours, a schedule which was found adequate to ensure a good homogeneity and fining. The glass compositions investigated are listed in Table I.

Table I. Nominal glass compositions (CM series).

	Composition (mol % (wt %))			
Sample	SiO_2	CaO	P_2O_5	MgO
CM1	31.1 (28.1)	58.3 (49.3)	10.6 (22.6)	0.0 (0.0)
CM2	31.1 (28.5)	52.9 (45.3)	10.6 (22.9)	5.4 (3.3)
CM3	31.1 (28.9)	47.5 (41.2)	10.6 (23.2)	10.8 (6.7)
CM4	31.1 (29.2)	42.3 (37.2)	10.6 (23.5)	16.0 (10.1)
CM5	31.1 (29.6)	37.0 (32.9)	10.6 (23.8)	21.3 (13.7)
CM6	31.1 (30.0)	31.7 (28.6)	10.6 (24.1)	26.6 (17.3)
CM7	31.1 (30.4)	26.4 (24.1)	10.6 (24.5)	31.9 (21.0)

Composition CM1 was used as a frit by quenching in water at room temperature. All other glasses were cast to blocks in metal molds, annealed for 30 minutes at the transition temperature, previously determined by differential thermal analysis, and slowly cooled to room temperature.

2.2 Glass analysis

To confirm the amorphous state all materials were analyzed by powder X-ray diffraction (XRD) using Cu K_α radiation.

The glass microstructures were observed by SEM using fractured samples.

Portions of about 500 mg of CM3 to CM7 glasses were digested for 24 hours in 20 ml HNO_3 1M solution at ca. 40 °C, under stirring. The solution was filtered through a

milipore with an aperture of 0.05 μm. The filtrate was used to evaluate the ionic concentration of Si, Ca, Mg and P by ICP emission spectroscopy; for reasons to be discussed the filtrate composition was assigned to the glass matrix. The amount of dispersed silica phase was then calculated by difference to the nominal glass composition. The insoluble residue was dried for further SEM observation and for chemical analysis by energy dispersive spectroscopy (EDS).

^{29}Si MAS NMR spectra of glasses CM1, CM4 and CM7 were recorded at 79.5 MHz on a spectrometer using 40° radio frequency pulses, spinning rates of 5.0 kHz, and a 240 s recycle delay. Chemical shifts were quoted in ppm from tetramethylsilane (TMS). The ^{31}P MAS NMR spectra of glasses were recorded at 161.97 MHz with 45° pulses, spinning rates of 10 kHz, a 45 s recycle delay and the chemical shift was quoted in ppm from phosphoric acid (85%).

3. Results

3.1 Glass Characterization

Because sample CM1 devitrified on pouring onto the metallic mold, it was necessary to quench the melt to enable the formation of an amorphous frit. Composition CM2 still showed some tendency for surface devitrification giving rise to slightly cloudy specimens. An increasingly white opaque color was exhibited by all glasses from CM2 to CM7. Compositions with MgO contents higher than that of CM7 did not melt up to 1550 °C. Powder XRD patterns of the base materials showed that all the samples were amorphous.

Transmission electron microscopy (TEM) observation did not reveal any heterogeneity in the CM1 frit indicating that phase separation did not occur, while a dispersed phase was present in all the other glasses of the series (as observed by SEM), mainly as aggregates.

Figure 1 shows SEM micrographs of the glasses CM3, CM5 and CM7. The micrographs clearly show that an increase in MgO content promotes a decrease in the number of aggregates per unit volume and a significant increase in their average size.

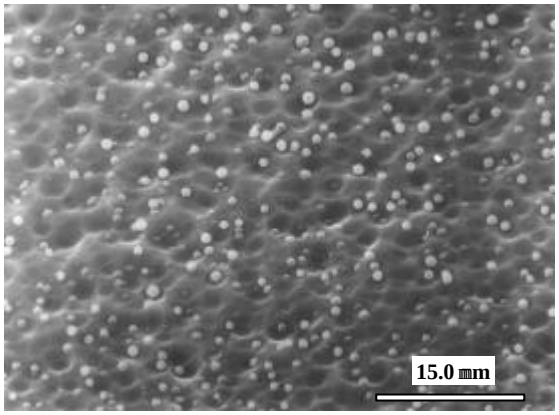

(a) CM3 etched

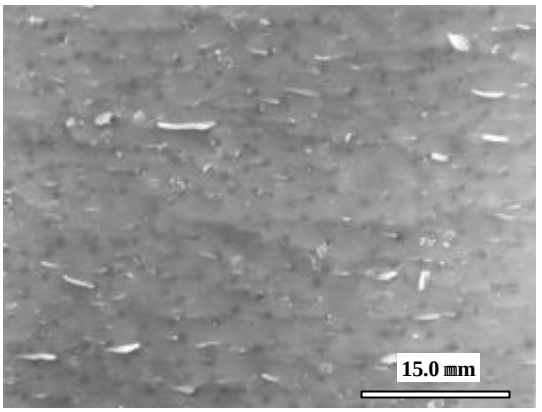

(b) CM3 non-etched

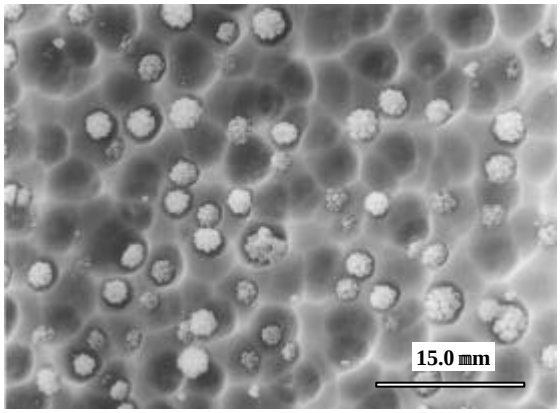

(c) CM5 etched

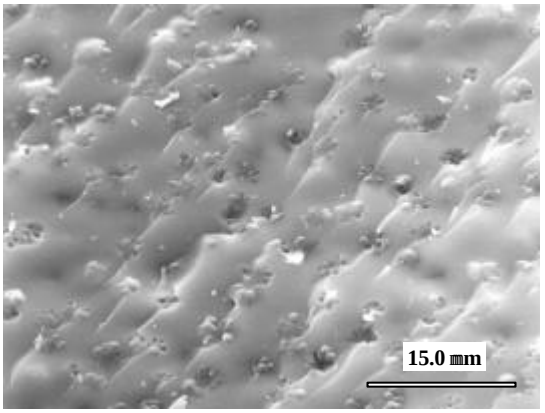

(d) CM5 non-etched

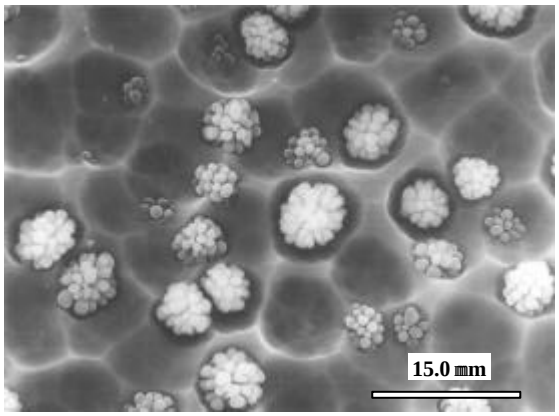

(e) CM7 etched

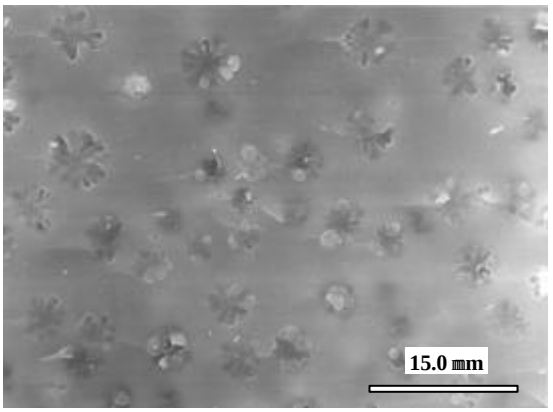

(f) CM7 non-etched

Fig. 1. SEM micrographs of CM3, CM5 and CM7 glasses. (a), (b) and (c) fractured and etched in 1 M HNO_3, 15 s; (d), (e) and (f) fractured, non-etched.

In a previous study, Oliveira *et al.*[31] showed that phase separation in glass CM6 occurred when it was melted at three different temperatures (1525 °C, 1560 °C and 1595 °C) and then quenched. The amount of dispersed phase was about the same at all temperatures and similar to that found in the as-cast samples. Temperature should thus have little effect on the amount of dispersed silica in CM6 and, presumably, in all other glasses of the present series. This means that the boundaries of the immiscibility dome are steep in the temperature range concerned.

The amount of dispersed phase was quantitatively determined in glasses CM3 to CM7 as described in section 2.

SEM observation of the residue from acid digestion of the glass showed that it consists only of dispersed phase (Fig. 2), and thus, that the chemical etching had selectively attacked the glassy matrix. EDS analysis of the residue confirmed that, within the experimental error, only two elements, silicon and oxygen, were present, as previously found by Oliveira *et al.*[31] on extraction replicas of non-etched fracture surfaces of glass CM6 examined by TEM/EDS. Therefore, it is assumed that the precipitates are pure silica. The compositions of the filtrates, assigned to the glass matrices, are shown in Table II, together with the amount of precipitated silica.

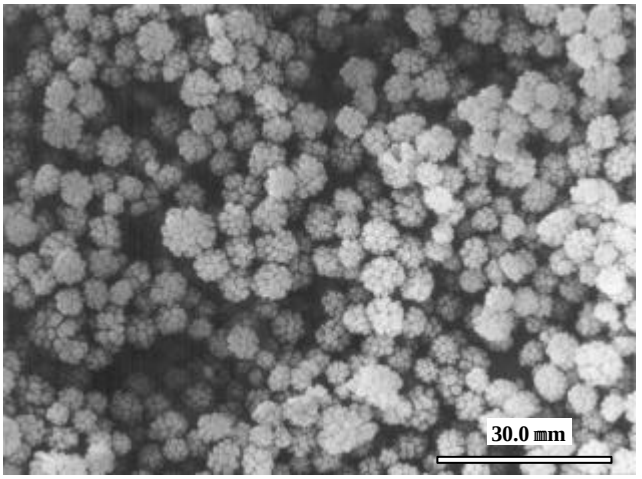

Fig. 2. SEM micrographs of the dispersed phase after chemical dissolution of the matrix.

Table II. Compositions determined by ICP.

Composition (mol % (wt %))					Calculated (mol % (wt %))
Sample	SiO_2	CaO	P_2O_5	MgO	Dispersed SiO_2
CM3	26.0±0.02	47.2±0.07	10.7±0.03	11.7±0.08	5.1± 0.02
	(24.4±0.12)	(41.4±0.19)	(23.8±0.20)	(7.4±0.10)	(4.5±0.12)
CM4	25.9±0.29	42.1±0.10	10.5±0.06	16.7±0.15	5.2±0.29
	(24.8±0.20)	(37.6±0.20)	(23.7±0.21)	(10.7±0.13)	(4.4±0.20)
CM5	25.5±0.14	37.1±0.24	10.6±0.11	21.3±0.23	5.6±0.14
	(24.6±0.20)	(33.5±0.13)	(24.1±0.19)	(13.8±0.18)	(5.0±0.20)
CM6	23.8±0.03	32.1±0.05	10.7±0.16	25.9±0.12	7.3±0.03
	(22.9±0.18)	(28.9±0.24)	(24.4±0.20)	(16.7±0.19)	(7.1±0.18)
CM7	21.9±0.12	26.7±0.08	10.8±0.05	31.6±0.24	9.2±0.12
	(21.6±0.16)	(24.6±0.12)	(25.0±0.15)	(20.9±0.12)	(8.8±0.16)

3.2 Glass structure: ^{29}Si and ^{31}P MAS NMR studies

^{29}Si MAS NMR spectra recorded for glasses CM1, CM4 and CM7, with respectively 0, 5 and 9 mol % of dispersed silica are shown in Fig. 3.

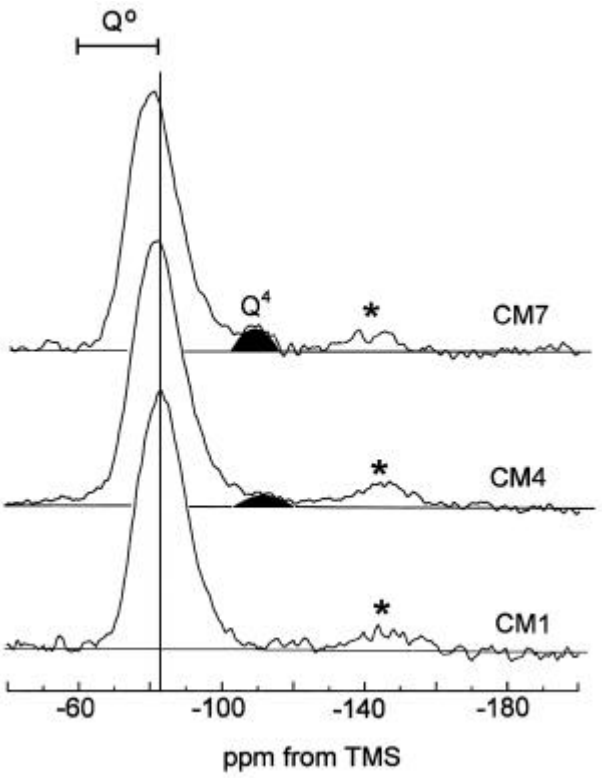

Fig. 3. ^{29}Si MAS NMR spectra of CM1, CM4 and CM7 glasses. The typical chemical shift range for Q^0 and Q^4 species in silicates is depicted. Asterisks denote spinning sidebands.

The main broad peak shifts from ca. -80 ppm to -83 ppm, with an accuracy of about 0.2 ppm. Although small, the observed shifts are considered meaningful because they appear to be related to structural differences in the three glass matrices, since the dispersed phase is apparently the same for all compositions.

The ^{31}P MAS NMR spectra for glasses CM1, CM4 and CM7 in Fig. 4, with peak position determined with an error of ± 0.1 ppm, suggest that phosphorus is present in all glasses as an orthophosphate, that is, monomeric units, and no evidence was found for the presence of Si-O-P bonds.

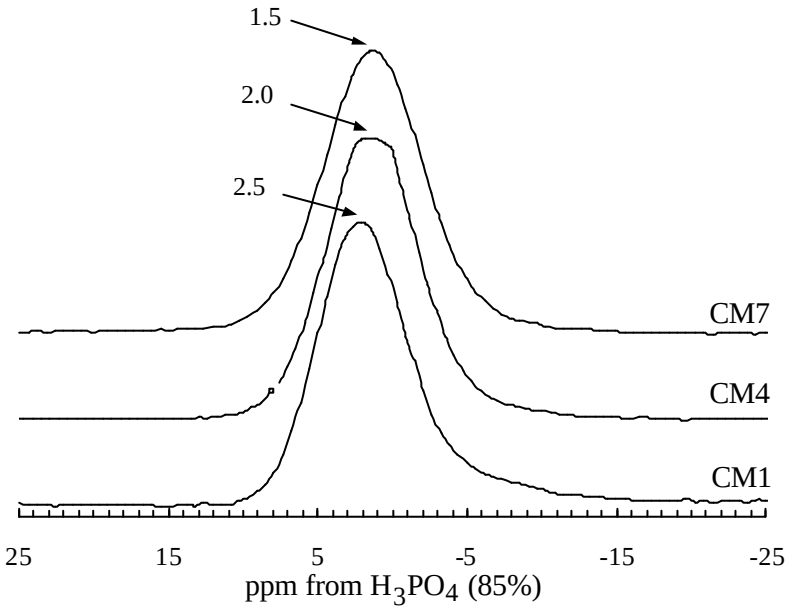

Fig. 4. ^{31}P MAS NMR spectra of CM1, CM4 and CM7 glasses.

4. Discussion

4.1 Glass Characterization

Comparing the results in Tables I and II it is clear that, within the experimental error, there is good agreement between the relative amounts of calcium, phosphorus and magnesium oxides in the nominal compositions and in the glassy matrix of the

separated glasses, but that a significant decrease in the silicon oxide content occurred. These results indicate that the amount of dispersed silica increases with the magnesium oxide content.

4.2 Glass structure: ^{29}Si and ^{31}P MAS NMR studies

Work in progress on the crystallization process of these glasses shows that bulk homogeneous nucleation occurs in all of them[32] and that the main crystalline silicates formed are wollastonite ($CaO\text{-}SiO_2$) and enstatite ($MgO\text{-}SiO_2$). The former is a three-ring silicate planar structure while the later is a single chain silicate, both consisting of Q^2 species. In the samples with higher MgO contents small amounts of forsterite ($2MgO\text{-}SiO_2$), characterized by Q^0 species, were also found.

Muller *et al.*[33] have shown that glasses with homogeneous nucleation have ionic arrangements resembling the corresponding crystal phases. The ^{29}Si MAS NMR chemical shift was reported to be -81.7 ppm in $CaO\text{-}SiO_2$ glass compositions[30], which crystallize as wollastonite. This finding suggests that "crystal-like" regions probably exist in the glass, thus favoring the subsequent crystallization of wollastonite. According to the above ideas one is led to admit that the peaks in Fig. 3 should be mainly attributed to Q^2 species, although other Q species, in smaller amounts, should also be present.

With increasing MgO content, that is, with increasing fraction of dispersed silica the ^{29}Si MAS NMR peak positions in the spectra shift towards higher frequencies. Interestingly, the glass transition temperature decreases with increasing MgO content from 745 °C in CM1 to 683 °C in CM7[34], indicating that the glassy matrix network becomes less cohesive as MgO replaces CaO. If the substitution of CaO by MgO is responsible for a gradual network weakening, then the number of non-bridging oxygens should be increasing. In these circumstances the ^{29}Si MAS NMR peak shift is attributed to a slight decrease in the average degree of polymerization (increasing number of non-bridging oxygens) of the matrix. This would correspond to a gradual rupture of the silicate chains by the Mg ions, rather than to a mere replacement of Ca by Mg at the existing non-bridging oxygen sites. An alternative explanation for the high-frequency shift of the ^{29}Si MAS NMR peaks as the MgO content increases, is the deshielding of the silicon nucleus, produced by the magnesium ions. This possibility could not be

experimentally supported. Galliano *et al.*[23] did not find any changes in the NMR spectra, when replacing Ca by Mg or Sr in a silica-phosphate glass containing alkaline earth ions. In their paper, however, it is not clear whether the glasses were monophasic or phase separated.

All glasses from CM2 to CM7 consist of two amorphous phases, one of which was experimentally identified as amorphous silica. It is expected that the environment of silicon in the dispersed phase is different from that in the surrounding glass matrix.

The absence of a peak around -200 ppm indicates that no 6-coordinated silicon exists[35]. However, in CM7 and CM4 glasses the peak around -110 ppm is a clear indication of the existence of a small amount of Q^4 species in the separated glass, which confirms the presence of amorphous silica. An evaluation of the peak area for Q^4 species in CM7 gives a value of ca. 8.5±0.2 mol % which agrees, within the experimental error, with the one calculated and shown in Table II. Hence, it is assumed that Q^4 species are essentially present in the dispersed phase.

With increasing MgO content the amount of dispersed silica increases and, thus, the number of Q^4 species. Since the total Si amount is constant throughout the series, there must be a transformation of part of the Q^2 species into Q^4 species. It is reported in the literature that the ^{29}Si NMR chemical shift for Q^0 species in silicates ranges from ca. -60 to -83 ppm[26]. Since the main ^{29}Si MAS NMR peak shifts to high frequency with decreasing CaO/MgO molar ratio it is possible that Q^0 species form simultaneously with Q^4 species (Fig. 3). Moreover, it was experimentally observed that forsterite (Q^0) started to crystallize, together with enstatite, in glasses of CM series with higher MgO content. In these circumstances the following disproportionation reaction:

$$2Q^2 \rightleftharpoons Q^0 + Q^4$$

is likely to occur, which is equivalent to:

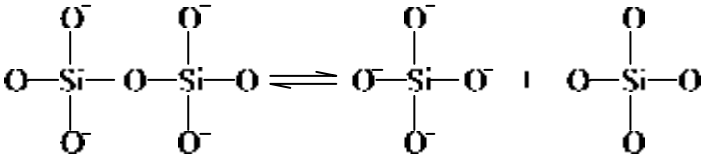

Therefore, the effect of increasing the MgO/CaO ratio in the glass composition is to break Si-O bonds, creating Q^4 species, Q^0 species and shorter Q^2 chains; Q^4 species are precipitated as amorphous silica and consequently, the $(CaO+MgO)/SiO_2$ ratio in the matrix increases.

The above reaction was first suggested by Murdoch *et al.*[36], although without any experimental NMR evidence. A similar reaction $2Q^m \rightleftharpoons Q^{m+1} + Q^{m-1}$ $(0<m<4)$ has been proposed for alkaline glasses[37], but little is known on the structural details of silicon Q species in alkaline-earth containing glasses.

The proposed local phosphorus structure is also supported by experimental evidence on the crystallization of glasses of the present series[32]. In fact, hydroxyapatite ($Ca_{10}(PO_4)_6(OH)_2$) is the main phosphate phase precipitating at lower MgO contents, but a Mg-substituted whitlockite ($Ca_7Mg_2P_6O_{24}$) is found instead in crystallized glasses of higher MgO contents. Since both are orthophosphates, and assuming that "crystal-like" regions already exist in the parent glass prior to crystallization, it seems obvious that Mg gradually occupies the Ca sites in the phosphorus environment.

5. Conclusions

^{29}Si and ^{31}P MAS NMR measurements performed on phase separated glasses of the series (mol %) $31SiO_2$-$11P_2O_5$-$(58-x)CaO$-xMgO, with x ranging from 0 to 32, suggested that in all glasses the Si ion is present in a fourfold coordination and P appears in an orthophosphate arrangement.

The peak shift in the ^{29}Si MAS NMR spectra towards higher frequencies as the MgO content increases, was attributed to a decrease in the average degree of polymerization of the Si network. It is proposed that Mg ions, acting as network modifiers, not only substitute Ca ions but also promote the disproportionation reaction $2Q^2 \rightleftharpoons Q^4 + Q^0$, thus disrupting Si-O-Si bonds.

The replacement of Ca by Mg in the glasses increases the amount of dispersed phase, identified as amorphous silica. In this phase Si atoms are arranged in Q^4 species,

while in the remaining glassy matrix Si appears as Q^2 species and, in small amounts, as Q^0 species.

In the P environment Mg ions directly replace Ca ions in an orthophosphate arrangement resulting in a low-frequency shift of the ^{31}P MAS NMR resonance.

References

[1] Ogino, M.; Hench, L. L. –"Formation of Calcium Phosphate Films on Silicate Glasses", *Journal of Non-Crystalline Solids*, 38&39, 1980, 673-678.

[2] Hench, L. L. – "Bioceramics: From Concept to Clinic", *Journal of the American Ceramic Society*, 74, 1991, 1487-1510.

[3] Kokubo, T.; Shigmatsu, M.; Nagashima, Y.; Tashiro, M.; Nakamura, T.; Yamamuro, T.; Higashi, S. – "Apatite and Wollastonite-containing Glass-ceramics for Prosthetic Application", *Bulletin of the Institute for Chemical Research Kyoto University*, 60, 1982, 260-268.

[4] Vogel, W. Hölland, W.; Naumann, K.; Grimmel, J. – "Development of Machineable Bioactive Glass-ceramics for Medical Uses", *Journal of Non-Crystalline Solids*, 80, 1986, 34-51.

[5] Brömer, H.; Deutsher, K.; Blencke, B.; Pfeil, E.; Strunz, V. – "Properties of the Bioactive Implant Material Ceravital", *Science of Ceramics*, 9, 1977, 219-225.

[6] Andersson, O. H.; Karlsson, K. H.; Kangasniemi, K. – "Calcium Phosphate Formation at the Surface of Bioactive Glass *In Vivo*", *Journal of Non-Crystalline Solids*, 119, 1990, 290-296.

[7] Oliveira, J. M.; Fernandes, M. H.; Correia, R. N. – "Development of a New Glass-ceramic in the System $MgO\text{-}3CaO.P_2O_5\text{-}SiO_2$ *in*: T. Yamamuro, T. Kokubo, T. Nakamura (Eds.), *Bioceramics*, 5, 1992, 7-14.

[8] Cao, W.; Hench, L. L. – "Bioactive Materials", *Ceramics International*, 22, 1996, 493-507.

[9] Kokubo, T.; Kushitani, K.; Sakka, S.; Kitsugi, T.; Yamamuro, T. – "Solutions Able to Reproduce *In Vivo* Surface-Structure Changes in Bioactive Glass-ceramic A-W", *Journal of Biomedical Materials Research*, 24, 1990, 721-734.

[10] Li, P.; Yang, Q.; Zhang, F.; Kokubo, T. – "The Effect of Residual Glassy Phase in a Bioactive Glass-ceramic on the Formation of its Surface Apatite Layer *In Vitro*", *Journal of Materials Science Materials in Medicine*, 13, 1992, 452-456.

[11] Andersson, O. H.; Karlsson, K. H. – "On the Bioactivity of Silicate Glass", *Journal of Non-Crystalline Solids*, 129, 1991, 145-151.

[12] Rawlings, R. D. – "Composition Dependence of the Bioactivity of Glasses", *Journal of Materials Science Letters*, 11, 1992, 1340-1343.

[13] Strnad, Z. – "Role of the Glass Phase in Bioactive Glass-ceramics", *Biomaterials*, 13, 1992, 317-321.

[14] Hill, R. – "An Alternative View of the Degradation of Bioglass", *Journal of Materials Science Letters*, 15, 1996, 1122-1125.

[15] Merzbacher, C.; White, W. B. – "The Structure of Alkaline Earth Aluminosilicate Glasses as Determined by Vibrational Spectroscopy", *Journal of Non-Crystalline Solids*, 130, 1991, 18-34.

[16] Gervais, F.; Blin, A.; Massiot, D.; Contures, J. P. – "Infrared Reflectivity Spectroscopy of Silicate Glasses", *Journal of Non-Crystalline Solids*, 89, 1997, 384-401.

[17] Hauret, G.; Vaills, Y.; Luspin, Y.; Gervais, F.; Coté, B. – "Similarities in the Behaviour of Magnesium and Calcium in Silicates Glasses", *Journal of Non-Crystalline Solids*, 170, 1994, 175-181.

[18] Cervinka, L.; Berghová, J.; Trojan, M. – "An X-Ray Study of Phosphate Glasses of the Composition $[M(PO_3)_2]n$ (M=Zn, Cu, Mn, Ca and Mg)", *Journal of Non-Crystalline Solids*, 192&193, 1995, 121-124.

[19] Hoppe, W.; Walter, G.; Knanold, R.; Stachel, D.; Baiz, A. – "The Dependence of Structural Peculiarities in Binary Phosphate Glasses on their Network Modifier Content", *Journal of Non-Crystalline Solids*, 192&193, 1995, 28-31.

[20] Hoppe, W. – "A Structural Model for Phosphate Glasses", *Journal of Non-Crystalline Solids*, 195, 1996, 138-147.

[21] Lockyer, M. E.; Holland, D.; Dupree, R. – "NMR Investigation of the Structure of Some Bioactive and Related Glasses", *Journal of Non-Crystalline Solids*, 188, 1995, 207-219.

[22] Hartmann, P.; Vogel, J.; Schnabel, B. – "NMR Study of Phosphate Glasses and Glass-ceramics Structures", *Journal of Non-Crystalline Solids*, 176, 1994, 157-163.

[23] Galliano, P. G.; Porto López, J. M; Varetti, E. L.; Sobrados, I.; Sanz, J. – "Analysis by Nuclear Magnetic Resonance and Raman Spectroscopies of the Structure of Bioactive Alkaline-Earth Silicophosphate Glasses", *Materials Research Bulletin*, 29, 1994, 1297-1306.

[24] Braun, M.; Jana, C. – "^{19}F and ^{31}P NMR Spectroscopy of Calcium Apatites"", *Journal of Materials Science Materials in Medine*, 6, 1995, 150-154.

[25] Vogel, J.; Jana, C.; Hartmann, P. – "Structural Investigations of SiO_2-Containing Phosphate Glasses", *Glastechnishe Berichte Glass Science and Technology*, 71, 1998, 97-101.

[26] Engelhardt, G.; Michel, D. – *High-Resolution Solid State NMR of Silicates and Zeolites*, New York, J. Wiley, 1987.

[27] Mägi, M.; Lippmaa, E.; Samoson, A.; Engelhardt, G.; Grimmer, A.-R. – "Solid State High Resolution Silicon-29 Chemical Shifts in Silicates", *The Journal of Physical Chemistry*, 88, 1984, 1518-15-22.

[28] Schneider, E.; Stebbins, J. F.; Pines, A. – "Speciation and Local structure in Alkali and Alkaline Earth Silicate Glasses: Constraints from ^{29}Si NMR Spectroscopy", *Journal of Non-Crystalline Solids*, 89, 1987, 371-383.

[29] Grimmer, A.-R.; Mägi, M.; Hähnert, M.; Stade, H.; Samoson, A.; Wieker, W.; Lippmaa, E. – "High-Resolution Solid-State ^{29}Si Nuclear Magnetic Resonance Spectroscopic Studies of Binary Alkali Silicate Glasses", *Physics and Chemistry of Glasses*, 25, 1984, 105-109.

[30] Yang, W.-R.; Kirkpatrick, R. J.; Turner, G. – "^{31}P and ^{29}Si Magic Angle Sample-Spinning NMR Investigation of the Structural Environment of Phosphorus in Alkaline-earth Silicate Glasses", *Journal of the American Ceramic Society*, 69, 1986, c222-c223.

[31] Oliveira, J. M.; Correia, R. N.; Fernandes, M. H. – "Formation of Convoluted Silica Precipitates during Amorphous Phase Separation in the $Ca(PO_4)_2$-SiO_2-MgO System", *Journal of the American Ceramic Society*, in press.

[32] Oliveira, J. M.; Correia, R. N., Fernandes, M. H., to be submitted.

[33] Muller, E.; Heide, K.; Zanotto, E. D. – "Molecular Structure and Nucleation in Silicate Glasses", *Journal of Non-Crystalline Solids*, 155, 1993, 56-66.

[34] Oliveira, J. M.; Correia, R. N.; Fernandes, M. H. – "Effect of MgO Additions on Amorphous Phase Separation in Silico-Phosphate Glasses", *Proceedings of the XVIII International Congress on Glass* (CD-ROM), Ohio, D5, 1998, 80-85.

[35] Dupree, R.; Holland, D.; Mortuza, M. – "Six-Coordinated Silicon in Glasses", *Nature*, 328, 1987, 416-417.

[36] Murdoch, J. B.; Stebbins, J. F.; Carmichael, I. S. – "High-Resolution ^{29}Si NMR Study of Silicate and Aluminosilicate Glasses: The Effect of Network-Modifying Cations", *American Mineralogist*, 70, 1985, 332-343.

[37] Matson, D. W.; Sharma, S. K.; Philpotts, J. A. – "The Structure of High-Silica Alkali-Silicate Glasses. A Raman Spectroscopic Investigation", *Journal of Non-Crystalline Solids*, 58, 1983, 323-352.

4 - COMPORTAMENTO *IN VITRO* DE VIDROS E VIDROS CERÂMICOS

4.1 - Introdução

Nesta secção apresentam-se, de forma concisa, os parâmetros considerados mais importantes para explicar o comportamento bioactivo dos materiais, vítreos ou vitrocerâmicos, e são passados em revista os artigos que o autor considerou terem contribuído de forma mais directa para a compreensão do mecanismo de formação superficial da apatite.

4.1.1 - A formação de apatite *in vitro* e mecanismos explicativos

Nos vidros ditos bioactivos quando testados *in vivo* verifica-se sempre o desenvolvimento de uma camada apatítica à sua superfície. No entanto, dada a dificuldade inerente a este tipo de ensaios, muitos destes biomateriais têm sido testados *in vitro* em soluções celulares ou acelulares. O recurso a soluções do tipo SBF[1] ("simulated body fluid"), cuja composição é semelhante à da parte inorgânica do plasma humano (ver Tabela 4.I), generalizou-se, sendo hoje um meio frequentemente utilizado em estudos de bioactividade. Os resultados a seguir apresentados baseiam-se em estudos realizados com a solução SBF, salvo alguma excepção que será assinalada.

Tabela 4.I. Concentrações iónicas nominais no plasma humano e numa solução sintética (SBF).[1]

	Na^+	K^+	Ca^{2+}	Mg^{2+}	Cl^-	HCO_3^-	HPO_4^{2-}	SO_4^{2-}
Plasma	142,0	5,0	2,5	1,5	103,0	27,0	1,0	0,5
SBF*	142,0	5,0	2,5	1,5	147,8	4,2	1,0	0,5

* - Tamponizada com 50mM tris-hidroxi-metil-aminometano (TRIS) e 45 mM HCl a pH 7,25. O TRIS é um tampão frequentemente utilizado em estudos *in vitro*; contudo, este composto pode acelerar a dissolução dos vidros através da formação de um complexo solúvel de cálcio[2].

Actualmente são quatro os mecanismos propostos para explicar o comportamento bioactivo dos vidros e dos vidros cerâmicos: o *mecanismo de Hench*, o *mecanismo de Kokubo*, o *mecanismo de Andersson* e o *mecanismo de Li.*

O mecanismo de Hench

Decorrente dos trabalhos realizados, em especial com o Bioglass® 45S5 (Tabela 1.I), Hench propôs um mecanismo para explicar a ligação entre o tecido ósseo e o material constituído por 12 etapas das quais as cinco primeiras, rápidas, ocorrem à superfície do material e são de natureza inorgânica, sendo as restantes de natureza orgânico-celular:[3-9]

1ª etapa – troca entre iões alcalinos do vidro e iões H^+ existentes na solução

$$Si–O–Na^+ + H^+_{(aq)} \rightarrow Si–OH + Na^+_{(aq)}$$

2ª etapa – dissolução da rede vítrea e formação de grupos silanol

$$Si–O–Si + H_2O \rightarrow Si–OH + OH–Si$$

3ª etapa – condensação de grupos silanol e formação de uma camada rica em sílica gel à superfície do vidro

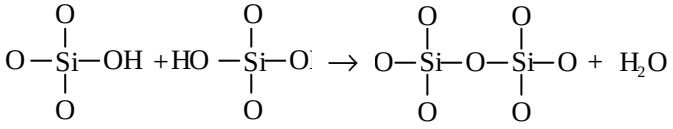

4ª etapa – adsorção de iões Ca^{2+} e PO_4^{3-} à superfície da camada de sílica gel, seguida de crescimento de um filme amorfo, rico em Ca-P, por incorporação de iões cálcio e fosfato da solução.

5ª etapa – formação de uma camada de hidroxi-carbonato-fluor-apatite por cristalização do filme amorfo, anteriormente formado, com incorporação de aniões OH^-, CO_3^{2-} ou F^-.

As reacções que constituem as etapas 1, 2 e 3 em nada diferem daquelas que ocorrem quando um vidro é imerso em soluções aquosas. A corrosão química de vidros alcalinos e alcalino-terrosos de sílica baseia-se no ataque protónico à rede vítrea, com a libertação de catiões modificadores, e a subsequente destruição das ligações Si-O-Si.

Desta ruptura da rede resulta a formação de grupos silanol, os quais por posterior condensação originam sílica gel.[10]

Associadas a todas estas trocas iónicas existem importantes variações de pH à superfície do material que possibilitam a deposição de apatite[11].

Muito embora Hench reconheça que existe uma forte dependência entre a cinética destas reacções e a composição vítrea[5], tal não é contemplado no mecanismo global.

O mecanismo de Kokubo

Os trabalhos realizados por Kokubo com o vidro base G-AW[iii] e os vidros cerâmicos derivados A-GC[iv], A.W-GC[v] (Cerabone A/W® - Tabela 1.I) e A.W.CP-GC[vi] permitiram encontrar uma explicação alternativa para o mecanismo responsável pela ligação bioactiva implante–tecido ósseo.[10,12-23]

No mecanismo proposto por Kokubo é de extrema importância a presença, no vidro, de dois iões: Ca^{2+} e Si^{4+}. A dissolução de Ca^{2+} aumenta o grau de saturação da solução SBF em relação à apatite e os iões Si^{4+} proporcionam, depois de adsorvidos à superfície do biomaterial, pontos de nucleação da apatite. Os iões fosfato necessários à formação de apatite provêm, essencialmente, da solução envolvente.[24,25,26] Mais tarde o próprio autor reconheceu que a saturação da solução não é um factor tão importante quanto a dissolução de Si^{4+}, pois o vidro $CaO.P_2O_5$ provoca um aumento do grau de saturação da solução SBF (por dissolução de iões fosfato) semelhante ao ocorrido com o vidro $CaO.SiO_2$ e só este, que dissolve Si^{4+}, é bioactivo.[27]

Em vidros do sistema $MgO\text{-}P_2O_5\text{-}SiO_2$ Kokubo detectou a formação superficial de uma camada de sílica gel, tal como previsto no modelo de Hench; contudo, este tipo de camada não foi detectado no vidro cerâmico A/W, o que levanta algumas questões relativas à aplicabilidade do mecanismo de Hench aos vidros cerâmicos do sistema $MgO\text{-}P_2O_5\text{-}SiO_2\text{-}CaO$.[28]

[iii] G – "Glass"; A – "Apatite"; W – "Wollastonite"
[iv] GC – "Glass-ceramic"
[v] W – "Wollastonite"
[vi] CP – "Whitlockite"

O conhecimento do papel desempenhado pelos iões de silício dissolvidos, esteve na base do desenvolvimento de um novo método para deposição de apatite em diferentes materiais – Método Biomimético. Este é um processo que se desenvolve em duas etapas: nucleação e crescimento. Numa primeira fase é colocado um substrato em contacto com um vidro à base de CaO e SiO_2, numa solução SBF, para que se promova o desenvolvimento de núcleos. O substrato previamente nucleado é depois imerso numa outra solução sobre-saturada em relação à apatite (tipicamente 1,5 SBF) e aqui tem lugar o rápido crescimento do filme apatítico. Este método foi aplicado com êxito no tratamento de diferentes tipos de substratos incluindo aço, titânio, platina, ouro, silício, carbono, alumina, zircónia, polimetilmetacrilato, etc.. O crescimento da camada de apatite é controlado por transporte de massa através da interface cristal-solução. Em relação à força de adesão substrato-apatite verifica-se uma grande variação em função do tipo de material que constitui o substrato.[29-34]

Nos trabalhos desenvolvidos por Kokubo foi reconhecida a importância da composição dos vidros no comportamento bioactivo dos materiais; no entanto, o mecanismo proposto não equaciona expressamente a sua influência.

O mecanismo de Andersson

Os trabalhos realizados por Andersson *et al.*[35,36,37] permitiram propor um novo mecanismo que, embora semelhante ao de Hench, apresenta algumas inovações. Segundo os autores, após uma troca iónica inicial entre um vidro e o meio envolvente a superfície vítrea transforma-se em sílica gel hidratada; a existência de um elevado número de oxigénios não ligantes no gel bem como a sua inerente flexibilidade favorecem a formação de complexos entre o silício e o fósforo. Segundo este mecanismo os iões cálcio libertam-se do vidro e, atravessando a camada de sílica gel, passam para a solução aquosa; só depois retornam à superfície por efeito de compensação de cargas.

A particularidade deste mecanismo reside no papel atribuído à sílica gel – a formação da camada de Ca-P ocorre em simultâneo com a camada de sílica gel e não sobre esta, como proposto por Hench.

Com base no comportamento *in vivo* de diversos vidros, Andersson correlacionou empiricamente a variação da bioactividade de um vidro com a sua composição[36], definindo o que denominou por "Reaction Number", RN, segundo a expressão:

$$RN = 88{,}3875 - 0{,}0116272[SiO_2]^2 - 0{,}980188[Na_2O] - 1{,}12306[CaO] - 1{,}20556[P_2O_5] - 0{,}560527[B_2O_3]^2 - 2{,}08689[Al_2O_3]$$

onde as composições dos diferentes compostos são expressas em percentagem ponderal. Neste modelo empírico, para que um vidro seja bioactivo RN tem de ser superior a 5.

Sendo um vidro um material amorfo, muitas das suas propriedades são aditivas, pelo que este modelo dá bons resultados para uma dada gama de composições. Contudo, apresenta limitações pois não considera os efeitos produzidos por alterações estruturais e a sua aplicabilidade está confinada ao sistema SiO_2-Na_2O-CaO-P_2O_5-B_2O_3-Al_2O_3.

<u>O mecanismo de Li</u>

Li[38] equacionou a importância da formação de grupos silanol e da natureza da carga superficial no desenvolvimento da camada de apatite.

Uma vez que em vidros bioactivos a formação de apatite é precedida pela formação de uma camada rica em silício, Li optou por realizar diversos trabalhos com sílica gel hidratada (pura). Estes estudos permitiram concluir que o material tem a capacidade de induzir a precipitação de apatite em meio SBF. Dada a ausência de elementos alcalinos e/ou alcalino-terrosos os mecanismos anteriormente apresentados não são, pelo menos nas primeiras etapas, aplicáveis. A capacidade de indução de apatite reside, segundo o autor, na elevada densidade de grupos silanol (Si–OH) existentes na superfície deste tipo de sílica que funcionam como pontos nucleantes, à semelhança do que foi proposto por Hench (etapa 3).[39-44]

No entanto, a capacidade de promover a precipitação de apatite não é exclusiva dos grupos Si-OH. Efectivamente, titânia gel e titânio também induzem a formação de

apatite, desde que as suas superfícies sejam suficientemente ricas em grupos Ti-OH.[45-47]

Poder-se-ia pensar que a existência/formação de grupos OH à superfície dos materiais é uma condição necessária e suficiente ao desenvolvimento espontâneo de apatite. Há com efeito materiais, como a alumina gel, que contêm um elevado número de grupos Al-OH à superfície mas não desenvolvem apatite quando imersos em SBF.[38] Assim, a existência de grupos OH pode ser uma condição necessária mas não é suficiente para a precipitação de apatite.

Li *et al*. [38,48] admitem que a natureza eléctrica das superfícies deve desempenhar um importante papel no mecanismo da bioactividade. Os materiais bioactivos apresentam superfícies electricamente negativas, o que não se passa com uma superfície do tipo alumina gel, a qual segundo os autores deve ser electricamente positiva a pH 7,4.

Em suma, o mecanismo proposto por Li refere que a presença de uma superfície electricamente negativa é necessária à adsorção de iões Ca^{2+} e a presença de grupos OH é necessária ao aprisionamento dos iões PO_4^{3-} através da formação de pontes de hidrogénio. Nestas circunstâncias pode-se atingir, nas vizinhanças da superfície do biomaterial, um grau de super saturação capaz de despoletar a precipitação espontânea de apatite.

Assim, segundo Li[38] para que um material seja bioactivo deve ter uma superfície electricamente negativa e dispor ou desenvolver à sua superfície grupos OH em elevadas quantidades.

Os pontos fundamentais dos vários mecanismos

Conciliando os diferentes mecanismos revistos podem-se encontrar muitos pontos em comum, nomeadamente os que decorrem do conhecido processo de corrosão química que os vidros e vidros cerâmicos sofrem quando imersos numa solução (Hench, Andersson e Kokubo), e algumas particularidades que os caracterizam. Os pontos fundamentais residem no processo de nucleação de apatite:

- Existência de uma camada rica em Si-OH à superfície dos vidros que proporciona pontos nucleantes (Hench e Andersson);
- Ausência de uma camada rica em Si-OH à superfície de vidros cerâmicos. Os pontos nucleantes são proporcionados pela existência de Si^{4+} adsorvidos à superfície (Kokubo);
- Preexistência ou formação de grupos OH em superfícies electricamente negativas que proporcionam pontos nucleantes (Li);

e na precipitação de apatite:

- Por adsorção de Ca^{2+} e PO_4^{3-} no topo da camada de sílica gel (Hench);
- Por adsorção de Ca^{2+} e PO_4^{3-} em simultâneo com a formação da camada de sílica gel (Andersson);
- Por adsorção de Ca^{2+} e PO_4^{3-} directamente à superfície de vidros cerâmicos (Kokubo);
- Por adsorção de Ca^{2+} e PO_4^{3-} nas superfícies electricamente negativas e ricas em OH (Li).

4.1.2 - A composição e o papel dos vários componentes do vidro

No início da investigação em biovidros as composições apresentavam invariavelmente pentóxido de fósforo, sílica e óxidos do tipo alcalino (frequentemente Na_2O) e alcalino-terroso (obrigatoriamente CaO). As quantidades de CaO e P_2O_5 eram, em muitas das situações, escolhidas de forma a que a razão atómica Ca/P fosse próxima de 1,67 (valor verificado na hidroxiapatite). Os iões alcalinos eram introduzidos com o objectivo de facilitar o processamento vítreo e de controlar a estabilidade química dos vidros. O papel de SiO_2 era exclusivamente o de formador de vidro.[5,7,49-59]

Os vidros cerâmicos eram desenvolvidos com o objectivo de melhorar as propriedades mecânicas dos vidros base e a hidroxiapatite devia ser uma das fases cristalinas, pois pensava-se que a sua presença era condição necessária e suficiente para garantir a bioactividade dos materiais.[60-63]

Com o evoluir da investigação, e graças às técnicas experimentais cada vez mais sofisticadas, foi possível atribuir outras funções aos vários óxidos constituintes dos

vidros e dos vidros cerâmicos, identificando um conjunto de parâmetros considerados hoje em dia fundamentais para explicar o fenómeno da bioactividade dos materiais.

O silício

A incorporação de sílica em biomateriais poderia parecer algo despropositada uma vez que a presença de silício em mamíferos não é abundante[39]. O silício parece ser bem tolerado no organismo humano desde que presente na forma de monómero ou numa fórmula solúvel, face à boa capacidade de excreção dos excedentes. Em relação aos tecidos ósseos, experiências realizadas em roedores e galináceos permitiram concluir que, embora em pequenas quantidades, o silício está presente em tecidos conjuntivos e ósseos jovens em pleno processo de calcificação. A sua ausência é associada a deficientes formações ósseas. Nestes casos é suposto que o papel do silício seja o de agente de nucleação na deposição de cálcio, sob a forma de silicato de cálcio.[64,65]

Sob o ponto de vista dos materiais, e independentemente das diferentes interpretações biológicas, viu-se anteriormente que em vidros é de extrema importância a presença de silício para a formação da camada apatítica.

Estudos no sistema SiO_2-CaO-Na_2O-P_2O_5 mostraram que vidros com elevada concentração de sílica (50 % ponderal < SiO_2 < 60 % ponderal) formam primeiro uma camada de sílica gel e só depois a camada de apatite sobre a primeira. Em vidros com baixa concentração de sílica (40 % ponderal < SiO_2 < 50 % ponderal) as duas camadas formam-se em simultâneo. Esta diferença de comportamento decorre da diferença nas respectivas durabilidades químicas dos vidros, i.e., na cinética de dissolução.[66] Segundo Filgueiras *et al.*[67] em vidros com um teor de sílica entre 40 % e 50 % ponderal um pequeno aumento desta concentração provoca uma diminuição na cinética das reacções envolvidas na etapa 3 do mecanismo de Hench, não tendo implicações ao nível das etapas 4 e 5. Porém, aumentando a quantidade de sílica para valores da ordem dos 60 % ponderal a etapa 3 é retardada e as seguintes são inibidas, perdendo-se a bioactividade.

O fósforo

O fósforo era inicialmente utilizado com o objectivo de aproximar a composição dos vidros da composição óssea. Em virtude desta suposição foram desenvolvidos vidros cerâmicos para aplicações clínicas à base de fósforo (livres de sílica)[68]. Rapidamente se percebeu que a sua importância era discutível. Kokubo[24] e Andersson[37] concluíram que os iões fosfato necessários à formação da apatite superficial provêm essencialmente da solução envolvente. Kokubo *et al*. desenvolveram vidros, sem fósforo, no sistema binário $CaO\text{-}SiO_2$ que se confirmou serem efectivamente bioactivos.[24,69-71]

Mais tarde concluiu-se que vidros do sistema convencional $Na_2O\text{-}CaO\text{-}SiO_2$ (utilizados no fabrico dos vidros de janela e de garrafa) podem também apresentar uma bioactividade tão elevada quanto a do Bioglass®.[72]

A realização de testes *in vitro* e *in vivo* mostrou que a adição de P_2O_5 a vidros do sistema $CaO\text{-}SiO_2$ provoca um aumento das suas reactividades superficiais e incrementa a força de ligação com os tecidos ósseos, respectivamente.[70,73] Assim, embora dispensável, a inclusão de fósforo na composição vítrea não é nociva à formação da camada de apatite. Pelo contrário, a sua presença pode ajudar a nucleação de fosfatos de cálcio à superfície.

Os outros elementos

Com base no sistema binário $CaO\text{-}SiO_2$ foi estudada a influência da adição de diferentes óxidos como Na_2O[70,73], MgO[70], B_2O_3[70,73], Al_2O_3[70,73,74] e Fe_2O_3[75] e também F^-[70,73] numa tentativa de compreender os seus efeitos.

Em testes *in vitro* em meio acelular verificou-se haver um aumento da reactividade dos vidros com a adição de Na_2O e uma diminuição com a adição de MgO, B_2O_3, F^-, Al_2O_3 e Fe_2O_3. Contudo, a realização de testes *in vivo* mostrou que apenas os vidros com boro e flúor formam uma forte ligação tecido ósseo-implante. Em vidros com sódio a fraca ligação do osso ao implante parece dever-se à formação de uma espessa camada de sílica gel. Já a adição de flúor ao Bioglass® apenas provoca uma alteração na

estrutura da camada apatítica formando-se fluorapatite em vez de hidroxiapatite; a força de ligação tecido ósseo-implante mantém-se inalterada[76].

A presença de alumina em biovidros e em biovidros cerâmicos é particularmente importante dada a sua capacidade para controlar a durabilidade química da fase vítrea.[10,77] Em alguns trabalhos foi indicado o teor máximo de alumina tolerado por um vidro bioactivo. Para que um vidro do sistema $CaO\text{-}SiO_2$ seja bioactivo a quantidade tolerada de Al_2O_3 não deve exceder 1,7 % mol, segundo Ohtsuki *et al.*[74]. Por outro lado Andersson[78] indica o valor de 1,5 % ponderal como o limite para além do qual um vidro perde a sua bioactividade. Este autor sugere que em vidros pouco solúveis a presença de alumina contribui para aumentar a sua resistência à dissolução e, por conseguinte, impede a formação *in vitro* da camada de sílica gel. No entanto, em vidros mais solúveis a sua presença parece contribuir para a estabilização da sílica gel hidratada, através da redução do número de oxigénios não ligantes, inibindo desta forma a precipitação da apatite. Em nenhum destes trabalhos foi feita qualquer discussão sobre a função estrutural desempenhada pelo alumínio.

Em relação ao boro os resultados conhecidos são aparentemente contraditórios. Enquanto que para Hench[5] a introdução de B_2O_3 no Bioglass® promove a sua reactividade, Kokubo *et al.* [79,80,81] observaram que a introdução de B_2O_3 no vidro cerâmico Cerabone A/W® não alterou a ligação tecido ósseo-implante. Contudo, no material de Kokubo B_2O_3 entrou a substituir CaF_2 e no de Hench substituiu SiO_2.

Como já referido, os biovidros apresentam um baixo teor de sílica e um elevado teor de elementos modificadores, pelo que a sua tendência para desvitrificarem é muito grande e pode levantar problemas de processamento. A partir do estudo de vidros do sistema $Na_2O\text{-}K_2O\text{-}MgO\text{-}CaO\text{-}B_2O_3\text{-}P_2O_5\text{-}SiO_2$, Brink[82] sugere que esta tendência pode ser minimizada. Segundo a autora, a redução da quantidade de elementos alcalinos, aliada à substituição de algum Na_2O por K_2O, e o aumento da quantidade de elementos alcalino-terrosos, aliado à substituição de algum CaO por MgO, não provocaram qualquer alteração significativa no comportamento *in vivo.*

Como se depreende dos parágrafos anteriores, o papel do magnésio em vidros não é consensual. Em termos de estrutura vítrea o magnésio é usualmente classificado como modificador; porém, há a possibilidade de entrar na estrutura vítrea em coordenação 4, i.e., como formador[83,84]. A introdução de magnésio em vidros de fósforo provoca

comportamentos anómalos em diversas propriedades[85,86,87]. Em biovidros existem também vários resultados aparentemente contraditórios. Kasuga *et al.*[50] verificaram que a adição de MgO em vidros cerâmicos desenvolvidos no sistema $CaO\text{-}P_2O_5\text{-}SiO_2$ provoca uma diminuição da capacidade de formação de apatite *in vitro*, inibindo-a para valores superiores a 8 % mol. Ebisawa *et al.*[70] referem também uma diminuição da capacidade de formação da apatite em vidros de $CaO.SiO_2$ por adição de MgO, justificando que esta se deve à superior resistência química dos vidros. Alguns dos vidros cerâmicos Bioverit (I e II) têm elevadas quantidades de magnésio na sua composição (6-28 % mol) e no entanto são bioactivos *in vivo* [88,89,90]. Outros autores, como Hench[5] e Moya[91], sugerem que o MgO tem um efeito desprezável na bioactividade. A capacidade dos iões Mg^{2+} para amorfizar a estrutura da hidroxiapatite é sobejamente conhecida na literatura.[92-96]

Também os catiões multivalentes Ta(V)[97], Ti(IV)[97], Sb(III)[97], Zr(IV)[97], La(III)[98,99] e Y(III)[98], dependendo da composição vítrea, podem inibir a formação da camada de apatite.

4.1.3 - O papel das fases vítreas e cristalinas

O papel na bioactividade das fases cristalinas presentes em vidros cerâmicos, nomeadamente apatite, é ainda objecto de discussão. Inicialmente pensava-se que a presença de apatite era, por si só, garante da bioactividade. O estudo do comportamento *in vitro* do vidro cerâmico A/W(Al), obtido por adição de 6,3 % ponderal de alumina ao vidro cerâmico Cerabone A/W® mostrou que este era um material não bioactivo. As fases que constituem este vidro cerâmico são as mesmas do Cerabone A/W® (hidroxiapatite, wollastonite e fase vítrea) que é bioactivo. O autor[24] concluiu assim que a presença de hidroxiapatite em vidros cerâmicos não é essencial para a bioactividade. A perda de bioactividade do vidro cerâmico A/W por adição de alumina foi atribuída à maior estabilidade química da fase vítrea, conferida pela presença da Al_2O_3 nessa fase.

Sabe-se que quer a estabilidade química quer a fracção amorfa da fase residual influenciam directamente a formação da camada de apatite, tornando-a tanto mais dificultada quanto mais estável a matriz vítrea ou quanto menor a fracção de fase

vítrea[100]. A dificuldade em determinar a composição da fase residual vítrea, aliada à diferente solubilidade das várias fases cristalinas, torna a previsão do comportamento bioactivo de vidros cerâmicos, com base na durabilidade química das fases, mais difícil que nos vidros.

A degradibilidade da fase vítrea como condição necessária à bioactividade justificou o desenvolvimento de muitos biocompósitos contendo vidros, quer como matriz quer como fase de reforço. A utilização de zircónia revelou-se particularmente eficiente no desenvolvimento de biocompósitos de matriz vítrea para aplicações onde a solicitação mecânica é muito elevada – a resistência à flexão destes materiais pode atingir cerca de 10 vezes a dos melhores vidros cerâmicos (400 a 1000 MPa). A bioactividade destes compósitos foi explicada recorrendo ao mecanismo proposto por Kokubo.[101-105] Interessante é também a tentativa, bem sucedida, de melhorar o desempenho bioactivo da hidroxiapatite por inclusão de vidros na microestrutura[106,107,108]. Neste caso a melhoria do comportamento bioactivo é atribuída quer à presença de β-fosfato tri-cálcico, formado por reacção entre o vidro e a hidroxiapatite durante a sinterização[109,110], quer à presença do próprio vidro[111].

4.1.4 - A topografia e as características químicas da superfície

Quando um vidro é imerso num meio agressivo sofre uma dissolução e as características da sua superfície são alteradas. Nestas circunstâncias, e sendo a bioactividade um processo essencialmente de superfície, é de admitir que a sua morfologia tenha também importância no processo. Esta possibilidade, referida por vários autores, foi experimentalmente verificada em sílica gel. O tempo necessário à formação da camada de apatite é, neste material, função do tamanho e do volume dos poros, diminuindo com o aumento destes parâmetros. [40,94,112-116]

Com base no conhecimento da importância da presença de grupos OH à superfície e também da importância da textura superficial dos materiais, foi possível transformar materiais não bioactivos ou de reduzida bioactividade em materiais bioactivos. As transformações foram induzidas por tratamentos de natureza química (meio ácido ou básico) e/ou térmica, tendo-se obtido bioactividade *in vitro* em materiais como vidros

cerâmicos inicialmente não bioactivos[117], titânio metálico[118,119,120,121,122], silicone[123], sílica gel[124], titanato de sódio e tântalo[125]. É também possível aumentar a eficiência de um processo biomimético, nomeadamente no que respeita à adesão da camada apatítica, através do tratamento químico (via HCl) da superfície do substrato, nomeadamente quando este é do tipo polimérico[126].

4.1.5 - A estrutura da matriz vítrea

Embora se reconheça que existe uma relação entre a bioactividade e a composição dos vidros e, consequentemente, a sua estrutura, os mecanismos mais divulgados não analisam explicitamente essa relação.

O modelo empírico de Andersson, que prevê a bioactividade a partir da composição vítrea, é bastante restrito. Strnad[127] calculou os parâmetros de Stevels Y e X (ver capítulo anterior – secção 3.1) para descrever o comportamento *in vitro* e *in vivo* de vidros e de vidros cerâmicos. Por exemplo, o vidro de composição $Na_2O.2SiO_2$ apresenta $Y = 3$ e no Bioglass® esse valor é 1,9. Segundo o autor, um vidro é bioactivo quando $Y < 3$ e deixa de o ser para valores superiores a 3. O valor óptimo sugerido é 2. Em relação aos vidros cerâmicos o autor sugere que o método é também aplicável, mas para tal é preciso conhecer a composição da fase residual amorfa.

Com o mesmo objectivo, Hill[128] calculou a conectividade da rede vítrea, valor igual ao de *Y*, de diferentes vidros bioactivos e concluiu que a etapa 2 do mecanismo de Hench depende do valor da conectividade da rede vítrea. Para valores de conectividade de rede superiores a 2 o desenvolvimento da referida etapa pode não ocorrer. Tomando por exemplo o Bioglass, o facto de a conectividade da rede vítrea ser 1,9 significa que as unidades estruturais de silicato presentes são de baixa massa molecular, ou seja no processo de dissolução dos vidros não é necessário quebrar um número elevado de ligações Si–O–Si. Este modelo prevê razoavelmente bem o carácter bioactivo de um vidro e os desvios registados envolvem vidros com fósforo e boro, elementos que têm um elevado potencial para evaporar durante a fusão e também para absorver água.

Uma situação interessante é a que se passa com a incorporação de alumina. O vidro $CaO.SiO_2$ (CS) é bioactivo com $Y = 2$ mas a incorporação de 3 % ponderal (3,4 % mol)

de alumina (vidro CSA) inibe este carácter, aumentando em 10 % o valor de Y (Y = 2,2). Como já referido, nestas circunstâncias a perda de bioactividade é directamente atribuída à presença da alumina[74]; contudo, esta suposição seria correcta se o valor de Y fosse o mesmo nos dois vidros, ou seja, para se estudar o efeito directo da alumina dever-se-ia substituir apenas o catião formador. Como na grande maioria das vezes a alumina actua como formador, a sua inclusão em vidros vai invariavelmente aumentar a conectividade da rede, i.e., em termos estruturais equivale a aumentar o conteúdo de sílica.

Uma das desvantagens deste tipo de abordagem é que não considera o diferente grau de estabilidade estrutural da rede proporcionado pelos iões alumínio ou pelos iões silício. Alguns autores referem que a presença de Al_2O_3 em vidros diminui cerca de 5 vezes a capacidade de libertação de iões silício (em soluções ácidas), i.e., um aumento de 1 % mol de Al_2O_3 corresponde a um aumento de 5 % mol de SiO_2[129]. Acresce ainda o facto de este modelo não distinguir a maior ou menor capacidade dos diferentes modificadores na quebra das ligações Si–O–Si (i.e., na prática um ião divalente equivale a dois iões monovalentes). No entanto, é conhecida a maior capacidade dos iões alcalinos em quebrar as referidas ligações, em detrimento dos alcalino-terrosos[130,131].

Outro problema deste modelo prende-se com o facto de a conectividade da rede ser um valor médio. Num vidro podem coexistir várias espécies Q^n, pelo que o conhecimento da conectividade pode não ser suficiente para uma correcta previsão da bioactividade de um vidro, como a seguir será discutido.

Referências Bibliográficas

[1] Kokubo, T.; Kushitani, H.; Sakka, S.; Kitsugi, T.; Yamamuro, T. – "Solutions Able to Reproduce i*n vivo* Surface-Structure Changes in Bioactive Glass-ceramic A-W", Journal of Biomedical Materials Research, 24, 1990, 721-734.

[2] Hlaváè, J.; Rohanová, D.; Helebrant, A. – "The Effect of Tris-Buffer on the Leaching Behaviour of Bioactive Glass-ceramics", *Ceramics – Silikáty*, 38, 1994, 119-122.

[3] Ogino, M.; Hench, L. L. – "Formation of Calcium Phosphate Films on Silicate Glasses", *Journal of Non-Crystalline Solids*, 38 & 39, 1980, 673-678.

[4] Kim, C. Y.; Clark, A. E.; Hench, L. L. – "Early Stages of Calcium-Phosphate Layer Formation in Bioglasses", *Journal of Non-Crystalline Solids*, 113, 1989, 195-202.

[5] Hench, L. L. – "Bioactive Glasses and Glass-ceramics: A Perspective", *in* Yamamuro, T.; Hench, L. L.; Wilson, J. – *CRC Handbook of Bioactive Ceramics*, 1, Boca Raton, CRC Press, 1990, 7-24.

[6] Hench, L. L.; Andersson, O. – "Bioactive Glasses" *in* Hench, L. L.; Wilson, J. – *An Introduction to Bioceramics*, 1, Singapore, World Scientific, 1993, 41-62.

[7] Hench, L. L. – "Bioceramics: From Concept to Clinic", *Journal of the American Ceramic Society*, 74, 1991, 1487-1510.

[8] Rehman, I.; Hench, L. L.; Bonfield, W.; Smith, R. – "Analysis of Surface Layers on Bioactive Glasses", *Biomaterials*, 15, 1994, 865-870.

[9] Rehman, I.; Knowles, J. C.; Bonfield, W. – "Analysis of In Vitro Reaction Layers Formed on Bioglass Using Thin-Film X-Ray Diffraction and ATR-FTIR Microspectroscopy", *Journal of Biomedical Materials Research*, 44, 1999, 162-166.

[10] Paul, A. – *Chemistry of Glasses*, New York, Chapman and Hall, 1982.

[11] Aza, P. N.; Guitian, F.; Merlos, A.; Lora-Tamayo, E.; Aza, S. – "Bioceramics - Simulated Body Fluid Interfaces: pH and its Influence of Hydroxyapatite Formation", *Journal of Materials Science: Materials in Medicine*, 7, 1996, 399-402.

[12] Kokubo, T.; Ito, S.; Sakka, S.; Yamamuro, T. – "Formation of a High-Strength Bioactive Glass-ceramic in the System MgO-CaO-SiO_2-P_2O_5", *Journal of Materials Science*, 21, 1986, 536-540.

[13] Kitsugi, T.; Nakamura, T.; Yamamuro, T.; Kokubo, T.; Takagi, M.; Shibuya,T. – "SEM-EPMA Observation of Three Types of Apatite-Containing Glass-ceramics Implanted in Bone: the Variance of a Ca-P-Rich Layer", *Journal of Biomedical Materials Research*, 21, 1987, 1155-1171.

[14] Kitsugi, T.; Yamamuro, T.; Nakamura, T.; Kokubo, T.; Takagi, M.; Shibuya, T.; Takeuchi, H.; Ono, M. – "Bonding Behavior Between Two Bioactive Ceramics *in vivo*", *Journal of Biomedical Materials Research*, 21, 1987, 1109-1123.

[15] Yoshii, S.; Kakutani, Y.; Yamamuro, T.; Nakamura, T.; Kitsugi, T.; Oka, M.; Kokubo, T.; Takagi, M. – "Strength of Bonding Between A-W Glass Ceramic and the Surface of Bone Cortex", *Journal of Biomedical Materials Research: Applied Biomaterials*, 22, 1988, 327-338.

[16] Ono, K.; Yamamuro, T.; Nakamura, T.; Kakutani, Y.; Kitsugi, T.; Hyakuna, K.; Kokubo, T.; Oka, M.; Kotoura, Y. – "Apatite-Wollastonite Containing Glass-ceramic-Fibrin Mixture as a Bone Defect Filler", *Journal of Biomedical Materials Research*, 22, 1988, 869-885.

[17] Kitsugi, T.; Yamamuro, T.; Nakamura, T.; Kokubo, T. – "Bone Bonding Behavior of MgO-CaO-SiO_2-P_2O_5-CaF_2 Glass (Mother Glass of A.W-Glass Ceramic)", *Journal of Biomedical Materials Research*, 23, 1989, 631-648.

[18] Neo, M.; Kotani, S.; Nakamura, T.; Yamamuro, T.; Ohtsuki, C.; Kokubo, T.; Bando, Y. – "A Comparative Study of Ultrastructures of the Interfaces Between four Kinds of Surface-Active Ceramic and Bone", *Journal of Biomedical Materials Research*, 26, 1992, 1419-1432.

[19] Neo, M.; Kotani, S.; Fujita, Y.; Nakamura, T.; Yamamuro, T.; Bando, Y.; Ohtsuki, C.; Kokubo, T. – "Differences in Ceramic-Bone Interface Between Surface-Active Ceramics and Resorbable Ceramics: A study by Scanning and Transmission Electron Microscopy", *Journal of Biomedical Materials Research*, 26, 1992, 255-267.

[20] Neo, M.; Nakamura, T.; Ohtsuki, C.; Kokubo, T.; Yamamuro, T. – "Apatite Formation on Three Kinds of Bioactive Material at an Early Stage *in vivo*: A Comparative Study by Transmission Electron Microscopy", *Journal of Biomedical Materials Research*, 27, 1993, 999-1006.

[21] Kokubo, T.; Kushitani, H.; Ohtsuki, C.; Sakka, S.; Yamamuro, T. – "Effects of Ions Dissolved from Bioactive Glass-ceramic on the Surface Apatite Formation", *Journal of Materials Science: Materials in Medicine*, 4, 1993, 1-4.

[22] Kokubo, T.; Ito, S.; Shigematsu, M.; Sakka, S.; Yamamuro, T. – "Mechanical Properties of a New Apatite-Containing Glass-ceramic for Prosthetic Application", *Journal of Materials Science*, 20, 1985, 2001-2004.

[23] Kokubo, T.; Ito, S.; Shigematsu, M.; Sakka, S.; Yamamuro, T. – "Fatigue and Life-Time of Bioactive Glass-ceramic A-W containing Apatite and Wollastonite", *Journal of Materials Science*, 22, 1987, 4067-4070.

[24] Kokubo, T. – "Surface Chemistry of Bioactive Glass-ceramics", *Journal of Non-Crystalline Solids*, 120, 1990, 138-151.

[25] Kokubo, T. – "Bioactive Glass-ceramics: Properties and Applications", *Biomaterials*, 12, 1991, 155-163.

[26] Kokubo, T.; Kushitani, H.; Ohtsuki, C.; Sakka, S.; Yamamuro, T. – "Chemical Reaction of Bioactive Glass and Glass-ceramics with a Simulated Body Fluid", *Journal of Materials Science: Materials in Medicine*, 3, 1992, 79-83.

[27] Ohtsuki, C.; Kokubo, T.; Yamamuro, T. – "Mechanism of Apatite Formation on CaO-SiO_2-P_2O_5 Glasses in a Simulated Body Fluid", *Journal of Non-Crystalline Solids*, 143, 1992, 84-92.

[28] Kokubo, T. – "A/W Glass-ceramics: Processing and Properties" *in* Hench, L. L.; Wilson, J. – *An Introduction to Bioceramics*, 1, Singapore, World Scientific, 1993, 75-88.

[29] Abe, Y.; Kokubo, T.; Yamamuro, Y. – "Apatite Coating on Ceramics, Metals and Polymers Utilizing a Biological Process", *Journal of Materials Science: Materials in Medicine*, 1, 1990, 233-238.

[30] Tanahashi, M.; Hata, K.; Kokubo, T.; Minoda, M.; Miyamoto, T.; Nakamura, T.; Yamamuro, T. – "Effect of Substrate on Apatite Formation by a Biomimetic Process", *in* Yamamuro, T.; Kokubo, T.; Nakamura, T. – *Bioceramics*, 5, Kyoto, Kobunshi Kankokai, 1992, 57-64.

[31] Tanahashi, M.; Yao, T.; Kokubo, T.; Minoda, M.; Myamoto, T.; Nakamura, T.; Yamamuro, T. – "Apatite Coating on Organic Polymers by a Biomimetic Process", *Journal of the American Ceramic Society*, 77, 1994, 2805-2808.

[32] Hata, K.; Kokubo, T.; Nakamura, T.; Yamamuro, T. – "Growth of a Bonelike Apatite Layer on a Substrate by a Biomimetic Process", *Journal of the American Ceramic Society*, 78, 1995, 1049-1053.

[33] Tanahashi, M.; Kokubo, T.; Nakamura, T.; Katsura, Y.; Nagano, M. – "Ultrastructural Study of an Apatite Layer Formed by a Biomimetic Process and ist Bonding to Bone", *Biomaterials*, 17, 1996, 47-51.

[34] Liu, G. J.; Miyaji, F.; Kokubo, T.; Takadama, H; Nakamura, T.; Murakami, A. – "Apatite-Organic Polymer Composites Prepared by a Biomimetic Process: Improvement in Adhesion of the Apatite Layer to the Substrate by Ultraviolet Irradiation", *Journal of Materials Science: Materials in Medicine*, 9, 1998, 285-290.

[35] Andersson, O. H.; Karlsson, K. H.; Kangasniemi, K. – "Calcium Phosphate Formation at the Surface of Bioactive Glass *in vivo*", *Journal of Non-Crystalline Solids*, 119, 1990, 290-296.

[36] Andersson, O. H.; Liu, G.; Karlsson, K. H.;Niemi, L.; Miettinen, J.; Juhanoja, J. – "*In vivo* Behaviour of Glasses in the SiO_2-Na_2O-CaO-P_2O_5-Al_2O_3-B_2O_3 System", *Journal of Materials Science: Materials in Medicine*, 1, 1990, 219-227.

[37] Andersson, O. H.; Karlsson, K. H. – "On the Bioactivity of Silicate Glass", *Journal of Non-Crystalline Solids*, 129, 1991, 145-151.

[38] Li, P. – In vitro *and* in vivo *Calcium Phosphate Induction on Gel Oxides*, PhDThesis, Leiden, 1993.

[39] Iler, R. K. – *The Chemistry of Silica*, New York, John Wiley &Sons, 1979.

[40] Li, P.; Ohtsuki, C.; Kokubo, T.; Nakanishi, K.; Soga, N.; Nakamura, T.; Yamamuro, T. – "Apatite Formation Induced by Silica Gel in a Simulated Body Fluid", *Journal of the American Ceramic Society*, 75, 1992, 2094-2097.

[41] Li, P.; Ohtsuki, C.; Kokubo, T.; Nakanishi, K.; Soga, N.; Nakamura, T.; Yamamuro, T. – "Process of Formation of Bone-like Apatite Layer on Silica Gel", *Journal of Materials Science: Materials in Medicine*, 4, 1993, 127-131.

[42] Cho, S.-B.; Nakanishi, K.; Kokubo, T.; Soga, N.; Ohtsuki, C.; Nakamura, T.; Kitsugi, T.; Yamamuro, T. – "Dependence of Apatite Formation on Silica Gel on Its Structure: Effect of Heat Treatment", *Journal of the American Ceramic Society*, 78, 1995, 1769-1774.

[43] Li, P; Kangasniemi, I.; De Groot; K.; Kokubo, T.; Yli-Urpo, A. U. – "Apatite Crystallization from Metastable Calcium Phosphate Solution on Sol-Gel-Prepared Silica", *Journal of Non-Crystalline Solids*, 168, 1994, 281-286.

[44] Cho, S.B.; Nakanishi, K.; Kokubo, T.; Soga, N.; Ohtsuki, C.; Nakamura, T. – "Apatite Formation on Silica Gel in Simulated Body Fluid: Its Dependence on Structures of Silica Gels Prepared in Different Media", *Journal of Biomedical Materials Research (Applied Biomaterials)*, 33, 1996, 145-151.

[45] Li, P; De Groot; K. – "Calcium Phosphate Formation within Sol-Gel Prepared Titania *in vitro* and *in vivo*", *Journal of Biomedical Materials Research*, 27, 1993, 1495-1500.

[46] Li, P; Kangasniemi, I.; De Groot; K. – "Bonelike Hydroxyapatite Induction by a Gel-Derived Titania on a Titanium Substrate", *Journal of the American Ceramic Society*, 77, 1994, 1307-1312.

[47] Li, P.; Ducheyne, P. – "Quasi-Biological Apatite Film Induced by Titanium in a Simulated Body Fluid", *Journal of Biomedical Materials Research*, 41, 1998, 341-348.

[48] Li, P; Zhang, F. – "The Electrochemistry of a Glass Surface and its Application to Bioactive Glass in Solution", *Journal of Non-Crystalline Solids*, 119, 1990, 112-118.

[49] Pernot, F.; Baldet, P.; Bonnel, F.; Zarzycki, J.; Rabischong, P. – "Development of Phosphate Glass-ceramics for Bone Implants", *Ceramics International*, 9, 1983, 127-131.

[50] Kasuga, T.; Nakagawa, K.; Yoshida, M.; Miyade, E. – "Compositional Dependence of Formation of an Apatite Layer on Glass-ceramics in Simulated Physiological Solution", *Journal of Materials Science*, 22, 1987, 3721-3724.

[51] Yunmao, L.; Zhangje, H.; Anyu, C. – "The Structure and Properties of a New, Biologically Active Glass-ceramics Used as Artificial Bones", *Journal of Non-Crystalline Solids*, 95&96, 1987, 1087-1094.

[52] Lin, F. H.; Hon, M. H. – "A Study on Bioglass Ceramics in the Na_2O-CaO-SiO_2-P_2O_5 System", *Journal of Materials Science*, 23, 1988, 4295-4299.

[53] Luhua, L.; Haihu, Y. – "Research on Bioactive Glass-ceramics", *Journal of Non-Crystalline Solids*, 112, 1989, 156-160.

[54] Shyu, J. J.; Wu, J. M. – "Crystallization of MgO-CaO-SiO_2-P_2O_5 Glass", *Journal of the American Ceramic Society*, 73, 1990, 1062-1068.

[55] Shyu, J. J.; Wu, J. M. – "Effects of Composition Changes on the Crystallization Behavior of MgO-CaO-SiO_2-P_2O_5 Glass-ceramics", *Journal of the American Ceramic Society*, 74, 1991, 2123-2130.

[56] Shyu, J. J.; Wu, J. M. – "Growth Kinetics of Spherulitic Apatite in Some MgO-CaO-SiO_2-P_2O_5 Glasses", *Journal of Materials Science*, 29, 1994, 3167-3171

[57] Berger, G.; Sauer, R.; Steinborn, G.; Wihsmann, F. G.; Thieme, V.; Kohler, S.; Dressel, H. – "Clinical Applications of Surface Reactive Apatite/Wollastonite Containing Glass-ceramic", *in* Mazurin, O. V. – *Proceedings of the XV International Congress on Glass*, 3(a), Leningrad, Nauka, 1989, 120-126.

[58] Liu, D.-M.; Chou, F.-M. – "Formation of a New Bioactive Glass-ceramic", *Journal of Materials Science: Materials in Medicine*, 5, 1994, 7-10.

[59] Pernot, F.; Zarzycki, J.; Bonnel, F.; Rabischong, P.; Baldet, P. – "New Glass-ceramics Materials for Prosthetic Applications", *Journal of Materials Science*, 14, 1979, 1694-1706.

[60] Vogel, W. – "Perspective of the Development of Bioactive Glass-Ceramics for Biomedical Applications, *Journal of Non-Crystalline Solids*, 73, 1985, 593-597.

[61] Vogel, W.; Holand, W. – "The Development of Bioglass Ceramics for Medical Applications" *Angewandte Chemie* (International Edition in English), 26(6), 1987, 526-544.

[62] Vogel, W.; Holand, W.; Naumann, K.; Gummel, J. – "Development of Machineable Bioactive Glass-Ceramics for Medical Uses", *Journal of Non-Crystalline Solids*, 80, 1986, 34-51.

[63] Holand, W.; Vogel, W.; Vogel, J.; Wange, P. – "Control of Apatite Crystallization in Bioactive Glass-Ceramics", *Science of Ceramics*, 14, 1988, 805-811.

[64] Karlsson, K. H.; "Bioactivity of Glass and its Relation to Glass Structure", *Glass Physics and Chemistry (Fizika i Khimiya Stekla)*, 24, 1998, 280-284.

[65] Iler, R. K. – *The Chemistry of Silica*, New York, John Wiley &Sons, 1979, 730-801.

[66] Kim, C. Y.; Clark, A. E.; Hench, L. L. – "Compositional Dependence of Calcium-Phosphate Layer Formation in Fluoride Bioglasses®", *Journal of Biomedical Materials Research*, 26, 1992, 1147-1161.

[67] Filgueiras, M. R.; La Torre, G.; Hench, L. L. – "Solution Effects on the Surface Reactions of a Bioactive Glass", *Journal of Biomedical Materials Research*, 27, 1993, 445-453.

[68] Wange, P.; Vogel, J.; Horn, L.; Holand, W.; Vogel, W. – "The Morphology of Phase Formations in Phosphate Glass-ceramics", *Silicates Industriels*, 7-8, 1990, 231-236.

[69] Ohura, K.; Nakamura, T.; Yamamuro, T.; Kokubo, T.; Ebisawa, Y.; Kotoura, Y.; Oka, M. – "Bone-Bonding Ability of P_2O_5-free $CaO.SiO_2$ Glasses", *Journal of Biomedical Materials Research*, 25, 1991, 357-365.

[70] Ebisawa, Y.; Kokubo, T.; Ohura, K.; Yamamuro, T. – "Bioactivity of $CaO.SiO_2$-based Glasses: *in vitro* Evaluation", *Journal of Materials Science: Materials in Medicine*, 1, 1990, 239-244.

[71] Branda, F.; Fresa, R.; Costantini, A.; Buri, A. – "Bioactivity of $1.25CaO.SiO_2$ Glass: an FTIR and X-Ray Study on Powdered Amples", *Biomaterials*, 17, 1996, 2247-2251.

[72] Kim, H.-M.; Miyaji, F.; Kokubo, T.; Ohtsuki, C.; Nakamura, T. – "Bioactivity of Na_2O-CaO-SiO_2 Glasses", *Journal of the American Ceramic Society*, 78, 1995, 2405-2411.

[73] Ohura, K.; Nakamura, T.; Yamamuro, T.; Ebisawa, Y.; Kokubo, T.; Kotoura, Y.; Oka, M. – "Bioactivity of CaO-SiO_2 Glasses Added with Various Ions", *Journal of Materials Science: Materials in Medicine*, 3, 1992, 95-100.

[74] Ohtsuki, C.; Kokubo, T.; Yamamuro, T. – "Compositional Dependence of Bioactivity of Glasses in the System CaO-SiO_2-Al_2O_3: Its *in vitro* Evaluation", *Journal of Materials Science: Materials in Medicine*, 3, 1992, 119-125.

[75] Ebisawa, Y.; Kokubo, T.; Ohura, K.; Yamamuro, T. – "Bioactivity of Fe_2O_3-Containing CaO-SiO_2 Glasses: *in vitro* Evaluation", *Journal of Materials Science: Materials in Medicine*, 4, 1992, 225-232.

[76] Clark, A. E.; Kim, C. Y.; West, J.; Wilson, J.; Hench, L. L. – "Reactions of Fluoride and Nonfluoride Containing Bioactive Glasses", *in* Yamamuro, T.; Hench, L. L.; Wilson, J. – *CRC Handbook of Bioactive Ceramics*, 1, Boca Raton, CRC Press, 1990, 73-87.

[77] Navarro, J. M.F. – *El Vidrio*, Madrid, C.S.I.C., 1991.

[78] Andersson, Ö. H.; Karlsson, K. H.; Kangasniemi, K.; Yli-Urpo, A. – "Models for Physical Properties and Bioactivity of Phosphate Opal Glasses", *Glastechnische Berichte Glass Science and Technology*, 61, 1988, 300-305.

[79] Kitsugi, T.; Yamamuro, T.; Nakamura, T.; Yoshii, S.; Kokubo, T.; Takagi, M.; Shibuya, T. – "Influence of Substituting B_2O_3 for CaF_2 on the Bonding Behaviour to Bone of Glass-ceramics Containing Apatite and Wollastonite", *Biomaterials*, 13, 1992, 393-399.

[80] Yoshii, S.; Yamamuro, T.; Kitsugi, T.; Nakamura, T.; Kokubo, T., Oka, M.; Shibuya, T.; Takagi, M. – "Bone-Bonding Capability and Mechanical Properties of Modified A-W Glass-ceramic (Animal Studies)", *in* Yamamuro, T.; Hench, L. L.; Wilson, J. – *CRC Handbook of Bioactive Ceramics*, 1, Boca Raton, CRC Press, 1990, 51-63.

[81] Kitsugi, T.; Yamamuro, T.; Yoshii, S.; Kokubo, T.; Takagi, M.; Shibuya, T. – "The Influence of Substituting B_2O_3 for CaF_2 on the Bonding Behavior of A-W Glass-ceramic to Bone Tissue", *in* Yamamuro, T.; Hench, L. L.; Wilson, J. – *CRC Handbook of Bioactive Ceramics*, 1, Boca Raton, CRC Press, 1990, 65-71.

[82] Brink, M. – "The Influence of Alkali and Alkaline Earths on the Working Range for Bioactive Glasses", *Journal of Biomedical Materials Research*, 36, 1997, 109-117.

[83] Merzbacher, C. I.; White, W. B. – "The Structure of Alkaline Earth Aluminosilicate Glasses as Determined by Vibrational Spectroscopy", *Journal of Non-Crystalline Solids*, 130, 1991, 18-34.

[84] Gervais, F.; Blin, A.; Massiot, D.; Coutures, J. P.; Chopinet, M. H.; Naudin, F. – "Infrared Reflectivity Spectroscopy of Silicate Glasses", *Journal of Non-Crystalline Solids*, 89, 1987, 384-401.

[85] Hauret, G.; Vaills, Y.; Luspin, Y.; Gervais, F.; Coté, B. – "Similarities in the Behaviour of Magnesium and Calcium in Silicates Glasses", *Journal of Non-Crystalline Solids*, 170, 1994, 175-181.

[86] Cervinka, L.; Bergerová, J.; Trojan, M. – "An X-Ray Study of Phosphate Glasses of the Composition $[M(PO_3)_2]$ (M=Zn, Cu, Mn, Ca and Mg)", *Journal of Non-Crystalline Solids*, 192&193, 1995, 121-124.

[87] Hoppe, U. – "A Structural Model for Phosphate Glasses", *Journal of Non-Crystalline Solids*, 195, 1996, 138-147.

[88] Vogel, W.; Holand, W. – "Development, Structure, Properties and Application of Glass-ceramics for Medicine", *Journal of Non-Crystalline Solids*, 123, 1990, 349-353.

[89] Wange, P.; Carl, G.; Naumann, K.; Vogel, J.; Vogel, W.; Gotz, W.; Holand, W. – "Development of Glass-ceramics and Ceramic Reinforced Glass-ceramics", *Silicates Industriels*, 1-2, 1991, 21-27.

[90] Holand, W.; Wange, P.; Naumann, K.; Vogel, J.; Carl, G.; Jana, C.; Gotz, W. – "Control of Phase Formation Processes in Glass-ceramics for Medicine and Technology", *Journal of Non-Crystalline Solids*, 129, 1991, 152-162.

[91] Moya, J. S.; Tomsia, A. P.; Pazo, A.; Santos, C.; Guitian, F.- "*In Vitro* Formation of Hydroxylapatite Layer in a MgO-Containing Glass", *Journal of Materials Science: Materials in Medicine*, 5, 1994, 529-532.

[92] Bigi, A.; Falini, G.; Foresti, E.; Gazzano, M.; Ripamonti, A.; Roveri, N. – "Magnesium Influence on Hydroxyapatite Crystallization", *Journal of Inorganic Biochemistry*, 49, 1993, 69-78.

[93] Okazaki, M. – "Crystallographic Properties of Heterogeneous Mg-containing Fluoridated Apatites Synthesized with a Two-Step Supply System", *Biomaterials*, 16, 1995, 703-707.

[94] Li, J.; Liao, H.; Sjostrom, M. – "Characterization of Calcium Phosphates Precipitated from Simulated Body Fluid of Different Buffering Capacities", *Biomaterials*, 18, 1997, 743-747.

[95] Ravaglioli, A.; Krajewski, A.; Celloti, G. C.; Piancastelli, A.; Bacchini, B.; Montanari, L.; Zama, G.; Piombi, L. – "Mineral Evolution of Bone", *Biomaterials*, 17, 1996, 617-622.

[96] Okazaki, M. – "Crystallographic Behaviour of Fluoridated Hydroxyapatites Containing Mg^{2+} and CO_3^{2-} Ions", *Biomaterials*, 12, 1991, 831-835.

[97] Cao, W.; Hench, L. L. – "Bioactive Materials", *Ceramics International*, 22, 1996, 493-507.

[98] Fresa, R.; Costantini, A.; Buri, A.; Branda, F. – "Apatite Formation on $(2-x)CaO.x/3M_2O_3$-$2SiO_2$ Glasses (M=La, Y; $0=<x=<0.6$) in a Simulated Body Fluid", *Biomaterials*, 16, 1995, 1249-1253.

[99] Costantini, A.; Fresa, R., Buri, A.; Branda, F. – "Effect of the Substitution of Y_2O_3 for CaO on the Bioactivity of $2.5CaO$-$2SiO_2$ Glass", *Biomaterials*, 18, 1997, 453-458.

[100] Li, P.; Yang, Q.; Zhang, F.; Kokubo, T. – "The Effect of Residual Glassy Phase in a Bioactive Glass-ceramic on the Formation of its Surface Apatite Layer In Vitro", *Journal of Materials Science: Materials in Medicine*, 3, 1992, 452-456.

[101] Kasuga, T.; Yoshida, M.; Uno, T.; Nakagima, K. – "Preparation of Zirconia-Toughened Bioactive Glass-ceramics", *Journal of Materials Science*, 23, 1988, 2255-2258.

[102] Kasuga, T.; Yoshida, M.; Ikushima, A.; Tuchiya, M.; Kusakari, H. – "Bioactivity of Zirconia-Thoughened Glass-ceramics", *Journal of the American Ceramic Society*, 75, 1992, 1884-1888.

[103] Kasuga, T.; Nakagima, K.; Uno, T.; Yoshida, M. – "Preparation of Zirconia-Toughened Bioactive Glass-ceramic Composite by Sinter-Hot Isostatic Pressing", *Journal of the American Ceramic Society*, 75, 1992, 1103-1107.

[104] Kasuga, T.; Yoshida, M.; Ikushima, A. J.; Tuchiya, M.; Kusakari, H. – "Stability of Zirconia-toughened Bioactive Glass-ceramics: *In vivo* Study Using Dogs", *Journal of Materials Science: Materials in Medicine*, 4, 1993, 36-39.

[105] Krajewski, A.; Ravaglioli, A.; Mazzocchi, M.; Fini, M. – "Coating of ZrO_2 Supports with a Biological Glass", *Journal of Materials Science: Materials in Medicine*, 9, 1998, 309-316.

[106] Santos, J. D.; Knowles, J. C.; Reis, R. L.; Monteiro, F. J.; Hastings, G. W. – "Microstructural Characterization of Glass-Reinforced Hydroxyapatite Composites", *Biomaterials*, 15, 1994, 5-10.

[107] Knowles, J. C.; Talal, S.; Santos, J. D. – "Sintering Effects in a Glass Reinforced Hydroxyapatite", *Biomaterials*, 17, 1996, 1437-1442.

[108] Knowles, J. C. – "Development of Hydroxyapatite with Enhanced Mechanical Properties: Effect of High Glass Additions on Mechanical Properties and Phase Stability of Sintered Hydroxyapatite", *British Ceramic Transactions*, 93, 1994, 100-103.

[109] Santos, J. D.; Jha, L. J.; Monteiro, F. J. – "*In vitro* Calcium Phosphate Formation on SiO_2-Na_2O-CaO-P_2O_5 Glass Reinforced Hydroxyapatite Composite: A Study by XPS Analysis", *Journal of Materials Science: Materials in Medicine*, 7, 1996, 181-185.

[110] Lopes, M. A.; Santos, J. D.; Monteiro, F. J.; Knowles, J. C. – "Glass-Reiforced Hydroxyapatite: A Comprehensive Study of the effect of Glass Composition on the Crystallography of the Composite", *Journal of Biomedical Materials Research*, 39, 1998, 244-251.

[111] Pazo, A.; Santos, C.; Guitian, F.; Tomsia, A. P.; Moya, J. S. – "HA-Bioactive Glass Composites: High Temperature Reactivity and *in vitro* Behavior", *Scripta Materialia*, 34, 1996, 1729-1733.

[112] Li, P.; Nakanishi, K.; Kokubo, T.; Groot, K. – "Induction and Morphology of Hydroxyapatite Precipitated from Metastable Simulated Body Fluid on Sol-Gel prepared Silica", *Biomaterials*, 14, 1993, 963-968.

[113] Gross, U. M.; Muller-Mai, C. M.; Voigt, C. – "The Interface of Calcium-Phosphate and Glass-ceramic in Bone, a Structural Analysis", *Biomaterials*, 11, 1990, 83-85.

[114] El-Ghannam, A.; Ducheyne, P.; Shapiro, I. M. – "Formation of Surface Reaction Products on Bioactive Glass and their Effects on the Expression of the Osteblastic Phenotype and the Deposition of Mineralized Extracellular Matrix", *Biomaterials*, 18, 1997, 295-303.

[115] Peltola, T.; Jokinen, M.; Rahiala, H.; Levänen, E.; Rosenholm, J. B.; Kangasniemi, I.; Yli-Urpo, A. – "Calcium Phosphate Formation on Porous Sol-Gel-Derived SiO_2 and CaO-P_2O_5-SiO_2 Substrates *in vitro"*, *Journal of Biomedical Materials Research*, 44, 1999, 12-21.

[116] Pereira, M. M.; Clarck, A. E.; Hench, L. L. – "Effect of Texture on the Rate of Hydroxyapatite Formation on Gel-Silica Surface", *Journal of the American Ceramic Society*, 78, 1995, 2463-2468.

[117] Cho, S.-B.; Miyaji, F.; Kokubo, T.; Nakamura, T. – "Induction of Bioactivity of a non-Bioactive Glass-ceramic by a Chemical Treatment", *Biomaterials*, 18, 1997, 1479-1485.

[118] Kokubo, T.; Miyaji, F.; Kim, H.M.; Nakamura, T. – "Spontaneous Formation of Bonelike Apatite Layer on Chemically Treated Titanium Metals", *Journal of the American Ceramic Society*, 79, 1996, 1127-1129.

[119] Kim, H. M.; Miyaji, F.; Kokubo, T.; Nakamuro, T. – "Apatite-forming Ability of Alkali-treated Ti Metal in Body Environment", *Journal of the Ceramic Society of Japan*, 105, 1997, 118-123.

[120] Kim, H.-M.; Miyaji, F.; Kokubo, T.; Nakamura, T. – "Bonding Strength of Bonelike Apatite Layer to Ti Metal Substrate", *Journal of Biomedical Materials Research: Applied Biomaterials*, 38, 1997, 121-127.

[121] Kim, H. M.; Miyaji, F.; Kokubo, T.; Nakamuro, T. – "Effect of Heat Treatment on Apatite-forming Ability of Ti Metal Induced by Alkali Treatment", *Journal of Materials Science: Materials in Medicine*, 8, 1997, 341-347.

[122] Wen, H. B.; Liu, Q.; Wijn, J. R.; Groot, K.; Cui.; F. Z. – "Preparation of Bioactive Microporous Titanium Surface by a New Two-Step Chemical Treatment", *Journal of Materials Science: Materials in Medicine*, 9, 1998, 121-128.

[123] Miyaji, F.; Iwai, M.; Kokubo, T.; Nakamura, T. – "Chemical Surface Treatment of Silicone for Induncing its Bioactivity", *Journal of Materials Science: Materials in Medicine*, 9, 1998, 61-65.

[124] Cho, S. B.; Miyaji, F.; kokubo, T.; Nakanishi, K.; Soga, N.; Nakamura, T. – "Apatite Formation on Silica Gel in Simulated Body Fluid: Effects of Structural Modification with Solvent-Exchange", *Journal of Materials Science: Materials in Medicine*, 9, 1998, 279-284.

[125] Kokubo, T.; Kim, H.-M.; Miyaji, F.; Miyazaki, T.; Nakamura, T. – "A Role of Amorphous Phase in Inducing Bioactivity" *in* Choudhary, M. K.; Huff, N. T.; Drummond III, C. H. – *Proceedings of the XVIII International Congress in Glass*, C5: Glass Surfaces-Chemical and Biological Interactions, The American Ceramic Society (CD-ROM), Ohio, 1998, 30-35.

[126] Tanahashi, M.; Yao, T.; Kokubo, T.; Minoda, M.; Myamoto, T.; Nakamura, T.; Yamamuro, T. – "Apatite Coated on Organic Polymers by Biomimetic Process: Improvement in Adhesion to Substrate by HCl Treatment", *Journal of Materials Science: Materials in Medicine*, 6, 1995, 319-326.

[127] Strnad, Z. – "Role of the Glass Phase in Bioactive Glass-ceramics", *Biomaterials*, 13, 1992, 317-321.

[128] Hill, R. – "An Alternative View of the Degradation of Bioglass", *Journal of Materials Science Letters*, 15, 1996, 1122-1125.

[129] Andersson, Ö. H.; Södergard, A. – "Solubility and Film Formation of Phosphate and Alumina Containing Glasses", *Journal of Non-Crystalline Solids*, 246, 1999, 9-15.

[130] Wallace, K. E.; Hill, R. G.; Pembroke, J. T.; Brown, C. J.; Hatton, P. V. – "Influence of Sodium Oxide Content on Bioactive Glass Properties", *Journal of Materials Science: Materials in Medicine*, 10, 1999, 697-701

[131] Lockyer, M. W.; Holland, D.; Dupree, R. – "NMR Investigation of the Structure of Some Bioactive and Related Glasses", *Journal of Non-Crystalline Solids*, 188, 1995, 207-219.

4.2 - Effects of Si Speciation on the *in vitro* Bioactivity of Glasses

J. M. Oliveira, R. N. Correia, M. H. Fernandes

UIMC, Department of Ceramics and Glass Engineering, University of Aveiro, 3810-193 Aveiro, PORTUGAL

(Biomaterials, submitted)

Abstract

The surface reactivity of glasses belonging to the (mol %) $31SiO_2$-$11P_2O_5$-(58-*x*)CaO-*x*MgO series, with *x* ranging from 0 to 32, was studied in Kokubo's simulated body fluid (SBF). Scanning electron microscopy (SEM), induced coupled plasma (ICP), and Fourier transform infrared (FTIR) spectroscopy were used to characterise the glass surface and the SBF compositional changes. All glasses develop surface layers rich in silica and calcium phosphate. An increasing surface activity with increasing MgO/CaO ratio was observed. In a previous investigation using magic-angle spinning (MAS) nuclear magnetic resonance (NMR) it was found that there is an increasing abundance of Q^0 species in the glass structure with increasing MgO content. The present work shows that, when immersed in SBF, Q^0-rich glasses are easily leached to form a silica gel layer. It is concluded that MgO in the glass indirectly improves the early stages of mineralization by favouring Q^0 speciation. This mechanism plays an important role in glass bioactivity.

Keywords*: Bioactive glasses, magnesium oxide, in vitro tests, apatite layer, glass speciation, biomineralization.*

1. Introduction

Nowadays, it is possible to find magnesium oxide in a considerable number of bioactive glasses and glass-ceramics, but the role of magnesium in their bioactivity is not completely clear.

The first bioactive glass - Bioglass® - developed by Hench *et al.*[1] was MgO-free, with composition (wt. %): 45 SiO_2, 24.5 CaO, 24.5 Na_2O and 6 P_2O_5. Based on its *in vitro* behaviour in inorganic media the authors proposed a five-stage interfacial reaction leading to calcium phosphate deposition. The mechanism involves surface leaching with sodium-proton exchange and loss of soluble silica, formation of silanol groups, formation of an hydrated silica gel film by polycondensation of silanols, development of an amorphous calcium phosphate layer onto the silica-rich layer and crystallization of hydroxycarbonate apatite (HCA) layer by incorporating OH^-, CO_3^{2-} and F^- ions. This HCA layer is necessary for the tissues to bond to the implant, being the bone bonding ratio dependent on its formation[2]. Later, Hench *et al.*[3] reported that substitution of CaO by MgO had little effect on bone bonding, while additions of 1-1.5 wt. % Al_2O_3 prevented it. West *et al.*[4] working with molecular orbital models proposed that only a special type of silanol groups (trigonal siloxane rings) would be able to induce apatite nucleation. Work done by Cho *et al.*[5-7] also suggests that only a certain type of structural unit of silanol groups is effective for apatite nucleation.

The first materials incorporating magnesium oxide were Ceravital® glasses and the resulting glass-ceramic materials[8]. The base Ceravital® glasses contain (wt. %) 40-50 SiO_2, 10-15 P_2O_5, 5-10 Na_2O, 0.5-3.0 K_2O and 2.5-5 MgO. From the set of Ceravital materials, glasses and glass ceramics KG Cera (2.9 wt. % MgO) and Mina (5 wt. % MgO) were prepared. The authors reported an intimate contact between living tissues and these materials (push-out strength of 4 MPa). From *in vivo* tests they also reported that small additions of Al_2O_3 inhibit bone bonding. The bone-bonding mechanism of Ceravital glass ceramics (KGS) involves the formation of an apatite layer[9].

Vogel *et al.*[10] developed the Bioverit family of glass ceramics in which MgO content is in the range 6-28 mol %. These glass-ceramics have apatite, mica and/or cordierite crystals in their structure. The authors reported a direct intergrowth between the materials and the living tissues.

In 1981 Kokubo *et al.*[11] working with glasses of the SiO_2-CaO-P_2O_5-MgO system developed the A-W.G glass containing (wt. %) 4.6 MgO, 44.7 CaO, 34 SiO_2 16.2 P_2O_5 and 0.5 CaF_2. An apatite and wollastonite-containing glass ceramic (A-W.GC) was obtained by crystallization of a glass powder compact. They also developed the A.GC and the A-W-CP.GC glass ceramics, being the first rich in apatite and the second in apatite, wollastonite and tri-calcium phosphate. When in contact with SBF solution these materials developed an HCA layer with compositional and structural characteristics similar to the one developed on the Bioglass surface[12]. Also, the glass A-W.G formed silica- and Ca,P- rich layers at the interface with bone tissues in 2 days after implantation[13]. From the set of Kokubo's materials the glass A-W.G is the one with lower bone bonding strength and thicker Si-layer, which led the authors to speculate about the role of this layer in providing the weakest interface. It is also reported that the presence of crystalline apatite is not necessary for the implant to bond to living tissues[14], the same applying to the presence of phosphorus in the composition[15]. Kokubo[16,17] proposed a mechanism to explain the bioactive behaviour of these materials based on glass-ceramic leaching with Ca^{2+} and Si^{4+} dissolution and increase in the local fluid supersaturation with respect to apatite, followed by nucleation of apatite on sites of the material surface provided by dissolution of the silicate ions. Later Ohtsuki *et al.*[18] working with CaO-SiO_2-P_2O_5 glasses, showed that the non-bioactive $CaO.P_2O_5$ composition increases the degree of supersaturation more than the bioactive $CaO.SiO_2$ glass, concluding that the degree of supersaturation may not be so important for apatite deposition as the formation of an hydrated silica layer on the glass. A non-bioactive alumina-containing glass-ceramic A-W(Al) developed an apatite rich-layer when immersed in a synthetic fluid with calcium and silicate ions added simultaneously, which means that soluble silicate ions play an important role in silica layer formation[19]. However, a silica layer was not detected on the A-W.GC surface tested in SBF solution.

Kasuga *et al.*[20] investigated the role of magnesium oxide in glasses and glass-ceramics of the system CaO-P_2O_5-SiO_2-MgO (Al_2O_3) in a pseudo-extracellular fluid (PECF). They found that the ability to form the apatite layer in glass-ceramics decreases with increasing MgO content, so that glass-ceramics with more than 8 wt. % MgO did not form such layer.

Ebisawa *et al.*[15] reported that the rate of apatite formation in SBF decreases with increasing MgO additions to $CaO.SiO_2$ glass and that this could be interpreted in terms of the suppressing effect of MgO on the dissolution of calcium, thus inhibiting the formation of the silica gel layer.

Moya *et al.*[21] working with a glass of nominal composition (wt. %) 54.5 SiO_2, 12.0 Na_2O, 4.0 K_2O, 15.0 CaO, 8.5 MgO and 6.0 P_2O_5 found that the role of Mg^{2+} in the formation of Ca-P rich layer was insignificant.

From an analogy with the silicon chemistry of diatoms and connective tissues Karlsson *et al.*[22] suggested that HCA develops from bidentate chelates between silica gel and phosphate. Later Andersson[23,24] working with MgO-free glasses suggested that, as phosphate in solution exists as HPO_4^{2-} ions, they would penetrate into the silica gel layer forming $Si\text{-}O\text{-}PO_3^{2-}$. This silica-phosphate gel layer would be stabilised with Ca^{2+}.

There are differences in the above mechanisms with respect to the role of silica. Kokubo suggested that dissolved silica has an active role on the formation of HCA. The other authors envisage mineralization as promoted by precipitated silica, either by accommodation of phosphate ions within the gel (Andersson) or by development of the HCA layer on top of the gel (Hench).

The presence of surface charges has also been considered to influence apatite formation on a bioactive glass[25]. In fact, not only silica gel induces apatite formation in SBF, due to the abundance of silanol groups on the material surface[26,27]; the ability of titania gel to develop an apatitic layer is attributed to the existence of Ti-OH groups responsible for nucleation[28]. However, Li[28] showed that there was no formation of a Ca-P rich layer on alumina gel. In these circumstances, it is clear that not all OH groups are apatite inducers and Li[28] proposed that the OH^- containing surfaces must develop a negative charge in order to promote apatite nucleation.

Another interesting approach to understand the bioactive behaviour of glasses and glass-ceramics was followed by Strnad[29] and Hill[30]. Strnad correlates the bioactive behaviour of glass-ceramics with the structural Stevels' parameter Y that corresponds to the mean number of bridging oxygens per polyhedron. Hill uses the network approach to inorganic glass structures and proposes the cross-linking density as a measure of the network connectivity, which, in turn, would condition glass reactivity.

Other factors also influence the bioactive behaviour of glasses and glass-ceramics. Li *et al.*[31] reported that in glass-ceramics the glassy phase controls the HCA rate formation since the crystalline phases have much lower dissolution rates. The influence of surface roughness was also reported and it can play a role in the bioactive properties of glasses and glass-ceramics[32,33].

The effect of MgO in bioactive glasses is somewhat controversial or ambiguous. Oliveira *et al.*[34] developed a glass with high magnesium oxide content (17.25 wt. %) that showed a Ca-P rich layer after immersion in a SBF solution. In the present paper the authors report the effect of magnesium on glass surface reactivity in SBF through its effect on glass structure.

2. Experimental Procedure

Seven glasses belonging to the (mol %) $31SiO_2$-$11P_2O_5$-(58-*x*)CaO-*x*MgO series were prepared as previously reported[35]. The investigated glass compositions are listed in Table I.

Table I. Glass compositions.

	Composition (mol %)			
Sample	SiO_2	CaO	P_2O_5	MgO
CM1	31.1	58.4	10.6	0.0
CM2	31.1	52.9	10.6	5.5
CM3	31.1	47.6	10.6	10.8
CM4	31.1	42.3	10.6	16.0
CM5	31.1	37.0	10.6	21.4
CM6	31.1	31.7	10.6	26.6
CM7	31.1	26.4	10.6	32.0

All glasses were cast into metal moulds, annealed at *Tg* temperatures for 30 minutes and slowly cooled to room temperature. Composition CM1 devitrified on casting and composition CM2 showed tendency for surface crystallization; they were not used in further tests.

Small pieces of glasses CM3 to CM7 were cut into prismatic specimens of about 7 x 7 x 1.3 mm^3. These were polished with 15 μm diamond paste and washed sequentially with water for 1 min and acetone for 5 min, in an ultrasonic cleaner. *In vitro* tests were carried out by immersing the specimens in flasks containing 20 ml of a synthesized solution with chemical composition close to the inorganic fraction of human blood plasma (Table II), buffered at pH 7.4 with trishydroxymethylaminomethane and hydrochloric acid. The flasks with the solution and the specimens were maintained at 37 °C for 3, 7 and 15 days during the *in vitro* experiments.

Table II. Ion concentration (mM) of simulated body fluid (SBF) and human blood plasma.

	Na^+	K^+	Ca^{2+}	Mg^{2+}	Cl^-	HCO^{3-}	HPO_4^{2-}	SO^{4-}
Plasma	142.0	5.0	2.5	1.5	103.0	27.0	1.0	0.5
SBF	142.0	5.0	2.5	1.5	148.8	4.2	1.0	0.5

After these periods the samples were removed, gently washed with deionised water, dried at room temperature and their surfaces observed by SEM on a Hitachi S-4100 and microanalysed by energy dispersive spectroscopy (EDS). The solution was analysed for Si, Ca, Mg and P by ICP emission spectroscopy using a Jobin-Yvon JY70 Plus spectrometer.

The deposited layer was detached and characterised by infrared absorption analysis in a computer-processed FTIR spectrometer Mattson 7000 using powder/KBr pellets. Spectra were obtained between 4000-400cm^{-1} wavenumber, with a resolution of 2 cm^{-1}.

3. Results

Figure 1 shows the microstructures of CM3, CM5 and CM7 etched for 15 s in 1M HNO_3. The glasses show a dispersed phase, consisting of amorphous silica[36] morular-like precipitates, whose contents increases with increasing MgO in the glass[35].

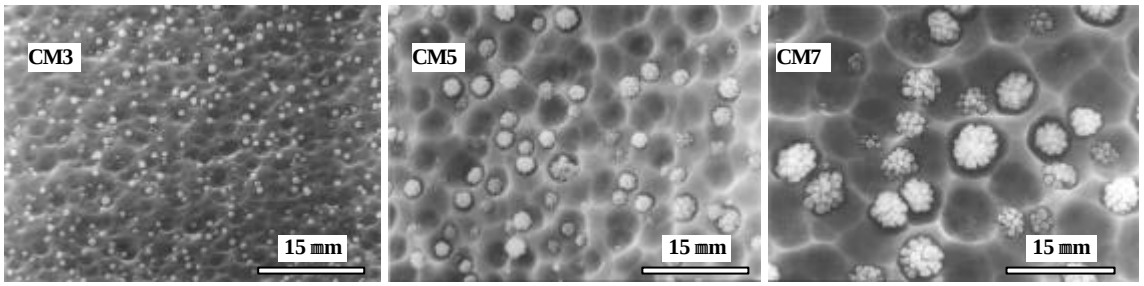

Fig. 1. SEM micrographs of glasses from the CM series.

After soaking in SBF solution all glasses present a surface layer with multiple cracks that was easily peeled out, especially for longer immersion times. The precipitated layer shows a tendency to become thicker for longer immersion times and higher MgO content in the glass.

Figure 2 shows the precipitate formed on specimens CM3 and CM7 after 3 and 15 days in SBF. EDS results indicate that the precipitated layer is Ca-P rich in the outside, with an Ca/P atomic ratio ranging 1.4-1.6, and Si-rich in its inner portion (close to the glass). No significant amounts of magnesium were detected in these layers, but it is likely that small amounts will be present in the outer part, due to the ability of alkaline-earth ions to interchange in calcium phosphate lattices[37]. The morphology of the calcium phosphate surface is quite similar for all materials, presenting particles tightly packed in spherical aggregates.

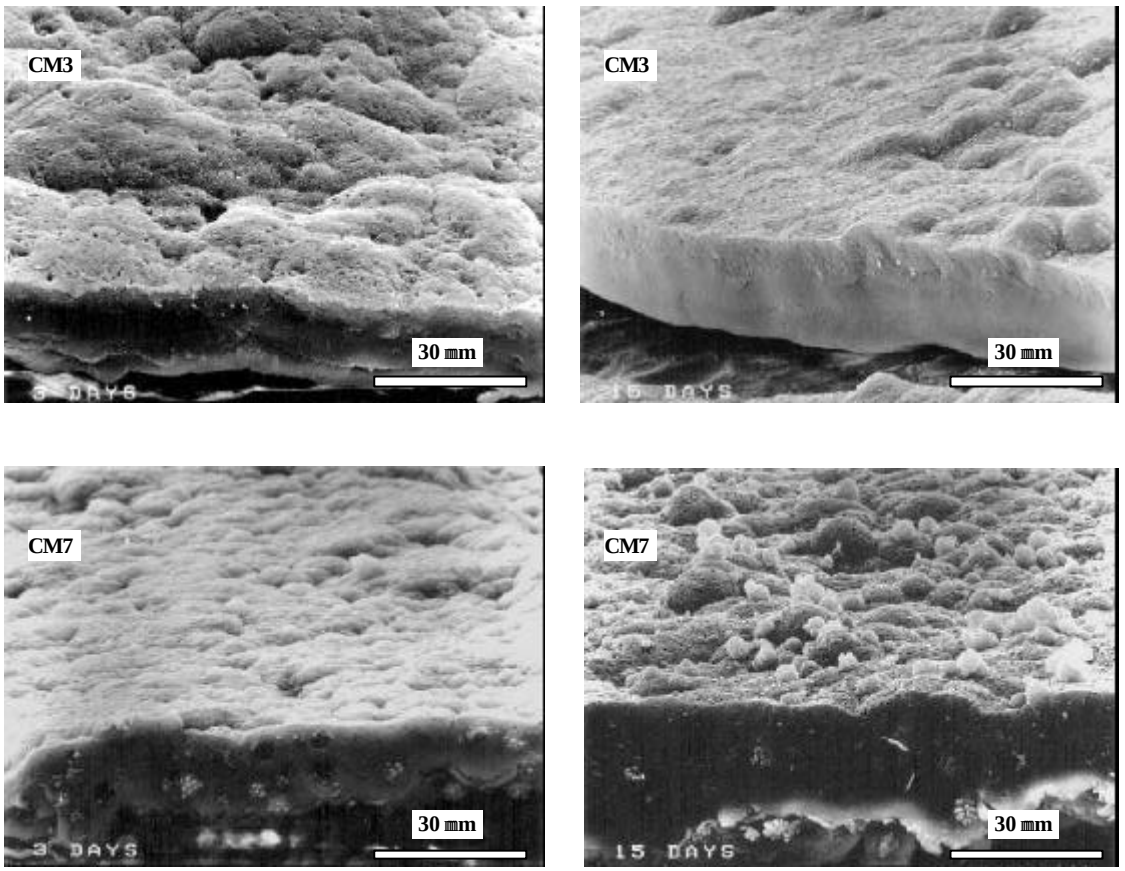

Fig. 2. SEM micrographs of the Ca-P rich layer formed onto CM3 and CM7 glasses after 3 and 15 days in SBF.

Figure 3 correlates the elemental concentrations of Si, Ca, P and Mg in SBF with the magnesium oxide content in glass, for different immersion times. Silicon concentration, taken as a measure of apparent solubility of CM glasses, and magnesium concentration show similar trends, increasing with MgO content in the glass, and more significantly so for 15 days tests. The calcium and phosphorus concentration changes shows also similarities between them, decreasing with increasing MgO content in glass. The depletion in calcium and phosphorus indicates that they are precipitating on the material surface.

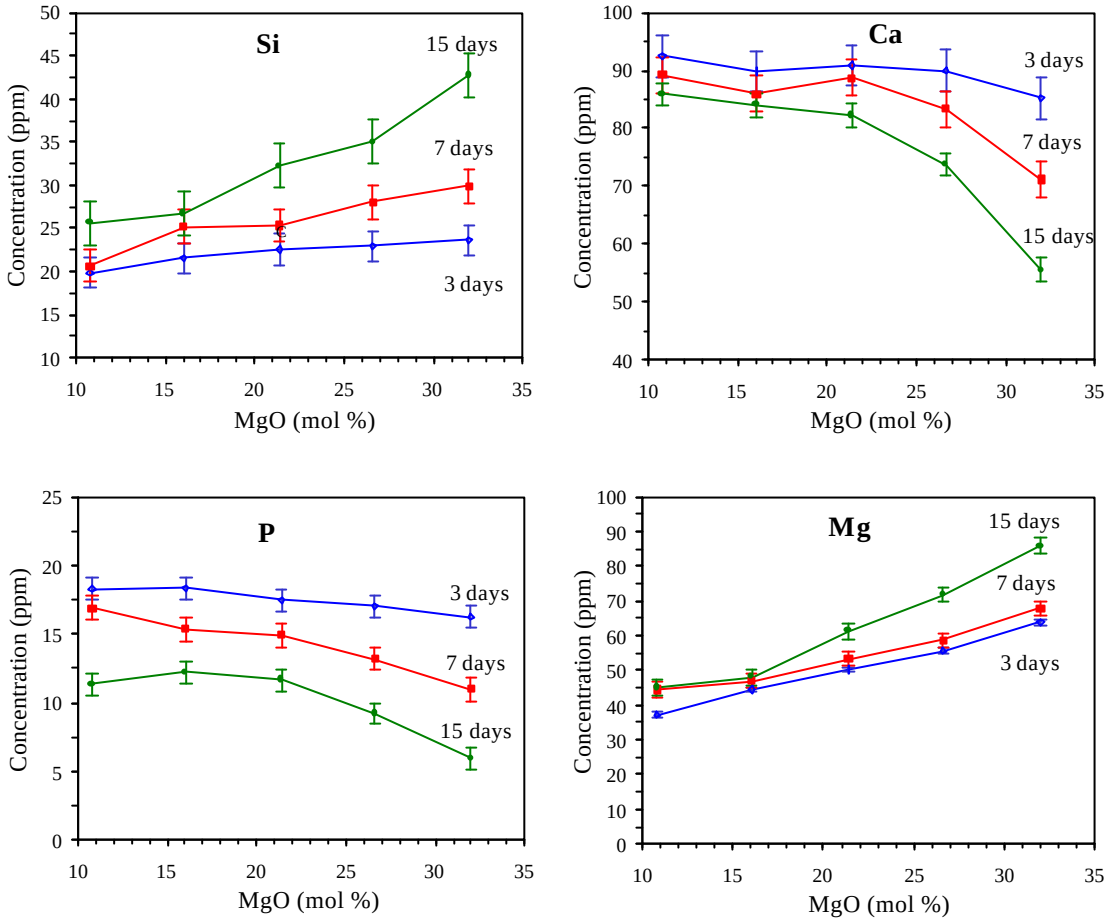

Fig. 3. Elemental concentrations in SBF after immersion of glass specimens with different MgO content for 3, 7, and 15 days.

For each glass sample silicon and magnesium concentrations gradually increase with immersion time while calcium and phosphorus concentrations decrease. The higher rates of change occur for the higher-MgO glasses (CM6 and CM7); therefore, these glasses present a higher surface activity.

In Figure 4 it is shown that the pH of the SBF solutions increases with MgO content in the glass, for each soaking time. For each glass composition the pH increases with soaking time.

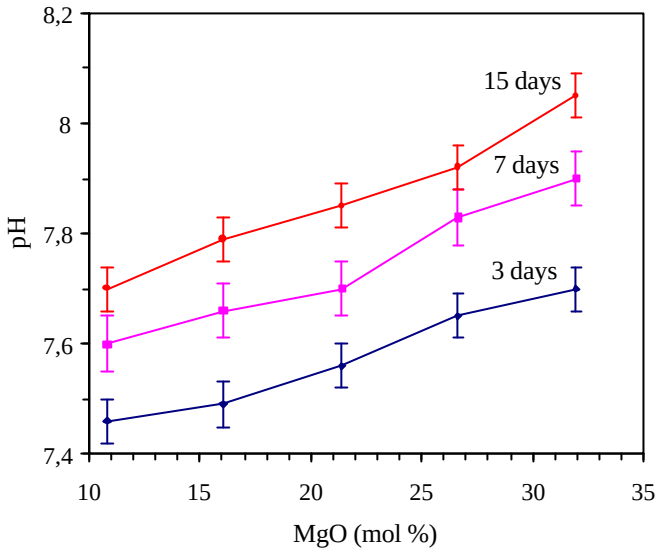

Fig. 4. pH of SBF solution after immersion of glass specimens with different MgO content for 3, 7, and 15 days.

Figure 5 shows the IR spectra of the detached precipitates formed on the glass surface after 3, 7 and 15 days in SBF. Bands were assigned on the basis on published data according to Table III.[38,39]

Table III. FTIR band assignment.

Wavenumber (cm^{-1})		Vibration Mode
This work	Published data[38,39]	
1460-1410	1415-1465	ν_3 (C-O stretch)
1100-1085	1095	ν_3 (Si-O-Si stretch)
1046-1036	1045, 1025	ν_3 (P-O stretch)
~960	960	ν_1 (P-O stretch)
875-870	878	ν_2 (C-O stretch)
805-795	800	ν_1 (Si-O bend)
602-600	602	ν_4 (P-O bend)
564-560	572	ν_4 (P-O bend)
476-473	455-470	ν_4 (Si-O-Si bend)

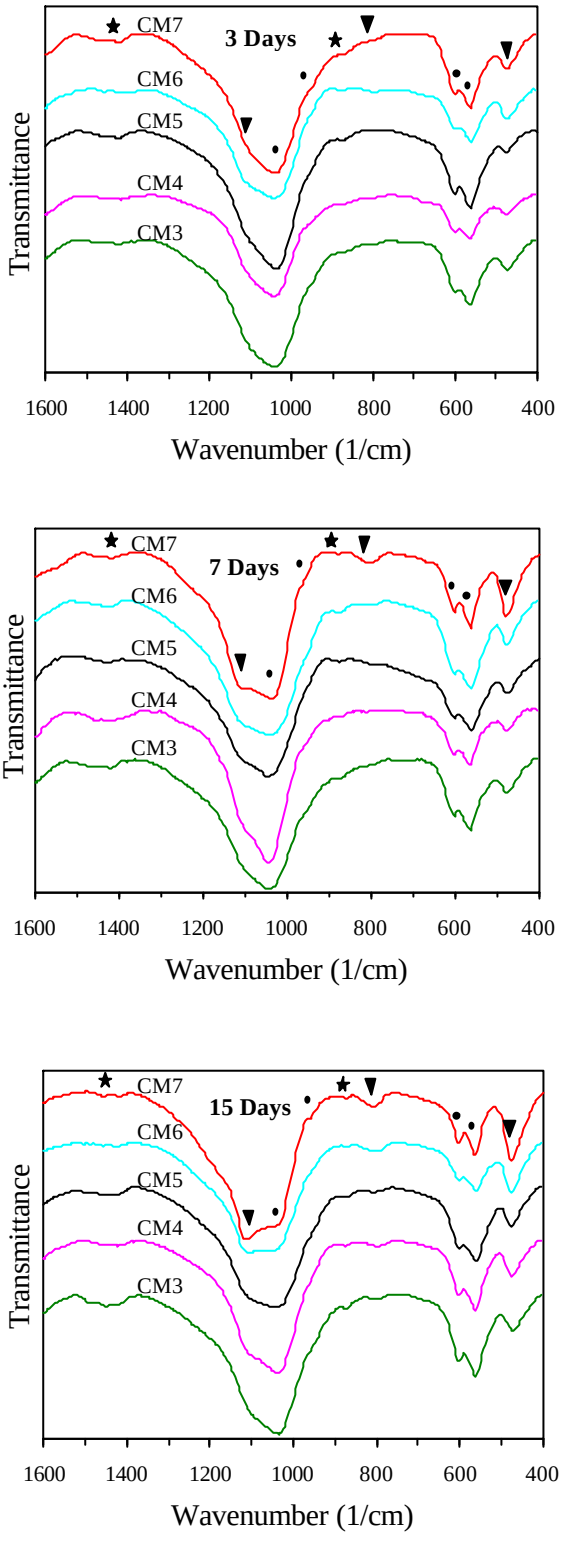

Fig. 5. FTIR spectra of CM glasses after 3, 7 and 15 days in SBF. ▼ - silica gel; ● - apatite; ★ - carbonate ion.

Roughly, all FTIR measurements yielded similar spectra, although with different band intensities. From the tabulated assignments it is clear that a silica-rich layer is present, together with a carbonate-containing hydroxyapatite layer. The small broad peak at 875-870 cm^{-1}, assigned to C-O vibrations in a CO_3^{2-} ion, could also be caused by HPO_4^{2-} ions but it seems that its intensity grows simultaneously with the one at 1460-1410 cm^{-1} and so it was assigned to CO_3^{2-} ion. The presence of two peaks at ~600cm^{-1} and 560cm^{-1} means that this layer is crystalline after 3 days. Peaks at ca. 1010 cm^{-1} (Si-O bonds with one non-bridging oxygen) and at ca. 920 cm^{-1} (Si-O bonds with two non-bridging oxygen) were not detected, indicating that the silica-rich layer is polymerised for the immersion times used[39]. In the 3 day-samples the layers are not so structurally different among them. However, in the 7 and 15 day-tests a progressive increase in the relative intensities of the Si-O bands is observed, especially between ν_4(Si-O)/ν_4(P-O) and ν_3(Si-O)/ν_3(P-O), showing an enrichment in silica gel.

4. Discussion

The CM glasses develop a dual silica-calcium phosphate layer in SBF. The following discussion will be based on the mechanism proposed by Hench[2-4] to explain the glass surface activity, namely, the existence of a silica gel layer as a supplier of calcium phosphate nucleation sites.

In this glass series the amount of (Ca+Mg) was kept constant, as well as the Si/(Ca+Mg) and P/(Ca+Mg) ratios. In general the extraction rate of alkaline-earth ions from a silicate glass decreases with decreasing ionic radius[40] and so reduction in CM glass leaching was expected as the MgO content increases. However, an increasing surface activity is observed instead. With increasing MgO content in the glass and for each immersion time FTIR spectra (Figure 5) show a more intense vibrational band for Si-O and Si-O-Si bonds, while Si^{4+} and Mg^{2+} ion concentration (Figure 3) and pH (Figure 4) changes indicate an increasing leaching; matching SEM images show a slight tendency for increasing layer thickness. Since it is known that silica gel thickness increases with glass surface leaching[41], those results enable us to conclude that the

amount of silica gel present in the precipitated layer increases with increasing MgO content in the glass. These findings are explained as follows.

In a previous work Oliveira *et al.*[35] showed that replacing CaO by MgO in this glass series promotes the disruption of Si-O-Si bonds and increases the amount of dispersed phase by means of a disproportionation reaction producing orthosilicate and silica, $2Q^2 \rightleftharpoons Q^0 + Q^4$, where Q represents the silicon atom and the exponent the number of bridging oxygens. Therefore, in CM series the glass matrices become more depolymerised as MgO content increases i.e. the glass matrix becomes richer in anionic species with relatively high charge density, $Q^0 = SiO_4^{4-}$, and the average chain length of Q^2 species becomes smaller. It may thus be inferred that the Mg^{2+} ion preferentially neutralises orthosilicate charges. In the same paper it was showed that Mg ions in a phosphorus environment directly replace Ca ions, keeping the orthophosphate arrangement.

There are reports in the literature[40,42] indicating that orthosilicates hydrolyse more rapidly than other silicate species (e.g. disilicates, chain silicates), i. e. bridging oxygens are much more resistant to attack than non-bridging oxygens. So, the presence of orthosilicate species will promote an easier glass leaching by exchanging H_3O^+ ions from solution with alkaline-earth ions concentrated in orthosilicate positions. In fact, Figures 3 and 4 show that increasing MgO content in the glass increases the dissolution of magnesium, with the corresponding rising in pH. At the same time, loss of soluble silicon occurs, which is supposed to enhance the repolymerization of the silica gel layer (Figure 5) according to the mechanism of silica gel formation[42]. Above pH=2 this mechanism involves polymerisation with condensation, catalysed by OH^- according to the following reaction:

$$2SiOH \overset{OH^-}{\rightleftharpoons} Si–O–Si + H_2O \qquad (1)$$

It is assumed that silica gel formation involves condensation between Si–OH groups formed at the material surface and Si–OH of the dissolved silicate present in SBF. In fact, Kokubo at al.[19] showed that when a non bioactive glass-ceramic was immersed in a silicate-containing SBF solution it could develop an apatite layer at the

surface, and Hayakawa *et al.*[43] also reported that condensation between the Si–OH units formed at a glass surface and dissolved Si–OH can be the dominant mechanism.

Thus, stages 1, 2 and 3 of the mechanism proposed by Hench[2] are thought to be enhanced as a result of a disproportionation by MgO in the glass, giving rise to an amorphous silica gel with an open arrangement necessary to accommodate Ca and P ions.

SBF depletion in Ca and P concentrations is observed (Figure 3). These changes are associated to the Ca-P rich layer formation. Figure 5 indicates that the apatite structure formed contains CO_3^{2-} ions but, especially in the case of 15-day tests, the layer become less crystallised as MgO in the glass increases, since the C-O and P-O band intensities show a slight tendency to broaden. This behaviour is attributed to increasing amounts of magnesium ions in the SBF solution. About the role of magnesium ions in solution, Filgueiras *et al.*[44] reported that stages 1-3 are not significantly affected by SBF composition, whereas stages 4 and 5 are retarded by the presence of magnesium in SBF. It is well known that biological apatites contain trace elements, among which Mg^{2+} is the most abundant; nevertheless, it promotes amorphization of the apatite structure, and increases its solubility[37,45].

It is worth noting that Karlsson speculated that Q^0 species may activate glass-bone bonding[46] and it is known that cations have a preference to bond to sites with higher negative charge density[47]. Kim *et al.*[39] reported that glasses with <50 mol % SiO_2 form a Ca-P rich layer and a Si layer simultaneously while glasses with >50 mol % SiO_2 form a Ca-P layer on the top of a Si-rich layer due to their different structures: the authors reported that the first one has an inverted glass structure and so it contains isolated SiO_4 tetrahedra.

All the CM glasses have the same average polymerisation, as calculated by their composition, being the Stevel's parameter[29], Y, 1.4. Therefore, although the average polymerisation of a glass can be theoretically calculated from its composition, the real distribution of silicon species may vary accordingly to equilibrium speciation reactions. These reactions are well known in alkaline silicate glasses[48], which, together with alkaline-earth silicate glasses, are being investigated since a long time ago for biomedical applications.

Apart from the measured rate of Si dissolution, evidence for an easier detachability of the mineralised layer with increasing MgO glass content was found. This is explained based on the development of the silica gel layer. Glasses richer in MgO develop a thicker gel, and this circumstance can play a decisive role in layer detachment through the gel in agreement with other results[13].

5. Conclusions

Glasses with increasing surface activity where developed by replacing calcium oxide by magnesium oxide in the (mol %) $31SiO_2$-$11P_2O_5$-(58-*x*)CaO-*x*MgO series. MgO disrupts the glass matrix network by means of a disproportionation reaction. It is concluded that glass speciation plays an important role in the bioactive behaviour of glasses, being Q0 species the more active in promoting stages 1-3 of Hench's mechanism.

By controlling the amount of MgO in the glass it is possible to control the thickness of the silica gel layer.

It is not correct to assume that MgO in glasses behaves always like CaO, even being both oxide glass network-modifiers

References

[1] Hench, L. L.; Splinter, R. J.; Allen W. C.; Greenlee, T. K. – "Bonding Mechanisms at the Interface of Ceramic Prosthethic Materials", *Journal of Biomedical Materials Research Symposium*, 36, 1971, 117-141.

[2] Hench, L. L. – "Bioceramics: from Concept to Clinic", *Journal of the American Ceramic Society*, 74, 1991, 1487-1510.

[3] Hench, L. L.; Andersson, O. – "Bioactive Glasses" *in* Hench, L. L.; Wilson, J. – *An Introduction to Bioceramics*, 1, Singapore, World Scientific, 1993, 41-62.

[4] West, J. K.; Hench, L. L. – "Reaction Kinetics of Bioactive Ceramics Part V: Molecular Orbital Modelling of Bioactive Glass Surface Reactions" *in* Yamamuro, T.; Kokubo, T.; Nakamura, T. – *Proceedings of the 5th International Symposium on Ceramics in Medicine*, *Bioceramics*, 5, Kyoto, Kobunshi Kankokai, 1992, 75-86.

[5] Cho, S.-B.; Nakanishi, K.; Kokubo, T.; Soga, N.; Ohtsuki, C.; Nakamura, T.; Kitsugi, T.; Yamamuro, T. – "Dependence of Apatite Formation on Silica Gel on its Structure: Effect of Heat Treatment", *Journal of the American Ceramic Society*, 78, 1995, 1769-1774.

[6] Cho, S.-B.; Nakanishi, K.; Kokubo, T.; Soga, N.; Ohtsuki, C.; Nakamura, T. – "Apatite Formation on Silica Gel in Simulated Body Fluid: its Dependence on Structures of Silica Gels Prepared in Different Media", *Journal of Biomedical Materials Research (Applied Biomaterials)*, 33, 1996, 145-151.

[7] Cho, S.-B,; Miyaji, F.; Kokubo, T.; Nakanishi, K.; Soga, N.; Nakamura, T. – "Apatite Formation on Silica Gel in Simulated Body Fluid: Effects of Structural Modification with Solvent-Exchange", *Journal of Materials Science: Materials in Medicine*, 9, 1998, 279-284.

[8] Bromer, H.; Deutscher, K.; Blencke, B.; Pfeil, E.; Strunz, V. – "Properties of the Bioactive Implant Material *Ceravital*", *Science of Ceramics*, 9, 1977, 219-225.

[9] Ohtsuki, C.; Kushitani, H.; Kokubo, T.; Kotani, S.; Yamamuro, T. – "Apatite Formation on the Surface of Ceravital-type Glass-ceramic in the Body", *Journal of Biomedical Materials Research*, 25, 199, 1363-1370.

[10] Vogel, W.; Holand, W. – "Development, Structure, Properties and Applications of Glass-ceramics for Medicine", *Journal of Non-Crystalline Solids*, 123, 1990, 349-353.

[11] Kokubo, T.; Shigematsu, M.; Nagashima, Y.; Tashiro, M.; Nakamura, T.; Yamamuro, T.; Higashi, S. – "Apatite- and Wollastonite-containing Glass-ceramic for Prosthetic Application", *Bulletin of the Institute for Chemical Research, Kyoto University*, 60, 1982, 260-268.

[12] Kokubo, T.; Kushitani, H.; Sakka, S.; Kitsugi, T.; Yamamuro, T. – "Solutions Able to Reproduce *in vivo* Surface-structure Changes in Bioactive Glass-ceramic A-W", *Journal of Biomedical Materials Research*, 24, 1990, 721-734.

[13] Kitsugi, T.; Yamamuro, T.; Nakamura, T.; Kokubo, T. – "Bone Bonding Behaviour of MgO-CaO-SiO_2-P_2O_5-CaF_2 Glass (Mother Glass of A*W-Glass Ceramic)", *Journal of Biomedical Materials Research*, 23, 1989, 631-648.

[14] Ohtsuki, C.; Kokubo, T.; Yamamuro, T. – "Compositional Dependence of Bioactivity of Glasses in the System CaO-SiO_2-Al_2O_3: its *in vitro* Evaluation", *Journal of Materials Science: Materials in Medicine*, 3, 1992, 119-125.

[15] Ebisawa, Y.; Kokubo, T.; Ohura, K.; Yamamuro, T. – "Bioactivity of CaO.SiO_2-based Glasses: *in vitro* Evaluation", *Journal of Materials Science: Materials in Medicine*, 1, 1990, 239-244.

[16] Kokubo, T. – "Surface Chemistry of Bioactive Glass-ceramics", *Journal of Non-Crystalline Solids*, 120, 1990, 138-151.

[17] Kokubo, T. – "Bioactive Glass-ceramics: Properties and Applications", *Biomaterials*, 12, 1991, 155-163.

[18] Ohtsuki, C.; Kokubo, T.; Yamamuro, T. – "Mechanism of Apatite Formation on CaO-SiO_2-P_2O_5 Glasses in a Simulated Body Fluid", *Journal of Non-Crystalline Solids*, 143, 1992, 84-92.

[19] Kokubo, T.; Kushitani, H.; Ohtsuki, C.; Sakka, S.; Yamamuro, T. – "Effects of Ions Dissolved from Bioactive Glass-ceramic on the Surface Apatite Formation", *Journal of Materials Science: Materials in Medicine*, 4, 1993, 1-4.

[20] Kasuga, T.; Nakagawa, K.; Yoshida, M.; Miyade, E. – "Compositional Dependence of Formation of an Apatite Layer on Glass-ceramics in Simulated Physiological Solution", *Journal of Materials Science*, 22, 1987, 3721-3724.

[21] Moya, J. S.; Tomsia, A. P.; Pazo, A.; Santos, C.; Guitian, F. – "*In vitro* Formation of Hydroxilapatite Layer in a MgO-containing Glass", *Journal of Materials Science: Materials in Medicine*, 5, 1994, 529-532.

[22] Karlsson, K. H.; Froberg, K.; Ringbom, T. – "A Structural Approach to Bone Adhering of Bioactive Glasses", *Journal of Non-Crystalline Solids*, 112, 1989, 69-72.

[23] Andersson, O. H.; Karlsson, K. H.; Kangasniemi, K. – "Calcium Phosphate Formation at the Surface of Bioactive Glass *in vivo*", *Journal of Non-Crystalline Solids*, 119, 1990, 290-296.

[24] Andersson, O. H.; Karlsson K. H. – "On the Bioactivity of Silicate Glass", *Journal of Non-Crystalline Solids*, 129, 1991, 145-151.

[25] Li, P.; Zhang, F. – "The Electrochemistry of a Glass Surface and its Application to Bioactive Glass in Solution", *Journal of Non-Crystalline Solids*, 119, 1990, 112-118.

[26] Li, P.; Ohtsuki, C.; Kokubo, T.; Nakaniishi, K.; Soga, N.; Nakamura, T.; Yamamuro, T. – "Apatite Formation Induced by Silica Gel in a Simulated Body Fluid", *Journal of the American Ceramic Society*, 75, 1992, 2094-2097.

[27] Li, P.; Ohtsuki, C.; Kokubo, T.; Nakanishi, K.; Soga, N.; Nakamura, T.; Yamamuro, T. – "Process of Formation of Bone-like Apatite Layer on Silica Gel", *Journal of Materials Science: Materials in Medicine*, 4, 1993, 127-131.

[28] Li, P. – "*In vitro* and *in vivo* Calcium Phosphate Induction on Gel Oxides", PhD Thesis, Leiden, 1993.

[29] Strnad, Z. – "Role of the Glass Phase in Bioactive Glass-ceramics", *Biomaterials*, 13, 1992, 317-321.

[30] Hill, R. – "An Alternative View of the Degradation of Bioglass", *Journal of Materials Science Letters*, 15, 1996, 112-1125.

[31] Li, P.; Ohtsuki, C.; Kokubo, T.; Nakanishi, K.; Soga, N.; Nakamura, T.; Yamamuro, T. – "Process of Formation of Bone-like Apatite Layer on Silica Gel", *Journal of Materials Science: Materials in Medicine*, 4, 1993, 127-131.

[32] Pereira, M. M.; Clark, A. E.; Hench, L. L. – "Effect of Texture on the Rate of Hydroxyapatite Formation on Gel-Silica Surface", *Journal of the American Ceramic Society*, 78, 1995, 2463-2468.

[33] Salinas. A.; Román, J.; Vallet, M.; Oliveira, J. M.; Correia, R. N.; Fernandes, M. H. – "*In vitro* Bioactivity of Glass and Glass Ceramics of the $3CaO.P_2O_5$-$CaO.SiO_2$-$CaO.MgO.2SiO_2$ System", *Biomaterials*, 21, 2000, 251-257.

[34] Oliveira, J. M.; Correia, R. N.; Fernandes, M. H. – "Surface Modifications of a Glass and a Glass-ceramic of the MgO-$3CaO.P_2O_5$-SiO_2 System in a Simulated Body Fluid", *Biomaterials*, 16, 1994, 849-854.

[35] Oliveira, J. M.; Correia, R. N.; Fernandes, M. H.; Rocha, J. – "Influence of the CaO/MgO Ratio on the Structure of Phase-Separated Glasses: a Solid State ^{29}Si and ^{31}P MAS NMR Study", *Journal of Non-Crystalline Solids*, 265, 2000, 221-229.

[36] Oliveira, J. M.; Correia, R. N.; Fernandes, M. H. – "Formation of Convoluted Silica Precipitates During Amorphous Phase Separation in the $Ca_3(PO_4)_2$-SiO_2-MgO System", *Journal of the American Ceramic Society*, 2000, *in press*.

[37] Bigi, A.; Falini, G.; Foresti, E.; Gazzano, M.; Ripamonti, A.; Roveri, N. – "Magnesium Influence on Hydroxyapatite Crystallization", *Journal of Inorganic Biochemistry*, 49, 1993, 69-78.

[38] Farmer, V. C. – *The Infrared Spectra of Minerals*, London, Mineralogical Society, 1974.

[39] Kim, C. Y.; Clark, A. E.; Hench, L. L. – "Compositional Dependence of Calcium Phosphate Layer Formation in Fluoride Bioglasses®", *Journal of Biomedical Materials Research*, 26, 1992, 1147-1161.

[40] Paul, A. – *Chemistry of Glasses*, London, Chapman and Hall,1982.

[41] Ebisawa, Y.; Kokubo, T.; Ohura, K.; Yamamuro, T. – "Bioactivity of Fe_2O_3-containing CaO-SiO_2 Glasses: *in vitro* Evaluation", *Journal of Materials Science: Materials in Medicine*, 4, 1992, 225-232.

[42] Iler, R. K. – *The Chemistry of Silica*, New York, John & Sons,1979.

[43] Hayakawa, S.; Tsuru, K.; Ohtsuki, C.; Osaka, A. – "Mechanism of Apatite Formation on a Sodium Silicate Glass in a Simulated Body Fluid", *Journal of the American Ceramic Society*, 82, 1999, 2155-2160.

[44] Filgueiras, M. R. T.; LaTorre, G.; Hench, L. L. – "Solution Effects on the Surface Reactions of Three Bioactive Glass Compositions", *Journal of Biomedical Materials Research*, 27, 1993, 1485-1493.

[45] Okazaki, M. – "Crystallographic Behaviour of Fluoridated Hydroxyapatites Containing Mg^{2+} and CO_3^{2-} Ions", *Biomaterials*, 12, 1991, 831-835.

[46] Karlsson, K. H. – "Bioactivity of Glass and its Relation to Glass Structure", *Glass Physics and Chemistry (Fizika i Khimiya Stekla)*, 24, 1998, 280-284.

[47] Merzbacher, C. I.; White, W. B. – "The Structure of Alkaline Earth Aluminosilicate Glasses as Determined by Vibrational Spectroscopy", *Journal of Non-Crystalline Solids*, 130, 1991, 18-34.

[48] Matson, D. W.; Sharma, S. K.; Philpotts, J. A. – "The Structure of High-Silica Glasses. A Raman Spectroscopic Investigation", *Journal of Non-Crystalline Solids*, 58, 1983, 323-352.

4.3 - *In vitro* Bioactivity of Glass and Glass-ceramics of the $3CaO.P_2O_5$-$CaO.SiO_2$-$CaO.MgO.2SiO_2$ System

A.J. Salinas, J. Roman, M. Vallet-Regi

Dept Quimica Inorganica y Bioinorganica, Facultad de Farmacia, UCM, 28040 Madrid, SPAIN

J. M. Oliveira, R. N. Correia, M. H. Fernandes

UIMC, Departamento de Engenharia Cerâmica e do Vidro, Universidade de Aveiro, 3810-193 Aveiro, PORTUGAL

(Biomaterials, 21(3), 2000, 251-257)

Abstract

A glass of nominal composition (wt %) 40.0 CaO-34.5 SiO_2-16.5 P_2O_5-8.5 MgO-0.5 CaF_2 has been obtained (G13). The glass showed *in vitro* bioactivity evidenced by the formation on its surface of a calcium phosphate-rich layer when soaked in a solution with ionic composition analogous to human plasma. By thermal treatments of G13, a glass-ceramic (GC13) containing apatite, diopside, althausite and akermanite as crystalline phases was developed. GC13 as-made did not show *in vitro* bioactivity. However, after chemical treatment of GC13 with HCl 1M (GC13-HCl), the *in vitro* studies showed the formation of an apatite-like layer covering certain areas of the material surface. The influence of both chemical and morphological factors on the *in vitro* bioactivity has been studied.

Keywords: *bioactive glasses, bioactive glass-ceramics, bioceramics, in vitro studies, surface morphology.*

1. Introduction

Bioceramics, including glasses and glass-ceramics, are currently used as implant materials, usually for bone substitution[1]. Since biomaterials contact with living tissues, their surface chemistry need to be optimised to meet the requirements of host tissues, being desirable that they are bioactive[2,3], i. e., form an interfacial bond with living tissues.

Bioactive implants should react chemically with body fluids in a manner compatible with the repair process of the tissues. First, an amorphous calcium phosphate (a-CaP) rich layer is formed on the surface of the bioactive materials when implanted. The initial a-CaP crystallizes to hydroxycarbonate apatite (HCA) analogous to that present in bones. The HCA crystals, together with collagen fibres form the bonding layer[1].

In the last years it has been observed that the calcium phosphate-rich layer also forms on the surface of bioactive ceramics when they are soaked in synthetic solutions simulating physiological plasma. For the *in vitro* study of Bioglass®, Hench *et al.* used the so-called Tris-buffered solution (Tris-buffer), i.e., distilled water buffered with tris-hydroxymethylaminomethane[4]. For the *in vitro* study of the glass-ceramic A-W Kokubo *et al*. proposed in 1990 the Tris-buffered Simulated Body Fluid (SBF) No.9[5] with an ion concentration nearly equal to that of human blood plasma. Since, unlike Tris-buffer alone, SBF contains calcium and phosphorus ions it can be used to study the *in vitro* bioactivity of a wider variety of materials. Therefore, the *in vitro* studies in SBF have become very popular as preliminary tests on new candidates to implant materials.

Glass-ceramics seem to be well-suited for use in biomedical applications. Natural bones and teeth are multiphase materials; their combination of properties probably can be simulated only by multiphase materials. Although composite fabrication appears as a possibility to create multiphase materials, crystallization of glasses seems to be a very effective way to simulate hard tissues for those applications where elastic modulus mismatch and toughness are not important.

A part of the glass-ceramics developed in the last years for biomedical applications is based on the CaO-MgO-P_2O_5-SiO_2 system[6-13]. Small amounts of other components like CaF_2[6-8,12] or TiO_2[10] have been added to the initial composition to facilitate

processing.

The occurrence of surface or bulk crystallization determines the way of processing the glass-ceramic. When the surface crystallization rate is low, the glass-ceramic may be obtained by thermal treatment of glass monoliths. However, when that rate is significant, glasses are generally ceramised via powder technology routes similar to those employed for ceramics, to avoid the formation of cracks in the glass-ceramic specimens[14]. Glasses of the above system have been crystallized either: as powder compacts [6-2,12] or in bulk form [9-13] depending on the composition studied. However, independently of the route used, two crystalline phases have been usually identified in the glass-ceramic materials: a silicate: wollastonite[6-8,12], diopside[9-11], akermanite[12] or enstatite[13] and a phosphate: apatite[6-8] or whitlockite [6-11,13].

One of the controversial topics in the study of bioactive glasses and glass-ceramics is the influence of the MgO content in the properties of these biomaterials. For glasses it is generally assumed that addition of MgO to their composition decreases the bioactivity, as reported by Ebisawa *et al.* [15] for a SiO_2-CaO based glass. However, preliminary results in the system MgO-CaO-P_2O_5-SiO_2 have shown that an increase of the MgO content on the glass could improve the ability to form the calcium and phosphorus-rich layer[16].

In this work, a glass (G13) with the same tricalcium phosphate content as the A/W composition [7] but with higher MgO content (13 mol-% instead of 7.2 mol-%) was prepared as part of an investigation on the role of MgO in the *in vitro* bioactivity of glasses and glass-ceramics of the system $3CaO.P_2O_5$-$CaO.SiO_2$-$CaO.MgO.2SiO_2$. G13 monoliths were processed to obtain a glass-ceramic (GC13). On the basis of recent studies by Cho *et al.*[17], GC13 was chemically treated with HCl (GC13-HCl), in order to improve its bioactivity. *In vitro* studies in SBF for G13, GC13 and GC13-HCl were performed.

2. Experimental procedure

Reagent-grade powders of $CaCO_3$, SiO_2, $Ca(H_2PO_4)_2$, MgO and CaF_2 were mixed in the required proportions to obtain a glass with the nominal composition (wt %) 40.0 CaO-34.5 SiO_2-16.5 P_2O_5-8.5 MgO and 0.5 CaF_2. The powders were ball milled in an agate mortar for 1 hour with ethanol and then dried in two steps at 60^0C for 12 h and 150^0C for l h, to drive of the volatile components. After each drying step the powder was reground to ensure homogeneity.

The dried powder was melted for two hours in a platinum crucible at 1475^0C and quenched in water.

After drying, 300 mg of glass powder with particle diameter below 45 μm were submitted to a Differential Thermal Analysis (DTA) test in an alumina crucible under atmospheric conditions at a heating rate of 10°C/min from room temperature up to 1100°C using calcined alumina powder as standard. DTA traces were used to determine the glass transition temperature and the temperatures at which crystallization of the relevant crystalline phases occurred.

The glass powder was melted again at 1475°C for 30 minutes and poured onto a metal plate. The glassy block was annealed for 30 minutes at 702°C and then slowly cooled to room temperature to obtain the cast glass (G13).

On the basis of the DTA results several heat treatments were performed to obtain a glass-ceramic. A crack-free glass-ceramic (GC13) was obtained by applying the heat treatment schedule shown in Fig. 1.

The parent glass and the glass-ceramic were cut by a low-speed diamond disc to prismatic pieces of dimensions 10x10xl.5 mm^3. These specimens were polished with α-alumina powder and washed sequentially with water and acetone for 15 minutes in an ultrasonic cleaner.

GC13 pieces were chemically treated with hydrochloric acid (HCl) 1M for ten minutes. After soaking, the pieces (GC13-HCl) were removed from the solution, washed with ion-exchanged distilled water and dried at room temperature.

Samples G13, GC13 and GC13-HCl were studied by X-Ray Diffraction (XRD) using a Philips X'Pert diffractometer with CuK_α radiation, by Scanning Electron Microscopy (SEM) on a Hitachi 54100, and by Energy Dispersive X-Ray Spectroscopy

(EDS) on a LINK AN10000 System connected to a JEOL 6400 SEM Microscope.

In vitro bioactivity tests of all the specimens were carried out in polyethylene containers soaking the samples at 37°C for different times in 45 ml of SBF, whose composition is shown in Table I. Pieces were mounted vertically in a special platinum scaffold to avoid deposition by gravity. Surface modifications of the materials were studied by XRD operating in (2θ, θ) and with low angle incidence (θ = 1°), SEM and EDS.

3. Results

3.1 Glass

3.1.1 XRD and DTA analyses

The XRD pattern of the cast glass G13 did not show any diffraction *maxima,* which confirms its amorphous nature. The DTA trace of the glass powder after the first melting is depicted in Fig. 2. An endothermal effect starting at 702°C corresponds to the glass transition. Thus, 702°C was used for annealing the glass block. In addition, the DTA curve indicated the formation of at least two crystalline phases, according to the exothermal peaks detected around 852°C and 891°C.

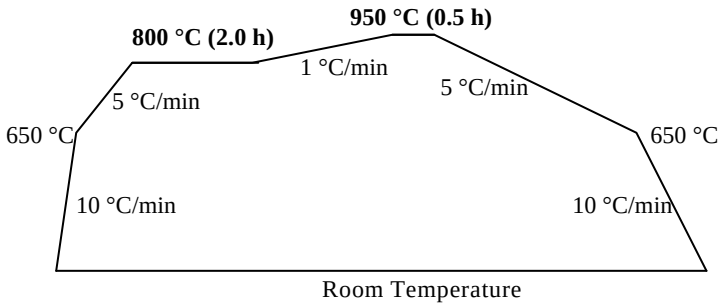

Fig. 1. Heat treatment schedule for ceramising the glass G13.

Table I. Ionic concentration (mM) in SBF and human plasma.

	Na^+	K^+	Ca^{2+}	Mg^{2+}	Cl^-	HCO_3^-	HPO_4^{2-}	SO_4^-
Plasma	142.0	5.0	2.5	1.5	103.0	27.0	1.0	0.5
SBF	142.0	5.0	2.5	1.5	148.8	4.2	1.0	0.5

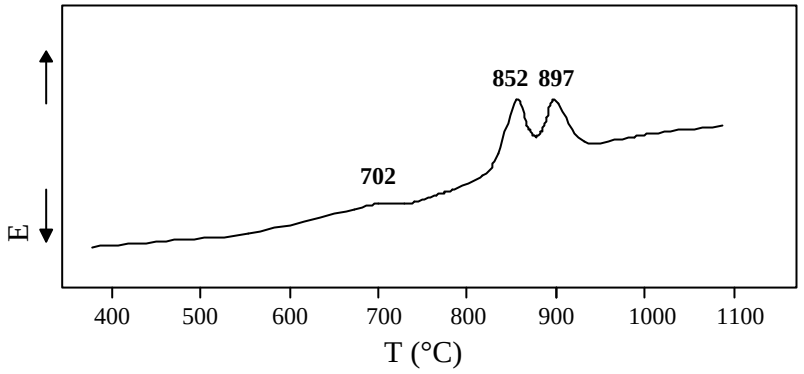

Fig. 2. DTA trace of G13.

3.1.2 In vitro studies

Figure *3* shows the G13 XRD pattern evolution with immersion time in SBF. The diffractographs obtained after 7 and 14 days in SBF are compared with that obtained in the as-annealed condition. After 7 days of soaking the (002) and (211) reflections of an apatite phase (PDF #9-432) were identified. After 14 days of soaking the intensity of reflections (002) and (211) increased while other apatite reflections (102), (202), (213) and (004) became evident.

Figure 4 shows a SEM micrograph of G13 after 14 days of immersion in SBF. It is observed that the initial polished surface of the glass was covered by a layer presenting some cracks.

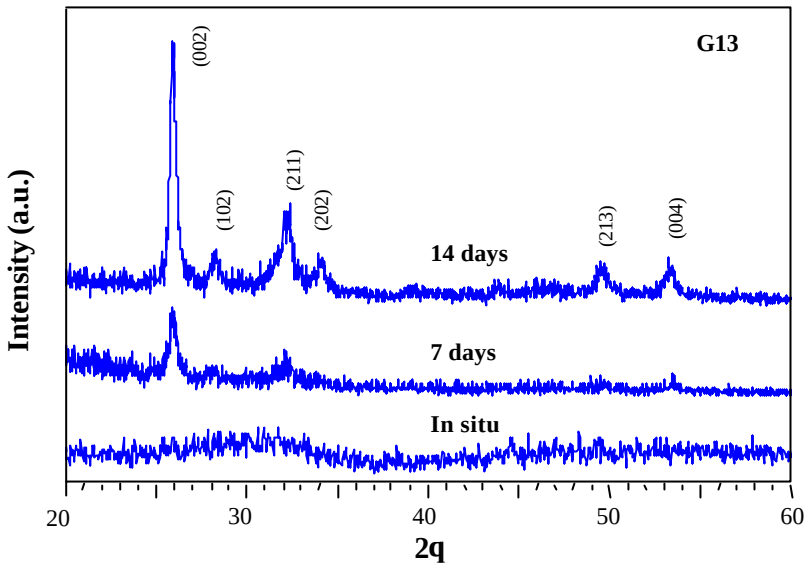

Fig. 3. XRD patterns of G13 before and after 7 and 14 days in SBF.

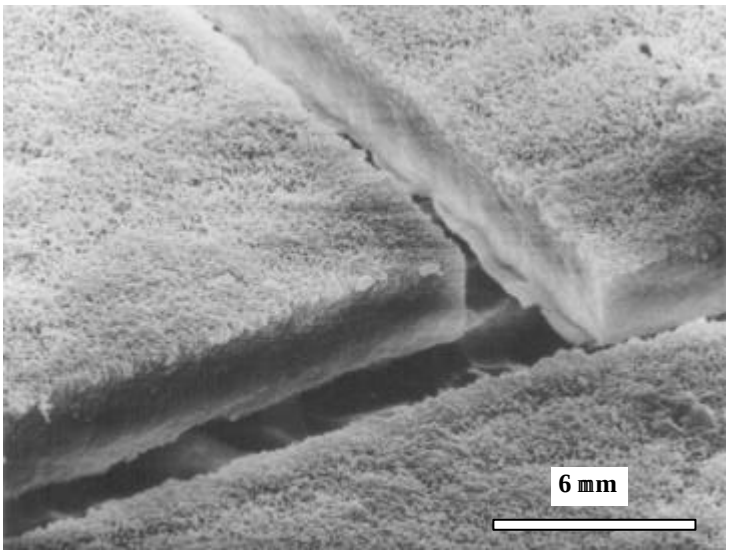

Fig. 4. SEM micrograph of G13 after 14 days in SBF.

Figure 5 shows for comparison the EDS spectra of G13 surface before (a) and after (b) soaking in SBF. It is observed that the newly formed layer was mainly composed by calcium and phosphorus, in a Ca/P ratio of 1.10.

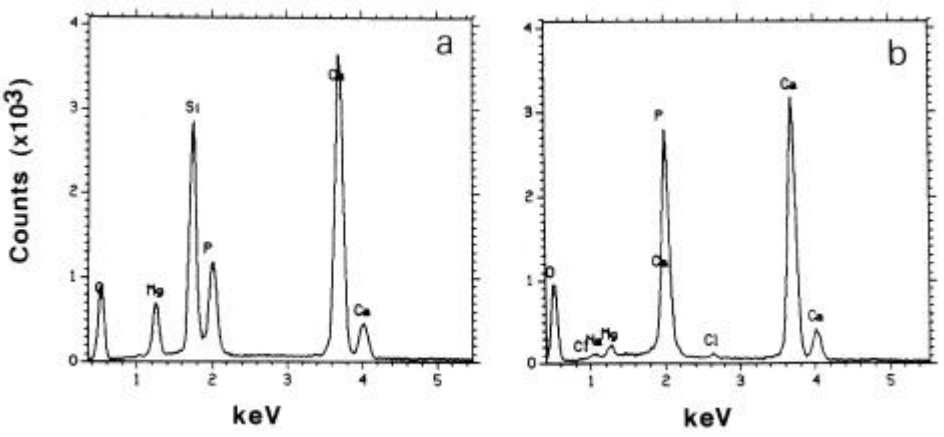

Fig. 5. EDS spectra of G13 (a) as-annealed and (b) after 14 d in SBF.

3.2. Glass-ceramic

3.2.1 XRD characterisation

The *XRD* pattern of GC13 (see Fig. 6) shows the presence of hydroxyapatite (PDF #9-432) $Ca_5(PO_4)_3OH$, diopside (PDF #11-654) $CaMg(SiO_3)_2$ and althausite (PDF #29-869) $Mg_2PO_4(OH)$ as crystalline phases. The unmarked low intensity *maxima* could correspond to an incipient crystallisation of akermanite (PDF #35-592) $Ca_2MgSi_2O_7$.

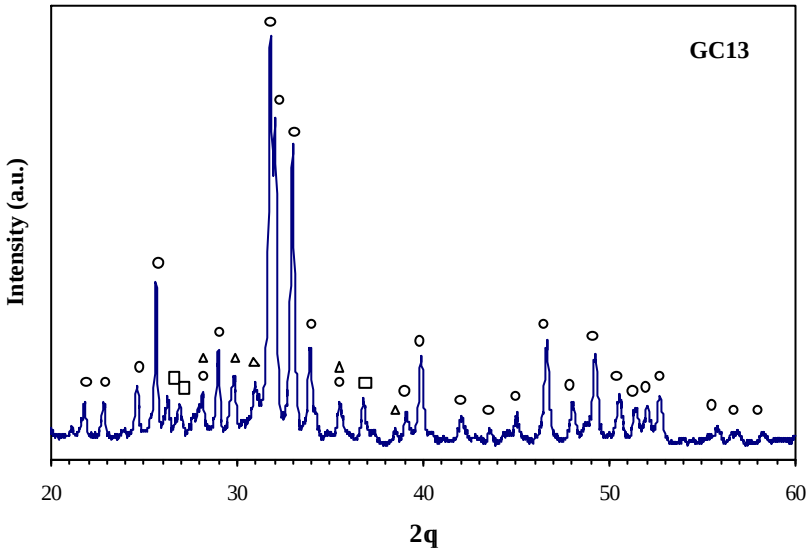

Fig. 6. XRD pattern of GC13 (O - apatite; Δ - diopside; - althausite).

3.2.2 SEM and EDS studies

Figure 7 shows the SEM micrograph of a polished surface of the glass-ceramic GC13. The microstructure is characterised by a three dimensional network of fibres. The network density is heterogeneous at larger scale. EDS scrutiny of the sample showed higher silicon/phosphorus ratio in regions where the fibre density is higher. Accounting for matrix effects, this suggests that the fibres are silicate and that phosphates are present in the interstices.

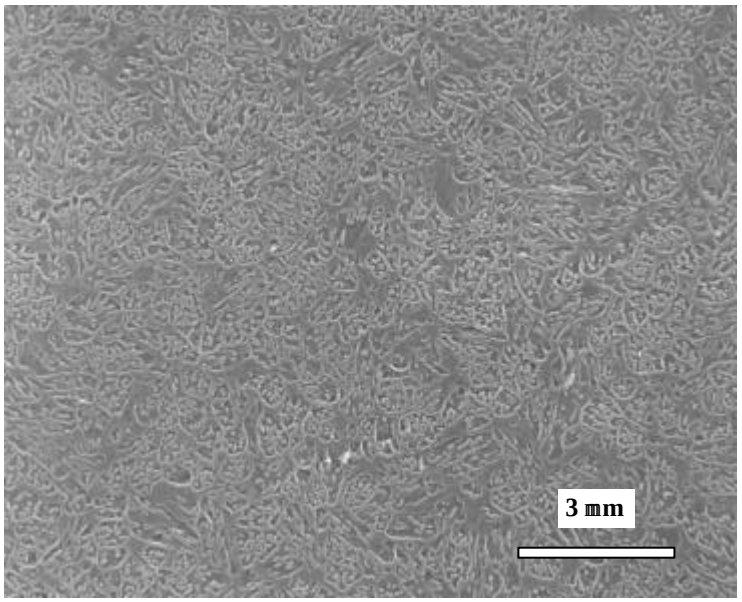

Fig. 7. SEM micrograph of GC13.

3.2.3 In vitro studies

The *in vitro* study in SBF demonstrated the unability of GC13 to form a Ca-P-rich layer since no changes were observed by XRD or SEM on the surface of GC13 after 6 weeks of soaking.

3.3. Glass-ceramic etched with HCl

3.3.1. Chemical treatment of the glass-ceramic

On the basis of a recent study of Cho *et al.*[17] and as a trial to induce bioactivity, GC13 was etched for 10 minutes with HCl 1M (GC13-HCl). A macroscopic

observation of GC13-HCl showed that acid attack had promoted a surface modification since the samples have changed from translucent to white opaque.

3.3.2 XRD studies

The XRD pattern of GC13-HCl is presented in Fig 8a. Comparing this diffractograph with that of GC13 before etching (Fig.6), it is observed that the diffraction *maxima* of the apatite phase practically disappeared, whereas those correspondent to the other crystalline phases remain almost unchanged. These results indicate that the apatite crystals near the surface of GC13 were dissolved in the acidic medium. At the same time, a careful comparison of the amorphous background of XRD patterns, before and after the chemical treatment, seems to indicate a decrease in the amount of the glassy phase in GC13-HCl which could indicate that a part of the vitreous phase on the surface of GC13 was also dissolved in HCl 1M.

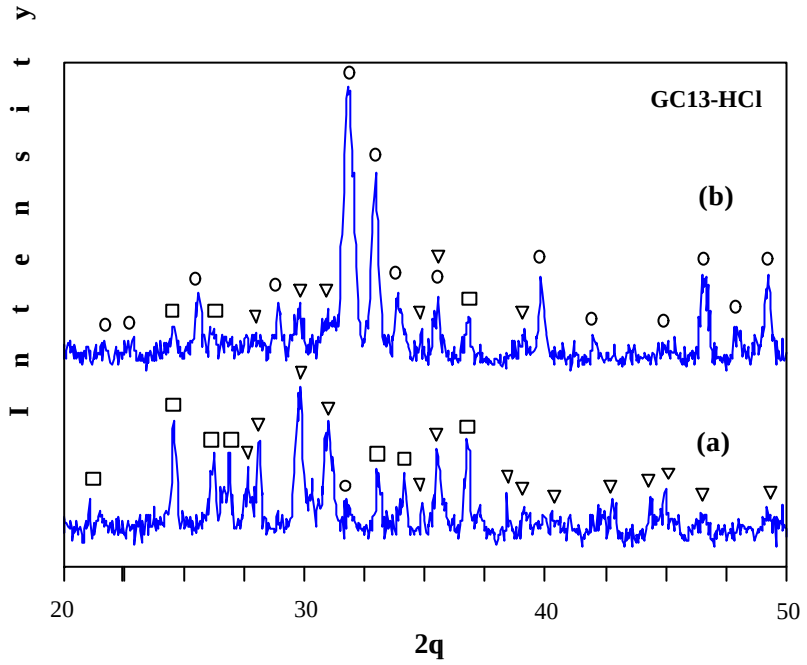

Fig. 8. XRD patterns of GCl3-HCl (a) before and (b) after 14 days in SBF. (O - apatite; ∇ - diopside; - althausite).

3.3.3 SEM and EDS studies

In Fig. 9 a SEM micrograph of GC13-HCl is shown. The heterogeneous distribution of fibres is evident as for GC13. Thus, some regions are smoother and with

higher fibre density (regions A in Fig. 9) while others appear to be rougher and with lower fibre density (regions B in Fig. 9). As mentioned, the HCl-dissolving phases are thought to be apatite and residual glass. In accordance with XRD findings, EDS analysis shows a decrease in calcium and phosphorus concentration in the attacked surface, from 6 mol-% to less than 1 mol-% (P) and from 16 mol-% to 7 mol-% (Ca).

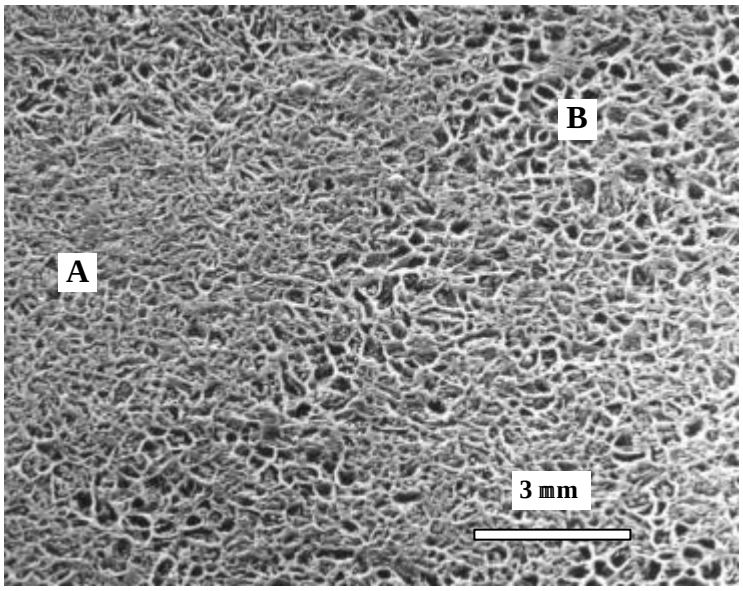

Fig. 9. SEM micrograph of GC13-HCl.

3.3.4 In vitro studies

Figure 8 shows the XRD patterns of GC13-HCl before (a) and after (b) 4 days soaking in SBF. As observed, the diffraction *maxima* of the apatite phase that disappeared after the chemical etch are again present after soaking. However, a decrease in the relative intensity of such reflections was observed.

Figure 10 shows SEM micrographs of GC13-HCl after 4 days in SBF at low (a) and high magnification (b and c). Regions with higher porosity resulting from acid attack were completely covered by needle-like crystals (Fig. l0b) of calcium phosphate, as confirmed by EDS. In darker, low porosity regions where roughness is less, only a few disperse crystal agglomerates were observed (Fig 10c). In the latter regions EDS analysis confirm a decrease in calcium and phosphorus and an increase in silicon and magnesium concentrations. The similarity of shape exhibited by the deposited crystals in both regions enables us to identify the sparse deposits as calcium phosphate.

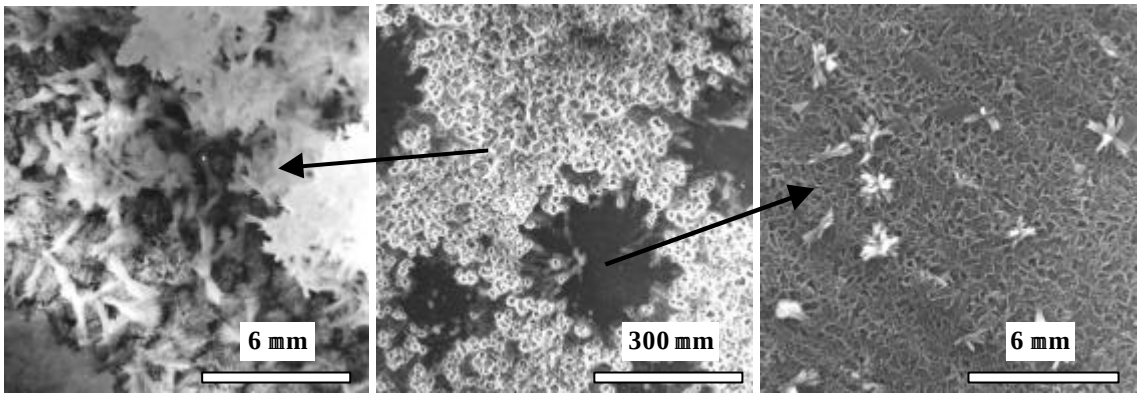

Fig. 10. SEM micrographs of GCI3-HCl after 4 days in SBF: (a) low magnification image; (b) and (c) higher magnification micrographs of regions with Ca-P layer and with a low amount of Ca-P formations, respectively.

4. Discussion

The *in vitro* study in SBF of the three samples: (i) the glass G13, (ii) the glass-ceramic GC13, obtained by thermal treatment of G13 and (iii) GC13-HCl obtained by chemically etching GC13 with HCl, allow to state that each one shows a different *in vitro* behaviour in SBF:

(i) G13 showed a high reactivity with SBF forming a calcium phosphate-rich layer on its surface in less than 7 days, as was confirmed by XRD, SEM and EDS.

(ii) GC 13 was not able to form a calcium phosphate-rich layer even after 6 weeks in SBF.

(iii) GC13-HCl showed regions of the surface in which the Ca-P rich layer was formed after 4 days in SBF, as detected by XRD SEM and EDS. However, in other regions of the surface only a minimum presence of Ca-P crystals was detected by SEM after 7 days of soaking.

The different behaviour of G13, GC13 and GC13-HCl in SBF could be due to differences in chemical composition and/or surface morphology.

In GC13, the formation of crystalline calcium-phosphates and silicates will produce a residual glassy phase with composition modified with regard to the parent glass G13. Depletion of the residual glass in Ca by crystallisation of diopside and apatite during heat treatment may have chemically stabilised it, thus hindering Ca^{2+} exchanges with H_3O^+ of SBF and subsequent formation of silanol groups which would explain the low

bioactivity of the glass-ceramic. This will be so in spite of the presence of diopside, reported as being a biodegradable phase[18].

Chemical etching in GC13-HC1 selectively dissolved the apatite phase. It might also have formed a silica-gel layer by attack on the silicate phases and the residual glass, which would explain the faster mineralization kinetics in SBF as compared with GC13.

The increase in surface area brought about by acid attack would also render GC13-HCl more susceptible to react with SBF. It was verified that apatite deposition in SBF was extensive in rougher regions of the surface and sparse in flatter regions. Pereira *et al.*[19] showed that the rate of HCA formation on a porous substrate depends on its texture and argued that pores may act as nucleation sites inside which the degree of supersaturation for precipitation of apatite is attained faster.

Probably, both chemical and/or morphological factors will be responsible for the different *in vitro* behaviour of these materials, all of them with a common precursor glass. The modification of the A/W composition[7] by increasing the MgO content of the silicate fraction in the $3CaO.P_2O_5$-$CaO.SiO_2$-$CaO.MgO.2SiO_2$ system was found not to necessarily decrease the *in vitro* bioactivity of the glass. However, the appearance of crystalline phases in the glass-ceramic GC13 (diopside, althausite and possibly akermanite instead of A/W wollastonite) was able to suppress the *in vitro* bioactivity. A chemical etch could restore the bioactive behaviour and more so in regions where the etching effect was greater.

5. Conclusions

a) A glass of the $3CaO.P_2O_5$-$CaO.SiO_2$-$CaO.MgO.2SiO_2$ system with relatively high MgO content (13 mol %) showed *in vitro* bioactivity in SBF.
b) However, the resultant bulk glass-ceramic containing diopside, althausite and possibly akermanite as crystalline silicates does not form a mineralized layer after 6 weeks in SBF.
c) The same glass-ceramic attacked with HCl 1M selectively deposits an apatite layer after 4 days in SBF. The kinetics of deposition is dependent on microstructural fluctuations in the material.

Acknowledgements

Financial support of CICYT, Spain, through research project No. MAT96-0919, and of the Spanish-Portuguese Integrated Actions HP-1996-0049 and HP-1997-0018 are gratefully acknowledged. We also thank F. Conde (CAI X-ray Diffraction, UCM) for valuable technical and professional assistance.

References

[1] Hench, L.L. – "Bioceramics", *Journal of the American Ceramic Society*, 81, 1998, 1705-1728.

[2] Vogel, W.; Holland, W. – "The Development of Bioglass-ceramics for Medical Applications", *Angewandte Chemie* (International Edition in English), 26, 1987, 527-544.

[3] Cao, W.; Hench, L. L. – "Bioactive Materials", *Ceramics International*, 22, 1996, 493-507.

[4] Pantano, C. O.; Clark, A. E.; Hench, L. L. – "Multilayer Corrosion Films on Bioglass Surfaces", *Journal of the American Ceramic Society*, 57, 1974, 412-413.

[5] Kokubo, T.; Kushitani, H.; Sakka, S.; Kitsugi, T.; Yamamuro, T. – "Solutions Able to Reproduce *in vivo* Surface-structure Changes in Bioactive Glass-ceramics A-W", *Journal of Biomedical Materials Research*, 24, 1990, 721-734.

[6] Kokubo, T.; Shigmatsu, M.; Nagashima, Y.; Tashiro, M.; Nakamura, T.; Yamamuro, T.; Higashi, S. – "Apatite and Wollastonite-containing Glass-ceramics for Prosthetic Application", *Bulletin of the Institute for Chemical Research Kyoto University*, 60, 1982, 260-268.

[7] Kokubo, T.; Ito, S.; Sakka, S.; Yamamuro, T. – "Formation of a High-strength Bioactive Glass-ceramic in the System MgO-CaO-SiO_2-P_2O_5", *Journal of Materials Science*, 21, 1986, 536-540.

[8] Kokubo, T. – "A/W Glass-ceramic: Processing and Properties" *in* Hench, L. L.; Wilson, J. – *An Introduction to Bioceramics*, 1, Singapore, World Scientific, 1993, 75-88.

[9] Shyu, J. J.; Wu, J. M. – "Crystallization of MgO-CaO-SiO_2-P_2O_5 Glass", *Journal of the American Ceramic Society*, 73, 1990, 1062-1068.

[10] Shyu, J. J.; Wu, J. M. – "Effect of TiO_2 Addition on the Nucleation of Apatite in an MgO-CaO-SiO_2-P_2O_5 Glass", *Journal of Materials Science Letters*, 10, 1991, 1056-1058.

[11] Shyu, J. J.; Wu, J. M. – "Growth Kinetics of Spherulitic Apatite in Some MgO-CaO-SiO_2-P_2O_5 Glasses", *Journal of Materials Science*, 29, 1994, 3167-3171.

[12] Liu, D. M.; Chou, H. M. – "Formation of a New Bioactive Glass-ceramic", *Journal of Materials Science: Materials in Medicine*, 5, 1994, 7-10.

[13] Oliveira, J. M.; Correia, R. N.; Fernandes, M. H. – "Surface Modifications of a Glass and a Glass-ceramic of the MgO-3CaO.P_2O_5-SiO_2 System in a Simulated Body Fluid", *Biomaterials*, 16, 1995, 849-854.

[14] Partridge, G. – "An Overview of Glass-ceramics. Part 1. Development and Principal Bulk Applications", *Glass Technology*, 35, 1994, 116-127.

[15] Ebisawa, Y.; Kokubo, T.; Ohura, K.; Yamamuro, T. – "Bioactivity of CaO-SiO_2-based Glasses: *in vitro* Evaluation", *Journal of Materials Science: Materials in Medicine*, 1, 1990; 239-244.

[16] Oliveira, J. M.; Correia, R. N.; Fernandes, M. H. – "Effects of Si Speciation on the *in vitro* Bioactivity of Glasses", *Biomaterials*, submitted.

[17] Cho, S.-B.; Miyaji, F.; Kokubo, T.; Nakamura, T. – "Induction of Bioactivity of a Non-bioactive Glass-ceramic by a Chemical Treatment", *Biomaterials*, 18, 1997, 1479-1485.

[18] Kobayashi, T.; Okada, K.; Kuroda, T.; Sato, K. – "Osteogenic Cell Cytotoxicity and Biomechanical Strength of the New Ceramic Diopside", *Journal of Biomedical Materials Research*, 37, 1997, 100-107.

[19] Pereira, M. M.; Clark, A. E.; Hench, L. L. – "Effect of Texture on the Rate of Hydroxyapatite Formation on Gel-silica Surface", *Journal of the American Ceramic Society*, 78, 1995, 2463-2468.

4.4 - Role of Acid Attack in the *in vitro* Bioactivity of a Glass-ceramic of the $3CaO.P_2O_5$-$CaO.SiO_2$-$CaO.MgO.2SiO_2$ System

J. Roman, A.J. Salinas, M. Vallet-Regi

Dept. Quimica Inorganica y Bioinorganica, Facultad de Farmacia, Universidad Complutense de Madrid, E-28040 Madrid, Spain. (Fax: +3491 394 1786)

J. M. Oliveira, R. N. Correia, M. H. Fernandes

UIMC, Departamento de Engenharia Cerâmica e do Vidro, Universidade de Aveiro, 3810-193 Aveiro, PORTUGAL

(Biomaterials, submitted)

Abstract

A non-bioactive glass-ceramic (GC13) that contains hydroxyapatite ($Ca_5(PO_4)_3OH$), diopside ($CaMg(SiO_3)_2$) and althausite (Mg_2PO_4OH) as crystalline phases has been obtained by thermal treatment of a parent bioactive glass (G13) of nominal composition (wt.%) 40.0 CaO - 34.5 SiO_2 - 16.5 P_2O_5 - 8.5 MgO - 0.5 CaF_2. To induce bioactivity, GC13 was chemically treated with 1M HCl for different times. After chemical etching the *in vitro* studies showed formation of an apatite like surface layer. In this article the influence of etching time both on the surface composition of the glass-ceramic and on the growth rate of the apatite layer is studied. It is concluded that the presence of hydroxyapatite in the glass-ceramic, associated to microstructural fluctuations, can favour apatite deposition *in vitro*.

***Keywords**: bioactive glass-ceramics, bioceramics, in vitro studies, bioactivity induction, surface morphology.*

Introduction

Together with the development of glasses and glass-ceramics for biomedical applications several efforts have been pursued in order to explain the mechanism responsible for their *in vitro* and *in vivo* behaviour.[1-3] The proposed mechanisms are based on the leaching ability of glasses or glassy phases in glass-ceramics and it is concluded that the necessary condition for glass and glass-ceramic bonding to living bone is the formation of a carbonate-containing hydroxyapatite (HCA) layer on their surfaces. Besides, it has been observed that the HCA layer formation, especially in glasses contacting physiological fluids *in vivo* or simulated body fluids *in vitro*, is preceded by formation of a silica gel layer. This layer results from the condensation and polymerisation of silanol groups formed by ion exchange with the surrounding medium and acts as nucleation sites for Ca-P layer development. However, due to the presence of crystalline phases, usually with high chemical stability in physiological fluids, the formation of a silica gel layer in glass-ceramics is more difficult, being then the glassy phase the sole responsible for bioactive behaviour[4,5].

The ability of Al_2O_3 to improve the chemical durability of glasses is known[6]. Kokubo[2,7] showed that apatite-containing $MgO.CaO.SiO_2.P_2O_5.Al_2O_3$ glass-ceramics can not develop an HCA layer after 6 days in a simulated body fluid (SBF) if the residual glassy phase is chemical stable, i.e. rich in Al_2O_3. Li[4] also showed that there is a direct relationship between the amount of soluble glassy phase and *in vitro* behaviour. Thus, the presence of crystalline phases can apparently be a hindrance to the bioactive behaviour of glass-ceramics.

Actually, the bioactive properties of glass-ceramics are more difficult to predict than those of glasses, especially *in vivo.* Hench[8] developed three different microstructural 45S5 compositions: glass, partially crystalline and fully crystalline, and after 6 weeks *in vivo* all the implants were bonded to the cortical bone of a rat femur. Kokubo's A/W glass-ceramic also bonds to living bone by means of a Ca-P rich layer, but with no silica gel layer detected at the implant - bone interface.

It is worth noting that Bioverit I, II and III bond to living tissues and all contain Al_2O_3[9], although retained in the crystalline phases. Bioverit I was developed from a silica-phosphate-based glass, Bioverit II from a silica-based glass and Bioverit III from

a silica free, phosphate-based glass. These glass-ceramics contain glassy and crystalline phases, of which apatite is present in Bioverit I and III, which are the most surface-active materials. *In vitro* tests performed with Bioverit I in Ringer's and in tris-buffered solutions and with Bioverit II in tris-buffered solution indicate ion exchange between the glass surface and the surrounding fluids[10]. *In vivo* experiments show that the materials bond to living bone, a small solubility of the glassy phase being recorded.

Other factors, like morphology and surface charge, can influence the bioactive behaviour of a material. Li *et al.*[11] proposed that in order to induce apatite formation a material must have, or develop a OH-rich, electrically negative surface. Other authors also showed that surface texture can influence apatite precipitation[12,13].

Recently, Cho *et al.*[14] showed that it is possible to induce bioactivity on a non-bioactive glass-ceramic of the MgO-CaO-SiO_2-P_2O_5-Al_2O_3 system containing apatite and wollastonite as crystalline phases. The authors concluded that the induction of bioactivity is due to the formation of a hydrated silica layer on the glass-ceramic surface when soaked in HCl aqueous solutions with concentrations higher than 0.1 M.

In a previous work[13] we studied the *in vitro* bioactivity of a glass and a glass-ceramic (G13 and GC13, respectively) of the CaO-MgO-SiO_2-P_2O_5-CaF_2 system containing 13 mol% MgO. Whereas G13 showed *in vitro* bioactivity, GC13 did not. After etching GC13 in a 1 M HCl solution for 10 minutes, non-uniform formation of apatite on the glass-ceramic surface was observed.

To advance in the knowledge of the mechanism responsible for bioactivity induction and to optimise the bioactive behaviour of GC13, the influence of etching time on the surface composition and on the growth rate of the apatite layer was studied in the present work.

2. Experimental Procedure

Glass-ceramic GC13 was prepared by thermal treatment of parent glass monoliths (G13) of nominal composition (wt %) 40.0 CaO -34.5 SiO_2 -16.5 P_2O_5 -8.5 MgO - 0.5 CaF_2, as previously reported[13].

The glass-ceramic was cut into prismatic pieces by a low-speed diamond disc, polished with α-alumina powder in distilled water and washed with ion-exchanged distilled water for 15 minutes in an ultrasonic cleaner.

GC13 pieces were chemically treated at room temperature in hydrochloric acid 1M for 1, 5, 10 and 20 minutes (GC13-1, GC13-5, GC13-10 and GC13-20, respectively) with continuous stirring. After soaking, the samples were removed from the solution, washed with ion-exchanged distilled water and dried at 60 °C.

After chemical etch the ionic concentrations of Si, Ca, Mg and P in the acidic solutions were determined by a inductively coupled plasma (ICP) emission spectroscopy using a Jobin-Yvon JY70 Plus spectrometer.

The etched samples were studied by X-Ray Diffraction (XRD) using a Philips X'Pert diffractometer with CuKα radiation, by Scanning Electron Microscopy (SEM) on a Hitachi S-4100, by Energy Dispersive X-Ray Spectroscopy (EDS) on a LINK AN10000 System connected to a JEOL 6400 SEM Microscope, and by Fourier-transformed infrared (FTIR) spectroscopy on a Brucker IFS88 spectrometer equipped with a SplitPea^{TM} cell.

In vitro bioactivity tests were carried out in polyethylene containers by soaking the samples at 37°C for 3, 7 and 14 days in 45 ml of tris-buffered SBF, whose composition is shown in Table I. Pieces were mounted vertically in a special platinum scaffold to avoid deposition by gravity. After soaking, surface modifications of the glass-ceramic pieces were studied by SEM.

Table I. Ionic concentration (mM) in SBF and human plasma.

	Na^+	K^+	Ca^{2+}	Mg^{2+}	Cl^-	HCO_3^-	HPO_4^{2-}	SO_4^{2-}
Plasma	142.0	5.0	2.5	1.5	103.0	27.0	1.0	0.5
SBF	142.0	5.0	2.5	1.5	148.8	4.2	1.0	0.5

3. Results

3.1 Glass-ceramic etching

3.1.1 ICP studies

Fig. 1 shows the evolution of ion extraction by the acid solution with etching time in relation to the initial elemental composition in the glass. A marked release of Ca and P ions takes place, whereas the release of Si and Mg ions was lower, the evolution of the pairs Ca:P and Si:Mg being similar. The amount of extracted Ca and P ions increases with etching time while the release of Si and Mg ions stays approximately constant after 5 minutes. After 20 minutes of etching time the amount of extracted Ca and P ions is 5-6 times greater than the extracted Si and Mg ions.

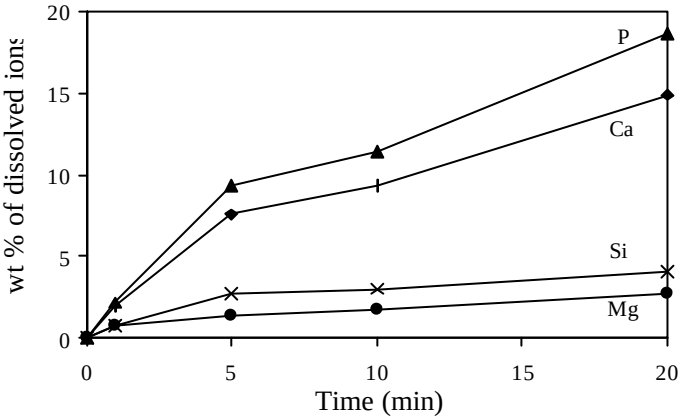

Fig. 1. Elemental concentrations in a 1M HCl solution during immersion of a specimen of GC13.

With increasing etching times the molar ratios of the dissolved ions, showed in Table II, become quite different from the initial glass stoichiometry, which indicates preferential phase etching.

Table II. Molar ratio between dissolved ions.

Time	Ca/P	Si/Mg	P/Mg	Ca/Si	Ca/Mg	Si/P
0	3.10	2.74	1.11	1.26	3.45	2.47
1	2.89	2.84	3.18	3.24	9.20	0.89
5	2.51	5.23	7.29	3.50	18.29	0.72
10	2.54	4.63	7.08	3.88	17.95	0.65
20	2.47	4.02	7.49	4.61	18.52	0.54

The Ca/P atomic ratio of the leached ions is higher than 2.4 for all etching times, indicating that calcium ions are released not only by the crystalline hydroxyapatite but also by other phases, since the stoichiometric Ca/P ratio in apatite is 1.67. By analysing the evolution of the Si/Mg ratio and knowing that in diopside that ratio is 2, it is concluded that silicate ions must also be provided by the glassy phase of the glass-ceramic.

3.1.2 DRX studies

Fig. 2 shows the XRD patterns of GC13, GC13-1, and GC13-10. XRD patterns of GC13-5 and GC13-20 are similar to that of GC13-10. The crystalline phases present in the glass-ceramic are mainly hydroxyapatite and diopside[13]. Althausite and an incipient crystallisation of akermanite are also detected.

In GC13-1 the intensity of apatite and althausite reflections decreased with respect to those of GC13, whereas the intensities of diopside peaks increased. For etching times greater than 1 min (GC13-5, GC13-10 and GC13-20) the reflections corresponding to phosphate phases disappeared and only those belonging to diopside (silicate phase) were detected. These results agree with those observed by ICP and confirm that, among the crystalline phases, phosphates are preferentially dissolved in HCl.

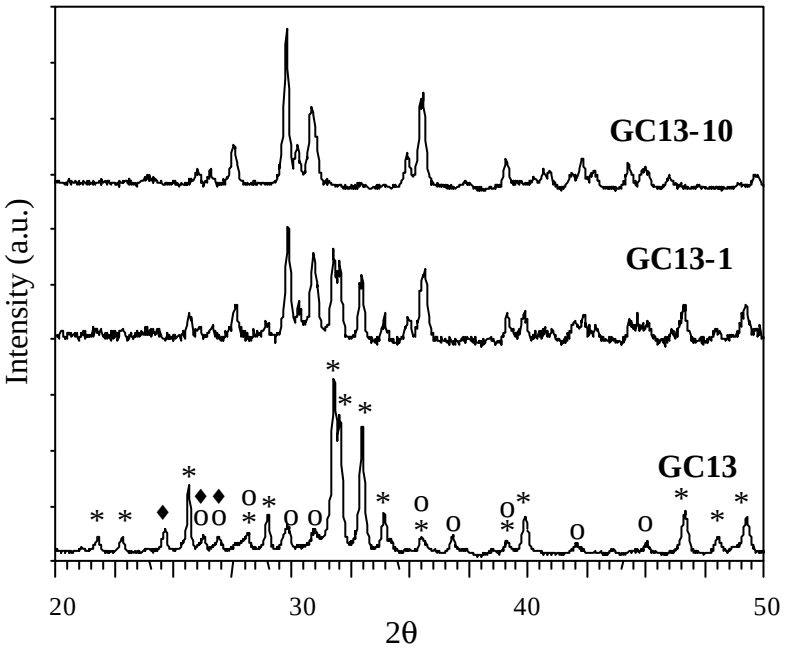

Fig. 2. XRD patterns of GC13 before and after 1 and 10 min. etching with HCl 1M (∗ - apatite; o - diopside; ♦ - althausite).

3.1.3 FTIR studies

Fig. 3 shows the FTIR spectra of GC13, GC13-1, GC13-5 and GC13-20. As in XRD patterns the presence of hydroxyapatite dominates the spectra of GC13 and GC13-1. The main FTIR peaks were assigned to the vibrational modes of the orthophosphate hydroxyapatite[15] and also to the single chain-silicate diopside[16,17]. The identified vibration peaks correspondent to the [PO_4] tetrahedron are the P–O asymmetric stretch (ν_3) at 1060 cm^{-1}, 1030 cm^{-1}, the P–O symmetric stretch (ν_1) at 940 cm^{-1} and P–O bending modes (ν_4) at 560 cm^{-1}, 575 cm^{-1} and 603 cm^{-1}. The crystalline silicate assignment was more difficult due to several overlaps with phosphate bond vibrations, however the main vibration modes were identified.

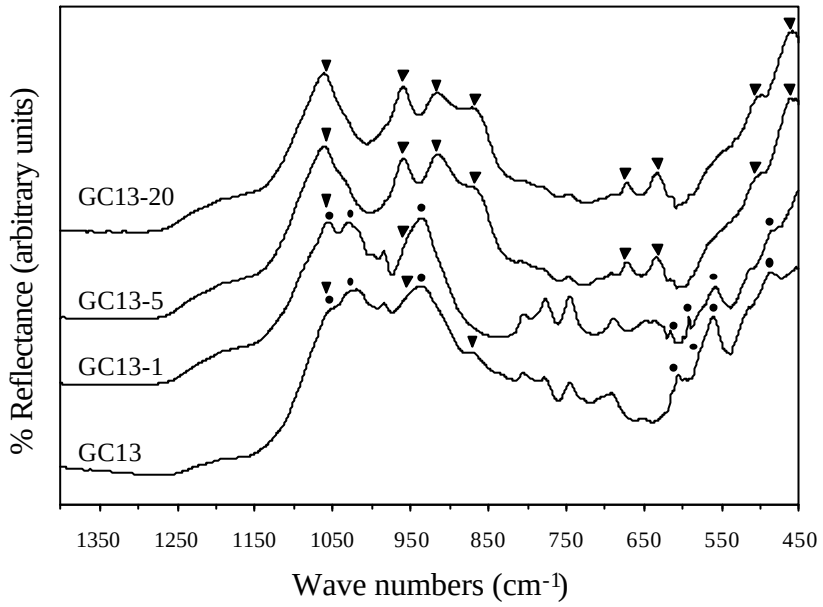

Fig. 3. FTIR spectra of the glass-ceramic surfaces after 0, 1, 5 and 20 min. in HCl 1M (▼ - silicate bond vibrations; • - phosphate bond vibrations).

The peaks in the envelope 700-810 cm^{-1} were assigned to Si–O–Si bending in polymerised silicates, due to the possibility of some silica surface devitrification, and to the presence of chain silicates.[18]

The GC13-1 sample spectrum is similar to the GC13. However, the higher intensity of the ~1060 cm^{-1} peak is most probably due to an overlap of the ν_3 vibrational mode in

P–O bonds and ν_3 vibrations in diopside[16] that began to become unmasked after the dissolution of hydroxyapatite.

After etching for 5 minutes the surface chemical characteristics markedly change, remaining unaltered for longer times. The peaks associated to crystalline hydroxyapatite almost disappear and new bands appear. According to published work[16,17] these bands were ascribed to diopside. The main peaks are the stretching Si–O bond vibrations at 1060 cm^{-1} and 960 cm^{-1}, and the Si–O bond vibrations with 2 non-bridging oxygens at 920 cm^{-1} and 865 cm^{-1}; the last 3 peaks are characteristic of diopside. The peaks at 670, 630, 510 and 460 cm^{-1} are due to bending vibrations in the silicate.

3.1.4 SEM results

Fig. 4 shows the SEM micrograph of a polished surface of the glass-ceramic GC13. The microstructure is characterised by a three-dimensional network of fibres. The network density is heterogeneous at larger scale. EDS scrutiny of the sample showed higher silicon/phosphorus ratio in the regions where the fibre density is higher. Accounting for matrix effects, this fact suggests that the fibres are silicate and that phosphates are present in the interstices.[13]

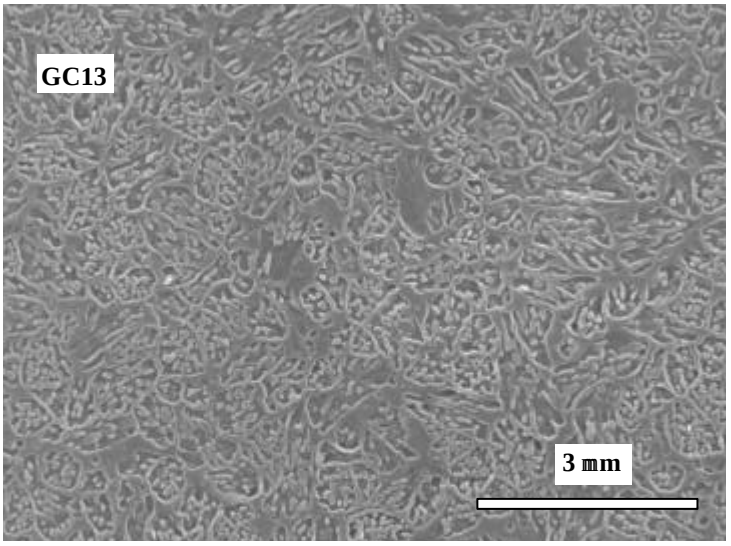

Fig. 4 – SEM micrograph of a polished GC13 surface.

In Fig. 5 a SEM micrograph of GC13-5 is shown. As for GC13 it is observed that some regions are smoother and with higher fibre density while others appear to be rougher and with lower fibre density. These results are similar for all samples after chemical etching. In spite of experimental errors due to the surface roughness, EDS analysis (Fig. 6) shows that the chemical etch produces an average marked decrease of Ca and P, simultaneously increasing the relative concentrations of Si and Mg. However, whereas phosphorus practically disappears from the surface, calcium remains in considerable concentrations.

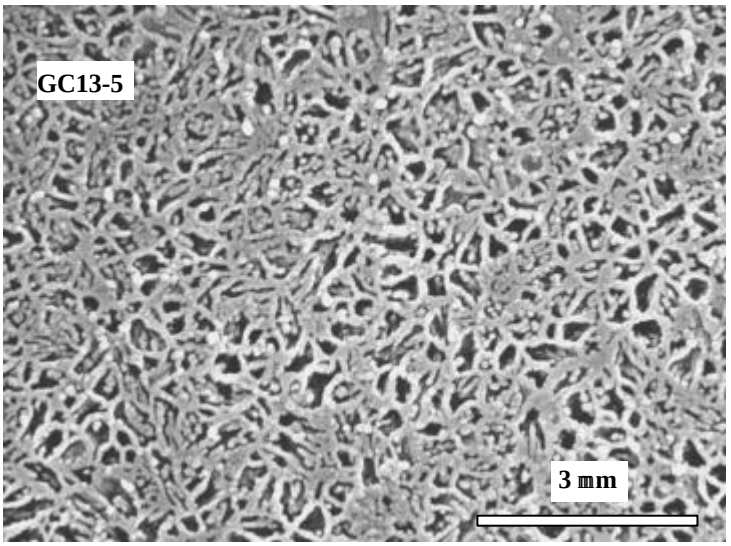

Fig. 5. SEM micrograph of GC13 etched for 5 min. in 1M HCl.

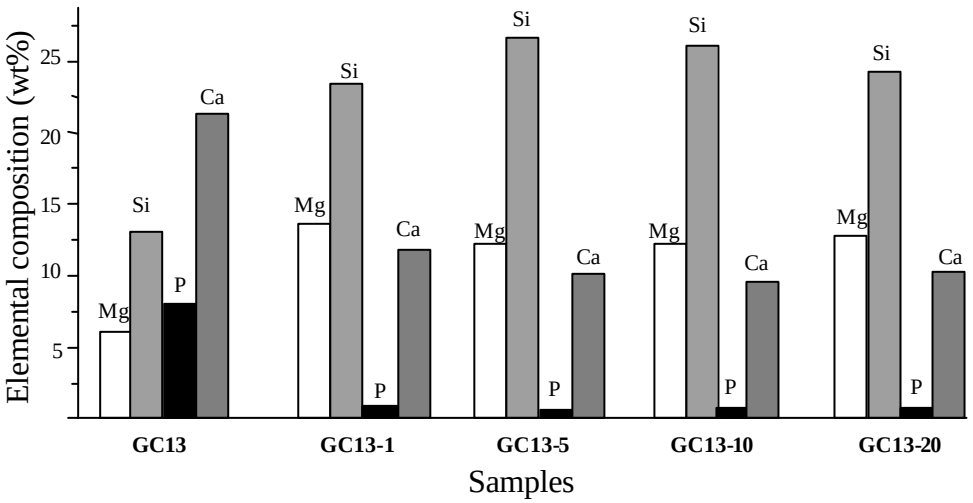

Fig. 6. Evolution of elemental concentrations (wt.%) obtained by EDS before and after 1M HCl treatment for 1, 5, 10 and 20 minutes.

3.2 In vitro studies

Fig. 7 shows SEM micrographs of GC13-1 after 7 days soaking in SBF and GC13-5, GC13-10 and GC13-20 after 14 days soaking. After 7 days soaking in SBF, the only sample totally covered by aggregates of apatite-like crystals is GC13-1. The morphology of the leaf-like apatite particles on GC13-1 surface was similar to that previously described for bone-like apatite formed *in vitro* on bioactive glasses and glass-ceramics.[2]

On the contrary, in glass-ceramics etched with HCl 1 M for times longer than 1 minute (GC13-5, GC13-10 and GC13-20) the surfaces were not totally covered. Apatite deposition is more intense in regions with higher porosity, as previously showed for GC13-10.[13] In these samples it is also observed (Fig. 7) that longer etching times lower the number density of apatite nuclei, which is particularly clear in regions with lower porosity.

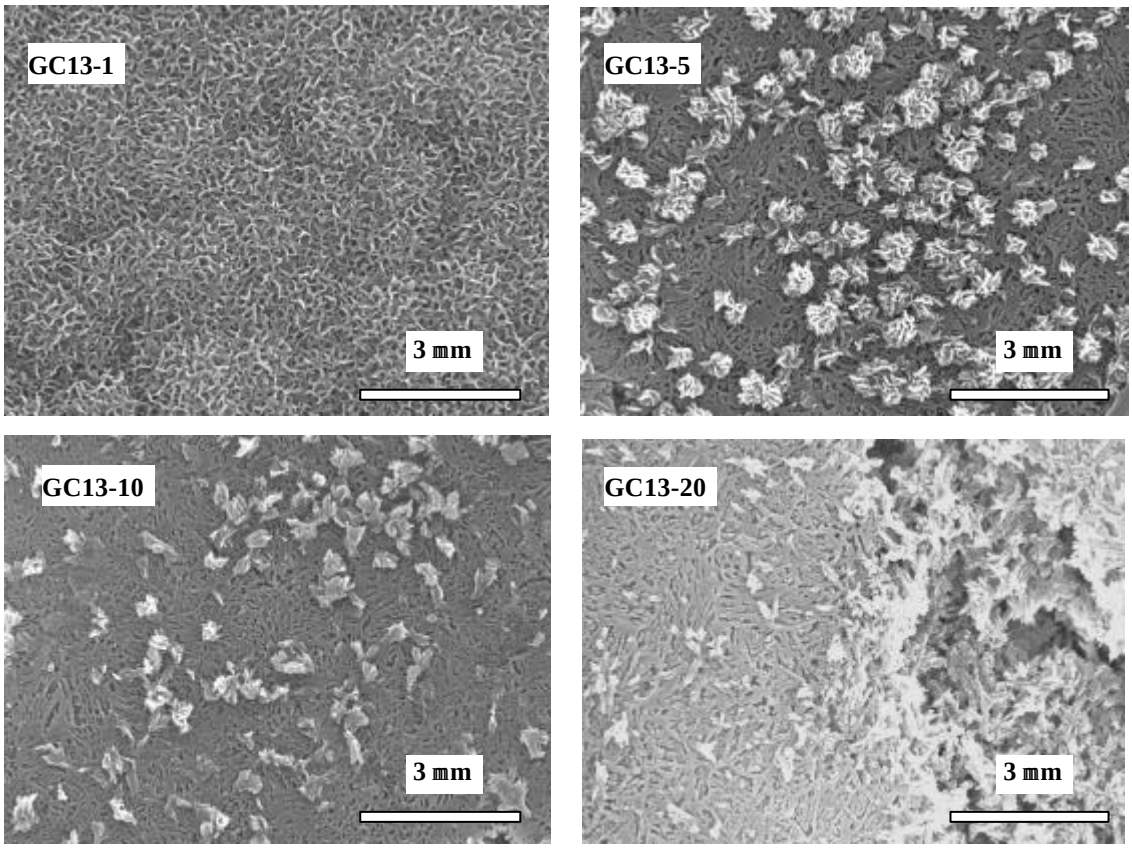

Fig. 7. SEM micrographs of GC13-1 after 7-day soaking and of GC13-5, GC13-10 and GC13-20 after 14-day soaking in SBF (low bioactivity regions were selected).

4. Discussion

Glass-ceramic GC13 did not develop an apatite layer when immersed in SBF for 6 weeks. However, after a chemical treatment with HCl 1M during 10 minutes a non-uniform deposition of apatite was achieved after 4 days in SBF. This behaviour was attributed to chemical or/and morphological factors[13].

Present results show that the GC13-1 sample not only was able to develop a Ca-P rich layer covering the entire surface, as it is the one with higher *in vitro* activity (Fig. 7). The other etched glass-ceramic specimens developed apatite in different amounts depending on their microstructural characteristics but their overall ability for mineralisation gradually decreases with increasing etching time. This behaviour is explained as follows.

ICP results (Fig. 1 and Table II) show that HCl treatment dissolves preferentially the crystalline phosphate and glassy phases present at the glass-ceramic surface. By removing the phosphate phases, long etching times will enrich the surface in crystalline silicates, due to their higher chemical resistance in acidic media. This interpretation is supported by the observation of Fig. 2, in which the relative intensity of the apatite phase decreases while the diopside phase increases with etching time. It should be noted, however, that after 1 minute etching the glass-ceramic surface is still composed of the same phases as the non-etched material (Fig. 2), although the surface is rougher (Fig. 5).

These observations agree with the FTIR results (Fig. 3). These still show a marked presence of crystalline phosphate groups after 1 minute etching together with a small increase in the intensity of the ~1060 cm^{-1} peak, assigned to unmasked Si–O vibrations from diopside. As etching time increases the surface becomes rich in diopside. Meanwhile the initial phosphate bond vibrations almost disappears for times longer than 5 minutes.

The matter of peak assignment deserves a comment. It is known that Si–OH stretching vibration in Bioglass® and fluoride Bioglass® compositions can occur in the range 1100-1000 cm^{-1} as well as the Si–O–Si bending vibration in the range 540-470 cm^{-1}.[19,20] However, Cho *et al.*[14] working with acid-etched samples of A-W(Al) glass-ceramic of composition close to G13, assigned a peak at 1200 cm^{-1} to Si–OH bond

vibrations. In GC13-1, GC13-5 and GC13-20 spectra no peak was identified at around 1200 cm^{-1}. The peak assignments to crystalline diopside were based on published data[16] according not only to peak positions but also to the very good fitting of the actual relative intensities with those published. So, among other peaks, the 1060 cm^{-1} and 460 cm^{-1} vibration modes were assigned to diopside, but it is not completely clear if a low amount of silica gel was formed.

As previously reported[13], acid attack increases the surface area of the GC13 sample. All etched samples show two distinct regions: one is smoother and with higher fibre density while the other appears to be rougher and with lower fibre density (Fig. 5). These results are similar for all etched samples, especially in the cases of GC13-5, GC13-10 and GC13-20. A drastic disappearance of apatite from the GC13-5, GC13-10 and GC13-20 material surfaces after chemical attack (Figs. 2 and 6) is the most striking experimental evidence. *In vitro* tests (Fig. 7) reveal that apatite deposition decreases with increasing etching time in both regions. It is also known that HCA formation depends on the texture of the substrate and it was argued that pores might act as nucleation sites[12].

In crystalline hydroxyapatite-containing rough regions the degree of supersaturation for apatite precipitation is thought to be attained faster by means of the mechanism that governs the bioactivity of dense hydroxyapatite ceramics[21]. So, microstructural and morphological factors associated to the presence of hydroxyapatite phase – acting as a nucleation site – can favour the higher bioactive behaviour of the GC13-1, rather than chemical factors related to ion exchange with the solution (namely, silanol formation).

In the work by Cho *2.*[14] the intensity of the silanol FTIR peak increases with increasing HCl concentration (0.01 M, 0.1 M, 1 M, 2 M, 4 M and 8 M), for a constant etching time of 10 minutes, but as we inferred from the analysis of their thin-film XRD patterns and FTIR spectra, the apatite deposition after 4 days in SBF seems to be more intense in glass-ceramic samples A-W(Al) etched with HCl 0.1M. This is even more interesting as the authors report a decrease in hydroxyapatite and an increase in wollastonite at the glass-ceramic surfaces, with increasing acid concentration.

Regarding the chemical factors, an apatite-wollastonite-containing glass-ceramic A-W(Al) is surface inactive at least for 6 days in SBF and, according to the authors[7] the main undesirable effect responsible for the lack of bioactivity is the superior chemical

resistance of the glassy phase (provided by alumina), which disables the leaching process i. e., the first step in the mechanism of apatite deposition in glasses and glass-ceramics. It is very important to note that the authors report that the A-W(Al) glass-ceramic "hardly showed any element concentration change" after 6 days in SBF. One must realise that a so high chemical resistance will basically maintain the surface characteristics, including roughness, and the small hydroxyapatite crystals (dimensions usually ranging from 0.1 μm to 1 μm) will stay partially masked.

It is commonly accepted that in glasses and glass-ceramics the development of silanol groups at surfaces and their subsequent polymerisation is responsible for the apatite layer development. However, this seems not to be case in every instance. The A-W glass-ceramic bonds to living bone by means of an apatite-rich layer. Although it was not possible to detect any silica gel formation, Kokubo explains the bonding mechanism through the fundamental role played by calcium and dissolved silicon ions in apatite precipitation, and also suggests that the dissolution of wollastonite and glassy phases gives rise to a rougher surface, mainly composed of hydroxyapatite, that provides favourable sites for further apatite deposition.[2] The silica-free Bioverit III is a phosphate glass-ceramic mainly constituted by apatite and the authors[9,22] report that after a initial dissolution, hence an increase in roughness, the material develops a bioactive bond with living tissues; no silanol formation can be invoked in this case. It is also worth noting that Ohtsuki *et al.*[23] showed that apatite crystal-free $CaO.P_2O_5$-based glasses do not develop an apatite layer 30 days in SBF.

5. Conclusions

a) Bioactivity has been induced in a non-bioactive glass ceramic GC13 by means of a chemical treatment with 1 M HCl.

b) Etching time influences the kinetics of growth of the apatite-like layer in SBF. The surface of GC13 etched for 1 minute (GC13-1) was fully covered by apatite after soaking seven days in SBF. The ability to form apatite under *in vitro* conditions decreased for longer etching times.

c) Microstructural and morphological factors associated to the presence of the hydroxyapatite crystals – acting as heterogeneous nucleation or growth sites – can favour the more bioactive behaviour of GC13-1 etched for 1 minute, rather than chemical factors like silanol group formation.

Acknowledgements

Financial support of CICYT, Spain through research projects MAT99-0466, MAT98-0746-C02-01, and of the Spanish-Portuguese Integrated Action HP1998-0079 is gratefully acknowledged. We thank also Dr. F. Conde (CAI DRX Complutense University), M. Ferro (University of Aveiro) and Dr. C. Ribeiro (University of Porto) for valuable technical assistance.

References

[1] Hench, L. L. – "Bioceramics: From Concept to Clinic", *Journal of the American Ceramic Society*, 74, 1991, 1487-1510.

[2] Kokubo, T. – "Surface Chemistry of Bioactive Glass-ceramics", *Journal of Non-Crystalline Solids*, 120, 1990, 138-151

[3] Andersson, O. H.; Karlsson, K. H. – "On the Bioactivity of Silicate Glass", *Journal of Non-Crystalline Solids*, 129, 1991, 145-151.

[4] Li, P.; Yang, Q.; Zhang, F.; Kokubo, T. – "The Effect of Residual Glassy Phase in a Bioactive Glass-ceramic on the Formation of its Surface Apatite Layer *in vitro*", *Journal of Materials Science: Materials in Medicine*, 3, 1992, 452-456.

[5] Strnad, Z. – "Role of the Glass Phase in Bioactive Glass-ceramics", *Biomaterials*, 13, 1992, 317-321.

[6] Paul, A. – *Chemistry of Glasses*, New York, Chapman and Hall, 1982.

[7] Kokubo, T.; Kushitani, H.; Ohtsuki, C.; Sakka, S.; Yamamuro. T. – "Chemical Reaction of Bioactive Glass and Glass-ceramics with a Simulated Body Fluid", *Journal of Materials Science: Materials in Medicine*, 3, 1992, 79-83.

[8] Hench, L. L. – "Bioactive Glasses and Glass-ceramics: A Perspective", *in* Yamamuro, T.; Hench, L. L.; Wilson, J. – *Handbook of Bioactive Ceramics*, 1, Boca Raton, CRC Press, 1990, 7-23.

[9] Vogel, W.; Hölland, W. – "The Development of BioGlass-ceramics for Medical Applications", *Angewandte Chemie* (International Edition in English), 26, 1987, 527-544.

[10] Hölland, W.; Völksch, G.; Naumann, K.; Carl, G.; Götz, W. – "Characterization of Bone-Glass-ceramic Interface", *in* Bonfield, W.; Hastings, G. W.; Tanner, K. E. – *Proceedings of the 4th International Symposium on Ceramics in Medicine, Bioceramics*, 4, London, Butterworth-Heinemann, 1991, 171-178.

[11] Li, P. – In vitro *and* in vivo *Calcium Phosphate Induction on Gel Oxides*, PhD Thesis, Leiden, 1993.

[12] Pereira, M. M.; Clark, A. E.; Hench, L. L. – "Effect of Texture on the Rate of Hydroxyapatite Formation on Gel-Silica Surface", *Journal of the American Ceramic Society*, 78, 1995, 463-2468.

[13] Salinas, A. J.; Román, J.; Vallet-Regi, M.; Oliveira, J. M.; Correia, R. N.; Fernandes, M. H. – "*In vitro* Bioactivity of Glass and Glass-ceramics of the $3CaO.P_2O_5$-$CaO.SiO_2$-$CaO.MgO.2SiO_2$ System", *Biomaterials*, 21, 2000, 251-257.

[14] Cho, S.-B.; Miyaji,F.; Kokubo, T.; Nakamura, T. – "Induction of Bioactivity of a Non-Bioactive Glass-ceramic by a Chemical Treatment", *Biomaterials*, 18, 1997, 1479-1485.

[15] Farmer, V. C. – *The Infrared Spectra of Minerals*, London, Mineralogical Society, 1974.

[16] Omori, K. – "Analysis of the Infrared Absorption Spectrum of Diopside", *The American Mineralogist*, 56, 1971, 1607-1616.

[17] Rutstein, M. S.; White, W. B. – "Vibrational Spectra of High-Calcium Pyroxenes and Pyroxenoids", *The American Mineralogist*, 56, 1971, 877-887.

[18] Wong, J.; Angell, C. A. – *Glass Structure by Spectroscopy*, New York, Marcel Dekker, 1976.

[19] Filgueiras, M. R.; La Torre, G.; Hench, L. L. – "Solution Effects on the Surface Reactions of a Bioactive Glass", *Journal of Biomedical Materials Research*, 27, 1993, 445-453.

[20] Kim, C. Y.; Clark, A. E.; Hench, L. L. – "Compositional Dependence of Calcium Phosphate Layer Formation in Fluoride Bioglasses ®", *Journal of Biomedical Materials Research*, 26, 1992, 1147-1161.

[21] LeGeros, R. Z.; LeGeros, J. P. – "Dense Hydroxyapatite" *in* Hench, L. L.; Wilson, J. – *An Introduction to Bioceramics*, 1, Singapore, World Scientific, 1993, 139-180.

[22] Hölland, W.; Vogel, W. – "Machineable and Phosphate Glass-ceramics" *in* Hench, L. L.; Wilson, J. – *An Introduction to Bioceramics*, 1, Singapore, World Scientific, 1993, 125-137.

[23] Ohtsuki, C.; Kokubo, T.; Yamamuro, T. – "Mechanism of Apatite Formation on CaO-SiO_2-P_2O_5 Glasses in a Simulated Body Fluid", *Journal of Non-Crystalline Solids*, 143, 1992, 84-92.

5 - CONCLUSÕES E SUGESTÕES

5.1 - Conclusões

As conclusões dos vários trabalhos foram sendo apresentadas e constam dos artigos que constituem esta tese. De seguida resumem-se por capítulo, os resultados considerados mais interessantes não só do ponto de vista da originalidade como também da importância que podem representar para a compreensão nomeadamente da bioactividade em vidros e em vidros cerâmicos.

ESTUDOS DE SEPARAÇÃO DE FASES E DE NUCLEAÇÃO E CRESCIMENTO DE CRISTAIS EM VIDROS

No estudo do processo de separação de fases identificaram-se estruturas morulares amorfas constituídas por sílica e determinou-se pela primeira vez os efeitos da temperatura e tempo de fusão, da taxa de arrefecimento do fundido e da viscosidade na formação dessas. Observou-se que, entre 1525 °C e 1590 °C, a cada temperatura de fusão corresponde um tamanho médio de gota da fase dispersa (sílica) cujas dimensões diminuem com o aumento da temperatura, sendo a quantidade de fase dispersa sensivelmente constante. Estes resultados sugeriram que a cúpula de imiscibilidade do diagrama de equilíbrio neste intervalo de temperatura deve ter uma inclinação quase-infinita. O tempo de fusão não provocou qualquer alteração no número e na quantidade de mórulas. A morfologia peculiar da fase dispersa foi explicada com base no processo de formação das mórulas atribuído a uma rápida coalescência de gotas isoladas, quase-esféricas, que ocorre durante o arrefecimento do fundido. Este processo é controlado pela diferença de viscosidades entre a fase dispersa e a matriz, sendo essa diferença no caso estudado de cerca de 6 a 8 ordens de grandeza.

O controlo do processo de cristalização em vidros é fundamental para o correcto desenvolvimento de vidros cerâmicos. Salvo raras excepções, essa cristalização ocorre a temperaturas superiores à temperatura de transição vítrea.

A adição de titânia a um vidro monofásico provocou imiscibilidade líquida e permitiu controlar o processo de cristalização. Com a adição até 3 % ponderal de TiO_2 obtiveram-se vidros cerâmicos, cristalizados em volume e livres de fissuras, em que as

principais fases cristalinas são um fosfato ($3CaO.P_2O_5$) e dois silicatos (clino-enstatite e forsterite).

Recorreu-se à técnica de análise térmica diferencial para estudar a cinética de cristalização de um vidro do sistema $3CaO.P_2O_5$-SiO_2-MgO (V4). Concluiu-se que o seu processo de cristalização é composto por duas etapas: nucleação e crescimento de cristais. A temperatura e o tempo para os quais o desenvolvimento de núcleos é máximo é 730 °C e para valores superiores a 2 horas, respectivamente. O crescimento de cristais ocorre a temperaturas superiores a 800 °C. A aplicação de diferentes modelos cinéticos adaptados às condições experimentais específicas permitiu ainda concluir que a energia de activação para o crescimento de cristais é de ≈ 763 kJ/mol, valor inferior à energia de activação de fluxo viscoso (~1000 kJ/mol). Em estudos de crescimento de cristais em vidros é usual admitir-se que as energias de activação para crescimento e para fluxo viscoso são as mesmas, uma vez que se assume que o transporte iónico através da interface cristal–líquido é cineticamente controlado pela viscosidade. Neste trabalho concluiu-se que o transporte é controlado por reacções de interface. Concluiu-se também ser necessário introduzir correcções nos modelos cinéticos por forma a que estes se adaptem às condições experimentais específicas.

ESTRUTURA VÍTREA

Partindo do estudo do efeito da sílica na separação de fases e com base em análises estruturais realizadas por espectroscopia de Raman foi desenvolvido um vidro monofásico cuja composição e estrutura são iguais às da matriz do vidro com separação de fases V4. Este vidro destina-se a dar seguimento aos estudos de cristalização.

Estudos estruturais realizados no sistema CaO-P_2O_5-SiO_2-MgO permitiram concluir, à semelhança do que sucede na grande maioria das composições sílico-fosfatadas, que os dois óxidos formadores (SiO_2 e P_2O_5) não se interligam. O silício constitui cadeias poliméricas dominadas por espécies Q^2, as quais, com o aumento da razão MgO/CaO, se decompõem em espécies Q^0 e Q^4 segundo a reacção de desproporcionação: $2Q^2 \rightleftharpoons Q^0 + Q^4$. As espécies Q^4 constituem a fase dispersa (sílica pura) e as espécies Q^0 e Q^2 (cujo comprimento médio da cadeia polimerizada diminui

com o aumento da razão MgO/CaO) permanecem na matriz. O fósforo está sempre presente como orto-fosfato e o seu ambiente apenas é perturbado pela presença crescente de iões magnésio quando se aumenta a razão MgO/CaO.

As reacções de desproporcionação: $2Q^n \rightleftharpoons Q^{n-1} + Q^{n+1}$ (n = 3, 2, 1) são amplamente conhecidas em vidros alcalinos de sílica; contudo, não se encontraram na literatura referências à ocorrência deste tipo de reacções em vidros de sílica contendo alcalino-terrosos. Acredita-se ter conseguido com este trabalho identificar experimentalmente pela primeira vez uma reacção de desproporcionação num sistema sem elementos alcalinos. A identificação das várias espécies na reacção de desproporcionação é sobretudo importante devido às implicações que poderá ter no comportamento *in vitro* de vidros, como a seguir se refere.

COMPORTAMENTO* IN VITRO *DE VIDROS E VIDROS CERÂMICOS

Foi experimentalmente verificada a importância do factor estrutural especiação no comportamento *in vitro* de vidros e de vidros cerâmicos. O estudo veio mostrar a possibilidade de se incorporar elevadas quantidades de MgO sem pôr em causa o carácter bioactivo dos vidros sílico-fosfatados do sistema SiO_2-CaO-P_2O_5-MgO. Com base no conhecimento do mecanismo de especiação do silício, estudos *in vitro* permitiram concluir que o aumento do grau de lixiviação dos vidros e a consequente formação de sílica gel – etapas 1 a 3 do mecanismo de Hench – são favorecidos pela maior solubilidade das espécies Q^0. Nestas circunstâncias, a presença de magnésio em vidros pode favorecer indirectamente o desenvolvimento da camada de sílica gel. Sendo esta camada o "ponto fraco" da ligação implante-tecido ósseo, o controlo da quantidade de magnésio pode ser determinante no projecto de vidros bioactivos no sistema SiO_2-P_2O_5-CaO-MgO.

A análise de vidros deste sistema, do tipo A/W enriquecidos com MgO, por substituição de CaO, revelou que o acréscimo de concentração de MgO usado não é nocivo para o desenvolvimento *in vitro* de apatite sobre o material vítreo (G13). A cristalização deste vidro que se revelou bioactivo originou contudo um vidro cerâmico (GC13) não bioactivo. Com o objectivo de promover o desenvolvimento de grupos

Si-OH, à superfície deste cerâmico não bioactivo, sujeitou-se o referido material a vários tratamentos em meio ácido. Observou-se a formação não uniforme de apatite *in vitro*, função de flutuações morfológicas provocadas pelo ataque químico. Efectivamente, zonas mais ricas em silicatos, de menor rugosidade, onde seria expectável uma maior abundância de grupos silanol e, portanto, maior formação de apatite *in vitro*, revelaram-se muito pouco bioactivas. Concluiu-se que a existência de flutuações morfológicas e microestruturais – que possibilitam a existência de locais onde o grau de super saturação da solução envolvente é mais rapidamente atingido – associada à presença de cristais de hidroxiapatite – que funcionam como pontos de nucleação heterogénea – pode ser mais importante na formação *in vitro* de apatite que a formação de grupos silanol.

Os trabalhos apresentados na última parte desta tese mostraram que a existência de fenómenos de especiação e factores de ordem morfológica e microestrutural condicionam o comportamento *in vitro* de vidros e de vidros cerâmicos, pelo que os mesmos devem ser considerados aquando do projecto destes materiais.

5.2 - Sugestões para trabalhos futuros

Das conclusões desta tese emergem várias possibilidades de realização de outros trabalhos entre os quais se consideram mais importantes os que se relacionam mais directamente com a compreensão do comportamento bioactivo de vidros e vidros cerâmicos.

Assim, o conhecimento do mecanismo de especiação será útil ao estudo da evolução da camada de sílica gel em outras composições vítreas, em especial em vidros de sílica contendo alcalinos. Sendo esta camada determinante na formação de apatite em vidros, seria interessante correlacionar a influência do desenvolvimento da camada de sílica gel no desenvolvimento da camada de apatite. A realização de testes *in vivo* seria útil para avaliar a força de ligação implante-tecido ósseo.

Face à importância da topografia da superfície na bioactividade seria importante analisar a capacidade de induzir a formação de apatite em outros materiais à base de cálcio e fósforo (como por exemplo vidros cerâmicos fosfatados) com diferentes tratamentos superficiais.

Finalmente e na sequência da experiência adquirida no estudo de vidros com elevado teor de MgO, julga-se possível desenvolver vidros em que o magnésio entre como formador, uma hipótese que ainda se mantém polémica no campo da estrutura do vidro. Este tipo de composições seria interessante não só para o estudo das propriedades bioactivas dos vidros mas sobretudo para o avanço global da ciência dos vidros. Num projecto com estas características seria útil utilizar espectroscopia de ressonância nuclear magnética ao núcleo ^{25}Mg que está actualmente em desenvolvimento.